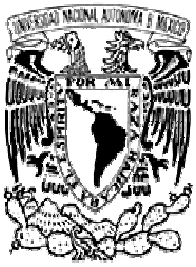

UNIVERSIDAD NACIONAL AUTÓNOMA DE MÉXICO

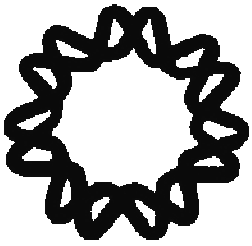

INSTITUTO DE BIOTECNOLOGÍA

"El papel de la fosfatasa alcalina de *Manduca sexta* en el mecanismo de toxicidad de la toxina Cry1Ab de *Bacillus thuringiensis*"

T E S I S

QUE PARA OBTENER EL GRADO DE

D O C T O R E N C I E N C I A S

P R E S E N T A

M. EN C. IVÁN ARENAS SOSA

DIRECTOR DE TESIS

DRA. ISABEL GÓMEZ GÓMEZ.

CUERNAVACA, MOR. **MAYO 2010.**

DEDICATORIA

Dedico este trabajo con todo mi amor a mi madre Rosa María Sosa Osorio y a mi padre Mario Arenas Anrubio que me han enseñado el significado de la palabra amor y que se han dado a la tarea de educarme para ser una persona de bien. Me siento muy orgulloso de ustedes.

A mi hermano Omar Arenas Sosa y su esposa Alejandra Castillo por apoyarme en todo momento.

A mis adorados abuelos Antonia Anrubio y Eusebio Triana que siempre tuvieron la paciencia de cuidarme cuando era necesario.

A mi tía Julia y su esposo Samuel junto con mis primos Juan y Samuel por todo el cariño que me han brindan.

A mis compadres Yazmin y Carlos por abrirme las puertas de su casa y permitirme ser quien guíe al pequeño Alan cuando así lo requieran.

A Mayra Avelar por compartir parte de su vida y de su amor conmigo a pesar de la distancia.

AGRADECIMIENTOS

Agradezco profundamente y con mucho cariño a la Dra. Isabel Gómez por todo el apoyo que me proporciono para la realización de este trabajo, por el tiempo dedicado a mi formación profesional y sobre todo por compartir su amistad conmigo. Muchas gracias.

Al Dr. Mario Soberón por permitirme pertenecer a su gran grupo de trabajo y sobre todo por estar al pendiente y aportar ideas para la realización de esta tesis.

A la Dra. Alejandra Bravo por todos sus comentarios para enriquecer este trabajo.

A los Doctores Humberto Lanz Mendoza y Lorenzo Segovia por pertenecer a mi comité tutoral y aportar ideas para mejorar mi trabajo.

A los Doctores Arturo Guevara, Alicia González, Federico Sánchez y Enrique Rudiño por darse el tiempo para revisar esta tesis.

A todos mis compañeros del laboratorio, por su amistad muchas gracias.

A mis amigos Héctor, Ángel, Javier, Alejando y Andrés por todos los momentos de felicidad que hemos pasado juntos en esta aventura.

A mis amigas Luz Adriana y Aimée por brindarme su amistad.

A la Universidad Nacional Autónoma de México por todo lo otorgado durante mis estudios de posgrado.

ESTE TRABAJO SE REALIZÓ EN EL DEPARTAMENTO

DE MICROBIOLOGÍA MOLECULAR DEL INSTITUTO

DE BIOTECNOLOGÍA DE LA UNAM BAJO LA DIRECCIÓN

DE LA DRA. ISABEL GÓMEZ.

TABLA DE CONTENIDO

ÍNDICE DE FIGURAS.

ÍNDICE DE TABLAS

LISTA DE ABREVIATURAS

ANS	8-anilino-1-nafatalenosultonato.
APN	Aminopeptidasa N.
BSA	Albúmina sérica bovina.
Bt-R_1	Caderina de *Manduca sexta*.
Bt-R_{175}	Caderina de *Bombix mori.*
DNA	Ácido desoxirribonucleico.
DTT	Ditiotritol.
EDTA	Ácido etilen diamino tetra-acético.
EGTA	N, N, N´, N´ ácido tetra acético etilen flyco-bis-(β aminoetil éter).
ELISA	Ensayo de inmunoabsorbencia ligado a enzimas.
GalNAc	N-acetil-galactosamina.
GPI	Glicosil-fosfatidil-inositol.
HEPES	Ácido 4-(2-hidroxi etil) piperanzina-1-etanol sulfónico.
IPTG	Isopopil-β-D- tiogalactopiranósido.
LB	Medio Luria-Bertoni.
PBS	Solución amortiguadora de fosfatos.
PDB	Banco de datos de proteínas.
PMSF	Fenil metanosulfonil fluoruro.
PVDF	Polivinilideno difluoruro.
RNA	Ácido ribonucleico.
RNAi	Silenciamiento con RNA interferente.
SDS PAGE	Electroforesis en gel de acrilamida en condiciones desnaturalizantes.
VMMA´s	Vesículas de la microvellosidad apical media.

ABSTRACT

The Cry toxins produced by *Bacillus thuringiensis* are an alternative for biological control of insects. In the case of Cry1A toxins, it has been proposed that after proteolytic activation of the Cry1A protoxin by midgut proteases, the monomeric form of the toxin binds to a transmembrane cadherine protein. This interaction promote the formation of an oligomeric form of the toxin that binds with high affinity to a glicosyl-phosphatidyl-inositol (GPI) anchored aminopeptidase N (APN) that facilitates the membrane insertion of the toxin. In *Manduca sexta* a second GPI-anchored protein (alkaline phosphatase, ALP) binds Cry1Ab toxin, however, the role of this protein in toxicity remains to be determined. In this work we analyzed the interaction of oligomeric and monomeric structures of Cry1Ab and of Cry1Ab mutants in domain II and domain III binding regions, with the midgut purified *M. sexta* ALP and APN to determine if these interactions are important for toxicity. Detection of Cry1Ab binding proteins by ligand blot assay revealed that ALP is preferentially expressed in earlier larval instars, whereas APN is preferentially expressed at later larval instars. This result suggests that ALP has an important role on Cry1Ab toxicity since Cry toxins are more effective when assayed with larvae from the first instars. The binding of oligomeric Cry1Ab to APN and ALP showed that this structure toxin interacts with both receptors with high affinity (apparent Kd= 0.6 nM and Kd= 0.5 nM, respectively) whereas the monomeric toxin showed lower affinity interactions (apparent Kd= 101.6 nM and 267.3 nM, respectively). Several Cry1Ab non-toxic mutants located in the exposed loop 2 of domain II or β16 domain III were affected in binding to APN and ALP, depending on their oligomeric state of the toxin. In particular, the monomeric non-toxic domain III mutant L511A did not bind to ALP, but retained APN binding, suggesting that initial monomer

interaction with ALP is critical for toxicity. Oligomers of the non-toxic domain II loop 2 mutants RR368-369AA and F371A were affected in the interaction with both receptors in contrast with toxin monomers that showed similar binding to both GPI anchored proteins as Cry1Ab wt toxin. These results suggest that the APN and ALP fulfill two roles in the mechanism of action of these toxins. First, the monomeric toxin binds to both GPI anchored proteins localized in the midgut microvilli before the toxin binds to cadherin. After cadherin interaction, the toxin forms the prepore oligomer and then binds with high affinity to APN and ALP mediating the oligomer insertion into the membrane. However, the expression pattern of these GPI-anchored receptors and the phenotype of L511A mutant suggest that ALP may have a predominant role in the toxicity than APN.

RESUMEN

Las toxinas Cry producidas por *Bacillus thuringiensis* son una elección importante en el control biológico de insectos. En el caso del mecanismo de acción de las toxinas Cry1A se ha demostrado que la toxina presenta dos interacciones sucesivas con aminopeptidasa. La primera interacción se da como monómero y la segunda después de que oligomeriza. Adicionalmente, en *M. sexta* se ha reportado una segunda proteína anclada por GPI como proteína de unión a la toxina Cry1Ab identificada como fosfatasa alcalina; sin embargo, su papel en la toxicidad no ha sido determinado. En este trabajo se analizó la interacción de la toxina Cry1Ab tanto en su conformación de monómero como de oligómero cuando se une a la aminopeptidasa y a la fosfatasa alcalina, para determinar si estas interacciones son importantes para la toxicidad y poder establecer el papel como receptor de la fosfatasa alcalina. El análisis de la expresión de los receptores en los diferentes estadíos del desarrollo muestra que la fosfatasa alcalina se expresa preferencialmente en los primeros estadíos y la aminopeptidasa se expresa después del tercer estadio de desarrollo. Esto indica que la fosfatasa alcalina es más abundante en los primeros estadíos cuando las larvas son más susceptibles a la toxina. La unión del oligómero de la toxina Cry1Ab a fosfatasa alcalina y aminopeptidasa purificadas muestran que la toxina interactúa con ambas proteínas con alta afinidad (0.5 nM y 0.6 nM, respectivamente), mientras que la afinidad del monómero es de 2 ó 3 órdenes de magnitud menor (267.3 nM y 101.6 nM, respectivamente). Algunas mutaciones que se encuentran localizadas en regiones expuestas del asa 2 del domino II y la β16 del dominio III afectan la capacidad de unión a los dos receptores dependiendo de la conformación de la toxina. Particularmente el monómero de la toxina L511A que no es tóxica, está afectada en la unión a fosfatasa alcalina pero sigue uniendo a aminopeptidasa. Lo que sugiere que la interacción inicial con fosfatasa alcalina

es crítica para la toxicidad. Las mutantes no tóxicas RR368-9AA y F371A se encuentran afectadas en la interacción con ambos receptores cuando la toxina se encuentra como oligómero, pero no como monómero. Estos datos sugieren que la aminopeptidasa y la fosfatasa alcalina juegan un papel doble en el mecanismo de acción. Primero, en las microvellosidades del intestino, el monómero de la toxina se une a la aminopeptidasa y a la fosfatasa alcalina y posteriormente, se da la interacción con el receptor caderina. El contacto con caderina induce la oligomerización de la toxina y permite nuevamente la unión aminopeptidasa y fosfatasa con alta afinidad, lo que medía la inserción de la toxina en la membrana. El fenotipo de la mutante L511A que está drásticamente afectada en la unión con fosfatasa alcalina y la toxicidad, además del patrón de expresión de los receptores, sugiere que la fosfatasa alcalina tiene un papel predominante en el mecanismo de las toxinas Cry.

INTRODUCCIÓN.

CARACTERÍSTICAS GENERALES.

Bacillus thuringiensis es miembro del grupo de *Bacillus cereus* que además incluye a *Bacillus anthracis* y a *Bacillus mycoides* (*1*). Las características que distinguen a *B. thuringiensis* de los demás miembros son sus propiedades entomopatógenas. *B. thuringiensis* es una bacteria ubicua gram positiva, formadora de esporas que durante la fase estacionaria de su crecimiento sintetiza cristales que están constituidos predominantemente de una o más proteínas llamadas Cry o Cyt. Estas proteínas son selectivamente tóxicas para diferentes insectos y son inocuas para humanos, invertebrados y plantas, además son completamente biodegradables. Debido a estas características, el uso de *B. thuringiensis* es una alternativa viable para el control de insectos plaga en la agricultura y para insectos vectores de enfermedades importantes en la salud pública.

A la fecha se han aislado numerosas cepas de *B. thuringiensis* a partir del suelo, hojas secas, insectos muertos, etc., que muestran actividad tóxica contra insectos lepidópteros, dípteros o coleópteros (*2*). Adicionalmente, en años recientes se han reportado cepas con actividad contra insectos himenópteros, homópteros, ortópteros y malófagos, así como contra ácaros y protozoarios (*3-4*).

DIVERSIDAD DE LA TOXINAS.

La gran variedad de toxinas de *B. thuringiensis* conocidas a la fecha es el resultado del interés y esfuerzos constantes internacionales para aislar y caracterizar nuevas cepas de *B. thuringiensis*, productoras de toxinas con nuevas propiedades que permitan su uso para el control agroquímico de insectos. Miles de cepas han sido seleccionadas y de éstas se han

aislado algunos cientos de toxinas de *B. thuringiensis* (http://www.lifesci.sussex.ac.uk/home/Neil_Crickmore/bt/). La extraordinaria diversidad de las toxinas Cry se debe al alto nivel de plasticidad genética de *B. thuringiensis*. Algunos de los genes de las toxinas están asociados a elementos de transposición que al promover la amplificación de los genes, da como resultado la evolución de nuevas toxinas (*5*). Adicionalmente, la mayoría de los genes de las toxinas Cry son funcionales en plásmidos y la transferencia horizontal puede resultar en la creación de nuevas cepas con combinatorias nuevas de genes Cry (*6-7*).

El gran número de proteínas Cry conocidas a la fecha ha permitido el análisis comparativo de secuencias, lo que ha ayudado a elucidar elementos importantes tanto en la función básica de la toxina, como en su especificidad. En 1989 Höfte y Whiteley realizaron el primer análisis detallado de la secuencia de las proteínas Cry e identificaron 5 bloques conservados de aminoácidos en la mayoría de las secuencias (*8*). El descubrimiento de nuevas proteínas Cry dio lugar a dos análisis más, el primero por Bravo y colaboradores (*9*) y el segundo por de Maag en el 2001 (*5*). En el análisis más reciente fueron analizadas las secuencias de Cry1 a Cry31. La mayoría de las toxinas presentan todos o algunos de los bloques conservados identificados en el trabajo de Höfte y Whiteley, sugiriendo que estas regiones pueden ser importantes en algunos aspectos de la estabilidad de la toxina o de la función. Además, fue evidente que las toxinas muestran diferentes tamaños, desde 70 kDa hasta 130-140 kDa (*8*). Los bloques conservados fueron observados en el amino terminal a lo largo de la toxina. Utilizando la información obtenida de la estructura cristalográfica de algunas toxinas activas (Cry1Aa, Cry2Aa, y Cry3Aa) fueron alineados cada uno de los tres dominios y se realizaron árboles filogenéticos para evaluar la contribución individual de

cada dominio a la especificidad (*5*). Los diferentes árboles mostraron que en general existe una correlación específica entre la identidad de la secuencia y el orden al que pertenece el insecto, pero que varios grupos no relacionados pueden tener algunas veces, la misma especificidad.

CLASIFICACIÓN DE LAS TOXINAS Cry.

El mayor determinante de las propiedades insecticidas de *B. thuringiensis* son las δ-endotoxinas (*2*). Estas endotoxinas forman dos familias multigénicas denominadas Cry o Cyt. Las proteínas Cry son tóxicas contra diferentes órdenes de insectos como lepidópteros, coleópteros, himenópteros y dípteros. En contraste, las toxinas Cyt son específicas contra dípteros aunque se han documentado algunas cepas que contienen proteínas Cyt que son específicas para coleópteros (*10*). Además de estas proteínas cristalinas, alguna cepas de *B. thuringiensis* y *B. cereus* producen un tercer grupo de proteínas insecticidas denominadas Vip (*11*). A diferencia de las proteínas Cry, estas proteínas son sintetizadas durante la fase vegetativa del desarrollo de la bacteria y secretadas al medio de cultivo sin la formación de cristales.

Las toxinas Cry comprenden 40 subgrupos con más de 200 miembros. La definición de toxina Cry es la siguiente: Cualquier proteínas paraesporal de *B. thuringiensis* que exhibe actividad tóxica contra un organismo blanco, verificable mediante bioensayo o cualquier otra proteína que tiene identidad en su secuencia de aminoácidos con alguna de las proteínas Cry (*3*). Las proteínas Cyt denotan a cualquier proteína de *B. thuringiensis* con actividad hemolítica o que tenga similitud a las proteínas Cyt. La nomenclatura de las proteínas Cry y Cyt está basada en la identidad de la secuencia primaria de las proteínas. Las proteínas reciben el mnemónico Cyt o Cry y cuatro rangos jerárquicos que consisten en

números, letras mayúsculas, letras minúsculas y números (por ejemplo Cry1Ab1). Los rangos están dados dependiendo de la identidad de la secuencia de aminoácidos que comparta con otras proteínas Cry o Cyt. Un número diferente (primer rango), está dado a una proteína que presenta menos del 45% de identidad con los demás miembros de las toxinas Cry (por ejemplo, Cry1, Cry2, etc.). La letra mayúscula (segundo rango), está dada si la proteína presenta menos del 78%, pero más del 45% de identidad con un grupo particular de toxinas Cry (por ejemplo, Cry1A, Cry1B, etc.). Un tercer rango está dado mediante letras minúsculas para distinguir proteínas que tienen más del 78%, pero menos del 95% de identidad con otras proteínas Cry (por ejemplo, la toxina Cry1Aa, Cry1Ab etc.). Finalmente se les da un número a las toxinas que comparten más del 95% de identidad, pero que no son idénticas o pueden ser variantes de la misma proteína (*3*). En esta nomenclatura no se toma en cuenta la especificidad de las toxinas y algunos subgrupos muestran toxicidad contra algunos otros órdenes de insectos. De esta manera, las toxinas Cry1 muestran toxicidad contra insectos lepidópteros y las toxinas Cry3 son tóxicas contra coleópteros. Para el caso de toxinas específicas contra dípteros, resulta interesante el alto número de proteínas con baja identidad en su secuencia de aminoácidos (por ejemplo, Cry1C, Cry2Aa, Cry4, Cry11, etc.).

ESTRUCTURA DE LAS TOXINAS Cry.

La mayoría de las proteínas Cry se sintetizan como protoxinas inactivas, que posteriormente son transformadas en toxinas activas por diferentes proteasas del intestino de diferentes insectos (*8*). Este proceso involucra una serie de cortes proteolíticos tanto en el extremo C- terminal, como en el N-terminal, hasta que se obtiene un fragmento resistente a proteasas (*12*). La estructura tridimensional de algunas toxinas Cry activadas ha sido

determinada mediante cristalografía de rayos X, tal es el caso de las toxinas Cry3Aa (*13*) y Cry3Bb1 (*14*) específicas para coleópteros, la toxina Cry1Aa específica para lepidópteros (*15*), la toxina Cry2Aa con actividad dual para lepidópteros y dípteros (*16*) y las toxinas Cry4Ba (*17*) y Cry4Aa con actividad contra dípteros (*18*). Estas toxinas muestran diferencias importantes en cuanto a su secuencia de aminoácidos y especificidad hacia diferentes insectos; sin embargo, todas ellas presentan una topología muy similar compuesta por 3 dominios (Figura 1).

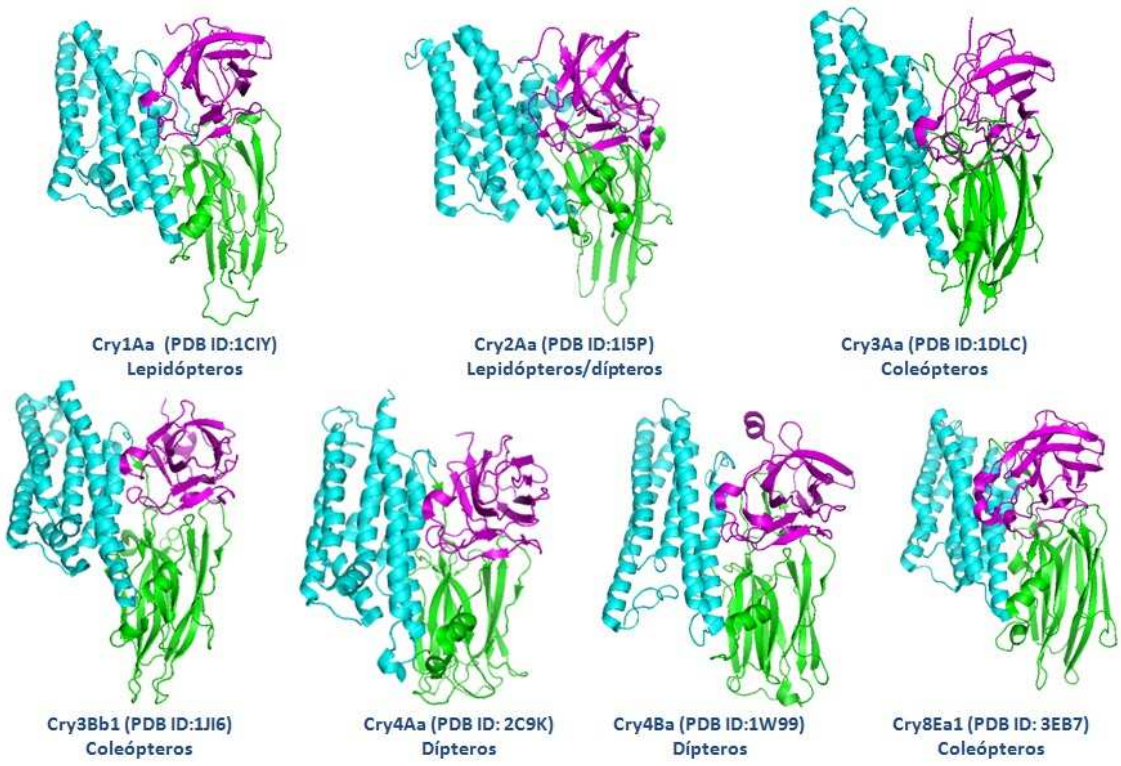

Figura 1. Estructura tridimensional de toxinas Cry. Se muestra la estructura tridimensional determinada por cristalografía de rayos X. El dominio I se muestra en color azul, el dominio II se muestra en color verde y en color morado se muestra el dominio III. Además se indica la especificidad y la clave correspondiente al PDB de cada una de las estructuras.

Dominio I.

El dominio I fue primero descrito en la toxina Cry3Aa y consiste de 7 hélices α, 6 de las cuales rodean a una hélice central (Figura 2). Cada una de las hélices es de naturaleza anfipática, en donde los residuos polares y cargados están generalmente expuestos al solvente y los residuos hidrofóbicos, típicamente de naturaleza aromática, se encuentran proyectados hacia la hélice central. Los grupos polares se encuentran presentes entre los espacios de las hélices y están involucrados en puentes de hidrógeno y puentes salinos. La mayoría de las hélices presentan una longitud de aproximadamente 30 Å y por su naturaleza, podrían atravesar una membrana hidrofóbica. Estas propiedades y la alta identidad en la estructura que presentan con otras toxinas formadoras de poro, como son la colicina Ia y la toxina de difteria, permiten suponer que el dominio I es el mayor determinante de la formación de poro en las toxinas Cry (*15, 19*). Además de esto, se han realizado experimentos con péptidos sintéticos de la hélice α5 de la toxina Cry3A, que demuestran que esta región de es capaz de formar poros en capas lipídicas en ausencia del receptor (*20*). Recientemente, se ha reportado otro papel de este dominio, en particular está involucrado en la oligomerización de la toxina. Mutaciones en la hélice α3 del dominio I de la toxina Cry1Ab, resultan en toxinas que pueden unir al receptor caderina, sin embargo, no son capaces de formar oligómero y pierden su actividad contra larvas de *M. sexta*, estos resultados sugieren que este dominio es importante para la oligomerización de la toxina(*21*). Mediante mutantes en la hélice α4 de la toxina Cry1Ab, se logró obtener toxinas con dominancia negativa, es decir, al hacer mezclas con la toxina silvestre se observó que tienen la propiedad de proteger a larvas de *M. sexta* y de evitar la formación de poro en membranas artificiales, demostrando que el proceso de oligomerización es determinante para la toxicidad de estas proteínas (*22*).

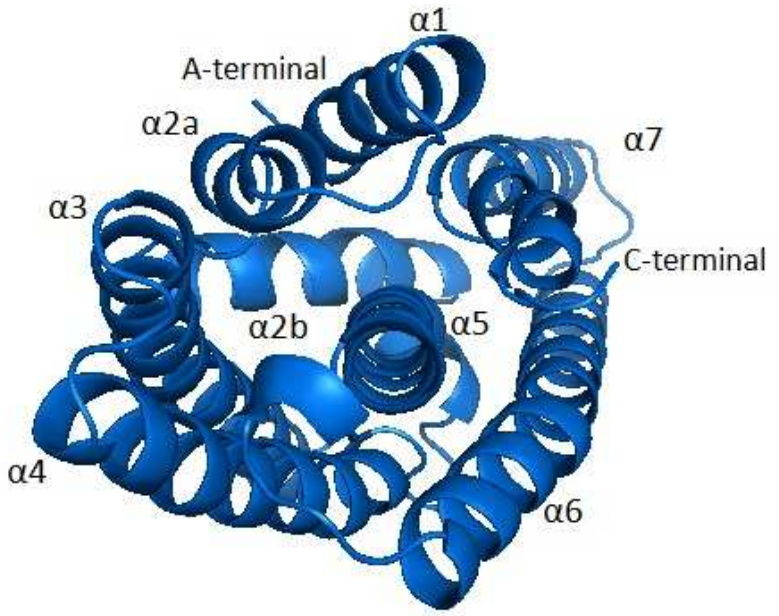

Figura 2. Estructura tridimensional del dominio I de la toxina Cry1Aa. El asa α5 de naturaleza hidrofóbica está rodeada por las demás asas que integran al dominio I.

Dominio II.

El dominio II está formado por tres láminas β antiparalelas empacadas en forma de un prisma β como se muestra en la Figura 3 (*13*). Dos de estas tres láminas β están compuestas de cuatro hojas empacadas en forma de llave griega y se encuentran expuestas al solvente. La tercera lámina β se encuentra empaquetada hacia el dominio I y está constituida por 3 hojas y una pequeña hélice α. Estructuralmente el dominio II es el más variable entre las diferentes toxinas y esto se debe a las asas que unen a estas láminas β (asa 1, asa 2 asa3 y asa α8), que difieren considerablemente en cuanto a longitud, conformación y secuencia (*17*). La similitud de las asas de este dominio, con las regiones determinantes de complementariedad de las inmunoglobulinas sugiere que este dominio es importante en la interacción con los receptores (*13*), estudios exhaustivos de mutagénesis en estas regiones

han aportado evidencia para comprobar esta hipótesis (*23*). La primera de estas asas es la α8. Un alelo de la toxina Cry1Ab, con sólo 2 cambios en los aminoácidos correspondientes a esta región, muestra un aumento en la afinidad de 9 veces a vesículas de la microvellosidad media apical (VMMA´s) de *Lymantria dispar* y presenta un aumento de diez veces en la toxicidad. Sin embargo, estos alelos no difieren en cuanto a su toxicidad o unión a *M. sexta* y *Spodoptera exigua* (*24*). Para el caso de la toxina Cry1Ab, se ha demostrado mediante competencias con péptidos sintéticos, que el asa α8 participa en la interacción con el receptor caderina de *M. sexta* (*25*). El asa siguiente es el asa 1 que no está específicamente implicada en la interacción para las toxinas Cry1A, sin embargo, una triple mutante en esta asa (R345A, Y350A y Y351A) de la toxina Cry3A, resulta en unión y toxicidad reducida en larvas del escarabajo *Tenebrio molitor*, lo que sugiere que esta región es importante en la interacción con el receptor para el caso de insectos coleópteros (*26*). Resulta interesante que cambios en estas posiciones (R354A, Y350F y Y351F), dan como resultado un aumento en la toxicidad de 10 veces con respecto a la toxina silvestre, en larvas de *T. molitor* (*27*). En el caso del asa 2, mutaciones en esta región de la toxina Cry1Ab afectan dramáticamente la unión a VMMA´s y la toxicidad en *Bombix mori* (*28*). De la misma manera, en la toxina Cry1Ab, mutaciones en los residuos ^{368}RRP^{370} resultan en la pérdida de unión a VMMA´s de *M. sexta* y *Heliothis virescens*. La doble mutante 368RR369 por alanina en la toxinas Cry1Ab y Cry1Ac, resulta en una toxina con defectos en la unión a VMMA´s de *M. sexta* y *L. dispar* (*29*). Una mutación con propiedades únicas es la F371A en la toxina Cry1Ab que muestra toxicidad reducida, pero no presenta diferencias en la unión a VMMA´s con respecto a la toxina silvestre (*30*). Sin embargo, esta mutación en la toxina Cry1Ac no altera la toxicidad de esta toxina en larvas de *L. dispar*, lo que sugiere que esta propiedad puede no estar conservada entre toxinas relacionadas con

diferentes insectos (*31*). Mediante el uso de la tecnología de despliegue en fago, se logró aislar un anticuerpo que reconoce el asa 2 del dominio II de la toxina Cry1Ab, que además mimetiza al receptor caderina y tiene la capacidad de inhibir el efecto tóxico de la toxina en bioensayos, la caracterización de este anticuerpo permitió determinar que el asa 2 es importante para la interacción con el receptor caderina en *M. sexta* (*25*). Finalmente, mutaciones en el asa 3 de las toxinas Cry1Aa y Cry1Ab resultan en toxinas con defectos en la unión a VMMA´s de *M. sexta* y *H. virescens* (*32*). Este resultado sugiere que esta región es importante en la interacción con los receptores. Mediante la caracterización de un anticuerpo que reconoce el asa 3 de la toxina Cry1Ab, que tiene la propiedad de evitar el efecto de la toxina en bioensayos con larvas de *M. sexta*, se demostró que esta región es importante en la interacción con el receptor caderina de este insecto (*33*). Si bien, este dominio ha sido el mejor caracterizado mediante mutaciones puntuales, aun falta determinar su relevancia en la interacción con los receptores anclados por GPI cuando la toxina se oligomeriza.

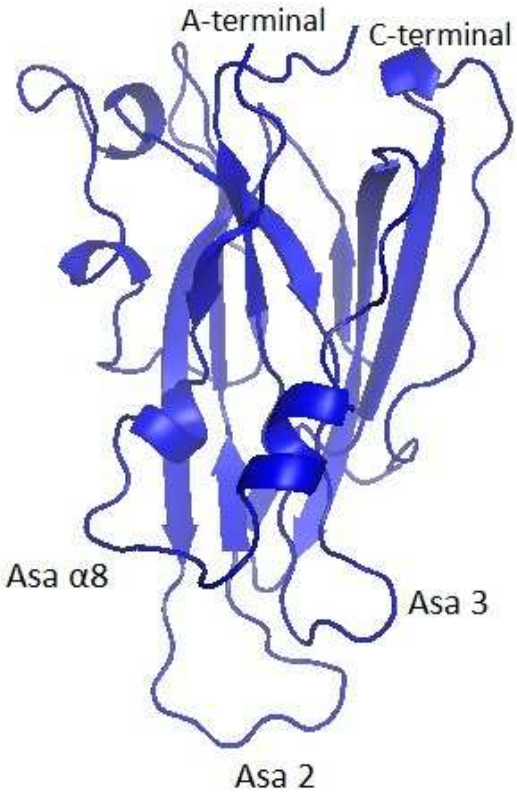

Figura 3. Estructura tridimensional del dominio II de la toxina Cry1Aa. Se muestran las asas (α8, 2 y 3) involucradas en la interacción del monómero con los receptores.

Dominio III.

El dominio III está constituido por dos láminas β antiparalelas y muestra menor variabilidad estructural que el dominio II, las diferencias más importantes se encuentran en la longitud, orientación y secuencia de las asas que unen estas láminas (Figura 4) (*17*). La importancia de estas diferencias resalta en las toxinas Cry1Aa y Cry1Ac, donde la extensión de una de estas asas en la toxina Cry1Ac forma un sitio único de unión al azúcar N-acetilgalactosamina (GalNAc) que se encuentra en el receptor aminopeptidasa de *M. sexta* (*34-36*). Mediante el intercambio de este dominio entre las toxinas Cry1Ab y Cry1C, se obtuvieron toxinas con actividad incrementada contra larvas de *S. exigua* con respecto a

la toxina Cry1Ab silvestre, lo que sugiere que este dominio juega un papel en la toxicidad (*37*). En el caso de la toxina Cry1Aa, se ha demostrado que este dominio interacciona directamente con la aminopeptidasa de *B. mori* (*38*). Más recientemente, la caracterización de un fago-anticuerpo seleccionado específicamente contra el dominio III de la toxina Cry1Ab, que tiene la capacidad de inhibir la interacción de la toxina con el receptor aminopeptidasa e inhibe la toxicidad en bioensayos con larvas de *M. sexta*, demostró que la β16 del dominio III está involucrada en la interacción del receptor aminopeptidasa (*33*). Todos estos experimentos demuestran que el dominio III está involucrado en la interacción con los receptores, sin embargo, hay que tomar en cuenta que todos los experimentos se han realizado con el monómero de la toxina y la interacción del oligómero no ha sido explorada a la fecha.

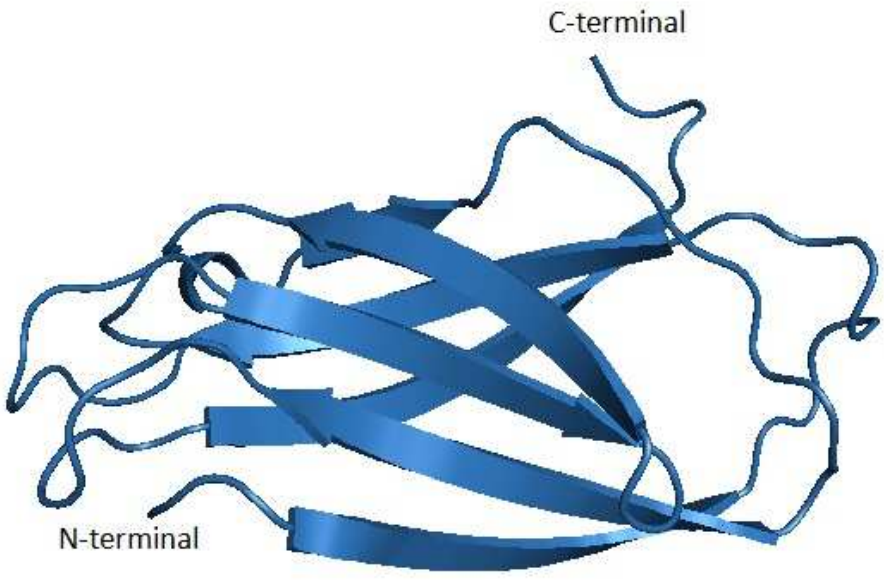

Figura 4. Estructura tridimensional del dominio III de la toxina Cry1Aa. Se muestran las láminas β que conforman al dominio III.

EVOLUCIÓN DE LAS TOXINAS Cry.

El incremento de toxinas Cry y la gran variedad de organismos blanco que estas proteínas matan, permite plantearse la pregunta de ¿cómo la evolución de esta familia de proteínas ha creado un amplio arsenal de toxinas? Se ha propuesto que las toxinas han coevolucionado con los insectos blanco (*5*); sin embargo, no hay estudios que correlacionen la distribución geográfica de las proteínas Cry que contienen las diversas cepas de *B. thuringiensis*, con la distribución de las diferentes especies de insectos blanco en la naturaleza. Un estudio realizado con una colección de cepas de *B. thuringiensis* provenientes de diferentes regiones climáticas de México, reveló que genes nuevos de toxinas Cry son encontrados más frecuentemente en cepas aisladas en regiones tropicales, en donde la diversidad de insectos es mayor (*39*). Adicionalmente, genes específicos para dípteros como Cry11 y Cyt, fueron encontrados más frecuentemente en regiones tropicales que en regiones semiáridas, lo que correlaciona con la distribución de dípteros (*39*). En otro estudio realizado por Bernhard en 1997 se mostró que un alto número de cepas de *B. thuringiensis* activas contra *H. virescens* fueron colectadas en norte América, en donde este insecto es la mayor plaga en la agricultura. Estos resultados sugieren que las toxinas Cry y los insectos blanco parecen estar presentes en el mismo lugar (*40*).

Análisis filogenéticos de toxinas o protoxinas, muestran una amplia correlación con la toxicidad (*9*), sin embargo, análisis filogenéticos de los dominios de las toxinas, muestran características interesantes en lo que se refiere a la evolución de esta familia de proteínas (*5, 9*). El análisis de los árboles filogenético de las secuencias de los dominio I y II por separado, reveló que estos dominios han coevolucionado (*9*). En el caso del dominio II, el análisis de los arboles filogenéticos muestra una topología que correlaciona con la

especificidad de estas proteínas. Este resultado no sorprende pues se sabe que el dominio II está involucrado en la unión al receptor y es un determinante de selectividad de los insectos (*5, 9*). Sorprendentemente, el análisis de los árboles filogenéticos del dominio I, que es el responsable de la formación de poro, mostró una topología que correlaciona con la selectividad de estas proteínas (*5, 9*). Esto sugiere que diferentes tipos de dominio I, han sido seleccionados para actuar en condiciones particulares de la membrana de sus insectos blanco. El análisis filogenético del dominio III, revela una topología diferente de los árboles filogenéticos de los dominios I y II, debido a intercambios del dominio III que se han dado en la naturaleza. Algunas toxinas con especificidad dual (coleópteros, lepidópteros), son claros ejemplos de intercambios del dominio III entre toxinas específicas contra lepidópteros y coleópteros. La toxina Cry1B es un claro ejemplo del intercambio del dominio III, en donde se han descrito 5 diferentes toxinas, que presentan el dominio I y II idénticos, sin embargo, el dominios III de estas toxinas muestra un proceso activo de intercambio de este dominio con el correspondiente de otras toxinas. Esta característica ha permitido el cambio de especificidad, por ejemplo, la toxina Cry1Ba es activa contra el coleóptero *Leptinotarsa decemlineata*, pero la toxina Cry1Bb, es activa contra el lepidóptero *Plutella xylostella*. Un análisis más profundo de las toxicidades de las toxinas Cry1B podría demostrar la relevancia del intercambio del dominio III en la toxicidad. *In vitro* se han realizado intercambios de dominios III de algunas toxinas Cry1, resultando en cambios en la especificidad. Un ejemplo es la construcción de una quimera que tiene el dominio I y II de la toxina Cry1Ab que no es tóxica para *S. exigua*, y el dominio III de la toxina Cry1C. La quimera muestra toxicidad contra *S. exigua* (*5, 41*). El análisis filogenético de la familia de las toxinas Cry, muestra que la gran variabilidad en la actividad insecticida de estas proteínas se debe fundamentalmente a dos procesos

evolutivos: La evolución independiente de los tres dominios estructurales y al intercambio horizontal del dominio III entre diferentes toxinas. Estos dos procesos han permitido la generación de proteínas con mecanismos de acción similares, pero con diferentes especificidades (*5*, *9*).

MECANISMO DE ACCIÓN DE LAS TOXINAS Cry.

La primera acción de las toxinas Cry es la de lisar las células epiteliales del intestino medio de insectos (*2*, *5*, *42*). Para obtener este efecto tóxico, las protoxinas Cry son modificadas para formar oligómeros que le permiten la inserción en la membrana y para causar la lisis de las células. Los cristales producidos por *B. thuringiensis* son ingeridas por el insecto blanco y se disuelven en el ambiente del intestino, las protoxinas inactivas son cortadas por proteasas propias del intestino, liberando una toxina de 60 kDa (*12*). La activación de la toxina involucra el corte proteolítico en la región N-terminal, de aproximadamente 25-30 aminoácidos para las toxinas Cry1 y aproximadamente la mitad del carboxilo terminal en protoxinas de 130 kDa. La toxina activa se une a receptores específicos localizados en la microvellosidad apical de las células columnares del intestino medio del insecto susceptible y posteriormente se inserta en la membrana (*2*). La inserción en la membrana da lugar a la formación de poros, la lisis celular y el rompimiento del epitelio intestinal, liberando el contenido celular que provee a las esporas de un medio rico, necesario para su germinación, causando una severa septicemia al insecto, que finalmente le causa la muerte (*2*, *5*).

Solubilización y activación proteolítica.

La solubilización de los cristales para liberar las protoxinas (130 kDa) depende del pH alcalino presente en el intestino los insectos lepidópteros y dípteros, a diferencia de los insectos coleópteros, que presentan un pH neutro o ligeramente ácido (*43*). El carboxilo

terminal de las protoxinas Cry contiene muchas regiones ricas en cisteínas, que forman puentes disulfuro cuando estás se encuentran en forma de cristales, por lo tanto, la reducción de estos puentes disulfuro es una paso necesario para su solubilización (*44*). Adicionalmente, el procesamiento proteolítico de estas toxinas es un paso crítico involucrado en la activación de la toxina. El pH del intestino de insectos lepidópteros y coleópteros define la población de proteasas que expresan. Se ha reportado que las serin-proteasas son abundantes en lepidópteros y dípteros, en contraste con los coleópteros que presentan cistein o aspartil-proteasas (*45*). Se ha reportado que la baja toxicidad de la toxina Cry1Ab a *S. frugiperda*, puede ser explicada en parte por la rápida degradación de la toxina, debido a que las proteasas propias de este insecto, a diferencia de la activación de la toxina en *M. sexta* cuyas proteasas intestinales son diferentes. Estos resultados sugieren que las proteasas de cada insecto son importantes para la activación correcta de la toxina (*46*). Para algunas toxinas la inactivación involucra un procesamiento intramolecular de la proteína (*12, 46*); sin embargo, en otras toxinas este proceso no está relacionado con la pérdida de toxicidad y en algunos casos, favorece la activación de la toxina (*47*). Con estos antecedes, se propone que el proceso proteolítico de diferentes insectos puede ser un paso limitante en la toxicidad de las proteínas Cry (*46*).

Unión al receptor, oligomerización y formación de poro.

La unión de las toxinas Cry a receptores en el epitelio intestinal del insecto es determinante en la toxicidad y en la especificidad. La correlación entre unión y toxicidad fue demostrada usando VMMA´s purificadas del intestino de algunos insectos, mediante una técnica desarrollada por Wolfersberger (*48*). Algunos estudios muestran que la toxina Cry1Ba tóxica para *Pieris brassicae* une específicamente a VMMA´s del insecto, pero no a

VMMA´s de rata. Posteriormente, se demostró que las toxinas Cry1Ab y Cry1Ba se unen específicamente a VMMA´s de *P. brassicae,* pero además, la toxina Cry1Ab une a VMMA´s purificadas de *M. sexta*. Como ambas proteínas son tóxicas para *P. brassicae*, pero sólo la toxina Cry1Ab es tóxica para *M. sexta*, esto demostró una correlación entre la unión y la toxicidad (*49*). Para las toxinas Cry se han descrito a la fecha 3 proteínas de unión en insectos lepidópteros, una proteína de la súper familia de las caderinas, una aminopeptidasa y una fosfatasa alcalina, ambas ancladas por GPI (glicosil-fosfatidil-inositol) y un glicoconjugado de 270 kDa (*50-53*). El papel de la interacción toxina-receptor ha sido examinado con mayor detalle en *M. sexta*, el modelo propuesto por Bravo y colaboradores, propone que una vez que la toxina es solubilizada y activada proteolíticamente, ésta se une como monómero al receptor caderina, la unión a esta proteína promueve cambios conformacionales en la toxina que la hacen susceptible a un segundo corte proteolítico, perdiendo la hélice α1 (*25, 46, 54-55*). Este corte permite la exposición de residuos hidrofóbicos y promueve la oligomerización de la toxina. La formación de oligómeros se ha reportado para diferentes toxinas Cry, entre ellas la Cry1Aa, Cry1Ab, Cry1Ca, Cry1Da, Cry1Ea y Cry1Fa, que son toxinas activas contra *M. sexta* y que forman oligómeros después de la activación con VMMA´s (*56-61*). Una vez formado el oligómero, se propone que éste se une a la aminopeptidasa que se encuentra localizada en balsas lipídicas, donde se lleva a cabo la formación de poro que causa un desbalance osmótico en la célula, llevando finalmente a la muerte del inserto (*62-63*). Recientemente, la caracterización de mutantes en el asa 3 del dominio II de la toxina Cry1Ab, dio como resultado la adición de más pasos en este mecanismo de acción (*64*). Con base en el mecanismo de acción de la aerolisina, con la que se ha demostrado que se une primero a moléculas de baja afinidad pero muy abundantes en sus células blanco, para

posteriormente, unirse a moléculas poco abundantes, pero de alta afinidad (*65*), se propone que una vez que los cristales son solubilizados y activados, el monómero de la toxina une primero a la aminopeptidasa con una baja afinidad (Kd= 100 nM) y posteriormente a la caderina con alta afinidad (kd= 1 nM); cabe mencionar que la aminopeptidasa es más abundante que la caderina en el intestino de *M. sexta*. Una vez que el monómero se une a caderina, éste sufre el corte de la hélice α1, lo que permite la formación del oligómero. Posteriormente, el oligómero se une nuevamente a la aminopeptidasa para insertarse en la membrana y formar el poro, que provocará la muerte del insecto (Figura 5) (*64*). La formación de poro es un paso determinante en el efecto tóxico de estas proteínas y con la evidencia que se tiene con otras toxinas bacterianas, se han propuesto dos modelos de inserción en la membrana, denominados como abrecartas y paraguas. El modelo de abrecartas, propone que las hélices α5 y 6 del dominio I se insertan en membrana como consecuencia de un cambio conformacional disparado por el receptor, sin participación de los dominio restantes. El modelo de paraguas plantea que una vez que la toxina se une al receptor, se insertan la región de la hélice α4-α5, mientras que el resto de la hélices se aplanan sobre la superficie de la bicapa lipídica, exponiendo hacia ella su cara hidrofóbica, de tal forma que la molécula queda en forma de paraguas (*66*). A la fecha los trabajos reportados respaldan el segundo modelo. Se ha demostrado mediante cambios por cisteínas en las hélices del dominio I, para evitar el movimiento de la hélice α5 mediante puentes disulfuro, que a diferencia de la toxina silvestre, las toxinas mutantes solo fueron capaces de formar poro en bicapas lipídicas cuando se les puso un agente reductor, como el β-mercaptoetanol que rompe los puentes disulfuro, lo que dejó ver la necesidad de que las hélices α4 y α5 conserven su flexibilidad para llevar a cabo la inserción y formación eficiente de poro (*67*).

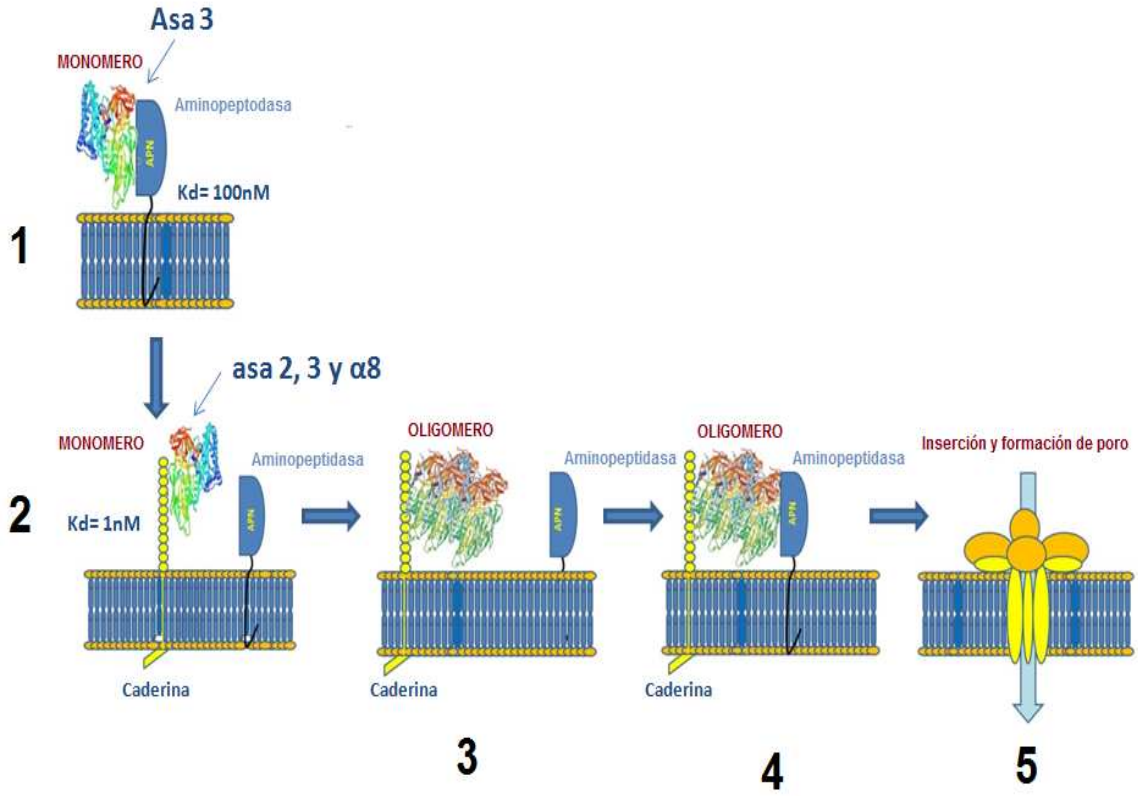

Figura 5. Mecanismo de acción propuesto de las toxinas Cry en *M. sexta*. Una vez que los cristales son solubilizado y activados, el monómero de la toxina se une al receptor aminopeptidasa con una afinidad de 100 nM (1). Posteriormente, el monómero se une a la caderina con alta afinidad (1 nM) mediante las asas del dominio II (2). Se corta el asa α1 y se exponen regiones hidrofóbicas que permiten la oligomerización de la toxina (3). El oligómero ahora se une al receptor aminopeptidasa (4) y se lleva a cabo la inserción y formación de poro que lleva a la muerte del insecto.

ANTECEDENTES

RECEPTORES Y PROTEÍNAS DE UNIÓN DE LAS TOXINAS Cry.

Como ya se mencionó, las toxinas Cry son altamente selectivas y matan diferentes especies de insectos. Esta selectividad está mediada por la interacción de las toxinas con proteínas localizadas en epitelio de las células del intestino. Se han realizado esfuerzos para identificar estas proteínas y en la actualidad se han descrito dos tipos: proteínas transmembranales como las caderinas, y proteínas ancladas a la membrana de las células por GPI.

La caderina fue la primera proteína descrita como proteína de unión de las toxinas Cry1A en *M. sexta* (*50, 68*). Posteriormente, se demostró que no sólo está involucrada en la unión a la toxina, sino que también es importante para que la toxina tenga su efecto tóxico en algunas especies de lepidópteros, como *B. mori* (*69*), *H. virescens* (*70*), *H. armiguera* (*71*), *Pectinophora gossypiella* (*72*), *Ostrinia nubilalis* (*73*) y en el díptero *Anopheles gambiae* (*74*). Las caderinas de insectos son proteínas modulares compuestas por tres dominios, el ectodominio que está compuesto por 11 ó 12 repetidos, el dominio transmembranal y el dominio intracelular. A diferencia de las caderinas de vertebrados que están involucradas en las uniones entre célula y célula, las caderinas de insectos están localizadas en la membrana basolateral del las células intestinales. En el caso de *M. sexta* y *A. gambiae*, se ha demostrado que la caderina se encuentra localizada en las microvellosidades de las células epiteliales del intestino medio (*74-75*). La caderina de *M. sexta* se ha expresado de manera heteróloga en líneas celulares de mamífero COS7 y HEK193, donde se ha demostrado que su presencia da susceptibilidad a estas células cuando se exponen a la

toxina Cry1Ab (*76*). Adicionalmente, la expresión de esta caderina en la líneas celulares de *Drosophila melanogaster* (S2) y de *Trichoplusa ni* (H5), resulta en células susceptibles a la toxina Cry1Ab en ambos casos, lo que sugiere que esta proteínas está involucrada en la toxicidad (*77*). En el caso de la caderina de *H. virescens*, ésta fue expresada en células S2 y, de la misma manera que sucede con la caderina de *M. sexta*, también confiere susceptibilidad a las toxinas Cry1A (*78*). Interesantemente, se ha reportado que pequeñas regiones del receptor caderina de *M. sexta* (R12), al ser expresadas en líneas celulares S2 dan como resultado a células susceptibles a la toxina Cry1Ab, este resultado sugiere que esta pequeña región es importante para mediar toxicidad (*79*). La caderina de *B. mori* se ha expresado en líneas celulares de insecto SF9 y de mamíferos HEK193, en ambos casos las líneas celulares fueron susceptibles a la toxina Cry1Aa (*80-81*). Es importante mencionar que estos trabajos se han realizado en líneas celulares y se requieren altas concentraciones de toxina para observar el efecto tóxico, a diferencia de las dosis que se utilizan en bioensayos con larvas de insectos. Sin embargo, estos datos dejan ver que las caderinas juegan un papel importante en la toxicidad de estas toxinas en diferentes insectos. También se han empleado otras metodologías para analizar el papel funcional de estas proteínas. En nuestro laboratorio se han aislado fago-anticuerpos que reconocen las asas 2 y 3 del dominio II y tienen la capacidad de inhibir la interacción de la toxina Cry1Ab con la caderina de *M. sexta*, en experimentos de unión a ligando, así mismo, cuando se alimentan larvas neonatas de *M. sexta* con la toxina preincubada con estos fago-anticuerpos, se observa que tienen la capacidad de proteger a las larvas del efecto de la toxina Cry1Ab. Esto demuestra por un lado, que las regiones que reconocen los anticuerpos en esta toxina (asa 2 y 3) están involucradas en la interacción con caderina y por otro, que esta interacción es importante para la toxicidad (*25, 33, 55*). Experimentos similares empleando un péptido

sintético correspondiente con la secuencia del asa α8, indicaron el mismo efecto (*25*). La interacción de la toxina con caderina es un proceso complejo, a la fecha se ha demostrado que existen 3 regiones en el receptor que están involucradas en la interacción con las asas del dominio II de la toxina Cry1Ab. El asa 2 de la toxina interacciona con los residuos ^{865}NITIHITDTNN^{875} localizado en el repetido 7, mientras que las asas 3 y α8 interaccionan con los residuos ^{1331}IPLPASILTVTV^{1342} localizados en el repetido 11 (*25*, *54*). Posteriormente, fue reportada una tercera región de interacción en el receptor que se localiza en el repetido 12 (*82*). A todos estos resultados, se suma la caracterización de diferentes poblaciones de insectos resistentes (*H. virescens*, *P. gossypiella y H. armiguera*), cuya resistencia se encuentra asociada con el receptor caderina (*70*). Finalmente, en el caso de *M. sexta*, el silenciamiento del transcrito de caderina mediante RNA de doble cadena resulta en larvas con resistencia a la toxina Cry1Ab (*83*). Este receptor además juega un papel adicional en la oligomerización de la toxina, la incubación de la protoxina con un fragmento de caderina y jugo gástrico *de M. sexta* promueve el corte de la hélice α1 del domino I de la toxina Cry1Ab, lo que permite la formación de un oligómero de aproximadamente 250 kDa que es competente para insertarse en las membranas del intestino (*56*). Resultados semejantes se han obtenido cuando se incuba la protoxina con jugo gástrico y VMMA´s, en donde la caderina se encuentra completa (*25*). Estos resultados indican que la presencia de caderina en el intestino del insecto es necesaria para que las toxinas Cry tengan su efecto tóxico.

En el caso de las proteínas ancladas por GPI, la primera reportada como proteína de unión de las toxina Cry fue la aminopeptidasa de *M. sexta* (*51*). La aminopeptidasa es una proteína glicosilada que se encuentra anclada a la membrana de las células mediante un

enlace GPI. A la fecha se han reportado diferentes aminopeptidasa en diversos insectos como *H. virescens* (*84*), *S. litura* (*85*), *H. armiguera* (*86*), *B. mori* (*87*), *L. dispar* (*88*) y *P. xylostella* (*89*). Análisis filogenéticos han demostrado que en insectos lepidópteros existen al menos 5 familias de aminopeptidasas y que de éstas, al menos 3 unen a las toxinas Cry en diferentes especies de insectos (*90*). Diversos estudios han explorado el papel de esta proteína como receptor de las toxinas Cry, entre los que incluyen el bloqueo de la interacción de la toxina con esta proteína. En *M. sexta* se logró aislar un fago-anticuerpo (M22), que une a la región β16-β22 del domino III de la toxina Cry1Ab, que tiene la capacidad de inhibir la interacción de la toxina con el receptor aminopeptidasa, pero no con caderina. En bioensayos con larvas de *M. sexta*. Este fago-anticuerpo inhibe el efecto tóxico de esta toxina (*33*). Con la toxina Cry1Ac, se ha demostrado que une a la aminopeptidasa de *M. sexta* a través de una cavidad presente en el dominio III y que esta interacción, está mediada por el azúcar N-aceltilgalactosamina (GalNAc) que se encuentra en el receptor; sin embargo, esta interacción no se ha reportado para ninguna otra proteína Cry (*91-92*). La caracterización de una población de *S. exigua* resistente a la toxina Cry1Ca, indicó que la resistencia estaba ligada a la falta del transcrito correspondiente a la aminopeptidasa, sugiriendo su papel en la toxicidad de esta toxina (*93*). Adicionalmente, en S*podoptera litura* se logró el silenciamiento de la aminopeptidasa mediante la inyección de RNA de doble cadena, lo que resultó en una baja susceptibilidad a la toxina Cry1Ca, lo que da a esta proteína un papel en la toxicidad de esta toxina (*94*). Mediante la expresión heteróloga de la aminopeptidasa de *M. sexta* en el intestino de *D. melanogaster*, se demostró que la presencia de esta proteína en el intestino de la mosca da como resultado susceptibilidad a la toxina Cry1Ac, mientras que las moscas silvestres no son susceptibles (*95*). Estos resultados sugieren que la aminopeptidasa juega un papel importante en la toxicidad de las

toxinas Cry, adicionalmente, la aminopeptidasa también ha sido implicada en la inserción de la toxina, pues el tratamiento de VMMA´s de *M. sexta* con fosfolipasa C, que corta el enlace GPI, disminuye substancialmente la incorporación de la toxina en balsas lipídicas de membrana (*96*). En *Trichoplusa ni*, se analizó la formación de poro en VMMA´s tratadas con fosfolipasa C y se observó una drástica reducción de la formación de poro en comparación con las VMMA´s no tratadas, lo que sugiere que la aminopeptidasa también está involucrada en la inserción de la toxina (*97*). Todos estos antecedentes aportan información que apoyan el papel de la aminopeptidasa como receptor de las toxinas Cry.

Recientemente se han reportado otras proteínas como posibles receptores o proteínas de unión a las toxinas Cry, sin embargo, en algunos casos no hay suficiente información para determinar si son receptores funcionales. La fosfatasa alcalina es una glicoproteína anclada por GPI y en *H. virescen*s es una proteína de 68 kDa que une a la toxina Cry1Ac (*98*). Esta unión fue demostrada en ensayos de unión a ligando y esta interacción es dependiente del azúcar GalNAc. Los niveles de expresión de fosfatasa alcalina en una población de *H. virescens* resistente a la toxina Cry1Ac se encuentran disminuidos, lo que sugiere que esta proteína puede estar involucrada en el mecanismo de toxicidad (*52*). La presencia de un anclaje GPI en la fosfatasa alcalina y la importancia del azúcar GalNac para esta interacción, sugieren una interacción similar a la de la aminopeptidasa con la toxina Cry1Ac. En *M. sexta*, mediante un análisis proteómico y experimentos de unión a ligando de VMMA´s con la toxina Cry1Ac, se identificó una proteína de 65 kDa como fosfatasa alcalina; sin embargo, no se tienen más datos que apoyen su papel como receptor de las toxinas Cry (*99*). Mediante experimentos de inmunolocalización se ha podido demostrar que la fosfatasa alcalina se encuentra distribuida en la microvellosidad del intestino medio

y que colocaliza con las regiones donde se une la toxina, lo que sugiere su posible participación en la toxicidad de Cry1Ac (*75*). De la misma manera que en *M. sexta*, en *H. armiguera* también se reportó una fosfatasa alcalina como proteína de unión y como posible receptor de la toxina Cry1Ac (*100*). En algunos insectos dípteros, también se han reportado algunas fosfatasas alcalinas con propiedades similares a las de lepidópteros. En *A. aegypti* se ha reportado una fosfatasa alcalina de aproximadamente 65 kDa que se encuentra anclada por GPI, estudios de inmunofluorescencia han demostrado que esta proteína se localiza en la ceca y en la región posterior del intestino medio, de la misma manera que ocurre con la fosfatasa alcalina de *M. sexta*, la localización de esta fosfatasa coincide con las regiones en las que se une la toxina Cry11Aa (*101*). Bioensayos realizados con toxina Cry11Aa en presencia de un fago-péptido que reconoce a la fosfatasa alcalina y que inhibe la unión con la toxina, mostraron que este fago-péptido puede disminuir la toxicidad de Cry11Aa, lo que sugiere que la fosfatasa alcalina juega un papel funcional en la toxicidad de esta toxina (*101*). En *A. aegypti* también se reportó a la fosfatasa alcalina como proteína de unión de la toxina Cry4Ba (*102*). En *Anopheles gambiae* se reportó una fosfatasa alcalina de 63 kDa que une a la toxina Cry11Ba, esta proteína al expresarse en *E. coli* mantiene su capacidad de unir a la toxina Cry11Ba con alta afinidad (23.9 nM), bioensayos realizados con ésta toxina, en presencia de la fosfatasa alcalina purificada, muestran que la toxicidad disminuye, lo que sugiere que la fosfatasa alcalina es un receptor de la toxina Cry11Ba en *A. gambiae* (*103*). Aunque estos antecedentes muestran que la fosfatasa alcalina es receptor de las toxinas Cry y es determinante de toxicidad en algunos insectos, en el caso de *M. sexta* falta explorar más al respecto.

También se ha reportado otra proteína de unión de las toxinas Cry en *Lymantria dispar*, una glicoproteína de aproximadamente 270 kDa que une a las toxinas Cry1Aa y Cry1Ab con alta afinidad, aunque une muy poco a la toxina Cry1Ac (*104*). A la fecha este es el único insecto donde se ha reportado y no se ha caracterizado más sobre él.

Todos los reportes anteriores dejan ver que la interacción de la toxina con sus receptores es un paso determinante en la toxicidad de las toxinas Cry, a la fecha las interacciones más estudiadas son las de los monómeros de las toxinas con algunas de las proteínas mencionadas anteriormente. En el caso de la toxina Cry1Ab, se ha reportado que puede interaccionar tanto con caderina, mediante las asas del dominio II como con aminopeptidasa, mediante el asa 3 del dominio II y la β16 del dominio III. Sin embargo, en el mecanismo de acción de las toxinas Cry en lepidópteros se propone que el oligómero de la toxina tiene interacciones con los receptores anclados por GPI, las cuales son importantes para la actividad insecticida de estas proteínas. A la fecha, el conocimiento sobre la interacción del oligómero con los receptores es muy escaso. En *M. sexta* se han realizado experimentos de inmunoprecipitación, donde se incubó al monómero y al oligómero de la toxina Cry1Ab de manera independiente con VMMA´s solubilizadas, posteriormente, fueron analizadas las proteínas que coprecipataron con cada una de las entidades de la toxina mediante anticuerpos específicos. Los resultados que se obtuvieron muestran que la caderina se une preferencialmente al monómero de la toxina y la aminopeptidasa se une preferencialmente al oligómero (*96*). Adicionalmente, se determinó la constante de afinidad aparente mediante ensayo de ELISA utilizando un extracto enriquecido en proteínas ancladas por GPI y se determinó que el oligómero se une con mayor afinidad a estas proteínas (kd= 0.75 nM), mientras que el monómero se une con menor afinidad (kd= 165

nM), sin embargo, este análisis se realizó utilizando una mezcla de proteínas obtenidas al tratar con fosfolipasa C las VMMA´s, lo que significa que está compuesto por una población de proteínas ancladas por GPI, por lo tanto, no se tiene la certeza de que esta interacción se deba exclusivamente a la aminopeptidasa o si también existen interacciones con la fosfatasa alcalina, la cual también es una proteína anclada por GPI. En este sentido, nos interesa estudiar la interacción del oligómero de la toxina Cry1Ab con las proteínas ancladas por GPI, particularmente con la aminopeptidasa y la fosfatasa alcalina. En el caso de la aminopeptidasa, ya se ha demostrado que es receptor de estas toxinas; sin embargo, los estudios reportados a la fecha se han realizado con el monómero de diferentes toxinas Cry, queda por estudiar esta misma interacción utilizando el oligómero de la toxina. Por otro lado, falta describir el papel de la fosfatasa alcalina, que a pesar de estar propuesta como proteína de unión para la toxina Cry1Ac en diferentes insectos y que en *H. virescens* se ha demostrado que está ligada a la resistencia, no se tienen datos para la toxina Cry1Ab. Para el caso de *M. sexta*, sólo se ha reportado que una fosfatasa alcalina de 65 kDa une a la proteína Cry1Ac en condiciones desnaturalizantes, sin embargo, se requiere explorar el papel de esta proteína en el mecanismo de toxicidad de las proteínas Cry. Se tienen algunos datos que apoyan a la fosfatasa alcalina como un receptor de las toxinas Cry: se ha reportado que una mezcla de aminopeptidasa y fosfatasa alcalina de *M. sexta*, al ser incorporadas en vesículas de lípidos, aumentan la unión de la toxina en un 35% y la formación de poro 100 veces, sin embargo, en este reporte no se determinó si el efecto es causado exclusivamente por una de las dos proteínas (*105*). También se sabe que la mutante R511A de la toxina Cry1Ac a pesar de ya no unir aminopeptidasa, sigue siendo tóxica en bioensayos con larvas de *M. sexta*, este resultado sugiere que probablemente hay otra proteína que participa en el mecanismo de toxicidad, probablemente esta proteína sea la

fosfatasa alcalina. Por esta razón, es importante determinar si la fosfatasa alcalina es sólo una proteína de unión o si tiene un papel funcional como receptor de la toxina Cry1Ac en *M. sexta*. Además, también se requiere determinar que regiones de la toxina son importantes para la interacción, lo que aportará información que pueda utilizarse en el diseño de toxinas más potentes o con características que puedan abatir la resistencia de algunos insectos.

HIPÓTESIS

La aminopeptidasa y la fosfatasa alcalina son componentes del epitelio intestinal de *M. sexta* que funcionan como receptores importantes para el mecanismo de acción de la toxina Cry1Ab.

OBJETIVO GENERAL

Caracterizar la unión de la toxina Cry1Ab con la fosfatasa alcalina y la aminopeptidasa de *M. sexta*.

OBJETIVOS PARTICULARES

- Purificar las proteínas aminopeptidasa y fosfatasa alcalina a partir el intestino de *M. sexta*.
- Caracterizar la unión *in vitro* del monómero y oligómero de la toxina Cry1Ab con aminopeptidasa y fosfatasa alcalina purificadas.
- Determinar regiones en la toxina que participan en la interacción con aminopeptidasa y fosfatasa alcalina.
- Describir el papel de la aminopeptidasa y fosfatasa alcalina como receptores de la toxina Cry1Ab en *M. sexta*.

MATERIALES Y MÉTODOS

Purificación y solubilización de VMMA´s.

Se disectan los intestinos de cada uno de los 5 estadíos de desarrollo larvario que presenta *M. sexta* y se les agrega la solución 1 (manitol 300 mM, Tris-HCl 17 mM, EGTA 5 mM, DTT 2 mM, HEPES 10 mM, EDTA 1 mM, PMSF 0.5 mM, leupeptina 100 μg/ml, pepstatina 100 μg/ml y neomicina 100 μg/ml, pH 7.4) en una proporción de 1:10 (intestino:solución 1). La mezcla se coloca en un homogenizador y se aplican 9 golpes con el émbolo a 2,250 rpm. Posteriormente, se agrega suavemente un volumen equivalente de solución de $MgCl_2$ 24 mM, se mezcla suavemente y se incuba durante 15 minutos en hielo. Esta solución se centrifuga a 4,500 rpm. a 4°C en un rotor de ángulo fijo (Beckman JA-20) y el sobrenadante se transfiere a un tubo limpio y se centrifuga a 16,000 rpm. por 30 min a 4°C. Descartar el sobrenadante y la pastilla se suspende en ½ volumen de la solución 1 y ½ volumen de $MgCl_2$ 24 mM. Se repiten los dos pasos de centrifugación descritos y la pastilla finalmente se resuspende en la solución 1 diluida con H_20 en una proporción 1:1.

Para solubilizar las VMMA's, primero se centrifugan a 70,000 rpm. y la pastilla se resuspende a una concentración final de 5 mg/ml en solución amortiguadora de solubilización (20 mM de Tris-HCl, pH. 8.5 con NaCl 100 mM, EDTA 5 mM EDTA, PMSF 1 mM y CHAPS 1%). La mezcla se incuba 2 horas a 4°C con agitación suave y se centrifuga a 70,000 rpm. por 40 minutos. La concentración de proteína en el sobrenadante se determina mediante Lowry (DC protein-dye, Bio-rad).

Purificación de aminopeptidasa.

La aminopeptidasa se purifica a partir de VMMA´s de larvas de 4º estadío de desarrollo. Las VMMA´s solubilizadas con CHAP´s se dializan en una solución compuesta de: Tris-HCl 20 mM pH. 8.5, $MgCl_2$ 2 mM y KCl 2 mM por 12 horas a 4°C. Posteriormente, la muestra se concentra por centrifugación en filtros Amicon YM-50 y se filtra en membranas millipore de 0.22 μm. Una alícuota de 2 ml se purifica mediante cromatografía de intercambio iónico en una columna mono-Q HR 5/10 (GE Healthcare) equilibrada con Tris-HCl 20 mM pH. 8.5, $MgCl_2$ 2 mM y KCl 2 mM (*106*). La muestra es eluída con una gradiente de NaCl (0.5-1 M) con un flujo de 1 ml/minuto por 40 minutos. Las fracciones que contienen la aminopeptidasa se unen y concentran. La muestra final es analizada en geles de acrilamida al 10% seguida por la tinción con plata utilizando el sistema SilverSnap Stain Kit II (Pierce) siguiendo las instrucciones del fabricante.

Purificación de fosfatasa alcalina.

La fosfatasa alcalina es purificada a partir de VMMA´s purificadas a partir de larvas de *M. sexta* de 3er estadio de desarrollo, mediante una cromatografía de afinidad en una columna de fosfatos (L-histidyl-diazo-benzyphosphonic acid agarosa). Las proteínas obtenidas de la solubilización con CHAP´s se dializan en solución A (Tris-HCl 20 mM pH 8.5 y $MgCl_2$ 1 mM) por 12 horas a 4°C. Posteriormente, la muestra se concentra por centrifugación con filtros Amicon YM-30 y se filtra en membranas millipore de 0.22 μm. Una muestra de 1 ml se purifica en la columna equilibrada con solución A y se realizan varios lavados con la misma solución. Finalmente, la muestra es eluída con solución A conteniendo KH_2PO_4 0.5 M. La muestra final es analizada en geles de acrilamida al 10% seguida de una tinción con plata como se mencionó anteriormente.

Determinación de concentración de proteína por el método de Bradford.

La determinación de proteína se realiza midiendo la absorbancia a una longitud de onda de 595 nm. Se toman 10 µl de las muestras y se llevan a un volumen final de 800 µl con H_2O. Posteriormente, se añaden 200 µl del reactivo de Bradford (bio-rad), se incuba por 5 minutos y se mide la absorbancia. Al mismo tiempo se prepara una curva estándar de referencia utilizando BSA.

Cuantificación de proteínas por el método de Lowry.

Se prepara una mezcla de la solución A y la solución S del sistema DC protein-dye (1 ml de solución A y 20 µl de solución S). Se toman 10 µl de muestra y se le agregan 125 µl de la mezcla preparada anteriormente, se incuba por 15 minutos a temperatura ambiente, se agrega 1 ml de la solución B y se incuba por 15 minutos. La absorbancia de las muestras se mide a 750 nm y los datos obtenidos fueron referenciados empleado una curva estándar de BSA.

Determinación de actividad enzimática específica.

Actividad de aminopeptidasa.

Se prepara el sustrato L-leucina-p-nitroanilida (LpNA) 100 mM (2.88 mg de LpNA (Sigma) en 1 ml de H_20). En un tubo eppendorf se mezclan los siguientes volúmenes: 650 µl de H_2O, 50 µl de NaCl 5 M, 200 µl de Tris-HCl pH 8 y 10 µl de la muestra. A la mezcla se le agregan 100 µl del sustrato, se mezcla y se registran las absorbancias a 405 nm cada 15 segundos de una cinética por 1 minuto para determinar la ΔAb. Para calcular la actividad específica, se consideró que el coeficiente de absorción de la p-nitroanilida es de 9.9×10^{-3}

mol 1^{-1} (*107*). Una unidad de actividad específica de aminopeptidasa se define como la cantidad de enzima que cataliza la hidrólisis de 1 μmol de LpNA min^{-1} mg de proteína^{-1}.

Actividad de fosfatasa alcalina.

Se prepara el sustrato p-nitrofenol fosfato 1 mg/ml en una solución de $MgCl_2$ 0.5 mM, Tris-HCl 100 mM pH 9.5. Se toman 500 μl de esta solución en un tubo eppendorf y se le agregan 5 μl de muestra, la mezcla se agita por inversión y se incuba por 15 minutos a temperatura ambiente. La reacción se detiene adicionando 500 μl de una solución de EDTA 250 nM pH 8 y se toma la absorbancia de la muestra a 405 nm. Los valores se refieren a una curva estándar de p-nitrofenol (Merck). La actividad enzimática específica se calcula considerando la cantidad de proteína necesaria para transformar 1 nmol de p-nitrofenol fosfato en un minuto.

Experimento de unión a ligando.

5 μg de VMMA´s purificadas de cada uno de los estadíos de desarrollo, se separan en un gel de acrilamida al 9%, las proteínas se electrotransfieren a una membrana PVDF. La membrana se lava con PBST (PBS 1x + Tween-20 0.1%) y se bloquea durante 1 hora con BSA 0.2% en PBST. La membrana se lava con PBST y se incuba por 2 horas con el monómero de la toxina Cry1Ab marcada con biotina en PBST con BSA 0.1%. Pasado el tiempo de incubación la membrana se lava nuevamente y se incuba con estreptavidina acoplada a peroxidasa por una 1 hora. Finalmente, la unión de la toxina se verifica mediante quimioluminiscencia (Pierce).

Experimentos de unión en ensayo de ELISA.

En una placa de ELISA se fija 1 ng por pozo de aminopeptidasa o fosfatasa alcalina en 100 µl de PBS durante 12 horas a 4°C. La placa se lava con PBS 3 veces y se agregan 200 µl de leche descremada al 2% en PBS y se incuba por 2 horas a 37°C. La placa se lava 4 veces con PBST y se incuba 1 hora a 37°C con diferentes concentraciones de monómero u oligómero según sea el caso, en 100 µl de PBST. El exceso de toxina es removido con 4 lavados con PBST y se agrega a la placa la dilución correspondiente de anticuerpo policlonal anti-Cry1Ab en una dilución 1:10,000. Se lava y se agrega el anticuerpo secundario (1:10,000) acoplado a peroxidasa, se incuba 1 hora. La unión se revela agregando 100 µl de sustrato (6 mg de o-fenilendiamina (Sigma) en 12 ml de amortiguador de fosfatos 0.1 M y 10 µl de H_2O_2), la reacción se detiene agregando 50µl de HCl 6M. Se registra la absorbancia a 490 nm.

Competencias homólogas y heterólogas.

Las competencias se realizaron mediante ensayos de ELISA preincubando la toxina (oligómero o monómero) con diferentes concentraciones del mismo receptor que se fijó en la placa (Competencia homóloga). Para el caso de las competencias heterólogas se fijó a la aminopeptidasa (1µg/pozo) y posteriormente se agregó la toxina (oligómero ó monómero) preincubada con varias concentraciones de fosfatasa alcalina y viceversa.

Mutagénesis dirigida de la toxina Cry1Ab.

Cepas y plásmidos.

E. coli DH5α Genotipo: F-Φ80*lac*ZΔM15 Δ (*lac*ZYA-*arg*F)U169 *deo*R *rec*A1 *end*A1 *hsd*R17(r_k^-, m_k^+) *pho*A *sup*E44 *thi*-1 *gyr*A96 *rel*A1 λ^- (Invitrogen).

E. coli SCS110, deficiente en dos sistemas de metilasas (Dam y Dcm); Genotipo: *rpsL* (Strr) *thr leu endA thi-1 lacY galK galT ara tonA tsx dam dcm supE44* Δ(*lac-proAB*) [F´ *traD36 proAB lacI*q*ZΔM15* (Stratagene).

B. thuringiensis 407 Cry^- acristalífera que carece de capacidad para sintetizar toxinas debido a la pérdida de los plásmidos Cry (Agaisse y Lereclus, 1995).

El plásmido pHT315 con el gen de la protoxina Cry1Ab (No de Acceso M13898) fue utilizado como templado para realizar la mutagénesis y a partir del mismo se diseñaron los oligonucleótidos (Tabla 1) para introducir los cambios deseados. Para introducir las mutaciones puntuales se utilizó el sistema *QuickChange™ Site-Directed Mutagenesis kit* de Stratagene siguiendo las instrucciones del fabricante.

Tabla 1. Oligonucleótidos diseñados para la generación de mutaciones.

Mutación	**Secuencia del oligonucleótido.**
RR368-9AA	**5´** CAT TAT CGT CCA CTT TAT ATG CAG CAC CTT TTA ATA TAG GGA TAA ATA ATC **3´**
F371A	**5´** CCA CTT TAT ATA GAA GAC CTG CTA ATA TAG GGA TAA ATA ATC **3´**
L511A	**5´** GGC CAG ATT TCA ACC GCG AGA GTA AAT ATT ACT GCA **3´**.

Fosforilación de oligonucleótidos para la mutagénesis.

La fosforilación es requerida para la ligación enzimática de ácidos nucleícos pues las ligasas requieren de un grupo fosfato en la posición 5'. Los oligonucleótidos liofilizados (Invitrogene) se resuspenden en 100 µl de agua Mili-Q y se toma un volumen de 1 µl (~300 pico mol de oligonucleótido) para una mezcla de reacción que contiene: 5 µl amortiguador de cinasa (más ATP) 10X, 1 µl PNK (Cinasa de polinucleótidos), 43 µl Agua MiliQ para un volumen final de 50 µl. La reacción se incuba a 37°C durante 30 minutos y a 68°C durante 35 minutos para inactivar a la enzima. La mezcla de polimerasas que contiene el sistema de mutagénesis de Stratagene permite generar un nuevo plásmido de doble cadena que contiene la mutación deseada. El programa de PCR utilizado en estos experimentos se muestra en la Tabla 2.

Para eliminar el ADN parental se digiere el producto de PCR obtenido con la enzima de restricción *Dpn I* (Stratagene), endonucleasa específica de ADN metilado y hemimetilado, por una hora a 37°C. Así se consigue seleccionar el ADN mutado que se transforma en la cepa de *E. coli* DH5α mediante electroporación.

Tabla 2. Programa de PCR para la introducción de mutaciones.

No de Ciclos	Temperatura (°C)	Tiempo (minutos)
1	**94**	**3**
35	**94**	**1**
	55	**1**
	65	**15**
1	**65**	**10**

Transformación por electroporación.

Se toman 2µl de ADN y se mezclan cuidadosamente con una alícuota de las células electrocompetentes DH5α. Las células más el ADN se transfirieren a celdas de 0.1cm (Bio-Rad) pre-enfriadas y se les da un choque de 2.5V a 25µF y 200Ω de resistencia. Inmediatamente después se agrega 1ml de medio SOC y se trasfirieren a tubos falcon estériles de 15 ml. Las células se incuban a 37°C con agitación durante 1 hora para su recuperación. Transcurrido el tiempo se sembraron 200µl de las células recuperadas en medio selectivo (LB-agar-ampicilina 200µg/ml) y se incuba a 37°C durante 12 horas. Para verificar las construcciones se toman colonias aisladas y se crecieron a 37°C durante 12 horas en 5 ml de medio LB-ampicilina (100µg/ml) líquido. Se purificaron los plásmidos correspondiente y la presencia de las mutaciones se confirmó mediante secuenciación de ADN. La composición de los medio y soluciones se muestran el la Tabla 3.

Preparación de células competentes.

Se inoculan 5 ml de medio LB líquido con una colonia de la cepa SCS110 y se deja crecer durante 12 horas a 37º C. Posteriormente se inoculan 100 ml de LB líquido con un volumen de 2 ml del pre-cultivo. Este cultivo se incuba a 37°C con agitación hasta alcanzar una $D.O._{600}$ de 0.60. El matraz se coloca en hielo durante 5 minutos. Se recuperan las células centrifugando en tubos estériles a 3,000 rpm durante 10 minutos, el sobrenadante se desecha. Las células se resuspenden en 10 ml de $CaCl_2$ 100 mM frío y se incubaron durante 30 minutos en hielo. Posteriormente las células se centrifugan a 3,000 rpm durante 10 minutos, se desecha el sobrenadante y la pastilla se resuspende en un volumen final de 2 ml de $CaCl_2$ 100 mM más 180 µl de DMSO. Se preparan alícuotas de 200 µl y se colocan en tubos eppendorf de 1.5 ml estériles. Las células se usan inmediatamente o se mantienen hasta su uso a -70°C.

Transformación por choque térmico.

Las células competentes se descongelan en hielo y se les añade un volumen de 5µl del ADN, se incuban durante 30 minutos en hielo y se les da un choque de calor (42°C) durante dos minutos. Posteriormente, se incuban en hielo durante 5 minutos y se les agrega 800µl de LB líquido sin antibiótico. Las células se dejan recuperar a 37°C con agitación durante una hora. 200µl de las células se esparcen en medio selectivo LB-agar suplementado con ampicilina (200µg/ml) y se incuban a 37°C durante 12 horas. Una colonia independiente se usó para inocular un volumen de 10 ml de medio LB-ampicilina (10 µg/ml) y el cultivo se incubó durante 12 horas a 37°C con agitación, para proceder a la purificación del ADN.

Secuenciación de ADN.

Las secuencias se realizaron en la Unidad de Secuenciación del Instituto de Biotecnología-UNAM.

Preparación y transformación de células vegetativas de *Bacillus thuringiensis* (407 Cry$^-$).

Se estría una caja petri con medio LB-agar sin antibiótico y se incuba 12 horas a 30°C, a partir de se toman colonias para extenderlas sobre una caja de LB-agar sin antibiótico fresca y se incuba a 30°C, hasta que se observan colonias transparentes (aproximadamente 3 horas). En este punto, las células se cosechan en su totalidad y se resuspenden en 500 µl de medio BHI y se homogenizan completamente con la ayuda de una pipeta. Se inocula un volumen de 100 ml de medio BHI y se incuba a 30°C con agitación hasta alcanzar una $D.O._{600}$ de 0.6. Posteriormente el cultivo se centrifuga a 5000 rpm durante 5 minutos. Se elimina el medio de cultivo y el paquete celular se resuspende en 50 ml de solución EB fría. Las células se centrifugan a 5000 rpm durante 5 minutos y se resuspenden en un volumen final de 3 ml de solución EB fría para preparar alícuotas de 300 µl en tubos eppendorf de 1.5 ml que se utilizan inmediatamente. Para la transformación se agregan 10µl de ADN, recuperados a partir de los cultivos de las mutantes en la cepa SCS1100 de *E. coli*. Se incuba durante 5 minutos en hielo, las células más el ADN fueron transferidos a celdas de 0.4 cm pre-enfriadas y se les aplicó un choque de 2.5V a 25µF y 1000Ω de resistencia. Las células electroporadas se incubaron en hielo durante 5 minutos y se les agregaron 700 µl de medio BHI. Estas alícuotas se transfieren a tubos falcon estériles de 15ml y se incuban a 30°C con agitación durante una hora para su recuperación. Se tomó un volumen de 250 µl

de las células recuperadas y se esparcieron en medio selectivo LB-agar-eritromicina (10 µg/ml).

Purificación de los cristales de la toxina Cry1Ab y las mutantes.

La cepa que expresa la toxina silvestre Cry1Ab y las mutantes construidas se crecieron en cajas petri con medio LB-agar suplementado con eritromicina (10 µg/ml) durante 12 horas a 30ºC. Posteriormente, se inoculó el medio de esporulación HCT líquido (50 ml) que contiene 10 µg/ml del antibiótico de selección (eritromicina), en el cual se sintetizan los cristales de las toxinas. El crecimiento se realizó a 30ºC con agitación hasta observar al microscopio los cristales correspondientes (72 horas aproximadamente).

Para recuperar los cristales de las toxinas primero se recupera la pastilla celular que contiene la mezcla de esporas-cristales por centrifugación a 10,000 rpm durante 15 minutos. Posteriormente se lava tres veces con solución de lavado (NaCl 5 M, EDTA 0.5 M pH 8). Se centrifuga a 10,000 rpm durante 15 minutos entre cada lavado. El sobrenadante se elimina y la pastilla se lava 3 veces más con una solución de PMSF 1 mM centrifugando a 10,000 rpm durante 15 minutos. Los cristales se purifican mediante un gradiente discontinuo de sacarosa de 84%, 79%, 72% y 67% complementado con amortiguador TTN (NaCl 10 mM, Tris-HCl 50 mM y Tritón X-100 0.01% pH 7.2). Las soluciones de mayor concentración se colocan en el fondo del tubo y por último la muestra de espora cristales es sonicada dando dos pulsos de 1 minuto con un minuto de descanso a 4°C. Los gradientes se centrifugan a 23000 rpm durante 30 minutos a 15°C en una ultracentrífuga Beckman. Las fracciones que contienen los cristales se identifican mediante observación al microscopio, se colectan por separado y se lavan con agua mili-Q más PMSF 1mM 3 veces, para eliminar el exceso de sacarosa. Se centrifuga a 10,000 rpm durante 15 minutos

entre cada lavado. Finalmente, los cristales se resuspenden en 1 ml de PMSF 1mM y se transfieren a tubos eppendorf y se almacenan a 4°C.

Bioensayos con larvas de *M. sexta*.

Los bioensayos se realizan con larvas neonatas de *M. sexta* por el método de contaminación de superficie. En placas de 24 pozos se coloca dieta artificial hasta llenar la mitad de cada pozo. Una vez que la dieta se seca, se agregan las diferentes dosis de la toxina en un volumen final de 35 µl con H_2O, las cajas se dejan secar y se coloca una larva en cada pozo. Después de 7 días se monitorea la mortalidad. Las concentración requerida para matar el 50% de la las larvas (LC_{50}) fue estimada mediante un análisis probit con el software Polo-PC Leotra.

Inmunoblot.

Las fracciones purificadas de los oligómeros de la toxina silvestre y las toxinas mutantes, se separan mediante SDS-PAGE y se transfieren a una membrana de nitrocelulosa. Posteriormente, después de bloquear la membrana por 1 hora con PBST y leche descremada al 5%, se incuba con un anticuerpo anti-cry1Ab (1:80,000) por una hora. La membrana se lava con PBST y se incuba con un anticuerpo anti-conejo acoplado a peroxidasa en una dilución 1:25,000 (Amersham) por una hora. Finalmente se detecta la toxina con un sistema de luminiscencia (Super signal chemiluminiscence, pierce).

Tabla 3. Composición de medios y soluciones

Nombre	Composición		Comentarios
Cloruro de Calcio	$CaCl_2 \cdot 2H_2O$	100 mM	Se esteriliza en autoclave.
Amortiguador EB	Sacarosa $MgCl_2$	0.625 M 1 mM	Se esteriliza en autoclave.
Solución I (para complementar el medio HCT)	KH_2PO_4	68 g /l	Se esteriliza en autoclave.
Solución II (para complementar el medio HCT)	$MgSO_4 \cdot 7H_2O$ $MnSO_4 \cdot H_2O$ $ZnSO_4 \cdot 7H_2O$	12.3 g/l 0.169 g/l 1.4 g/l	Se esteriliza en autoclave.
Solución III (para complementar el medio HCT)	$FeSO_4 \cdot 7H_2O$ H_2SO_4	2 g/l 100 ml/l	Se esteriliza en autoclave.
Solución IV (para complementar el medio HCT)	$CaCl_2 \cdot 2H_2O$	14.7 g/l	Se esteriliza en autoclave.

Amortiguador de Laemli 4X	Tris-HCl 1.5 M pH 6.8 Glicerol SDS Azul de bromofenol β-mercaptoetanol	5 ml/10 ml 4 ml/10 ml 0.4 g/10 ml 0.1% 1ml/10 ml	Disolver y mantener a 4ºC.
Amortiguador de corrida TGS	Tris Glicina SDS	144 g/l 30 g/l 10g/l	Filtrar en membranas millipore de 0.22 μm.
Medios para Bacterias			
Nombre	**Composición**		**Comentarios**
LB	Bacto Triptona Extracto de levadura NaCl	10 g/l 5 g/l 10 g/l	Ajustar el pH a 7 con NaOH y esterilizar en autoclave.
LBagar	Medio LB pH 7.0 Agar	1l 15 g	Se esteriliza en autoclave y se dejar enfriar hasta ~50ºC y añadir, si procede, el antibiótico de selección. Distribuir en cajas petri y dejar solidificar. Conservar a 4ºC
SOC	Bacto Triptona Extracto de levadura	20 g/l 5 g/l	Se ajusta el pH a 7.0 con NaOH y se esteriliza en autoclave. Antes de usar agregar 10 ml/l de una

	NaCl KCl	0.5 g/l 0.186 g/l	solución de $MgCl_2$ 2M y 10 ml de Glucosa 1M ambas previamente esterilizadas en autoclave.
BHI	Infusión cerebro-corazón	37 g/l	Se esteriliza en autoclave.
HCT	Bacto Triptona Casa-amino-ácidos	5 g/l 2 g/l	Ajustar el pH a 7.25 con KOH y se esteriliza en autoclave. Antes de usar complementar con 50 ml de la Sol I, 1 ml de la Sol II, 10 ml de la Sol III, 10 ml de la Sol IV y 30 ml de Glucosa al 10% por cada litro.

RESULTADOS.

PURIFICACIÓN DE AMINOPEPTIDASA Y FOSFATASA ALCALINA.

Actividad enzimática en las VMMA´s de cada uno de estadíos larvarios de *M. sexta*.

Para obtener las proteínas necesarias para este trabajo primero se determinó el estadío de desarrollo más adecuado para purificar las proteínas. Se sabe que las larvas son menos susceptibles a las toxinas Cry conforme van creciendo, por lo que se decidió recuperar intestinos de *M. sexta* de los diferentes estadíos de desarrollo, a partir de una colonia del laboratorio que se mantiene con dieta artificial. El ciclo larvario de este insecto comprende 5 estados larvarios que van de 3 a 5 días dependiendo del estadío de desarrollo y de las condiciones ambientales. A partir de larvas de cada uno de los estadíos se disectaron intestinos, para purificar VMMA´s mediante precipitación diferencial con Mg^2 (*48*). En las VMMA´s, se determinaron las actividades enzimáticas específicas de la fosfatasa alcalina y de la aminopeptidasa utilizando como sustratos ρ-nitrofenol-fosfato y L-leucina-ρ-nitroanilida, respectivamente. Una gráfica con los resultados de actividad obtenidos para estas dos enzimas se presenta en la Figura 6.

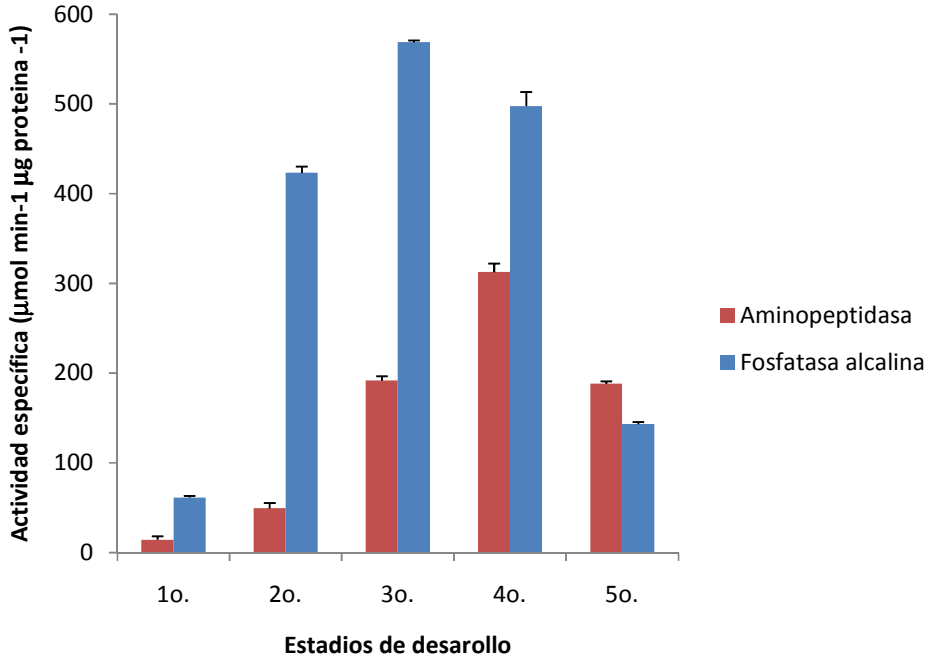

Figura 1. Actividad específica de aminopeptidasa y fosfatasa alcalina en los diferentes estadíos de desarrollo de larvas de *M. sexta*.

Brevemente se observa, que existen diferencias en cuanto a los niveles de la actividad de cada una de las enzimas en cada uno de los estadíos de desarrollo. Ambas actividades aumentan conforme avanza el desarrollo de las larvas; sin embargo la actividad de la fosfatasa alcalina es mayor a la de la aminopeptidasa. También se puede notar que el nivel máximo de actividad para la aminopeptidasa se alcanza en el cuarto estadío de desarrollo y posteriormente, disminuye en el último estadio de desarrollo. En el caso de la fosfatasa alcalina, es en el tercer estadío en donde se encuentra la mayor actividad enzimática, disminuyendo en el cuarto y quinto estadío. Hay que tomar en cuenta que se analizó la actividad total de las enzimas y no se puede concluir cuanta corresponde a la proteína que

puede unir a la toxina Cry1Ab. Es claro que en todos los estadíos de desarrollo hay actividad enzimática de ambas proteínas, pero en diferentes niveles.

Ensayo de unión de la toxina Cry1Ab a VMMA´s de los 5 estadíos de desarrollo.

Para determinar si las actividades enzimáticas específicas de cada una de la enzimas coinciden con la unión de la toxina Cry1Ab a la VMMA´s se realizó un ensayo de unión a ligando. 2.5 µg de proteína total de VMMA´s se separaron en un gel de acrilamida y se transfirieron a una membrana de PVDF. La membrana fue incubada con 2.5 nM de la toxina Cry1Ab marcada con biotina y la unión se verificó mediante estreptavidina acoplada a peroxidasa. En la Figura 7 se muestra el resultado en donde se aprecia que la toxina Cry1Ab se une a una proteína de aproximadamente 65 kDa en las muestras correspondientes a los primeros estadíos de desarrollo, siendo en el primer estadío, donde notamos la mayor unión de la toxina. En contraste, en los estadíos cuarto y quinto, se observa que la toxina se une preferencialmente a una proteína de aproximadamente 120 kDa que corresponde al peso molecular de la aminopeptidasa. En estos últimos estadíos no se observa la unión a la proteína de 65 kDa. Con base a estos resultados se determinó purificar la aminopeptidasa de larvas de cuarto estadío de desarrollo y la fosfatasa alcalina a partir de larvas de tercer estadío de desarrollo, en la decisión también influyo el tamaño de las larvas y la cantidad de material que se puede recuperar.

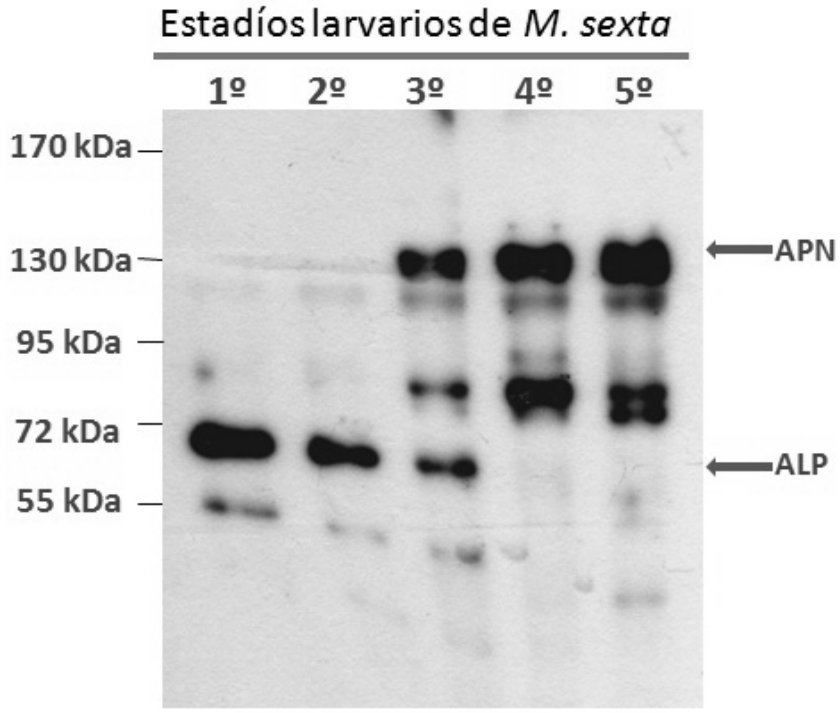

Figura 2. Unión de la toxina Cry1Ab a VMMA´s de los diferentes estadíos de desarrollo de *M. sexta*.

CARACTERIZACIÓN DE LA AMINOPEPTIDASA Y FOSFATASA ALCALINA PURIFICADAS.

Para poder analizar la interacción de la toxina Cry1Ab en su conformación de monómero u oligómero con la aminopeptidasa y fosfatasa alcalina, se procedió a purificar ambas proteínas a partir de VMMA´s solubilizadas con detergente. La aminopeptidasa y la fosfatasa alcalina fueron purificadas por cromatografía de intercambio iónico y de afinidad, respectivamente. Las fracciones recuperadas se caracterizaron mediante actividad enzimática específica, los rendimientos de cada proceso de purificación se resumen en las Tablas 4 y 5. Para la aminopeptidasa se observó un enriquecimiento en la actividad enzimática de 4.3 a 78.2 U/mg entre las VMMA´s y la fracción purificada, con un

rendimiento de recuperación del 19 % aproximadamente (Tabla 4). Para la fosfatasa alcalina se observó un enriquecimiento en la actividad específica de 3.5 a 11.3 U/mg entre las VMMA´s y la fracción purificada, con un rendimiento del 3.8 % (Tabla 5).

Tabla 1. Purificación de aminopeptidasa a partir del VMMA´s de larvas de *M. sexta* de cuarto estadío de desarrollo.

Fracción	Actividad total (U)	Proteína total (mg)	Actividad específica	Rendimiento (%)
VMMA´s	**87.3**	**20**	**4.3**	**100**
VMMA´s/CHAP´s	**49.3**	**5.4**	**9.1**	**56.4**
Mono Q	**16.6**	**0.212**	**78.2**	**19.01**

Tabla 2. Purificación de la fosfatasa alcalina a partir del VMMA´s de larvas de *M. sexta* de tercer estadío de desarrollo.

Fracción	Actividad total (U)	Proteína total (mg)	Actividad específica	Rendimiento (%)
VMMA´s	33.6	10	3.56	100
VMMA´s/CHAP´s	21.6	4.5	4.8	60.6
Columna de fosfato	1.135	0.1	11.35	3.18

Evaluación de la eficiencia de purificación.

La pureza de las muestras recuperadas se evaluó en gel de poliacrilamida (SDS-PAGE) y se realizó una tinción con plata como se describe en materiales y métodos. En los carriles 1 y 2 de la Figura 8 se muestran las fracciones correspondientes a aminopeptidasa (120 kDa) y fosfatasa alcalina (65 kDa), respectivamente. Se nota que para la aminopeptidasa se logró un mayor grado de purificación ya que en el caso de la fracción que corresponde a la fosfatasa alcalina, se observan algunas bandas adicionales de aproximadamente 60 kDa que se han reportado como producto de degradación de la de 65 kDa.

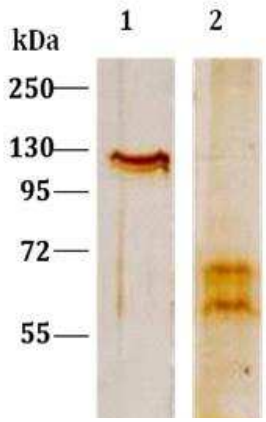

Figura 3. Tinción con plata de las proteínas purificadas. La aminopeptidasa se muestra en el carril 1 y la fosfatasa alcalina en el carril 2.

Ensayo de unión de la toxina Cry1Ab con las fracciones purificadas.

Para determinar si en el proceso de purificación se afectó las propiedades de las proteínas para unir a la toxina Cry1Ab, se realizó un ensayo de unión a ligando, incubando una membrana PVDF conteniendo las fracciones purificadas con la toxina Cry1Ab marcada con biotina. La unión se verificó con estreptavidina acoplada a peroxidasa. Los resultados obtenidos se muestran en la Figura 9, donde se observa que las fracciones correspondientes a aminopeptidasa (carril 1) y fosfatasa alcalina (carril 2) unen a la toxina Cry1Ab. Esto resultados confirman que ambas proteínas purificadas mantienen su capacidad de unión a la toxina.

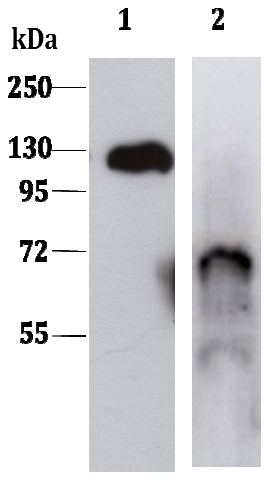

Figura 4. Unión de la toxina Cry1Ab a los receptores purificados. En el carril 1 se muestra la unión a aminopeptidasa y en el carril 2 la unión a fosfatasa alcalina.

LA FOSFATASA ALCALINA Y LA AMINOPEPTIDASA SON RECEPTORES DE LA TOXINA Cry1Ab.

Caracterización de la unión del monómero de la toxina Cry1Ab a la aminopeptidasa y fosfatasa alcalina.

La cinética de interacción del monómero de la toxina Cry1Ab con la aminopeptidasa y fosfatasa alcalina purificadas, se realizó mediante ensayo de ELISA, fijando ambas proteínas purificadas de manera independiente, en cajas de 96 pozos de ELISA, que fueron incubadas con diferentes concentraciones de monómero de la toxina, obtenida mediante la activación de la protoxina con tripsina. Con los datos obtenidos se realizó un análisis de Scatchard para determinar la constante de disociación aparente de las interacciones. En la Figura 10 se presentan las cinéticas de unión del monómero con la aminopeptidasa y la fosfatasa alcalina. Ambas interacciones son dependientes de la concentración y saturables, lo que indica que ambas proteínas pueden unir a la toxina Cry1Ab en forma de monómero.

Mediante el análisis de Scatchard se determinó que la constante de disociación para la interacción del monómero de la toxina con la aminopeptidasa es de 101.6 nM, que coincide con la afinidad reportada por otros grupos para esta interacción en experimentos de SPR (*68*). Para la interacción del monómero de la toxina Cry1Ab con la fosfatasa alcalina se determinó una constante de disociación de 267.3 nM, siendo este dato el primer reporte de este tipo de interacción.

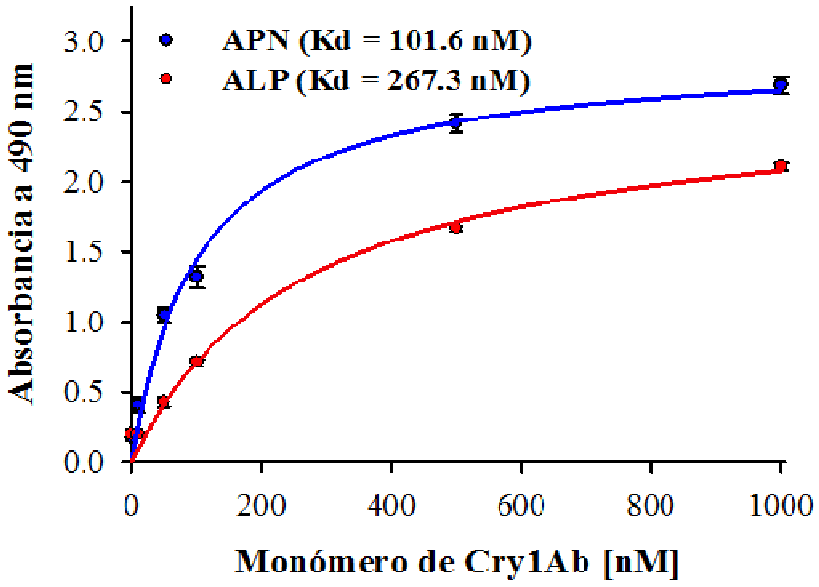

Figura 5. Unión del monómero de la toxina Cry1Ab a la aminopeptidasa y fosfatasa alcalina. La constante de disociación aparente se obtuvo mediante análisis de Scatchard.

Caracterización de la unión del oligómero de la toxina a la aminopeptidasa y a la fosfatasa alcalina.

En el mecanismo de acción propuesto para las toxinas Cry se indica que el oligómero es importante en la interacción con las proteínas ancladas por GPI, de tal manera, que las propiedades de unión de ambas proteínas con el oligómero de la toxina Cry1Ab se determinó mediante ensayos de ELISA de manera similar a como se hizo con el monómero. La unión se verificó de la misma manera que en el experimento con el monómero y los datos se analizaron mediante Scatchard, como en el caso del monómero. Como se muestra en la Figura 10, la unión del oligómero con aminopeptidasa y la fosfatasa alcalina también es saturable y dependiente de concentración, sin embargo, las constantes de disociación para esta interacción son de 0.6 y 0.5 nM, respectivamente. Indicando claras diferencias en cuanto a la interacción del monómero y el oligómero de la toxina Cry1Ab. El oligómero se une con mayor afinidad a las proteínas ancladas por GPI, lo que coincide con el mecanismo de acción reportado, donde la toxina se une primero como monómero a aminopeptidasa con baja afinidad y posteriormente, existe una segunda unión con alta afinidad, pero ya en forma de oligómero. Estos datos concluyen que además de la aminopeptidasa, la fosfatasa alcalina también es un receptor de las toxinas Cry y puede participar tanto en la interacción con el monómero (con baja afinidad) así como con el oligómero de la toxina (alta afinidad).

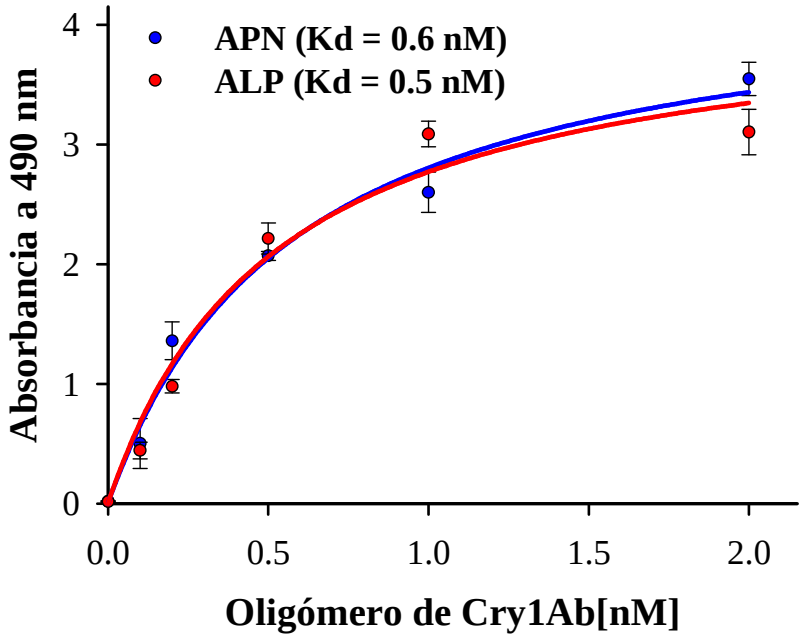

Figura 6.Unión del oligómero de la toxina Cry1Ab a la aminopeptidasa y fosfatasa alcalina. La constante de disociación aparente se obtuvo mediante análisis de Scatchard.

Competencias homólogas de la unión del oligómero y monómero.

Para determinar si la unión de la toxina en sus dos conformaciones (monómero u oligómero) es específica, se realizaron competencias homólogas en ensayos de ELISA. Para estos experimentos, se fijó a la aminopeptidasa o a la fosfatasa alcalina a las cajas de ELISA a las que posteriormente, se agregó el monómero o el oligómero de la toxina preincubado con diferentes concentraciones de la proteína que fue fijada en la placa. Como se muestra en la Figura 12 la unión del monómero, tanto a la aminopeptidasa como a la fosfatasa alcalina, se abate al competirla con la misma proteína. En el caso del oligómero también se observó competencia (Figura 13). Estos resultados confirman que ambas interacciones descritas son específicas.

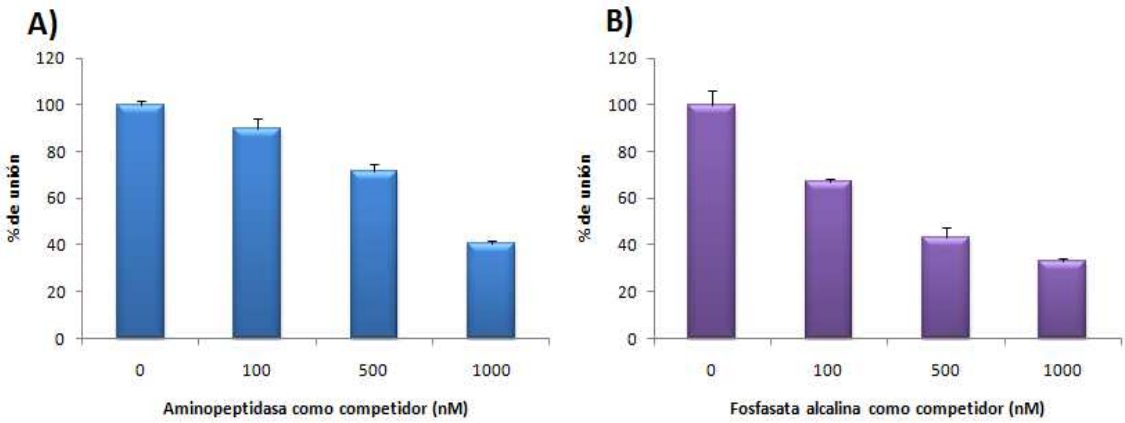

Figura 7. Competencias homólogas de la unión del monómero de la toxina Cry1Ab con aminopeptidasa y fosfatasa alcalina purificadas. Unión con aminopeptidasa (A) y fosfatasa alcalina (B) compitiéndose con el mismo receptor.

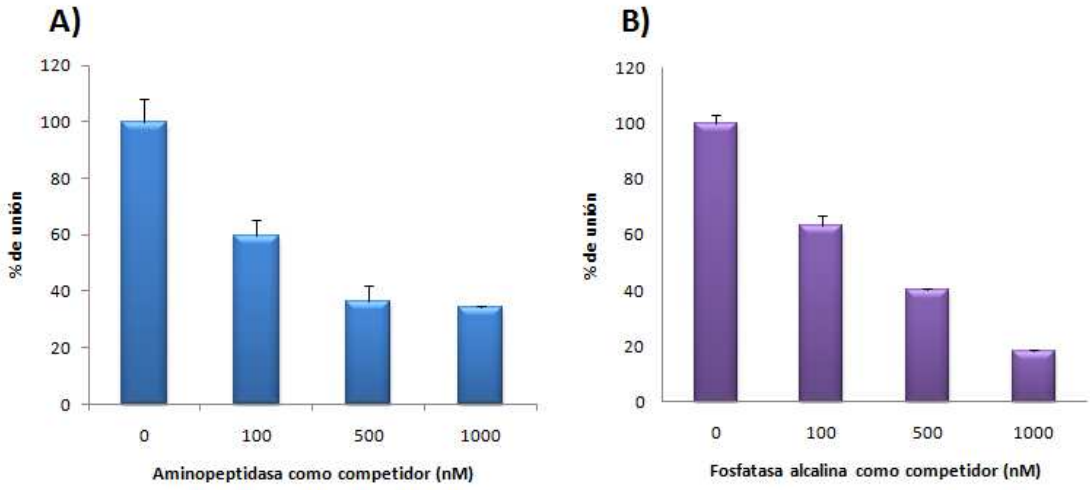

Figura 8. Competencia homóloga de la interacción del oligómero de la toxina Cry1Ab con la aminopeptidasa y fosfatasa alcalina purificadas. Unión con aminopeptidasa (A) y fosfatasa alcalina (B) compitiéndose con el mismo receptor.

LA AMINOPEPTIDASA Y LA FOSFATASA ALCALINA COMPARTEN SITIOS DE INTERACCIÓN CON EL OLIGÓMERO DE LA TOXINA.

Competencia heteróloga del oligómero de la toxina con aminopeptidasa y fosfatasa alcalina.

De acuerdo a los resultados presentados, surgió la pregunta sobre si estas proteínas comparten sitios de interacción con la toxina. Para contestarla se realizaron competencias heterólogas similares a las descritas, pero retando las placas con el oligómero de la toxina preincubada con diferentes concentraciones de la proteínas que no se fijó en la placa. Los resultados obtenidos muestran que la aminopeptidasa tiene la capacidad de inhibir la unión del oligómero con fosfatasa alcalina y la fosfatasa alcalina tiene la capacidad de inhibir la interacción del oligómero con aminopeptidasa (Figura 14). Sin embargo, la fosfatasa alcalina es menos eficiente para competir la unión con aminopeptidasa, que por su parte compite muy bien la unión de la toxina con fosfatasa alcalina. Posiblemente esto se debe a que en la interacción del oligómero con aminopeptidasa pudiese estar mediada por 2 sitios de interacción y uno de estos se comparta con la fosfatasa alcalina. Para determinar cuáles son estas regiones en el receptor se deberán realizar más experimentos.

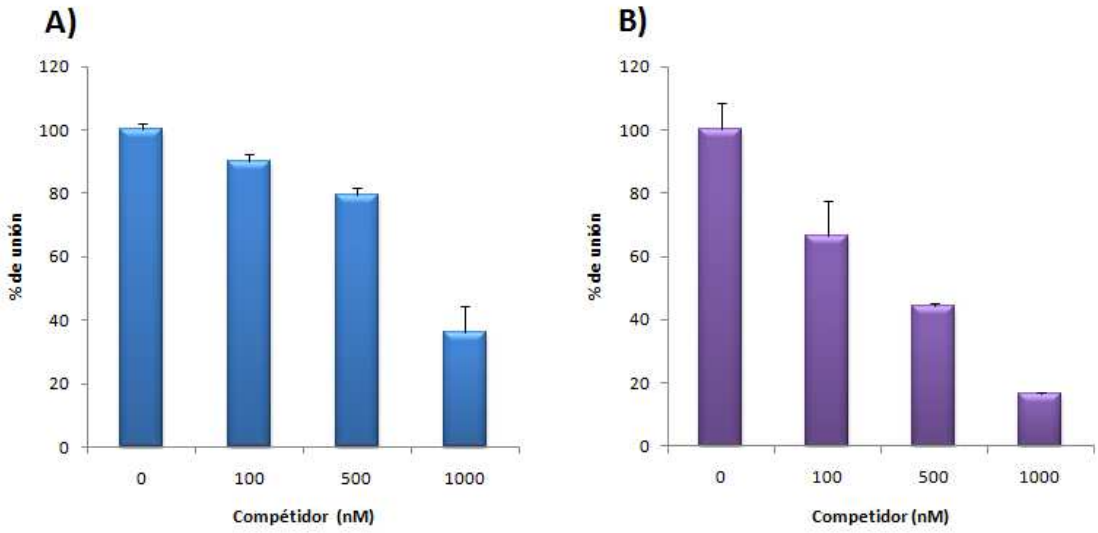

Figura 9. Competencias heterólogas de la unión del oligómero de la toxina Cry1Ab. Unión del oligómero a aminopeptidasa compitiendo con fosfatasa alcalina (A) y la unión del oligómero de la toxina con fosfatasa alcalina compitiendo con aminopeptidasa (B).

IDENTIFICACIÓN DE REGIONES EN LA TOXINA Cry1Ab IMPORTANTES PARA LA INTERACCIÓN CON LA AMINOPEPTIDASA Y FOSFATASA ALCALINA.

La interacción toxina-receptor es un paso determinante para el efecto tóxico de las toxinas Cry, se ha reportado que la mayoría de los mecanismos de resistencia a estas proteínas se dan por defectos en la unión con el receptor. Por lo tanto, es importante obtener información acerca de la naturaleza de estas interacciones que nos pueda ser útil para diseñar toxinas que puedan abatir la resistencia o dirigir su toxicidad. Con esta idea, se analizó la interacción de la toxina con la aminopeptidasa y la fosfatasa alcalina, con versiones mutantes de la toxina Cry1Ab que se encuentran afectadas en toxicidad contra larvas de *M. sexta*. Para analizar la interacción del oligómero de la toxina con

aminopeptidasa y fosfatasa alcalina, se generaron 2 mutantes en el dominio II (RR368-9AA y F371A) y una mutante en la β16 del dominio III (L511A) de la toxina Cry1Ab.

Caracterización de mutantes en el dominio II y III de la toxina Cry1Ab.

Activación de las toxinas mutantes y tipo silvestre.

Lo primero que se analizó fue que las mutaciones no hubiesen provocado cambios importantes en la estructura tridimensional que afectaran su activación. Los cristales de cada mutante fueron solubilizados en amortiguador de carbonatos y activados con tripsina comercial por 1 hora a 37°C, la reacción se paró con PMSF y la mezcla resultante se analizó mediante SDS-PAGE. Como se muestra en la Figura 15 la activación de las toxinas mutantes es similar a la de la toxina tipo silvestre, en todos los casos se obtuvo una proteína de 65 kDa que corresponde con el peso molecular de la toxina tipo silvestre, indicando que las mutaciones no afectan su activación, ni tampoco inducen su degradación.

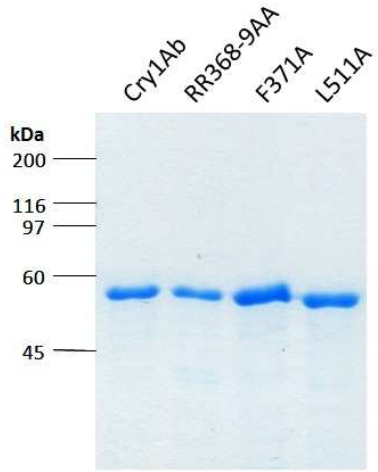

Figura 10. Activación con tripsina de la toxina Cry1Ab y las mutantes del dominio II y dominio III.

Toxicidad de las mutantes de los dominios II y III de la toxina Cry1Ab.

La toxicidad de las mutantes contra larvas de *M. sexta,* se determinó mediante un bioensayo, en el que se probaron diferentes dosis para determinar los valores de dosis letal media para cada una de las toxinas mutantes y tipo silvestre. Como se observa en la Tabla 6 ninguna de las mutantes fue tóxica para las larvas, por lo que resultan útiles para determinar si la pérdida de toxicidad puede asociarse a la unión de estas mutantes, con la aminopeptidasa y fosfatasa alcalina.

Tabla 3. Toxicidad de la toxina Cry1Ab y las toxinas mutantes a larvas de *M. sexta* de primer estadio de desarrollo.

Toxina	LC_{50} (ng/cm^2)[a]	Toxicidad relativa[b]
Cry1Ab	**3.9 (2.2-6.6)**	**1**
RR368-9AA	**>1000**	**>260**
F371A	**>1000**	**>260**
L511A	**>1000**	**>260**

a. Concentración que mata el 50% de las larvas. Los números entre paréntesis muestran el 95% del límite de confianza de la LC_{50}.
b. LC_{50} de la toxina silvestre/LC_{50} de la toxina mutante.

Obtención de oligómero.

Para analizar la unión del oligómero de las toxinas Cry1Ab mutantes y tipo silvestre, se realizaron activaciones en presencia de un fragmento de caderina (fragmento 7-12) que promueve la formación de los oligómeros. Para comprobar la presencia de oligómeros, después de la activación se realizó un inmunoblot con los oligómeros purificados mediante cromatografía de exclusión molecular, los resultados se muestran en la Figura 16.

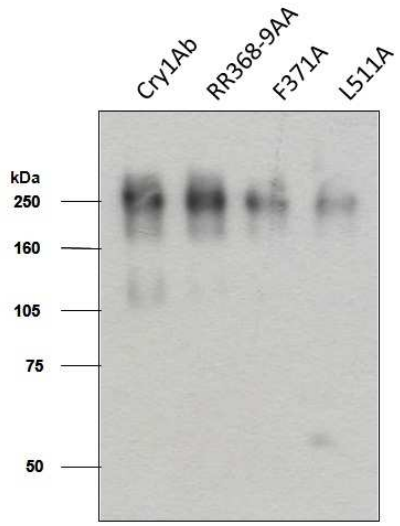

Figura 11. Oligómeros purificados de la toxina Cry1Ab y las mutantes de los dominios II y III.

Como se puede ver en la Figura 16 aunque la producción de oligómero de las mutantes fue menor, tanto en la toxina silvestre como en las mutantes, se lograron purificar los oligómeros correspondientes, mismos que fueron concentrados y cuantificados para su uso en los experimentos posteriores.

EL DOMINIO II ES IMPORTANTE PARA LA INTERACCIÓN DEL OLIGÓMERO CON LOS RECEPTORES.

Unión del oligómero de las mutantes en el dominio II y III.

La determinación de la participación del dominio II y dominio III de la toxina Cry1Ab en la interacción del oligómero de la toxina con los receptores aminopeptidasa y fosfatasa alcalina, se realizó mediante ensayo de ELISA en placas en donde ambas proteínas fueron fijadas de manera independiente e incubadas con los oligómeros de las toxinas mutantes y tipo silvestre purificados. Los resultados de la interacción se muestran en la Figura 17, donde se ve que los oligómeros de las mutantes RR368-9AA y F371A, están afectadas en la unión en más del 50%, con respecto a la unión que muestra el oligómero de la toxina tipo silvestre, mientras que la mutante L511A, sólo muestra una pequeña disminución en su capacidad de unión. Estos resultados indican que los residuos del asa 2 del dominio II están involucrados en la interacción del oligómero de la toxina Cry1Ab con los receptores aminopeptidasa y fosfatasa alcalina, mientras que el dominio III no parece ser determinante para esta interacción.

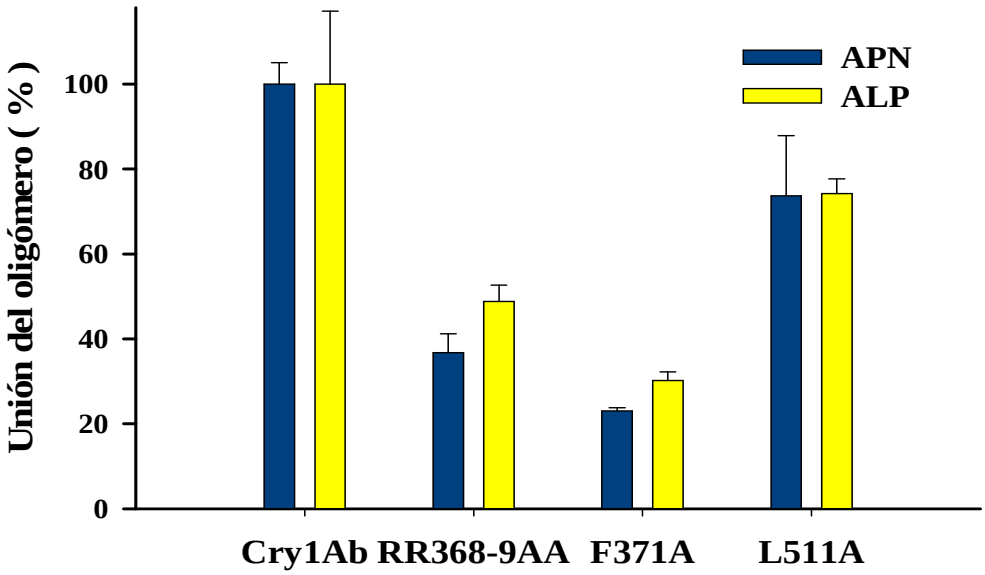

Figura 12. Unión del oligómero de la toxina Cry1Ab y de las toxinas mutantes a la aminopeptidasa y fosfatasa alcalina.

EL DOMINIO III ES IMPORTANTE PARA LA INTERACCIÓN DEL MONÓMERO CON LOS RECEPTORES.

Unión del monómero de las mutantes en el dominio II y III.

Para comparar si los sitios de interacción del oligómero de la toxina son los mismos sitios de interacción que los del monómero, se realizó un experimento de ELISA con los monómeros purificados de las mutantes y la toxina tipo silvestre (Figura 18).

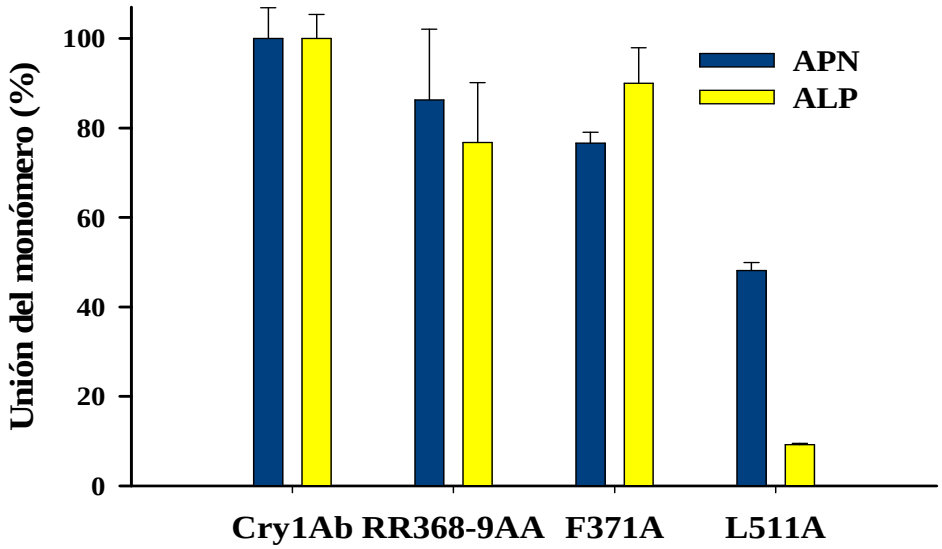

Figura 13. Unión del monómero de la toxina Cry1Ab y las toxinas mutantes a aminopeptidasa y fosfatasa alcalina.

Los resultados muestran que los monómeros de las mutantes RR368-9AA y la F371A no se encuentran afectados en la unión a aminopeptidasa y fosfatasa alcalina, sin embargo, la mutante L511A si se encuentra severamente afectada en la unión a fosfatasa alcalina (más del 80%) y también se encuentra afectada, aunque en menor grado en la unión a aminopeptidasa (cerca del 50%). Estos resultados sugieren que el dominio III es importante para la interacción del monómero con los receptores aminopeptidasa y fosfatasa alcalina, a diferencia de cuando la toxina se encuentra en forma de oligómero que interacciona con esos receptores mediante el dominio II. Estos resultados son evidencia de que además de la aminopeptidasa la fosfatasa alcalina es un receptor de las toxinas Cry1Ab en *M. sexta*.

DISCUSIÓN.

Las toxinas Cry son una alternativa viable para el control biológico de insectos plaga importantes en la agricultura o de insectos vectores de enfermedades en humanos, debido a su alta toxicidad y especificidad contra diferentes órdenes de insectos. Sin embargo, la mayor limitante sobre el uso de estas toxinas es el riesgo a la aparición de poblaciones resistentes, tal y como ha sucedido con los insecticidas químicos que se utilizan a la fecha en el campo. En la actualidad se han reportado algunos casos de insectos resistentes a las toxinas Cry y se ha demostrado que en la mayoría de los casos la resistencia está ligada a defectos en la interacción con los receptores (*108*). Para combatir esta resistencia es necesario conocer a fondo el mecanismo de acción de estas toxinas y mapear las regiones importantes para su interacción con sus receptores, lo que permitirá el diseño de toxinas mejoradas que puedan abatir la resistencia. El mecanismo de acción propuesto a la fecha para *M. sexta*, involucra varios pasos secuenciales comenzando con la ingestión de los cristales, solubilización y activación proteolítica, que dan como resultado el monómero de la toxina, que se une a aminopeptidasa con baja afinidad para localizarse en la membrana y posteriormente se une al receptor caderina, lo que promueve un segundo corte proteolítico que conlleva a la oligomerización de la toxina. Una vez que se forma el oligómero, se propone que este se une a proteínas ancladas por GPI, adicionalmente se lleva a cabo la inserción de la toxina y la formación de poro, que finalmente lleva a la muerte del insecto. El papel que juega el oligómero en la toxicidad se ha demostrado en diferentes experimentos. Se ha reportado que mutantes en la hélice α3 del dominio I de la toxina Cry1Ab, que mantienen su capacidad de unión a caderina, son incapaces de formar oligómeros y no son tóxicas para larvas de *M. sexta* (*21*). Por otro lado, se ha demostrado

que el oligómero de la toxina es más eficiente en la formación de poro que el monómero en membranas artificiales (*56*). Adicionalmente, mutantes en la α4 del dominio I de la toxina Cry1Ab resultan en toxinas dominantes negativas, que al formar hetero-oligómeros con la toxina tipo silvestre inhiben el efecto tóxico de esta proteína (*22*). Estos datos sugieren que el oligómero es una identidad importante en la toxicidad, sin embargo, hasta este trabajo no se había explorado la manera en que interacciona con los receptores anclados por GPI, como se propone aquí el mecanismo de acción. En este sentido, se analizó la interacción del oligómero de la toxina Cry1Ab con dos proteínas ancladas por GPI, la aminopeptidasa de 120 kDa y la fosfatasa alcalina de 65 kDa, del insecto lepidóptero *M. sexta*. La aminopeptidasa es la proteína más caracterizada y ha sido reportada como receptor de las toxinas Cry. Se han realizado experimentos con la proteína pura para determinar su papel en la toxicidad y para determinar su afinidad por la toxina; sin embargo, todos los trabajos reportados están realizados con el monómero de la toxina. A la fecha, el único reporte de la interacción de esta proteína con el oligómero de la toxina se realizó mediante experimentos de inmunoprecipitación determinándose que el oligómero presenta una unión preferencial con aminopeptidasa, mientras que el monómero presenta una unión preferencial por caderina, sin embargo, en este estudio no se analizó la unión con la fosfatasa alcalina (*63*). A pesar de que existen reportes que le dan un papel funcional a la aminopeptidasa en el mecanismo de acción de estas toxinas, también hay datos que sugieren que esta proteína no es importante para la toxicidad. Se han reportado mutantes en el dominio III de la toxina Cry1Ac afectadas en la unión a aminopeptidasa, pero que siguen siendo tóxicas para las larvas de *M. sexta* (*109*). Estos datos dan la pauta para pensar que existen receptores alternativos que podrían jugar el mismo papel que la aminopeptidasa. Por su parte, la fosfatasa alcalina se ha reportado como proteína de unión de la toxina Cry1Ac en *M. sexta*

y *H. armiguera*, sin embargo, exclusivamente en *H. vierescens* se le ha dado el papel de receptor, pues se ha demostrado que su baja expresión resulta en la resistencia del insecto. En el caso de *M. sexta*, no se sabe si esta proteína funciona como receptor o simplemente es una proteína de unión (*52, 99-100*). En este trabajo se analizó la unión del oligómero y del monómero de la toxina Cry1Ab con aminopeptidasa y fosfatasa alcalina purificadas. Los resultados muestran que el monómero de la toxina se une tanto a aminopeptidasa como a fosfatasa alcalina, con afinidades aparentes de 101.6 nM y 267.3 nM, respectivamente. La afinidad que se determinó en este trabajo es muy parecida a la reportada para la unión del monómero de la toxina con aminopeptidasa purificada (100 nM) en análisis con resonancia de plasmones (*109*) y a la calculada mediante competencia en ensayo de ELISA para la unión del monómero con extractos ricos con proteínas ancladas por GPI (*63*).Para la fosfatasa alcalina no se ha reportado ninguna afinidad, por lo que éste es el primer reporte de la afinidad del monómero por esta proteína. Cuando se analizó la interacción del oligómero con aminopeptidasa y fosfatasa alcalina se determinó un aumento en la afinidad de más de 200 veces, con respecto a las obtenidas con el monómero de la toxina. Para el caso de la unión del oligómero con aminopeptidasa, se determinó una afinidad aparente de 0.6 nM y para el caso de la fosfatasa alcalina de 0.5 nM. Estos resultados sugieren que deben existir cambios conformacionales en la toxina que permiten que, una vez que el oligómero se forme, se aumente su afinidad por las proteínas ancladas por GPI. En este sentido, ya se ha reportado que existen cambios estructurales entre el oligómero y el monómero de la toxina. Experimentos con ANS, que es un colorante que emite fluorescencia cuando se une a regiones hidrofóbicas, mostraron que el oligómero de la toxina muestra una mayor hidrofobicidad con respecto al monómero (*56*). También se sabe que la conformación del monómero es diferente a la del oligómero, porque un anticuerpo

monoclonal, aislado mediante la metodología de Despliegue en Fagos, que reconoce específicamente al asa 2 de la toxina en su conformación de monómero, no une a la toxina en su conformación de oligómero. Todos estos resultados sugieren que tanto la aminopeptidasa, como la fosfatasa alcalina, pueden ser receptores de la toxina Cry1Ab en *M. sexta*. La unión del oligómero con la fosfatasa alcalina puede ser competida por la aminopeptidasa y viceversa, aunque con menor eficiencia. Este dato sugiere que ambas proteínas comparten al menos un sitio de interacción con el oligómero de la toxina. Adicionalmente, en este trabajo se caracterizó la unión de dos mutantes de la toxina Cry1Ab localizadas en el asa 2 (RR368-9AA y F371A), con los receptores aminopeptidasa y fosfatasa alcalina. Las dos toxinas mutantes se unen de la misma manera que la toxina tipo silvestre a aminopeptidasa y fosfatasa alcalina cuando se encuentran como monómeros. Sin embargo, se encuentran severamente afectadas en la unión en forma de oligómeros. Estos resultados sugieren que el asa 2 del dominio II de la toxina Cry1Ab, es un epítope importante en la interacción del oligómero de la toxina con estos dos receptores. En un trabajo previo se reportó que la mutante F371A no se encuentra afectada en la interacción con aminopeptidasa, pero si estaba afectada en la toxicidad. Este resultado causó controversia, pues como la unión no correlacionaba con la toxicidad, se sugería que algún otro receptor podría estar involucrado, si bien los estudios se realizaron exclusivamente con el monómero de la toxina (*109*). En este trabajo se demuestra, que efectivamente que la unión del monómero no está afectada como se había reportado, sin embargo, la unión de la mutante como oligómero se encuentra severamente afectada, lo que correlaciona con la pérdida de toxicidad. Interesantemente la mutante se encuentra afectada de manera similar en la unión tanto a aminopeptidasa como a fosfatasa alcalina y aparentemente, los defectos en la unión no permiten la inserción de la toxina en la membrana para la formación de poro,

por lo que no es tóxica para la larvas. Recientemente se reportó un mecanismo de acción que involucra a la aminopeptidasa en dos pasos. El primero se da cuando el monómero de la toxina se une a este receptor, vía el asa 3 del dominio II para localizarse en el intestino, se propone que esta unión es de baja afinidad, pero con abundantes sitios de interacción, ya que esta proteína es muy abundante en el intestino del insecto. El segundo se da cuando se forma el oligómero de la toxina (después de contacto con caderina) y se propone que es de alta afinidad (*64*). En nuestro trabajo, se demostró por un lado, que la fosfatasa alcalina también se puede unir de manera similar al monómero y al oligómero de la toxina, como lo hace la aminopeptidasa y por otro, que la interacción del oligómero de la toxina con ambos receptores, se da mediante el asa 2 del dominio II. Interesantemente, mutantes en el asa 3 se encuentran afectadas en la interacción con aminopeptidasa cuando se encuentran como monómeros, sin embargo, no se encuentran afectadas en la unión cuando se encuentran como oligómeros (*64*). Estos resultados sugieren un papel secuencial de las asas, cuando la toxina se encuentra como monómero, se une mediante el asa 3 y cuando se encuentra como oligómero, se une por el asa 2. Adicionalmente, los cambios en las afinidades de la interacción del monómero con respecto al oligómero correlacionan con el mecanismo de acción propuesto, en donde el monómero se une con baja afinidad, mientras que el oligómero se une con alta afinidad a las proteínas ancladas por GPI. En el caso de la interacción del dominio III con los receptores, se ha demostrado mediante la caracterización de un anticuerpo que reconocen esta región de la toxina, que la β16 está involucrada en la interacción con el receptor aminopeptidasa, sin embargo, no se determinó si esta región también es importante en la interacción del oligómero o si esta región es importante en la interacción con la fosfatasa alcalina. Aquí se caracterizó la unión de la mutante L511A, localizada en la β16 con los receptores anclados por GPI. Los resultados

obtenidos muestran que cuando se probó la unión del oligómero de esta mutante con los receptores purificados, no se observaron defectos en la unión, sin embargo, cuando se probó la unión del monómero, sí se observaron defectos en la unión, pero estos defectos son particulares para cada receptor. En el caso de la unión con aminopeptidasa, se observó una ligera disminución en la unión, mientras que la unión con la fosfatasa alcalina está severamente afectada. Estos datos corroboran que la unión del monómero con aminopeptidasa se da mediante la β16 del dominio III, epítope que parece no ser importante en la interacción cuando la toxina se oligomeriza, como sucede con el asa 2. La falta de toxicidad de esta mutante no puede justificarse con los defectos en la unión con aminopeptidasa, sin embargo, si se justifica con los defectos en la unión con fosfatasa alcalina. Estos resultados sugieren que la fosfatasa alcalina juega un papel más importante que la aminopeptidasa en la toxicidad. Otra observación que soporta la importancia de la fosfatasa es la unión de la toxina a las VMMA´s de los diferentes estadíos, donde la unión de la toxina en los primeros estadíos está o puede estar mediada por la fosfatasa alcalina y no por la aminopeptidasa. El papel exacto de estas dos proteínas, en cada uno de los pasos en el mecanismo de acción de las toxinas, podrá ser determinado mediante otras metodologías como el silenciamiento genético con RNA de doble cadena o mediante la caracterización de líneas celulares de insecto que expresen los receptores de manera independiente. Los datos obtenidos en este trabajo aportan más información al mecanismo de acción denominado como “ping-pong”(*64*). En primer lugar, una vez que la toxina es activada después de la solubilización de los cristales, el monómero se une a aminopeptidasa, como se había reportado, pero también a la fosfatasa alcalina, mediante el asa 3 del dominio II y la β16 del dominio III. Las afinidades de unión para aminopeptidasa y para fosfatasa alcalina son de 101.6 nM y 267.3 nM, respectivamente. Posteriormente, la

toxina se une a la caderina mediante el dominio II (con una afinidad de 1 nM), para sufrir una segunda activación que permite la oligomerización. En este paso de oligomerización aparentemente existen cambios conformacionales en el dominio II de la toxina que incrementan la afinidad de la toxina por los receptores anclados por GPI. En el caso de aminopeptidasa, de 101.6 nM como monómero a 0.6 nM cuando se oligomeriza, para la fosfatasa alcalina, de 267.3 nM como monómero a 0.5 nM cuando se oligomeriza. Una vez formado el oligómero, éste se une a aminopeptidasa y a fosfatasa alcalina, que se localiza en balsas lipídicas, donde se lleva a cabo la inserción de la toxina (Figura 19).

CONCLUSIONES.

- La unión del monómero de la toxina cambia a lo largo de los estadíos de desarrollo, en los primeros estadíos se une a fosfatasa alcalina y en los estadíos tardíos se une a la aminopeptidasa.
- La toxina Cry1Ab se une a aminopeptidasa y fosfatasa alcalina con diferentes afinidades dependiendo de su conformación. El monómero se une con una afinidad de 101.6 nM a aminopeptidasa y con una afinidad de 267.3 nM a fosfatasa alcalina. Cuando la toxina se oligomeriza aumenta su afinidad en más de 200 veces por ambos receptores, 0.6 nM para aminopeptidasa y 0.5 nM para fosfatasa alcalina.
- Dos mutantes en el asa 2 RR368-9AA y F371A, están afectadas en la toxicidad contra larvas de *M. sexta* debido a defectos en su interacción con aminopeptidasa y fosfatasa alcalina cuando la toxina se encuentra como oligómero. Dado que cuando está como monómero la unión no se ve afectada, se sugiere que la interacción del oligómero con los receptores es importante en la toxicidad y que esta interacción está dada mediante el asa 2 de la toxina.
- La mutación L511A en la β16 del dominio III afecta drásticamente la toxicidad, aparentemente debido a la pérdida de unión del monómero a fosfatasa alcalina. El papel de la fosfatasa alcalina es más importante en la toxicidad de las toxinas Cry, pues esta proteína es abundante en los estadios tempranos y la mutante L511A al perder la unión con esta proteína, pierde la toxicidad.
- Los resultados contribuyen y soportan el mecanismo de acción denominado ping-pong.

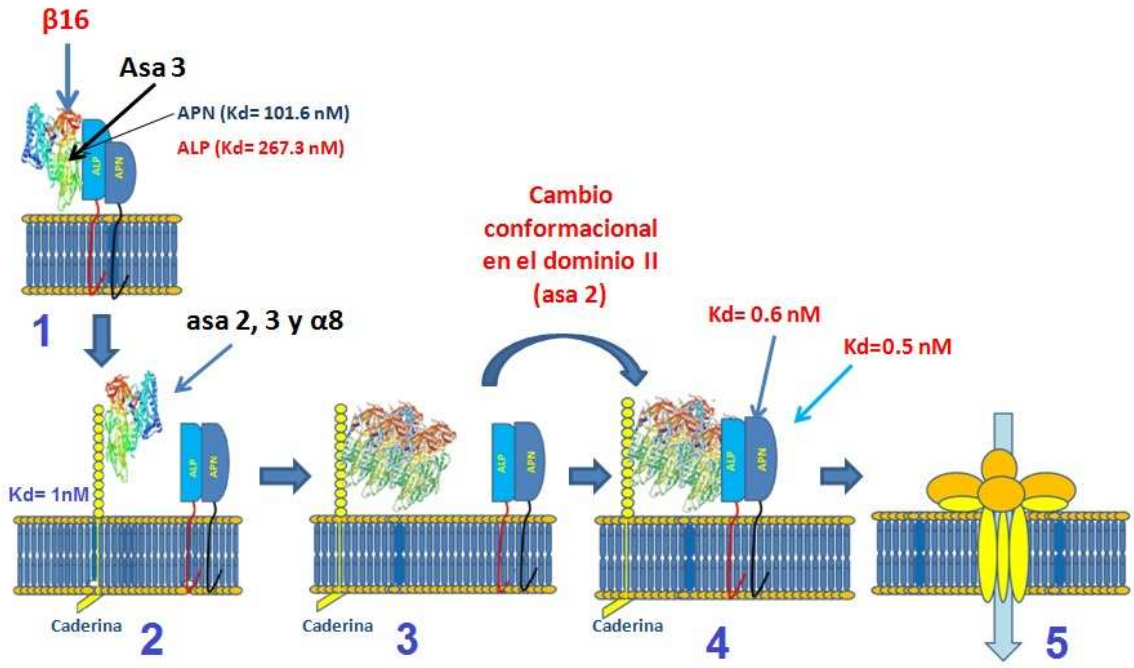

Figura 1. Mecanismo de acción para las toxinas Cry. 1) Después de que los cristales de la toxina son solubilizados y activados proteolíticamente se libera al monómero de la toxina que se une con los receptores anclados por GPI fosfatasa alcalina y aminopeptidasa a través de el asa 3 del Dominio II de la región la β16 del Dominio III con afinidades de 267.3 nM y 101.6 n M, respectivamente; 2) La toxina se une con alta afinidad (1 nM) al receptor caderina a través de las asas 2, 3 y α8; 3) La toxina sufre nuevamente un procesamiento proteolítico perdiendo la hélice α1, lo que permite la formación del oligómero de la toxina; 4) La formación del oligómero conlleva cambios conformacionales que permiten un aumento de afinidad (0.6 nM para aminopeptidasa y 0.5 nM para fosfatasa alcalina) y la unión con los receptores anclados por GPI; 5) Posteriormente se lleva a cabo la inserción de la toxina, la formación de poro que causa el desbalance osmótico que lleva a la muerte del insecto.

PERSPECTIVAS.

- Determinar los parámetros cinéticos de las interacciones entre la toxina en sus dos conformaciones estructurales, con los receptores anclados por GPI en tiempo real utilizando la técnica de SPR (Resonancia de plasmones).

- Demostrar la funcionalidad *in vivo* de la aminopeptidasa y fosfatasa alcalina en larvas de *M. sexta*, mediante interferencia con RNA de doble cadena.

- Disectar el papel de la aminopeptidasa ó fosfatasa alcalina en la toxicidad mediada por monómero u oligómero de la toxina, a través de la construcción de líneas celulares de insecto que expresen a los receptores de manera independiente.

- Determinar regiones de interacción en cada uno de los receptores, analizando la unión de la toxina con fragmentos de aminopeptidasa y fosfatasa alcalina expresados heterólogamente.

BIBLIOGRAFÍA.

1. Helgason, E., Okstad, O. A., Caugant, D. A., Johansen, H. A., Fouet, A., Mock, M., Hegna, I., and Kolsto, A.-B. (2000) *Bacillus anthracis*, *Bacillus cereus*, and *Bacillus thuringiensis* One Species on the Basis of Genetic Evidence, *Appl. Environ. Microbiol. 66*, 2627-2630.
2. Schnepf, E., Crickmore, N., Van Rie, J., Lereclus, D., Baum, J., Feitelson, J., Zeigler, D. R., and Dean, D. H. (1998) Bacillus thuringiensis and Its Pesticidal Crystal Proteins, *Microbiol. Mol. Biol. Rev. 62*, 775-806.
3. Crickmore, N., Zeigler, D. R., Feitelson, J., Schnepf, E., Van Rie, J., Lereclus, D., Baum, J., and Dean, D. H. (1998) Revision of the Nomenclature for the Bacillus thuringiensis Pesticidal Crystal Proteins, *Microbiol. Mol. Biol. Rev. 62*, 807-813.
4. Wei, J.-Z., Hale, K., Carta, L., Platzer, E., Wong, C., Fang, S.-C., and Aroian, R. V. (2003) Bacillus thuringiensis crystal proteins that target nematodes, *Proc. Natl. Acad. Sci. USA 100*, 2760-2765.
5. de Maagd, R. A., Bravo, A., and Crickmore, N. (2001) How *Bacillus thuringiensis* has evolved specific toxins to colonize the insect world, *Trends. Genet. 17,* 193 - 199.
6. Thomas, D. J. I., Morgan, J. A. W., Whipps, J. M., and Saunders, J. R. (2001) Plasmid Transfer between *Bacillus thuringiensis* subsp. israelensis Strains in Laboratory Culture, River Water, and Dipteran Larvae, *Appl. Environ. Microbiol. 67*, 330-338.
7. Thomas, D. J. I., Morgan, J. A. W., Whipps, J. M., and Saunders, J. R. (2000) Plasmid Transfer between the *Bacillus thuringiensis* Subspecies kurstaki and tenebrionis in Laboratory Culture and Soil and in Lepidopteran and Coleopteran Larvae, *Appl. Environ. Microbiol. 66*, 118-124.
8. Hofte, H., and Whiteley, H. (1989) Insecticidal crystal proteins of *Bacillus thuringiensis*, *Microbiol. Rev. 52*, 242–255.
9. Bravo, A. (1997) Phylogenetic relationships of *Bacillus thuringiensis* delta-endotoxin family proteins and their functional domains, *J. Bacteriol. 179*, 2793-2801.
10. Guerchicoff, A., Delecluse, A., and Rubinstein, C. P. (2001) The *Bacillus thuringiensis* cyt Genes for Hemolytic Endotoxins Constitute a Gene Family, *Appl. Environ. Microbiol. 67*, 1090-1096.
11. Estruch, J. J., Warren, G. W., Mullins, M. A., Nye, G. J., Craig, J. A., and Koziel, M. G. (1996) Vip3A, a novel *Bacillus thuringiensis* vegetative insecticidal protein with a wide spectrum of activities against lepidopteran insects, *Proc. Natl. Acad. Sci. USA 93*, 5389-5394.
12. CHOMA, C. T., SUREWICZ, W. K., CAREY, P. R., POZSGAY, M., RAYNOR, T., and KAPLAN, H. (1990) Unusual proteolysis of the protoxin and toxin from *Bacillus thuringiensis*, *Euro. J. Bioch. 189*, 523-527.
13. Li, J., Carroll, J., and Ellar, D. J. (1991) Crystal structure of insecticidal δ-endotoxin from *Bacillus thuringiensis* at 2.5 A resolution, *Nature 353*, 815-821.

14. Galitsky, N., Cody, V., Wojtczak, A., Ghosh, D., Luft, J. R., Pangborn, W., and English, L. (2001) Structure of the insecticidal bacterial δ-endotoxin Cry3Bb1 of *Bacillus thuringiensis*, *Acta Cryst. D 57*, 1101-1109.
15. Grochulski, P., Masson, L., Borisova, S., Pusztai-Carey, M., Schwartz, J.-L., Brousseau, R., and Cygler, M. (1995) *Bacillus thuringiensis* CrylA(a) Insecticidal Toxin: Crystal Structure and Channel Formation, *J. Mol. Biol. 254*, 447-464.
16. Morse, R. J., Yamamoto, T., and Stroud, R. M. (2001) Structure of Cry2Aa Suggests an Unexpected Receptor Binding Epitope, *Structure 9*, 409-417.
17. Boonserm, P., Davis, P., Ellar, D. J., and Li, J. (2005) Crystal Structure of the Mosquito-larvicidal Toxin Cry4Ba and Its Biological Implications, *J. Mol. Biol. 348*, 363-382.
18. Boonserm, P., Mo, M., Angsuthanasombat, C., and Lescar, J. (2006) Structure of the Functional Form of the Mosquito Larvicidal Cry4Aa Toxin from *Bacillus thuringiensis* at a 2.8-Angstrom Resolution, *J. Bacteriol. 188*, 3391-3401.
19. Parker, M. W., Postma, J. P. M., Pattus, F., Tucker, A. D., and Tsernoglou, D. (1992) Refined structure of the pore-forming domain of colicin A at 2.4 Å resolution, *J. Mol. Biol. 224*, 639-657.
20. Gazit, E., Bach, D., Kerr, I. D., Sansom, M. S., Chejanovsky, N., and Shai, Y. (1994) The alpha-5 segment of *Bacillus thuringiensis* delta-endotoxin: in vitro activity, ion channel formation and molecular modelling, *Biochem. J 304 (Pt 3)*, 895-902.
21. Jimenez-Juarez, N., Munoz-Garay, C., Gomez, I., Saab-Rincon, G., Damian-Alamazo, J. Y., Gill, S. S., Soberon, M., and Bravo, A. (2007) *Bacillus thuringiensis* Cry1Ab mutants affecting oligomer formation are non toxic to *Manduca sexta* larvae, *J. Biol. Chem. 282*(29), 21222-21229.
22. Rodriguez-Almazan, C., Zavala, L. E., Munoz-Garay, C., Jimenez-Juarez, N., Pacheco, S., Masson, L., Soberon, M., and Bravo, A. (2009) Dominant negative mutants of *Bacillus thuringiensis* Cry1Ab toxin function as anti-toxins: demonstration of the role of oligomerization in toxicity, *PLoS One 4*, e5545.
23. Rajamohan, F., lee, M. K., and Dean, D. (1998) *Bacillus thuringiensis* insecticidal proteins: molecular mode of action, *Prog. Nucleic Acid. Res. Mol. biol. 60*, 1-27.
24. Lee, M. K., and Dean, D. H. (1996) Inconsistencies in Determining *Bacillus thuringiensis* Toxin Binding Sites Relationship by Comparing Competition Assays with Ligand Blotting, *Bioch. Biophys. Res. Commun 220*, 575-580.
25. Gomez, I., Dean, D. H., Bravo, A., and Soberon, M. (2003) Molecular Basis for *Bacillus thuringiensis* Cry1Ab Toxin Specificity: Two Structural Determinants in the *Manduca sexta* Bt-R_1Receptor Interact with Loops α8 and 2 in Domain II of Cy1Ab Toxin, *Biochem. 42*, 10482-10489.
26. Wu, S.-J., and Dean, D. H. (1996) Functional Significance of Loops in The Receptor Binding Domain of *Bacillus thuringiensis* CryIIIA δ-Endotoxin, *J. Mol. Biol. 255*, 628-640.
27. Wu, S.-J., Koller, C. N., Miller, D. L., Bauer, L. S., and Dean, D. H. (2000) Enhanced toxicity of *Bacillus thuringiensis* Cry3A δ-endotoxin in coleopterans by mutagenesis in a receptor binding loop, *FEBS Letters 473*, 227-232.
28. Lu, H., Rajamohan, F., and Dean, D. H. (1994) Identification of amino acid residues of *Bacillus thuringiensis* delta-endotoxin CryIAa associated with membrane binding and toxicity to *Bombyx mori*, *J. Bacteriol. 176*, 5554-5559.

29. Lee, M. K., Jenkins, J. L., You, T. H., Curtiss, A., Son, J. J., Adang, M. J., and Dean, D. H. (2001) Mutations at the arginine residues in α8 loop of *Bacillus thuringiensis* δ-endotoxin Cry1Ac affect toxicity and binding to *Manduca sexta* and *Lymantria dispar* aminopeptidase N, *FEBS Letters 497,* 108-112.
30. Rajamohan, F., Alcantara, E., Lee, M. K., Chen, X. J., Curtiss, A., and Dean, D. H. (1995) Single amino acid changes in domain II of *Bacillus thuringiensis* CryIAb δ-endotoxin affect irreversible binding to *Manduca sexta* midgut membrane vesicles, *J. Bacteriol. 177,* 2276-2282.
31. Rajamohan, F., Cotrill, J. A., Gould, F., and Dean, D. H. (1996) Role of Domain II, Loop 2 Residues of *Bacillus thuringiensis* CryIAb δ-Endotoxin in Reversible and Irreversible Binding to *Manduca sexta* and *Heliothis virescens*, *J. Biol. Chem. 271,* 2390-2396.
32. Rajamohan, F., Hussain, S.-R. A., Cotrill, J. A., Gould, F., and Dean, D. H. (1996) Mutations at Domain II, Loop 3,of *Bacillus thuringiensis* CryIAa and CryIAb δ-Endotoxins Suggest Loop 3 Is Involved in Initial Binding to Lepidopteran Midguts, *J. Biol. Chem. 271,* 25220-25226.
33. Gomez, I., Arenas, I., Benitez, I., Miranda-Rios, J., Becerril, B., Grande, R., Almagro, J. C., Bravo, A., and Soberon, M. (2006) Specific Epitopes of Domains II and III of B*acillus thuringiensis* Cry1Ab Toxin Involved in the Sequential Interaction with Cadherin and Aminopeptidase-N Receptors in *Manduca sexta*, *J. Biol. Chem. 281,* 34032-34039.
34. Derbyshire, D. J., Ellar, D. J., and Li, J. (2001) Crystallization of the *Bacillus thuringiensis* toxin Cry1Ac and its complex with the receptor ligand N-acetyl-d-galactosamine, *Acta Crystallogr. Sec. D 57,* 1938-1944.
35. Burton, S. L., Ellar, D. J., Li, J., and Derbyshire, D. J. (1999) N-acetylgalactosamine on the putative insect receptor aminopeptidase N is recognised by a site on the domain III lectin-like fold of a *Bacillus thuringiensis* insecticidal toxin, *J. Mol. Biol. 287,* 1011-1022.
36. de Maagd, R. A. d., Bakker, P. L., Masson, L., Adang, M. J., Sangadala, S., Stiekema, W., and Bosch, D. (1999) Domain III of the *Bacillus thuringiensis* delta-endotoxin Cry1Ac is involved in binding to *Manduca sexta* brush border membranes and to its purified aminopeptidase N, *Mol. Microbiol. 31,* 463-471.
37. de Maagd, R., Kwa, M., van der Klei, H., Yamamoto, T., Schipper, B., Vlak, J., Stiekema, W., and Bosch, D. (1996) Domain III substitution in *Bacillus thuringiensis* δ-endotoxin CryIA(b) results in superior toxicity for *Spodoptera exigua* and altered membrane protein recognition, *Appl. Environ. Microbiol. 62,* 1537-1543.
38. Atsumi, S., Mizuno, E., Hara, H., Nakanishi, K., Kitami, M., Miura, N., Tabunoki, H., Watanabe, A., and Sato, R. (2005) Location of the *Bombyx mori* Aminopeptidase N Type 1 Binding Site on *Bacillus thuringiensis* Cry1Aa Toxin, *Appl. Environ. Microbiol. 71,* 3966-3977.
39. Bravo, A., Sarabia, S., Lopez, L., Ontiveros, H., Abarca, C., Ortiz, A., Ortiz, M., Lina, L., Villalobos, F. J., Pena, G., Nunez-Valdez, M.-E., Soberon, M., and Quintero, R. (1998) Characterization of cry Genes in a Mexican *Bacillus thuringiensis* Strain Collection, *Appl. Environ. Microbiol. 64,* 4965-4972.
40. Bernhard, K., Jarrett, P., Meadows, M., Butt, J., Ellis, D. J., Roberts, G. M., Pauli, S., Rodgers, P., and Burges, H. D. (1997) Natural Isolates of *Bacillus thuringiensis*:

Worldwide Distribution, Characterization, and Activity against Insect Pests, *J. Invertebr. Pathol. 70*, 59-68.

41. de Maagd, R. A., Weemen-Hendriks, M., Stiekema, W., and Bosch, D. (2000) B*acillus thuringiensis* Delta-Endotoxin Cry1C Domain III Can Function as a Specificity Determinant for *Spodoptera exigua* in Different, but Not All, Cry1-Cry1C Hybrids, *Appl. Environ. Microbiol. 66*, 1559-1563.
42. Aronson, A. I., and Shai, Y. (2001) Why *Bacillus thuringiensis* insecticidal toxins are so effective: unique features of their mode of action, *FEMS Microbiol. Lett. 195*, 1-8.
43. Dow, J. A. T. (1986) Insect midgut function, In *Advances in Insect Physiology* (Evans, P. D. a. W. B. W., Ed.), pp 187–328, Academic Press, London.
44. Du, C., Martin, P., and Nickerson, K. (1994) Comparison of Disulfide Contents and Solubility at Alkaline pH of Insecticidal and Noninsecticidal *Bacillus thuringiensis* Protein Crystals, *Appl. Environ. Microbiol. 60*, 3847-3853.
45. Terra, W. R. a. C. F. (1994) Insect digestive enzymes: properties, compartmentalization and function, *Com. Biochem. Physiol. 109*, 1-62.
46. Miranda, R., Zamudio, F. Z., and Bravo, A. (2001) Processing of Cry1Ab δ-endotoxin from *Bacillus thuringiensis* by *Manduca sexta* and *Spodoptera frugiperda* midgut proteases: role in protoxin activation and toxin inactivation, *Insect Biochem. Mol. Biol. 31*, 1155-1163.
47. Dai, S.-m., and Gill, S. S. (1993) In vitro and in vivo proteolysis of the *Bacillus thuringiensis* subsp. israelensis CryIVD protein by *Culex quinquefasciatus* larval midgut proteases, *Insect Biochem. Mol. Biol. 23*, 273-283.
48. Wolfersberger, M. G., Luethy, P., Muarer, A.,Parenti, P.,Sacchi, F. V., Giordana, B. and Hanozett, G. M. (1987) Preparation and partial characterization of amino acid transporting brush border membrane vesicles from the larval midgut of the cabbage butterfly (*Pieris brassicae*). *Comp. Biochem. Physiol. 86*, 301–308.
49. Hofmann C, V. H., Höfte H, Van Rie J, Jansens S, Van Mellaert H. (1988) Specificity of *Bacillus thuringiensis* δ-endotoxins is correlated with the presence of high-affinity binding sites in the brush border membrane of target insect midguts, *Proc. Natl. Acad. Sci. USA 85*, 7844-7848.
50. Vadlamudi, R., Ji, T., and Bulla, L. (1993) A specific binding protein from Manduca sexta for the insecticidal toxin of Bacillus thuringiensis subsp. berliner, *J. Biol. Chem. 268*, 12334 - 12340.
51. Knight, P., Crickmore, N., and Ellar, D. (1994) The receptor for *Bacillus thuringiensis* CryIA(c) delta-endotoxin in the brush border membrane of the lepidopteran *Manduca sexta* is aminopeptidase N, *Mol. Microbiol. 11*, 429 - 436.
52. Jurat-Fuentes, J. L., and Adang, M. J. (2004) Characterization of a Cry1Ac-receptor alkaline phosphatase in susceptible and resistant *Heliothis virescens* larvae, *Eur. J. Biochem. 271*, 3127-3135.
53. Valaitis, A., Jenkins, J., Lee, M., Dean, D., and Garner, K. (2001) Isolation and partial characterization of gypsy moth BTR-270, an anionic brush border membrane glycoconjugate that binds *Bacillus thuringiensis* Cry1A toxins with high affinity, *Arch. Insect Biochem. Physiol. 46*, 186 - 200.
54. Gomez, I., Miranda-Rios, J., Rudino-Pinera, E., Oltean, D. I., Gill, S. S., Bravo, A., and Soberon, M. (2002) Hydropathic Complementarity Determines Interaction of Epitope 869HITDTNNK876 in *Manduca sexta* Bt-R1 Receptor with Loop 2 of

Domain II of *Bacillus thuringiensis* Cry1A Toxins, *J. Biol. Chem. 277*, 30137-30143.

55. Gomez, I., Oltean, D. I., Gill, S. S., Bravo, A., and Soberon, M. (2001) Mapping the Epitope in Cadherin-like Receptors Involved in *Bacillus thuringiensis* Cry1A Toxin Interaction Using Phage Display, *J. Biol. Chem. 276*, 28906-28912.
56. Gomez, I., Sanchez, J., Miranda, R., Bravo, A., and Soberon, M. (2002) Cadherin-like receptor binding facilitates proteolytic cleavage of helix α1 in domain I and oligomer pre-pore formation of *Bacillus thuringiensis* Cry1Ab toxin, *FEBS Lett. 513*, 242-246.
57. Rausell, C., Munoz-Garay, C., Miranda-CassoLuengo, R., Gomez, I., Rudino-Pinera, E., Soberon, M., and Bravo, A. (2004) Tryptophan Spectroscopy Studies and Black Lipid Bilayer Analysis Indicate that the Oligomeric Structure of Cry1Ab Toxin from *Bacillus thuringiensis* Is the Membrane-Insertion Intermediate, *Biochem. 43*, 166-174.
58. Muñoz-Garay, C., Sánchez, J., Darszon, A., de Maagd, R. A., Bakker, P., Soberón, M., and Bravo, A. (2006) Permeability Changes of *Manduca sexta* Midgut Brush Border Membranes Induced by Oligomeric Structures of Different Cry Toxins, *J. Membr. Biol. 212*, 61-68.
59. Aronson, A. I., Geng, C., and Wu, L. (1999) Aggregation of *Bacillus thuringiensis* Cry1A Toxins upon Binding to Target Insect Larval Midgut Vesicles, *Appl. Environ. Microbiol. 65*, 2503-2507.
60. Tigue, N. J., Jacoby, J., and Ellar, D. J. (2001) The alpha Helix 4 Residue, Asn135, Is Involved in the Oligomerization of Cry1Ac1 and Cry1Ab5 *Bacillus thuringiensis* Toxins, *Appl. Environ. Microbiol. 67*, 5715-5720.
61. Herrero, S., Gonzalez Cabrera, J., Ferre, J., Bakker, P. L., and de Maagd, R. A. (2004) Mutations in the *Bacillus thuringiensis* Cry1Ca toxin demonstrate the role of domains II and III in specificity towards *Spodoptera exigua* larvae, *Biochem. J. 384*, 507 - 513.
62. Gomez, I., Arenas, I., Benitez, I., Miranda-Rios, J., Becerril, B., Grande, R., Almagro, J. C., Bravo, A., and Soberon, M. (2006) Specific epitopes of domains II and III of *Bacillus thuringiensis* Cry1Ab toxin involved in the sequential interaction with cadherin and aminopeptidase-N receptors in *Manduca sexta*, *J. Biol. Chem. 281*, 34032-34039.
63. Bravo, A., Gomez, I., Conde, J., Munoz-Garay, C., Sanchez, J., Miranda, R., Zhuang, M., Gill, S. S., and Soberon, M. (2004) Oligomerization triggers binding of a *Bacillus thuringiensis* Cry1Ab pore-forming toxin to aminopeptidase N receptor leading to insertion into membrane microdomains, *Biochim. Biophy. Acta 1667*, 38-46.
64. Pacheco, S., Gomez, I., Arenas, I., Saab-Rincon, G., Rodriguez-Almazan, C., Gill, S. S., Bravo, A., and Soberon, M. (2009) Domain II loop 3 of *Bacillus thuringiensis* Cry1Ab toxin is involved in a "ping pong" binding mechanism with *Manduca sexta* aminopeptidase-N and cadherin receptors, *J. Biol. Chem. 284*, 32750-32757.
65. Abrami, L., Fivaz, M., Glauser, P.-E., Sugimoto, N., Zurzolo, C., and van der Goot, F. G. (2003) Sensitivity of Polarized Epithelial Cells to the Pore-Forming Toxin Aerolysin, *Infect. Immun. 71*, 739-746.

66. Knowles, B. H. (1994) Mechanism of Action of *Bacillus thuringiensis* Insecticidal δ-Endotoxins, In *Advances in Insect Physiology* (Evans, P. D., Ed.), pp 275-308, Academic Press.
67. Schwartz, J.-L., Juteau, M., Grochulski, P., Cygler, M., Préfontaine, G., Brousseau, R., and Masson, L. (1997) Restriction of intramolecular movements within the Cry1Aa toxin molecule of *Bacillus thuringiensis* through disulfide bond engineering, *FEBS Lett. 410*, 397-402.
68. Vadlamudi, R. K., Weber, E., Ji, I., Ji, T. H., and Bulla, L. A., Jr. (1995) Cloning and Expression of a Receptor for an Insecticidal Toxin of *Bacillus thuringiensis*, *J. Biol. Chem. 270*, 5490-5494.
69. Nagamatsu, Y., Toda, S., Yamaguchi, F., Ogo, M., Kogure, M., Nakamura, M., Shibata, Y., and Katsumoto, T. (1998) Identification of *Bombyx mori* midgut receptor for *Bacillus thuringiensis* insecticidal CryIA(a) toxin, *Biosci. Biotechnol. Biochem. 62*, 718 - 726.
70. Gahan, L. J., Gould, F., and Heckel, D. G. (2001) Identification of a Gene Associated with Bt Resistance in *Heliothis virescens*, *Science 293*, 857-860.
71. Xu, X., Yu, L., and Wu, Y. (2005) Disruption of a Cadherin Gene Associated with Resistance to Cry1Ac δ-Endotoxin of *Bacillus thuringiensis* in *Helicoverpa armigera*, *Appl. Environ. Microbiol. 71*, 948-954.
72. Morin, S., Biggs, R. W., Sisterson, M. S., Shriver, L., Ellers-Kirk, C., Higginson, D., Holley, D., Gahan, L. J., Heckel, D. G., CarriÃ¨re, Y., Dennehy, T. J., Brown, J. K., and Tabashnik, B. E. (2003) Three cadherin alleles associated with resistance to *Bacillus thuringiensis* in pink bollworm, *Proc. Natl. Acad. Sci. USA. 100*, 5004-5009.
73. Flannagan, R. D., Yu, C.-G., Mathis, J. P., Meyer, T. E., Shi, X., Siqueira, H. A. A., and Siegfried, B. D. (2005) Identification, cloning and expression of a Cry1Ab cadherin receptor from European corn borer, *Ostrinia nubilalis* (Hübner) (Lepidoptera: Crambidae), *Insect Biochem. Mol. Biol. 35*, 33-40.
74. Hua, G., Zhang, R., Abdullah, M. A., and Adang, M. J. (2008) *Anopheles gambiae* cadherin AgCad1 binds the Cry4Ba toxin of *Bacillus thuringiensis* israelensis and a fragment of AgCad1 synergizes toxicity, *Biochem. 47*, 5101-5110.
75. Chen, J., Brown, M. R., Hua, G., and Adang, M. J. (2005) Comparison of the localization of *Bacillus thuringiensis* Cry1A δ-endotoxins and their binding proteins in larval midgut of tobacco hornworm, *Manduca sexta*, *Cell Tissue Res. 321*, 123-129.
76. Dorsch, J. A., Candas, M., Griko, N. B., Maaty, W. S. A., Midboe, E. G., Vadlamudi, R. K., and Bulla, L. A. (2002) Cry1A toxins of *Bacillus thuringiensis* bind specifically to a region adjacent to the membrane-proximal extracellular domain of BT-R1 in *Manduca sexta*: involvement of a cadherin in the entomopathogenicity of *Bacillus thuringiensis*, *Insect Biochem. Mol. Biol. 32*, 1025-1036.
77. Zhang, X., Candas, M., Griko, N. B., Rose-Young, L., and Bulla, L. A. (2005) Cytotoxicity of *Bacillus thuringiensis* Cry1Ab toxin depends on specific binding of the toxin to the cadherin receptor BT-R1 expressed in insect cells. *Cell Death Differ. 12*, 1407-1416.

78. Jurat-Fuentes, J. L., and Adang, M. J. (2006) The *Heliothis virescens* cadherin protein expressed in Drosophila S2 cells functions as a receptor for *Bacillus thuringiensis* Cry1A but not Cry1Fa toxins, *Biochem. 45*, 9688-9695.
79. Hua, G., Jurat-Fuentes, J. L., and Adang, M. J. (2004) Bt-R1a Extracellular Cadherin Repeat 12 Mediates *Bacillus thuringiensis* Cry1Ab Binding and Cytotoxicity, *J. Biol. Chem. 279*, 28051-28056.
80. Nagamatsu, Y., Toda, S., Koike, T., Miyoshi, Y., Shigematsu, S., and M, K. (1998) Cloning, sequencing, and expression of the *Bombyx mori* receptor for *Bacillus thuringiensis* insecticidal CryIA(a) toxin, *Biosci. Biotechnol. Biochem. 62*, 727-734.
81. Tsuda Y, N. F., Hashimoto K, Ikawa S, Matsuura C, Fukada T, Sugimoto K, Himeno M. (2003) Cytotoxic activity of *Bacillus thuringiensis* Cry proteins on mammalian cells transfected with cadherin-like Cry receptor gene of *Bombyx mori* (silkworm), *Biochem. J. 1*, 697-703.
82. Hua, G., Jurat-Fuentes, J. L., and Adang, M. J. (2004) Bt-R1a Extracellular Cadherin Repeat 12 Mediates *Bacillus thuringiensis* Cry1Ab Binding and Cytotoxicity, *J. Biol. Chem. 279*, 28051-28056.
83. Soberon, M., Pardo-Lopez, L., Lopez, I., Gomez, I., Tabashnik, B. E., and Bravo, A. (2007) Engineering Modified Bt Toxins to Counter Insect Resistance, *Science 318*, 1640-1642.
84. Gill, S. S., Cowles, E. A., and Francis, V. (1995) Identification, Isolation, and Cloning of a *Bacillus thuringiensis* CryIAc Toxin-binding Protein from the Midgut of the Lepidopteran Insect *Heliothis virescens*, *J. Biol. Chem. 270*, 27277-27282.
85. Agrawal, N., Malhotra, P., and Bhatnagar, R. K. (2002) Interaction of Gene-Cloned and Insect Cell-Expressed Aminopeptidase N of *Spodoptera litura* with Insecticidal Crystal Protein Cry1C, *Appl. Environ. Microbiol. 68*, 4583-4592.
86. Rajagopal R, A. N., Selvapandiyan A, Sivakumar S, Ahmad S, Bhatnagar RK. (2003) Recombinantly expressed isoenzymic aminopeptidases from *Helicoverpa armigera* (American cotton bollworm) midgut display differential interaction with closely related *Bacillus thuringiensis* insecticidal proteins. *Biochem. J. 370*, 971-978.
87. Yaoi, K., Kadotani, T., Kuwana, H., Shinkawa, A., Takahashi, T., Iwahana, H., and Sato, R. (1997) Aminopeptidase N from *Bombyx mori* as a candidate for the receptor of *Bacillus thuringiensis* Cry1Aa toxin, *Eur. J. Biochem. 246*, 652 - 657.
88. Garner, K., Hiremath, S., Lehtoma, K., and Valaitis, A. (1999) Cloning and complete sequence characterization of two gypsy moth aminopeptidase-N cDNAs, including the receptor for *Bacillus thuringiensis* Cry1Ac toxin, *Insect Biochem. Mol. Biol. 29*, 527 - 535.
89. Nakanishi, K., Yaoi, K., Nagino, Y., Hara, H., Kitami, M., Atsumi, S., Miura, N., and Sato, R. (2002) Aminopeptidase N isoforms from the midgut of *Bombyx mori* and *Plutella xylostella* their classification and the factors that determine their binding specificity to *Bacillus thuringiensis* Cry1A toxin, *FEBS Lett. 519*, 215-220.
90. Pigott, C. R., and Ellar, D. J. (2007) Role of Receptors in *Bacillus thuringiensis* Crystal Toxin Activity, *Microbiol. Mol. Biol. Rev. 71*, 255-281.
91. Masson, L., Lu, Y.-j., Mazza, A., Brousseau, R., and Adang, M. J. (1995) The CryIA(c) Receptor Purified from *Manduca sexta* Displays Multiple Specificities, *J. Biol. Chem. 270*, 20309-20315.

92. Cooper MA, C. J., Travis ER, Williams DH, Ellar DJ. (1998) *Bacillus thuringiensis* Cry1Ac toxin interaction with *Manduca sexta* aminopeptidase N in a model membrane environment, *Biochem. J. 333*, 677-683.
93. Herrero, S., Gechev, T., Bakker, P., Moar, W., and de Maagd, R. (2005) *Bacillus thuringiensis* Cry1Ca-resistant *Spodoptera exigua* lacks expression of one of four Aminopeptidase N genes, *BMC Genomics 6*, 96.
94. Rajagopal, R., Sivakumar, S., Agrawal, N., Malhotra, P., and Bhatnagar, R. K. (2002) Silencing of midgut aminopeptidase N of *Spodoptera litura* by double-stranded RNA establishes its role as *Bacillus thuringiensis* toxin receptor, *J. Biol. Chem. 277*, 46849 - 46851.
95. Gill, M., and Ellar, D. (2002) Transgenic Drosophila reveals a functional in vivo receptor for the *Bacillus thuringiensis* toxin Cry1Ac1, *Insect Mol. Biol. 11*, 619 - 625.
96. Bravo, A., Gómez, I., Conde, J., Muñoz-Garay, C., Sánchez, J., Miranda, R., Zhuang, M., Gill, S. S., and Soberón, M. (2004) Oligomerization triggers binding of a *Bacillus thuringiensis* Cry1Ab pore-forming toxin to aminopeptidase N receptor leading to insertion into membrane microdomains, *Biochi. Biophys. Acta 1667*, 38-46.
97. Lorence, A., Darzon, A., and Bravo, A. (1997) Aminopeptidase dependent pore formation of *Bacillus thuringiensis* Cry1Ac toxin on *Trichoplusia ni* membranes, *FEBS Lett. 414*, 303 - 307.
98. Jurat-Fuentes, J. L., Gould, F. L., and Adang, M. J. (2002) Altered Glycosylation of 63- and 68-Kilodalton Microvillar Proteins in *Heliothis virescens* Correlates with Reduced Cry1 Toxin Binding, Decreased Pore Formation, and Increased Resistance to *Bacillus thuringiensis* Cry1 Toxins, *Appl. Environ. Microbiol. 68*, 5711-5717.
99. McNall, R. J., and Adang, M. J. (2003) Identification of novel Bacillus thuringiensis Cry1Ac binding proteins in *Manduca sexta* midgut through proteomic analysis, *Insect Biochem. Mol. Biol. 33*, 999-1010.
100. Sarkar, A., Hess, D., Mondal, H. A., Banerjee, S., Sharma, H. C., and Das, S. (2009) Homodimeric Alkaline Phosphatase Located at *Helicoverpa armigera* Midgut, a Putative Receptor of Cry1Ac Contains α-GalNAc in Terminal Glycan Structure as Interactive Epitope, *J. Proteome Res. 8*, 1838-1848.
101. Fernandez, L. E., Aimanova, K. G., Gill, S. S., Bravo, A., and Soberon, M. (2006) A GPI-anchored alkaline phosphatase is a functional midgut receptor of Cry11Aa toxin in *Aedes aegypti* larvae, *Biochem. J. 394*, 77-84.
102. Bayyareddy, K., Andacht, T. M., Abdullah, M. A., and Adang, M. J. (2009) Proteomic identification of *Bacillus thuringiensis* subsp. israelensis toxin Cry4Ba binding proteins in midgut membranes from *Aedes* (Stegomyia) *aegypti* Linnaeus (Diptera, Culicidae) larvae, *Insect Biochem. Mol. Biol. 39*, 279-286.
103. Hua, G., Zhang, R., Bayyareddy, K., and Adang, M. J. (2009) *Anopheles gambiae* alkaline phosphatase is a functional receptor of *Bacillus thuringiensis* jegathesan Cry11Ba toxin, *Biochem. 48*, 9785-9793.
104. Valaitis, P., Jenkins, L., Lee, K., Dean, H., and Garner, J. (2001) Isolation and partial characterization of gypsy moth BTR-270, an anionic brush border membrane glycoconjugate that binds *Bacillus thuringiensis* Cry1A toxins with high affinity, *Arch. Insect Biochem. Physiol. 46*, 186-200.

105. Sangadala, S., Walters, F. S., English, L. H., and Adang, M. J. (1994) A mixture of *Manduca sexta* aminopeptidase and phosphatase enhances *Bacillus thuringiensis* insecticidal CryIA(c) toxin binding and 86Rb(+)- K+ efflux in vitro, *J. Biol. Chem. 269*, 10088-10092.
106. Valaitis, A. P. (1995) Gypsy moth midgut proteinases: Purification and characterization of luminal trypsin, elastase and the brush border membrane leucine aminopeptidase, *Insect Biochem. Mol. Biol. 25*, 139-149.
107. Bravo, A., Miranda, R., Gomez, I., and Soberon, M. (2002) Pore formation activity of Cry1Ab toxin from *Bacillus thuringiensis* in an improved membrane vesicle preparation from *Manduca sexta* midgut cell microvilli, *Biochim. Biophys. Acta 1562*, 63-69.
108. Tabashnik, B. E., Unnithan, G. C., Masson, L., Crowder, D. W., Li, X., and Carriere, Y. (2009) Asymmetrical cross-resistance between *Bacillus thuringiensis* toxins Cry1Ac and Cry2Ab in pink bollworm, *Proc. Natl. Acad. Sci. USA 106*, 11889-11894.
109. Jenkins, J. L., Lee, M. K., Sangadala, S., Adang, M. J., and Dean, D. H. (1999) Binding of *Bacillus thuringiensis* Cry1Ac toxin to *Manduca sexta* aminopeptidase-N receptor is not directly related to toxicity, *FEBS Lett. 462*, 373-376.

ANEXO I

Publicación derivada directamente de este proyecto.

Role of alkaline phosphatase from *Manduca sexta* in the mechanism of action of *Bacillus thuringiensis* Cry1Ab toxin.

Arenas, I., Bravo, A., Soberón, M. and Gómez, I.

Journal of Biological Chemistry. (2010). 285 (17):12497-503.

THE JOURNAL OF BIOLOGICAL CHEMISTRY VOL. 285, NO. 17, pp. 12497–12503, April 23, 2010

Role of Alkaline Phosphatase from *Manduca sexta* in the Mechanism of Action of *Bacillus thuringiensis* Cry1Ab Toxin*

Received for publication, November 14, 2009, and in revised form, January 14, 2010 Published, JBC Papers in Press, February 22, 2010, DOI 10.1074/jbc.M109.085266

Iván Arenas, Alejandra Bravo, Mario Soberón, and Isabel Gómez[1]

From the Departamento de Microbiología Molecular, Instituto de Biotecnología, Universidad Nacional Autónoma de México, Cuernavaca, Morelos 62250, México

Cry toxins produced by *Bacillus thuringiensis* have been recognized as pore-forming toxins whose primary action is to lyse midgut epithelial cells in their target insect. In the case of the Cry1A toxins, a prepore oligomeric intermediate is formed after interaction with cadherin receptor. The Cry1A oligomer then interacts with glycosylphosphatidylinositol-anchored receptors. Two *Manduca sexta* glycosylphosphatidylinositol-anchored proteins, aminopeptidase (APN) and alkaline phosphatase (ALP), have been shown to bind Cry1Ab, although their role in toxicity remains to be determined. Detection of Cry1Ab binding proteins by ligand blot assay revealed that ALP is preferentially expressed earlier during insect development, because it was found in the first larval instars, whereas APN is induced later after the third larval instar. The binding of Cry1Ab oligomer to pure preparations of APN and ALP showed that this toxin structure interacts with both receptors with high affinity (apparent K_d = 0.6 nM), whereas the monomer showed weaker binding (apparent K_d = 101.6 and 267.3 nM for APN and ALP, respectively). Several Cry1Ab nontoxic mutants located in the exposed loop 2 of domain II or in β-16 of domain III were affected in binding to APN and ALP, depending on their oligomeric state. In particular monomers of the nontoxic domain III, the L511A mutant did not bind ALP but retained APN binding, suggesting that initial interaction with ALP is critical for toxicity. Our data suggest that APN and ALP fulfill two roles. First APN and ALP are initial receptors promoting the localization of toxin monomers in the midgut microvilli before interaction with cadherin. Then APN and ALP function as secondary receptors mediating oligomer insertion into the membrane. However, the expression pattern of these receptors and the phenotype of L511A mutant suggest that ALP may have a predominant role in toxin action because Cry toxins are highly effective against the neonate larvae that is the target for pest control programs.

The Cry toxins produced by *Bacillus thuringiensis* are used worldwide as effective biological control agents for many species of insects including agricultural and forest pests and several vectors of human and animal diseases. Its insecticidal property results from crystalline inclusions produced during sporulation that are formed by δ-endotoxins known as Cry toxins (1).

The Cry protein family is composed of more than 54 groups, among which the three-domain Cry family forms the major group, having members that show toxicity to different insect orders and to nematodes. The crystal structure has been solved for six three-domain Cry toxins and one protoxin that display different insect specificities (2). The activated Cry toxins are globular molecules consisting of a bundle of seven α-helices (domain I), a three-β-sheet prism (domain II), and a β-sandwich (domain III) (3, 4). The N-terminal domain I is involved in oligomer formation, membrane insertion, and pore formation (5–8). Domain II and III are involved in the recognition and binding interaction with receptors in midgut cells (9–11).

The mode of action of Cry toxins has been extensively studied in lepidopteran insects and to some extent in coleopteran, dipteran, and nematodes. In the case of lepidopteran insects, a sequential binding of Cry1A toxins with at least two receptor molecules located in the midgut epithelium cells was proposed that resulted in toxin insertion into the membrane, pore formation, and cell death (12, 13). Susceptible larvae ingest Cry1A crystals formed of 130-kDa protoxins that after solubilization in the gut lumen are subject to proteolysis by midgut proteases, resulting in a 60-kDa toxic fragment composed of the three-domain structure described above. Cry1A monomers then bind to the primary receptor that has been identified in several species as a cadherin protein that is located in the microvilli of columnar midgut cells. This interaction provokes a conformational change of the toxin that facilitates further proteolytic cleavage of the domain I N-terminal helix α-1, resulting in toxin oligomerization (14, 15). In favor of this model, engineered modified Cry1Ab and Cry1Ac toxins lacking helix α-1 have been shown to retain toxicity to resistant insects that have mutations affecting the cadherin gene (16). The oligomer gains binding affinity to a second receptor that is anchored to the membrane by GPI[2] and located in lipid rafts (13). Two proteins have been identified as secondary receptors, APN and ALP (17). Binding of the oligomeric toxin to the GPI-anchored receptors results in the insertion of the oligomer into the membrane and formation of pores, resulting in osmotic shock and cell death (13, 18).

Although APN was the first Cry1Ac-binding molecule identified in *Manduca sexta* (19, 20), its role as functional receptor is

* This work was supported, in whole or in part, by National Institutes of Health Grant 1R01 AI066014. This work was also supported by Consejo Nacional de Ciencia y Tecnología Grants 83135 and 81639, Dirección General de Asuntos del Personal Académico–UNAM Grants IN218608 and IN210208, and United States Department of Agriculture Grant 2207-35607-17780.

[1] To whom correspondence should be addressed. Tel./Fax: 52-777-3291624; E-mail: isabelg@ibt.unam.mx.

[2] The abbreviations used are: GPI, glycosylphosphatidylinositol; APN, aminopeptidase-N; ALP, alkaline phosphatase; BBMV, brush border membrane vesicles; CHAPS, 3-[(3-cholamidopropyl)dimethylammonio]-1-propanesulfonate; ELISA, enzyme-linked immunosorbent assay; BBMV, brush border membrane vesicle(s); PBS, phosphate-buffered saline; CR, cadherin repeat(s).

still controversial. Incorporation of *M. sexta* APN-1 in black lipid bilayers enhanced the Cry1Aa pore formation activity (21). Also, the transgenic expression of *M. sexta* APN-1 in *Drosophila melanogaster* resulted in sensitivity to Cry1Ac toxin (22). Nevertheless, Cry1Ac mutants in domain III that are affected in binding to APN-1 had a marginal effect on toxicity against *M. sexta* larvae (23). Also, in the case of *Bombyx mori*, it was shown that anti-cadherin antibodies protected detached midgut cells from the toxic effects of Cry1Aa, in contrast to anti-APN antibodies that had no effect on the toxicity of Cry1Aa (24). These apparently contradictory data could be explained if an additional secondary receptor could play the same role as APN in *M. sexta* midgut cells. In this regard, a GPI-anchored ALP was also identified as a binding protein of Cry1Ac toxin in *M. sexta*, although its role as a Cry1A receptor has not been analyzed until now (25, 26).

To determine whether the GPI-anchored ALP could act as a functional receptor of Cry1Ab toxin in *M. sexta*, we compared the binding interaction of monomeric and oligomeric forms of Cry1Ab toxin to pure preparations of both APN and ALP enzymes. Also, we analyzed the binding of Cry1Ab mutants located in regions of domain II and domain III previously characterized as APN-binding epitopes (27, 28). Our data suggest that both APN and ALP are functional receptor molecules that bind the oligomeric structure of Cry1Ab toxin with high affinity, facilitating membrane insertion and pore formation, and we also found that ALP may a have a predominant and more important role in Cry1Ab toxicity at earlier stages of larval development.

EXPERIMENTAL PROCEDURES

M. sexta Midgut BBMV Purification and Solubilization—Larvae of *M. sexta* were from a laboratory colony maintained on an artificial diet. BBMV were prepared from midgut tissue from each of the different larval instar by the magnesium precipitation method (29). The BBMV were centrifuged at 70,000 rpm for 40 min at 4 °C and suspended at 5 mg/ml in 20 mM Tris-HCl pH 8.5 buffer containing 100 mM NaCl, 5 mM EDTA, 1 mM phenylmethylsulfonyl fluoride, and 1% CHAPS for detergent solubilization. After 2 h at 4 °C, the solution was centrifuged at 70,000 rpm for 40 min. Protein content in the supernatant was measured by the DC protein dye method (Bio-Rad) using bovine serum albumin as a standard (Pierce).

Purification of Aminopeptidase-N—The APN protein was purified from fourth instar BBMV. The BBMV proteins that were solubilized with CHAPS as stated above were concentrated by Amicon YM-50 ultrafiltration, and a 2-ml aliquot was applied to a HR 5/10 Mono Q (GE Healthcare) column equilibrated with 20 mM Tris-HCl pH 8.5 buffer containing 2 mM $MgCl_2$, 2 mM KCl (28, 30). The column was eluted with a gradient of NaCl (0.5–1 M) with a flow rate of 1 ml/min for 40 min. Fractions containing APN activity were pooled and concentrated by Amicon YM-50 ultrafiltration. The final sample was analyzed by SDS-PAGE and silver staining using the SilverSNAP II stain kit (Pierce) following the manufacturer's instructions.

Purification of Alkaline Phosphatase—ALP was purified by affinity chromatography using L-histidyl-diazo-benzylphosphonic acid agarose (Sigma) (31, 32). CHAPS-solubilized proteins from BBMV of third instar larvae were concentrated by Amicon YM-30 ultrafiltration, and a 1-ml aliquot was loaded into the column equilibrated with 20 mM Tris-HCl pH 8.5 buffer containing 1 mM $MgCl_2$. After a washing step with the same buffer, ALP was eluted using 0.5 M KH_2PO_4. The final sample was analyzed by SDS-PAGE and silver staining as mentioned above.

Enzyme Assays—APN activity was assayed using L-leucine-*p*-nitroanilide as substrate, and ALP activity was assayed using *p*-nitrophenyl phosphate as substrate (33). Protein content was measured by the DC protein dye method (Bio-Rad) using bovine serum albumin as a standard (Pierce). The initial rate at 405 nm (Ultrospec II spectrophotometer; GE Healthcare) was used to calculate specific enzymatic activity of both enzymes. The absorption coefficient of *p*-nitroanilide used was 9.9×10^{-3} mol l^{-1}. One unit of specific APN activity was defined as the amount of enzyme catalyzing the hydrolysis of 1 μmol of L-leucine-*p*-nitroanilide min^{-1} mg of $protein^{-11}$ at 25 °C. One unit of specific ALP activity was defined as the amount of enzyme producing 1 μmol of nitrophenol min^{-11} mg of $protein^{-11}$ at 25 °C. Nitrophenol concentration was calculated by using a standard curve of 4-nitrophenol in 0.5 mM $MgCl_2$, 100 mM Tris, pH 9.5.

Construction of Cry1Ab Mutants—Substitutions R368A/R369A, F371A, and L511A were produced by site-directed mutagenesis (QuikChange; Stratagene) using the pHT315Ab plasmid harboring the *cry1Ab* gene as template and the corresponding mutagenic primers: R368A/R369A, 5′-CAT TAT CGT CCA CTT TAT ATG CAG CAC CTT TTA ATA TAG GGA TAA ATA ATC-3′; F371A, 5′-CCA CTT TAT ATA GAA GAC CTG CTA ATA TAG GGA TAA ATA ATC-3′; and L511A, 5′-GGC CAG ATT TCA ACC GCG AGA GTA AAT ATT ACT GCA-3′. Automated DNA sequencing at facilities of the Instituto de Biotecnología-Universidad Nacional Autónoma de México verified the single-point mutations. Acrystalliferous *B. thuringiensis* strain 407 was transformed with the recombinant plasmids containing the mutated *cry1Ab* genes as reported (34) and selected in Luria broth at 30 °C supplemented with 10 μg ml^{-1} of erythromycin.

Cry1Ab Toxin Purification—Crystal inclusions of Cry1Ab toxin and their mutants were produced in *B. thuringiensis* strains described above. The cells were grown for 3 days at 30 °C in nutrient broth sporulation medium supplemented with erythromycin at 10 μg ml^{-1}. After complete sporulation, the crystal inclusions were purified using discontinuous sucrose gradients, and the protein concentration was determined by the protein dye method of Bradford (35).

The monomeric toxins were obtained by trypsin activation in a mass ratio of 1:50 (1 h at 37 °C). Phenylmethylsulfonyl fluoride (final concentration, 1 mM) was added to stop proteolysis. The oligomeric Cry1Ab structure was produced by incubation of the crystals for 1 h with cadherin fragment CR7-CR12 (residues Met^{810}–Ala^{1485}) in a mass ratio 1:1 and digestion with midgut juice (5%) for 1 h at 37 °C in extraction buffer (50 mM Na_2CO_3 at pH 10.5, 0.02% mercaptoethanol). Phenylmethylsulfonyl fluoride (1 mM) was added to stop the reaction (36). Purification of monomeric and oligomeric structures of Cry1Ab toxin was

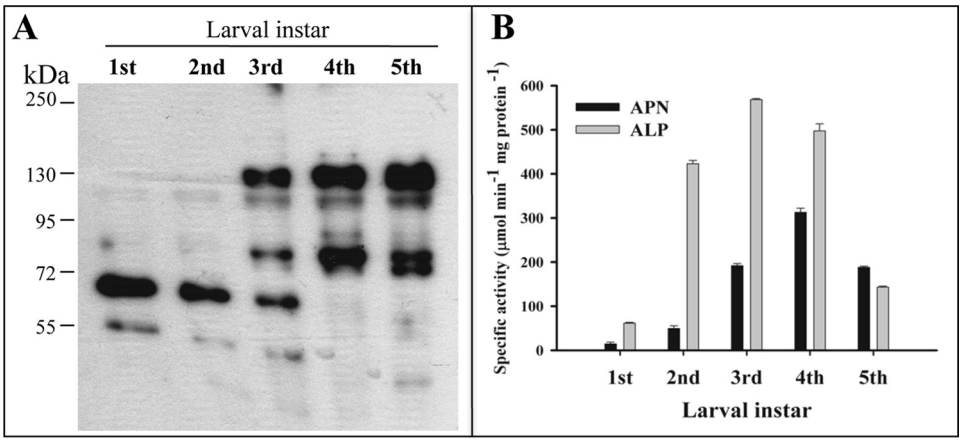

FIGURE 1. **Expression of aminopeptidase N and alkaline phosphatase during larval development.** *A*, ligand blot analysis of biotin-labeled Cry1Ab toxin to BBMV proteins from *M. sexta* larvae isolated from each instar larvae (first through fifth indicated). *B*, specific enzymatic activities of APN (*black bars*) and ALP (*gray bars*) determined in BBMV from each larval instar.

achieved by size exclusion chromatography using a Superdex 200 HR 10/30 column on an AKTA Explorer (GE Healthcare) as reported previously (15).

Western Blots of Cry1Ab Toxin—Fractions of the purified toxin oligomers were separated in SDS-PAGE and transferred onto nitrocellulose membrane. The proteins were detected with polyclonal anti-Cry1Ab (1/80,000; 1 h) and a goat anti-rabbit secondary antibody coupled with horseradish peroxidase (Amersham Biosciences) (1/10,000; 1 h), followed by Super Signal chemiluminescence substrate (Pierce) as indicated by the manufacturer.

Ligand Blot—Cry1Ab toxin was biotinylated using biotinamidocaproate *N*-hydroxysuccinamide ester (Amersham Biosciences) according to the manufacturer's instructions. Samples of 5 μg of BBMV were separated by SDS-PAGE (9%) and transferred to polyvinylidene difluoride; after renaturation and blocking, the blots were incubated for 2 h with 10 nM of biotinylated Cry1Ab toxin in washing buffer (0.05% Tween 20 in PBS) at room temperature. Unbound toxin was removed by washing three times for 10 min in washing buffer, and bound toxin was identified by incubating the blots in PBS containing streptavidin-peroxidasa conjugate (1:5000 in PBS) for 1 h. The excess of streptavidin was removed by washing in three changes of washing buffer, and the membrane-bound complex was visualized by Super Signal chemiluminescence substrate (Pierce) as indicated by the manufacturer.

Toxicity Assays—Bioassays were performed with *M. sexta* neonate larvae by a surface contamination method. Toxin solution was poured on the diet surface and allowed to dry. Neonate *M. sexta* larvae were placed on the dried surface, and the mortality was monitored after 7 days. The lethal concentration required to kill 50% of the larvae (LC_{50}) was estimated by Probit analysis (Polo-PC LeOra Software).

ELISA Binding Assays—One ng/well of purified APN or ALP was suspended in PBS buffer and used to coat a 96-well ELISA plate. After overnight incubation at 4 °C, 200 μl of PBS containing 2% skim milk was added to each well and incubated at 37 °C for 2 h. Then each well was washed three times with PBS buffer followed by incubation with different Cry1Ab toxin dilutions in PBS buffer (monomeric or oligomeric structures) at 37 °C. Excess toxin was removed by washing, and each well was incubated with anti-Cry1Ab antibody (1/10,000) for 1 h at 37 °C. After washing, peroxidase-conjugated rabbit antibody was added and incubated again at 37 °C for 1 h. After washing, substrate solution was added, and absorbance at 490 nm was measured. The data were analyzed using SigmaPlot version 10.

RESULTS

Expression of Aminopeptidase and Alkaline Phosphatase Proteins in M. sexta Larvae—The expression of both APN and ALP in the different states of larval development was determined by ligand blot assays using biotinylated Cry1Ab toxin. The BBMV were isolated from midgut tissue of insects at different larval instar. Fig. 1*A* shows that Cry1Ab bound preferentially to a 65-kDa protein, previously identified as ALP (25) in BBMV isolated from first and second instar larvae. In contrast, these assays revealed that at the latter stages of larval development, such as the fourth and fifth instar, only the 120-kDa corresponding to APN protein but not the 65-kDa band was observed. However, it is important to mention that both proteins, APN and ALP, are present during all instar stages, although at different levels. Overexposure of the ligand blots revealed detectable low levels of APN in the first and second instar larvae and detectable low levels of ALP in the fourth and fifth instar larvae (data not shown). APN and ALP specific activities were determined in BBMV obtained from larvae in the different instars showing higher ALP enzymatic activity than APN during the first instars, whereas APN activity increased after the third instar, showing higher APN activities than ALP in the fifth instar (Fig. 1*B*).

Analysis of Binding of Cry1Ab Oligomer and Monomer to APN and ALP—To determine the role of *M. sexta* ALP in Cry1Ab toxicity, we decided to analyze the binding of Cry1Ab oligomer to pure ALP preparations and compare it with the binding to pure APN samples. APN was purified from fourth instar larvae to avoid ALP contamination, and ALP was purified from third instar larvae because first and second instar larvae are too small. The BBMV were solubilized with detergent, and APN and ALP were purified by ion exchange and affinity chromatography, respectively, as described under "Experimental Procedures." The purified fractions containing only APN or ALP activity were examined by SDS-PAGE and silver staining to assess their quality (Fig. 2, *lanes 1* and *2*). APN appears as a single band at ~120 kDa, whereas ALP appeared as two bands of ~65 and 60 kDa. The purity of both receptors was further examined by a Cry1Ab toxin ligand blot showing that both the 120-kDa APN and the 65-kDa ALP bound Cry1Ab (Fig. 2, *lanes 3* and *4*). Tables 1 and 2 show the results of representative purification experiments of APN and ALP, respectively. These data

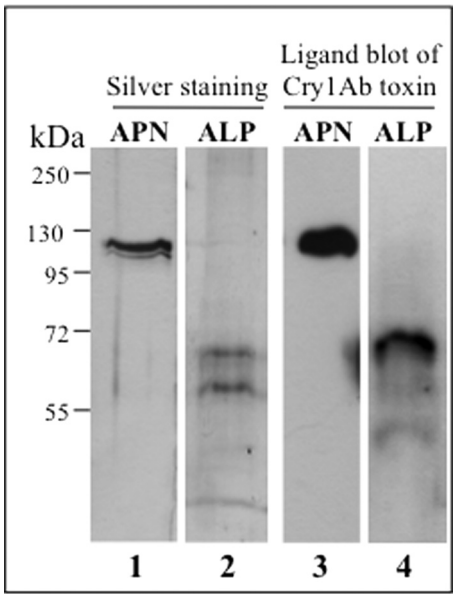

FIGURE 2. **Purification of *M. sexta* APN and ALP proteins.** Silver stain 10% SDS-PAGE of APN (*lane 1*) and ALP (*lane 2*) pure fractions from Mono Q (Table 1) and affinity chromatography (Table 2), respectively, are shown. Ligand blots with biotin-labeled Cry1Ab toxin of APN (*lane 3*) and ALP (*lane 4*) fractions are shown. Molecular mass markers are shown at the *left* of the figure.

TABLE 1

Purification of aminopeptidase-N from midgut brush border membrane vesicles of fourth instar *M. sexta* larvae

Fraction	Total activity	Total protein	Specific activity	Recovery
	units	*mg*	*units/mg*	*%*
BBMV	87.3	20	4.3	100
BBMV/CHAPS	49.3	5.4	9.1	56.4
Mono Q[a]	16.6	0.212	78.2	19.01

[a] Fig. 2 (*lane 1*) shows the protein profile of purified APN.

TABLE 2

Purification of alkaline phosphatase from midgut brush border membrane vesicles of third instar *M. sexta* larvae

Fraction	Total activity	Total protein	Specific activity	Recovery
	units	*mg*	*units/mg*	*%*
BBMV	35.6	10	3.56	100
BBMV/CHAPS	21.6	4.5	4.8	60.6
Affinity column[a]	1.135	0.1	11.35	3.18

[a] Fig. 2 (*lane 2*) shows the protein profile of purified ALP.

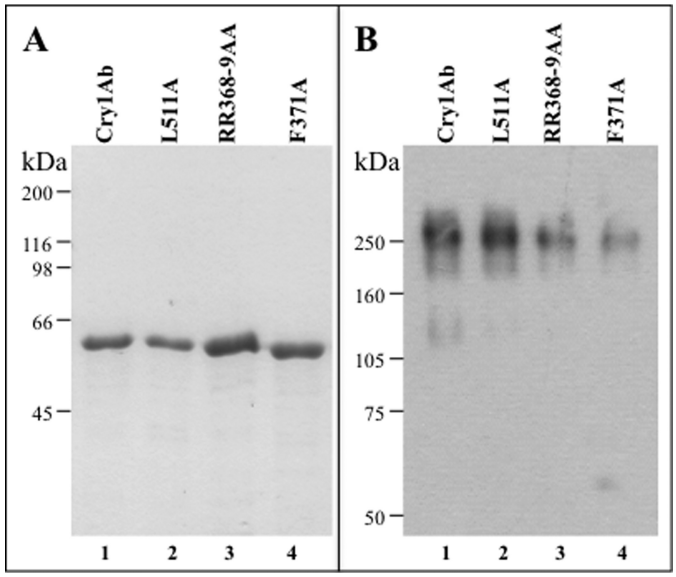

FIGURE 3. **Cry1Ab domain II loop 2 and domain III mutants are structurally stable.** *A*, SDS-PAGE electrophoresis pattern of trypsin activated Cry1Ab (*lane 1*), L511A (*lane 2*), R368A/R369A (*lane 3*), and F371A (*lane 4*) toxins. *B*, Western blot of pure oligomer samples obtained after size exclusion chromatography of toxin samples activated in the presence of cadherin fragment CR7-CR12. Cry1Ab (*lane 1*), L511A (*lane 2*), R368A/R369A (*lane 3*), and F371A (*lane 4*) toxins are shown. Molecular mass markers are shown at the *left* of the figure.

also indicate that the 65- and 120-kDa bands previously identified by Cry1Ab binding in BBMV samples (Fig. 1*A*) correspond to ALP and APN proteins, respectively. The identity of the 65-kDa band as ALP protein was confirmed by mass spectrometry analysis (data not shown).

We then analyzed the interaction of the two Cry1Ab structures, corresponding to the oligomeric or monomeric Cry1Ab structures, with both receptors, APN or ALP. The Cry1Ab oligomers were purified by size exclusion chromatography from Cry1Ab protoxin samples activated with *M. sexta* midgut juice in the presence of a cadherin fragment that contains cadherin repeats (CR) 7–12, whereas monomeric Cry1Ab was prepared by activating Cry1Ab protoxin with trypsin as described under "Experimental Procedures." Fig. 3 shows the Cry1Ab trypsin-activated 60-kDa monomer and the 250-kDa oligomer after purification (Fig. 3, *A* and *B*, respectively, *lanes 1*).

Specific binding of Cry1Ab oligomer to both receptors, APN and ALP, proved to be concentration-dependent and saturable. Oligomer binding to APN was saturated at 1 nM (Fig. 4*A*), whereas saturable binding of Cry1Ab monomer was observed with a much higher toxin concentration, 400 nM (Fig. 4*B*). Determination of binding parameters indicated that the oligomer structure bound APN and ALP with an apparent binding affinity (K_d) in the range of 0.5–0.6 nM, whereas the monomer bound APN or ALP molecules with an apparent binding affinity of 100 and 260 nM, respectively. These results suggest that the Cry1Ab oligomeric structure gains at least 200-fold higher affinity to both APN and ALP proteins in comparison with the Cry1Ab monomeric structure.

Cry1Ab-binding Regions Involved in APN and ALP Interaction—Domain II loop 2 and 3 mutants were previously shown to be affected in APN binding (27, 37, 38). Also, a scFv antibody that bound the domain III β16-β22 region competed the binding of Cry1Ab to APN (10). However, the role of these binding regions in the interaction of Cry1Ab oligomer with APN has not been analyzed, nor whether the same regions are involved in the interaction with ALP. To gain insight on the role of these Cry1Ab epitopes in the binding interaction of Cry1Ab oligomer with both APN and ALP, we characterized the binding of monomeric and oligomeric structures of three Cry1Ab mutants to APN and ALP. Two mutants were located in loop 2 of domain II (R368A/R369A and F371A), and the third mutant was located in the β-16 of domain III (L511A). Toxicity assays showed that the three mutants were not toxic to *M. sexta* (Table 3). The protoxins of the three Cry1Ab mutants characterized produced a 60-kDa protein after trypsin activation, indicating no major structural constraints for these mutants (Fig. 3*A*). Although

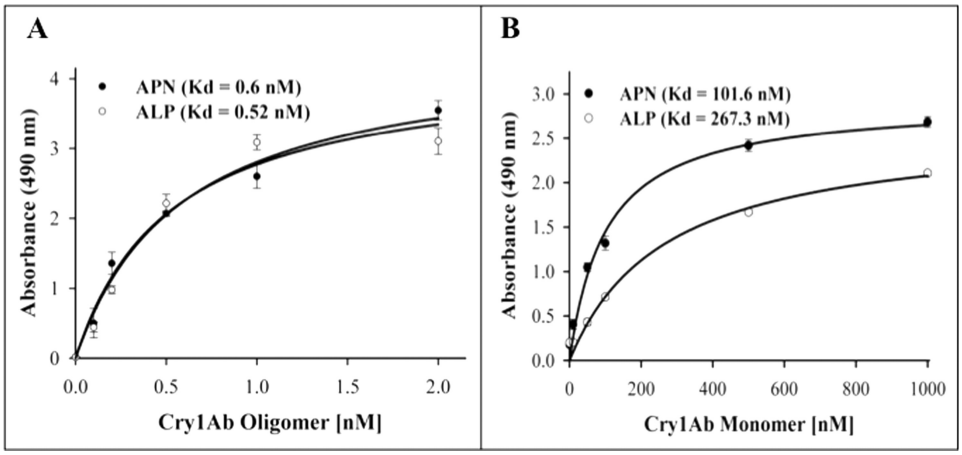

FIGURE 4. **Binding of Cry1Ab oligomer and monomer structure to APN and ALP proteins.** The purified APN (Table 1) and ALP (Table 2) were immobilized on ELISA plates and incubated with Cry1Ab oligomer (*A*, 0–2 nM) or monomer (*B*, 0–1000 nM). K_d values obtained by Scatchard analysis are indicated inside the graphs.

TABLE 3
Toxicity of Cry1Ab and mutant toxins to *M. sexta* larvae

Toxin	LC_{50}[a]	Relative toxicity[b]
	ng/cm²	
Cry1Ab	3.9 (2.2–6.6)	1
R368A/R369A	>1000	>260
F371A	>1000	>260
L511A	>1000	>260

[a] LC_{50} indicates the concentration required to kill 50% of the tested larvae. The numbers in parentheses are 95% confidence limits.
[b] LC_{50} mutant/LC_{50} wild type.

the loop 2 mutants produced lower amounts of oligomer after proteolytic activation in the presence of the cadherin fragment CR7-CR12, enough oligomer was obtained to perform binding assays (Fig. 3*B*).

ELISA binding assays of monomeric (25 nM) or oligomeric (0.1 nM) structures of Cry1Ab mutants to APN and ALP were performed under nonsaturated conditions. These studies showed that the monomeric structure of the L511A mutant, located in domain III, was severely affected in binding to ALP protein (Fig. 5*A*). In contrast, it is clear in this figure that this mutant retained significant binding to APN (Fig. 5*A*). Fig. 5*A* also shows that monomeric structures of the domain II loop 2 mutants, F371A and R368A/R369A, were not affected in their binding interaction with both APN and ALP. The binding of oligomeric structures of the Cry1Ab mutants to both APN and ALP revealed that domain II loop 2 mutations are affected on binding to both receptors, whereas the domain III mutant L511A had just a marginal effect in its interaction with both receptors (Fig. 5*B*).

DISCUSSION

In the pore forming model describing the mode of action of Cry1Ab toxin (33), binding to cadherin receptor results in a conformational change that allows further toxin proteolysis, this cleavage induces the formation of a toxin prepore structure. Then the GPI-anchored receptors, APN and ALP, have been proposed to bind the prepore oligomeric structure and drive it into lipid rafts where pore formation takes place (12, 13, 33, 39). The role of the prepore oligomeric structure in Cry1A toxicity was demonstrated by isolation of single-point mutations in helix α-3, which were affected in oligomerization and were severally affected in toxicity. Also, it was reported that Cry1Ab mutants in helix α-4 were affected in pore formation activity and were inactive. The mutants in helix α-4 are dominant-negative inhibitors of Cry1Ab toxin (5, 40).

We previously reported that the Cry1Ab oligomeric structure bound a protein extract enriched in *M. sexta* APN activity with an apparent binding affinity of 1 nM, in contrast with the monomeric toxin that bound this protein extract with 160 nM apparent binding affinity. The protein extract was enriched in GPI-anchored proteins because it was prepared by treatment of *M. sexta* BBMV with phospholipase-C that cleaves out GPI-anchored proteins (13). Nevertheless, we did not rule out the contribution of GPI-anchored ALP to the binding of the Cry1Ab oligomer to that protein extract. To directly determine the properties of toxin receptor binding interaction, the GPI-anchored APN and ALP receptors were purified, and their interaction with Cry1Ab oligomeric or monomeric structures was analyzed. We found that Cry1Ab oligomer bound to APN and ALP from *M. sexta* with similar high affinities, suggesting that both proteins could act as receptors for Cry1Ab toxin. These results suggest that both APN and ALP could have a similar role in the binding of Cry1Ab prepore oligomer and in mediating toxicity. However, it was also reported that APN and ALP are differentially expressed within *M. sexta* gut, because APN was preferentially expressed in the posterior part of the gut, whereas ALP was expressed at similar levels through out the gut (41). Interestingly, we show in this work that both APN and ALP have also a differential expression through larval development. ALP was expressed at higher levels than APN in the two first larval instars, whereas APN was the predominant GPI-anchored Cry1Ab binding protein in the fourth and fifth instar (Fig. 1*A*). The identities of both the 65- and 120-kDa proteins as ALP and APN were confirmed by purification of these proteins and determination of their enzymatic activities (Tables 1 and 2). In addition the 65-kDa band was confirmed to be ALP by mass spectrometry analysis (data not shown). Overall, these data suggest that ALP could have a predominant role in toxicity because toxicity bioassays are performed with neonate larvae where ALP is highly abundant and present in the anterior region of the gut. The susceptibility of *M. sexta* larvae to Cry1Ab is greatly diminished through larval development, showing lower susceptibility to this toxin in higher instars (42), and these data correlate with the developmental expression pattern of ALP protein (Fig. 1*A*).

We characterized two Cry1Ab mutants, located in domain II loop 2 (R368A/R369A and F371A), with respect to their binding interaction with APN and ALP. Accordingly, we found that the monomeric structures of these nontoxic mutants were not affected in their binding interaction with APN or ALP. How-

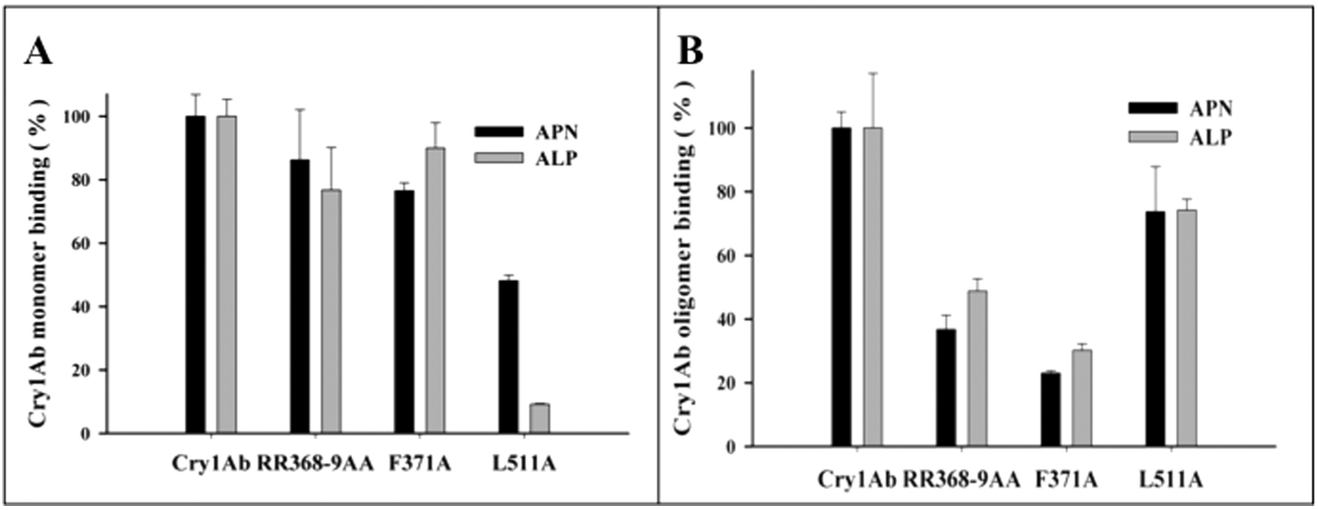

FIGURE 5. **Binding analysis of Cry1Ab and loop 2 and domain III mutants to APN or ALP.** *A*, ELISA binding assays of 25 nM of monomeric structures of Cry1Ab and mutant toxins to APN (*black bars*) or ALP (*gray bars*). *B*, ELISA binding assays of 0.1 nM of oligomeric structures of Cry1Ab and mutant toxins to APN (*black bars*) or ALP (*gray bars*). Standard deviations from three replica plates were obtained.

ever, these mutations had an important effect on the binding of their corresponding oligomeric structure to APN or ALP. These results show that domain II loop 2 of Cry1Ab oligomer is an important epitope in the interaction with APN and ALP receptors. It was previously reported that F371A mutation did not affect APN binding, but these studies were done only with the monomeric structure of the mutant toxin (37). Also it was proposed that this mutant was affected in membrane insertion, and this effect was used as an argument to say that domain II loop 2 may be participating in triggering membrane insertion (43). Here we show that F371A mutation greatly affects binding of the oligomeric structure to both APN and ALP. Because it was shown that binding of the Cry1A oligomer to APN facilitates insertion of the toxin into the membrane (18), the results presented here suggest that the previously observed effect of F371A mutation in regard to its membrane insertion is due to the severe effects of this mutation on the binding interaction of the oligomeric structure with APN and ALP.

Recently we proposed that APN fulfills two roles in the mode of action of Cry1Ab: first as a low affinity and highly abundant binding site that locates monomeric toxin in the vicinity of the microvilli before cadherin binding and second as a secondary high affinity receptor that mediates insertion of the oligomeric Cry1Ab structure into the membrane, suggesting a ping-pong binding mechanism (38). Interestingly, characterization of nontoxic domain II loop 3 mutants revealed an opposite phenotype when compared with the loop 2 mutations regarding the binding of monomeric or oligomeric Cry1Ab to APN. Domain II loop 3 mutants affected monomer binding to APN in contrast to the binding of the oligomeric structure that was not affected (38). Here we show that the monomeric structures of domain II loop 2 mutations had no effect on their binding to APN or ALP, whereas oligomer binding to both GPI-anchored molecules was greatly affected. These results show that domain II loops 2 and 3 mediate different steps of Cry1Ab interaction with GPI-anchored receptors depending on their oligomeric state.

In relation to the interaction of domain III with APN and ALP, previous work identified domain III β-16 of Cry1Ab as an important binding determinant to *M. sexta* APN (10). The nontoxic L511A mutant is located in this β16, and this mutant was specially affected in its interaction with ALP retaining significant binding to APN (Fig. 5*A*). The severe effect on toxicity shown by L511A mutant indicates an important role for ALP binding in *vivo* and suggests that ALP has a predominant role, in comparison with APN, on Cry1Ab toxicity. Nevertheless, the precise role of both GPI-anchored proteins on Cry1Ab toxicity should be determined in the future; probably toxicity assays of larvae that are specifically silenced by RNA interference for either APN or ALP could help in answering this specific question.[3]

Acknowledgments—We thank Josué Océlotl for isolation of Cry1Ab L511A mutant and Jorge Sánchez and Lizbeth Cabrera for technical assistance.

REFERENCES

1. Schnepf, E., Crickmore, N., Van Rie, J., Lereclus, D., Baum, J., Feitelson, J., Zeigler, D. R., and Dean, D. H. (1998) *Microbiol. Mol. Biol. Rev.* **62,** 775–806
2. Guo, S., Ye, S., Liu, Y., Wei, L., Xue, J., Wu, H., Song, F., Zhang, J., Wu, X., Huang, D., and Rao, Z. (2009) *J. Struct. Biol.* **168,** 259–266
3. de Maagd, R. A., Bravo, A., Berry, C., Crickmore, N., and Schnepf, H. E. (2003) *Annu. Rev. Genet.* **37,** 409–433
4. Bravo, A., Gill, S. S., and Soberón, M. (2007) *Toxicon* **49,** 423–435
5. Jiménez-Juárez, N., Muñoz-Garay, C., Gómez, I., Saab-Rincon, G., Damian-Almazo, J. Y., Gill, S. S., Soberón, M., and Bravo, A. (2007) *J. Biol. Chem.* **282,** 21222–21229
6. Gazit, E., La Rocca, P., Sansom, M. S., and Shai, Y. (1998) *Proc. Natl. Acad. Sci. U.S.A.* **95,** 12289–12294
7. Grochulski, P., Masson, L., Borisova, S., Pusztai-Carey, M., Schwartz, J. L., Brousseau, R., and Cygler, M. (1995) *J. Mol. Biol.* **254,** 447–464
8. Rausell, C., Pardo-López, L., Sánchez, J., Muñoz-Garay, C., Morera, C., Soberón, M., and Bravo, A. (2004) *J. Biol. Chem.* **279,** 55168–55175
9. Herrero, S., González-Cabrera, J., Ferré, J., Bakker, P. L., and de Maagd, R. A. (2004) *Biochem. J.* **384,** 507–513

[3] B. Flores-Escobar, A. Bravo, M. Soberón, and I. Gómez, personal communication.

10. Gómez, I., Arenas, I., Benitez, I., Miranda-Ríos, J., Becerril, B., Grande, R., Almagro, J. C., Bravo, A., and Soberón, M. (2006) *J. Biol. Chem.* **281,** 34032–34039
11. Rajamohan, F., Lee, M. K., and Dean, D. H. (1998) *Prog. Nucleic Acid Res. Mol. Biol.* **60,** 1–27
12. Jurat-Fuentes, J. L., and Adang, M. J. (2006) *J. Invertebr. Pathol.* **92,** 166–171
13. Bravo, A., Gómez, I., Conde, J., Muñoz-Garay, C., Sánchez, J., Miranda, R., Zhuang, M., Gill, S. S., and Soberón, M. (2004) *Biochim. Biophys. Acta* **1667,** 38–46
14. Gómez, I., Pardo-López, L., Muñoz-Garay, C., Fernandez, L. E., Pérez, C., Sánchez, J., Soberón, M., and Bravo, A. (2007) *Peptides* **28,** 169–173
15. Gómez, I., Sánchez, J., Miranda, R., Bravo, A., and Soberón, M. (2002) *FEBS Lett.* **513,** 242–246
16. Soberón, M., Pardo-López, L., López, I., Gómez, I., Tabashnik, B. E., and Bravo, A. (2007) *Science* **318,** 1640–1642
17. Pigott, C. R., and Ellar, D. J. (2007) *Microbiol. Mol. Biol. Rev.* **71,** 255–281
18. Pardo-López, L., Gómez, I., Rausell, C., Sanchez, J., Soberón, M., and Bravo, A. (2006) *Biochemistry* **45,** 10329–10336
19. Knight, P. J., Crickmore, N., and Ellar, D. J. (1994) *Mol. Microbiol.* **11,** 429–436
20. Sangadala, S., Walters, F. S., English, L. H., and Adang, M. J. (1994) *J. Biol. Chem.* **269,** 10088–10092
21. Schwartz, J. L., Lu, Y. J., Söhnlein, P., Brousseau, R., Laprade, R., Masson, L., and Adang, M. J. (1997) *FEBS Lett.* **412,** 270–276
22. Gill, M., and Ellar, D. (2002) *Insect Mol. Biol.* **11,** 619–625
23. Jenkins, J. L., Lee, M. K., Sangadala, S., Adang, M. J., and Dean, D. H. (1999) *FEBS Lett.* **462,** 373–376
24. You, T. H., Lee, M. K., Jenkins, J. L., Alzate, O., and Dean, D. H. (2008) *BMC Biochem.* **9,** 3
25. McNall, R. J., and Adang, M. J. (2003) *Insect Biochem. Mol. Biol.* **33,** 999–1010
26. Krishnamoorthy, M., Jurat-Fuentes, J. L., McNall, R. J., Andacht, T., and Adang, M. J. (2007) *Insect Biochem. Mol. Biol.* **37,** 189–201
27. Lee, M. K., Rajamohan, F., Jenkins, J. L., Curtiss, A. S., and Dean, D. H. (2000) *Mol. Microbiol.* **38,** 289–298
28. Jenkins, J. L., Lee, M. K., Valaitis, A. P., Curtiss, A., and Dean, D. H. (2000) *J. Biol. Chem.* **275,** 14423–14431
29. Wolfersberger, M. G. (1993) *Arch. Insect Biochem. Physiol.* **24,** 139–147
30. Valaitis, A. P., Lee, M. K., Rajamohan, F., and Dean, D. H. (1995) *Insect Biochem. Mol. Biol.* **25,** 1143–1151
31. Landt, M., Boltz, S. C., and Butler, L. G. (1978) *Biochemistry* **17,** 915–919
32. Asgeirsson, B., Adalbjörnsson, B. V., and Gylfason, G. A. (2007) *Biochim. Biophys. Acta* **1774,** 679–687
33. Bravo, A., Miranda, R., Gómez, I., and Soberón, M. (2002) *Biochim. Biophys. Acta* **1562,** 63–69
34. Lereclus, D., Arantès, O., Chaufaux, J., and Lecadet, M. (1989) *FEMS Microbiol. Lett.* **51,** 211–217
35. Bradford, M. M. (1976) *Anal. Biochem.* **72,** 248–254
36. Pacheco, S., Gómez, I., Gill, S. S., Bravo, A., and Soberón, M. (2009) *Peptides* **30,** 583–588
37. Jenkins, J. L., and Dean, D. H. (2000) in *Genetic Engineering: Principles and Methods* (Setlow, J. K., ed) Vol. 22, pp. 33–54, Plenum Press, New York
38. Pacheco, S., Gómez, I., Arenas, I., Saab-Rincon, G., Rodríguez-Almazán, C., Gill, S. S., Bravo, A., and Soberón, M. (2009) *J. Biol. Chem.* **284,** 32750–32757
39. Zhuang, M., Oltean, D. I., Gómez, I., Pullikuth, A. K., Soberón, M., Bravo, A., and Gill, S. S. (2002) *J. Biol. Chem.* **277,** 13863–13872
40. Rodríguez-Almazán, C., Zavala, L. E., Muñoz-Garay, C., Jiménez-Juárez, N., Pacheco, S., Masson, L., Soberón, M., and Bravo, A. (2009) *PloS One* **4,** e5545
41. Chen, J., Brown, M. R., Hua, G., and Adang, M. J. (2005) *Cell Tissue Res.* **321,** 123–129
42. Griko, N., Zhang, X., Ibrahim, M., Midboe, E. G., and Bulla, L. A., Jr. (2008) *Comp. Biochem. Physiol. B Biochem. Mol. Biol.* **151,** 59–63
43. Nair, M. S., Liu, X. S., and Dean, D. H. (2008) *Biochemistry* **47,** 5814–5822

ANEXO II

Colaboración del estudiante en otros proyectos.

Domain II loop 3 of *Bacillus thuringiensis* Cry1Ab toxin is involved in the "ping-pong" binding mechanism with *Manduca sexta* aminopeptidase N and cadherin receptors.
Pacheco, S., Gómez, I., **Arenas, I**., Saab-rincon, G., Rodriguez-Almazan, C., Gill, S.S., Bravo, A. and Soberón, M.

Journal of Biological Chemistry. (2009). 284, 32750-32757.

Characterization of the mechanism of action of the genetically modified Cry1AbMod toxin that is active against Cry1Ab-resistant insects.
Muños-Garay, C., Portugal, L., Pardo-López, L., Jimenez-Juarez, N., **Arenas, I**., Gómez. I., Sanchez-Lopez, R., Arrollo, R., Holzenburg, A., Savva, C. G., Soberón, M. and Bravo, A.

Biochemical Et Biophysical Acta-Biomembranes. (2009). 1788, 2229-2237.

Employing phage display to study the mode of action of *Bacillus thuringiensis* Cry toxins.
Fernandez, L.E., Gómez, I., Pacheco, S., **Arenas, I**., Gill, S. S., Bravo, A. and Soberón, M.

Peptides. (2008).29, 324-329.

Specific epitopes of domain II and III of *Bacillus thuringiensis* Cry1Ab toxin involved in the sequential interaction with cadherin and aminopeptidase-N receptors in *Manduca sexta*.
Gómez, I., **Arenas, I**., Benítez, I., Miranda-Ríos, J., Becerril, B., Grande, R., Almagro, J.C., Bravo, A. and Soberón, M.

Journal of Biological Chemistry. (2006). 281, 34032-34039.

THE JOURNAL OF BIOLOGICAL CHEMISTRY VOL. 284, NO. 47, pp. 32750–32757, November 20, 2009

Domain II Loop 3 of *Bacillus thuringiensis* Cry1Ab Toxin Is Involved in a "Ping Pong" Binding Mechanism with *Manduca sexta* Aminopeptidase-N and Cadherin Receptors*

Received for publication, May 25, 2009, and in revised form, September 22, 2009 Published, JBC Papers in Press, October 6, 2009, DOI 10.1074/jbc.M109.024968

Sabino Pacheco[‡], Isabel Gómez[‡], Ivan Arenas[‡], Gloria Saab-Rincon[‡], Claudia Rodríguez-Almazán[‡], Sarjeet S. Gill[§], Alejandra Bravo[‡], and Mario Soberón[‡1]

From the [‡]Instituto de Biotecnología, Universidad Nacional Autónoma de México, Apdo. Postal 510-3, Cuernavaca 62250, Morelos, Mexico and the [§]Department of Cell Biology and Neuroscience, University of California, Riverside, California 92506

Bacillus thuringiensis **Cry toxins are used worldwide as insecticides in agriculture, in forestry, and in the control of disease transmission vectors. In the lepidopteran *Manduca sexta*, cadherin (Bt-R_1) and aminopeptidase-N (APN) function as Cry1A toxin receptors. The interaction with Bt-R_1 promotes cleavage of the amino-terminal end, including helix α-1 and formation of prepore oligomer that binds to APN, leading to membrane insertion and pore formation. Loops of domain II of Cry1Ab toxin are involved in receptor interaction. Here we show that Cry1Ab mutants located in domain II loop 3 are affected in binding to both receptors and toxicity against *Manduca sexta* larvae. Interaction with both receptors depends on the oligomeric state of the toxin. Monomers of loop 3 mutants were affected in binding to APN and to a cadherin fragment corresponding to cadherin repeat 12 but not with a fragment comprising cadherin repeats 7–12. In contrast, the oligomers of loop 3 mutants were affected in binding to both Bt-R_1 fragments but not to APN. Toxicity assays showed that either monomeric or oligomeric structures of Cry1Ab loop 3 mutations were severely affected in insecticidal activity. These data suggest that loop 3 is differentially involved in the binding with both receptor molecules, depending on the oligomeric state of the toxin and also that possibly a "ping pong" binding mechanism with both receptors is involved in toxin action.**

Bacillus thuringiensis is a bacterium that produces crystalline inclusions formed by insecticidal proteins, called Cry toxins, during the sporulation phase of growth. Cry toxins are toxic to different insect orders as well as to other invertebrates, such as nematodes, mites, and protozoa (1). Cry toxins have been used worldwide in the control of insect pests in agriculture, either as transgenic crops or as spray formulations.

The molecular mechanism proposed to describe the action of Cry1A toxins, which are active against different lepidopteran insect species, involves several steps. After larval ingestion of the crystalline inclusions, these are solubilized in midgut lumen and activated by proteases releasing a toxic 65-kDa fragment that binds, in a sequential manner, with at least two receptors located in midgut microvilli. The first interaction occurs with cadherin protein (Bt-R_1[2] in the case of *Manduca sexta*). This interaction promotes further proteolytic processing of the N-terminal end, including helix α-1 of the toxin, resulting in the formation of a prepore oligomeric structure (2). The oligomer has higher affinity to secondary receptors, which are anchored by glycosylphosphatidylinositol, such as aminopeptidase-N (APN) or alkaline phosphatase in the case of *M. sexta* or *Heliothis virescens*, respectively (3, 4). Glycosylphosphatidylinositol-anchored receptors are located in specific membrane regions called lipid rafts, where the oligomer inserts into the membrane-forming pores, disrupting the osmotic equilibrium and leading to cell death (1, 5). Although this mechanism of action is generally accepted, it may involve additional binding molecules, such as glycolipids, or more than one glycosylphosphatidylinositol-anchored receptor (5, 6). Furthermore, it was shown that Bt-R_1 that is normally not located in lipid rafts changes its location to lipid rafts after treatment of *M. sexta* microvilli membranes with Cry1Ab protoxin, suggesting that it remains attached to toxin oligomer after binding to APN (3).

The three-dimensional structures of several Cry toxins with different insect specificity have been solved, including Cry1Aa, Cry2Aa, Cry3Aa, Cry3Ba, Cry4Aa, and Cry4Ba (for a review, see Ref. 1). Overall, these proteins show a similar organization in three different domains, suggesting a conserved mode of action as follows. Domain I contains seven α-helixes and is involved in oligomer formation, insertion into the membrane, and pore formation (1, 7); domain II consists of three antiparallel β-sheets, and its structure is the most variable of three domains and is implicated in receptor recognition; and domain III is composed of two antiparallel β-sheets and is also involved in receptor binding (1).

Cry1A toxins bind to cadherin proteins of at least six lepidopteran species, *M. sexta*, *Bombyx mori*, *H. virescens*, *Helicoverpa armigera*, *Pectinophora gossypiella*, and *Ostrinia nubilalis* (8–13). Insect cadherins are composed of an ectodomain

* This work was supported, in whole or in part, by National Institutes of Health Grant 1R01 AI066014. This work was also supported by Consejo Nacional de Ciencia y Tecnologia Grants 83135 and 81639, DGAPA-UNAM Grants IN218608-3 and IN210208, and United States Department of Agriculture Grant 2207-35607-17780.

[1] To whom correspondence should be addressed. E-mail: mario@ibt.unam.mx.

[2] The abbreviations used are: Bt-R_1, cadherin receptor; APN, aminopeptidase-N; CR, cadherin repeat; BBMV, brush border membrane vesicle(s); ELISA, enzyme-liked immunosorbent assay; scFv, single-chain Fv; MS, single mutant; MD, double mutant; MT, triple mutant; PBS, phosphate-buffered saline; CHAPS, 3-[(3-cholamidopropyl)dimethylammonio]-1-propanesulfonic acid.

formed by 11 or 12 cadherin repeats (CRs), a transmembrane domain, and an intracellular domain (14). The exposed loops of Cry1A domain II have been directly involved in binding with cadherin in *M. sexta*, *H. virescens*, and *B. mori* (15–18). Three Cry1Ab binding sites were mapped in CR7, CR11, and CR12 of the *M. sexta* Bt-R_1 (15, 19). The interaction between Cry1Ab/Cry1Ac toxins and *H. virescens* cadherin was analyzed, showing that loop 3 of domain II binds to CR12 of this receptor (17). Accordingly, loop 3 of Cry1Aa binds the corresponding site of *B. mori* cadherin (Bt-R_{175}) (18). Cry1Ab loop α-8 and loop 2 bind with *M. sexta* Bt-R_1 CR7 and CR11 epitopes (15).

Regarding interaction of Cry1A toxins with the second receptor, Cry1Ac toxin binds to APN by means of domain III, which recognizes *N*-acetylgaloctosamine moieties in the receptor (20). Also, recent reports indicate that the region $\beta16-\beta22$ located in domain III of Cry1Aa and Cry1Ab toxins is involved in the interaction with *B. mori* and *M. sexta* APNs, respectively (16, 21). In addition, domain II is involved in Cry1A toxin interaction with APN because mutations in domain II loop regions that affected toxicity were shown to affect binding of Cry1Ac or Cry1Ab to *M. sexta* and *Lymantria dispar* APNs (22, 23). It is important to mention that these binding studies were performed with monomeric toxins, and these mutations could also affect binding to the cadherin receptor. In another study, scFv antibodies that bind specifically to Cry1Ab domain II loop 2 or loop 3 or to domain III ($\beta16-\beta22$ region) were used to show that these domain II loop regions, in contrast to domain III, undergo a conformational change upon oligomerization, suggesting that this structural change may be involved in the sequential interaction of the Cry1Ab toxin with cadherin and APN receptors (16).

To determine the role of domain II loop 3 residues in the sequential interaction of Cry1Ab toxin with cadherin and APN receptors, we characterized Cry1Ab domain II loop 3 mutants. We analyzed the ability of either monomers or oligomers of these mutants to bind Bt-R_1 and APN and analyzed their effect on toxicity. Our data show that mutations in domain II loop 3 differentially affect the binding with both receptors, depending on the oligomeric state of the toxin. We propose that possibly a "ping pong" binding mechanism with both receptors is involved in toxin action.

MATERIALS AND METHODS

Site-directed Mutagenesis—pHT315-Cry1Ab was used as a template for site-directed loop 3 mutagenesis using QuikChange® Multi following the manufacturer's instructions (Stratagene).

Purification and Activation of Cry1Ab Toxins—The acrystalliferous *B. thuringiensis* strain 407$^-$ was transformed with pHT315-Cry1Ab or the same plasmid containing loop 3 substitutions. *B. thuringiensis* transformant strains were grown for 3 days at 30 °C in LB medium supplemented with 10 μg/ml erythromycin. After sporulation, crystals were purified by sucrose gradients. For monomer production, Cry1Ab crystals were solubilized in alkaline buffer and activated by trypsin as reported previously (24). In order to obtain oligomeric structure, the crystals were activated with 5% *M. sexta* midgut juice in the presence of scFv73 antibody as described (16). The oligomers were purified by size exclusion chromatography with a Superdex 200HR 10/30 (Amersham Biosciences) fast protein liquid chromatography system. Protein concentration was determined by the Bradford assay, using bovine serum albumin as a standard and the extinction coefficient method, where E_M^{280} = 82,280 M^{-1}/cm^{-1} for Cry1Ab toxin.

Expression and Purification of Cadherin Proteins—Fragments of cadherin protein (CR7–CR12 or CR12) were cloned into pET22b vector as reported previously (7, 25, 26). These constructions were transformed into *Escherichia coli* ER2566 cells; protein expression was induced by the addition of 1 mM isopropyl-thio-β-galactopyranoside. Proteins expressed as inclusion bodies were solubilized with 8 M urea solution. Bt-R_1 peptides were purified with nickel affinity columns according to the manufacturer's instructions (Qiagen) and eluted with 250 mM imidazole in PBS buffer to eliminate urea.

Secondary Structure Analysis of CR12 and CR7–CR12 by CD Spectroscopy—CD spectra were recorded with a JASCO model J-715 spectropolarimeter equipped with a Peltier temperature control supplied by Jasco. Spectra were collected from 200 to 240 nm. Buffer conditions were 10 mM potassium phosphate, pH 7.6, and 25 °C. Eight replicate spectra were collected on each sample to improve signal/noise ratio. The final purified protein (CR12 or CR7–CR12) concentration was 0.3 mg/ml, and spectra were collected in a 0.01-cm path length cell. The secondary structure prediction was performed using the CDSSTR algorithm, which requires data from 200 to 240 nm (27–29).

Expression and Purification of scFv Antibodies—The soluble scFv73 and scFv3L3 antibodies were expressed in *E. coli* BL21 (DE3) cells and purified (16, 24).

Preparation of BBMV—Insect midguts of fourth instar *M. sexta* larvae were dissected and used to prepare brush border membrane vesicles by differential precipitation using $MgCl_2$ (30) and stored at −70 °C until use.

Toxin Overlay Assay—One hundred micrograms of BBMV protein were loaded in a single long lane, separated by 9% SDS-PAGE, and electrotransferred to polyvinylidene difluoride membrane (Amersham Biosciences). Single gel blots were incubated with different Cry1Ab proteins using the PR 150 Mini Deca-Probe (Amersham Biosciences) that was designed to incubate each lane of the blot in different conditions, avoiding the need of cutting lanes for different conditions. Ten parallel troughs milled in one side of the upper plate become individual incubation chambers when the unit is assembled. After blocking with PBS-M (PBS, 5% skim milk), the membrane was incubated with 5 nM wild type or mutant Cry1Ab toxins. Unbound toxins were removed by washing the membrane with PBS-T (PBS, 0.1% Tween 20). The membrane was then incubated with rabbit anti-Cry1Ab antibody followed by secondary anti-rabbit antibody conjugated with horseradish peroxidase (Amersham Biosciences). Blots were visualized using luminol (ECL™, Amersham Biosciences).

Binding Assay of Cry1Ab Toxins with BBMV—For binding assays of wild type and mutant Cry1Ab toxins to BBMV, 10 μg of BBMV protein were incubated in binding buffer (PBS, 0.1% bovine serum albumin, 0.1% Tween 20) with 5 nM Cry1Ab or loop 3 mutants. The unbound toxin was removed by centrifugation (10 min at 14,000 rpm). BBMV were washed three times with binding buffer and suspended in 10 μl of PBS, 3 μl of

Laemmli sample buffer 4× (0.125 M Tris/HCl, 4% SDS, 20% glycerol, 10% β-mercaptoethanol, 0.01% bromphenol blue). The samples were separated by 10% SDS-PAGE and electrotransferred to polyvinylidene difluoride membrane. The membrane was revealed using rabbit anti-Cry1Ab (1:5000) and secondary anti-rabbit (1:5000) conjugated with horseradish peroxidase antibodies.

For competition binding assays, Cry1Ab toxin was labeled with biotin using biotinyl-*N*-hydroxysuccinimide ester according to the manufacturer's instructions (Amersham Biosciences). Ten micrograms of BBMV protein were incubated in binding buffer (PBS, 0.1% bovine serum albumin, 0.1% Tween 20) with 5 nM biotinylated Cry1Ab toxin in the presence or absence of a severalfold molar excess of unlabeled wild type or Cry1Ab-activated mutants. The unbound toxin was removed by centrifugation (10 min at 14,000 rpm). BBMV were washed three times with binding buffer and suspended in 10 μl of PBS, 3 μl of Laemmli sample buffer 4×. The samples were separated by 10% SDS-PAGE and electrotransferred to polyvinylidene difluoride membrane. The membrane was incubated with streptavidin-peroxidase conjugate (Amersham Biosciences) for 1 h, and blots were visualized using luminol (Amersham Biosciences).

APN Purification—Aminopeptidase-N was purified from BBMV of fifth instar *M. sexta* larvae as reported (31). BBMV were incubated in solubilization buffer (1% CHAPS, 5 mM EDTA, 0.1 M NaCl, 1 mM phenylmethylsulfonyl fluoride, 20 mM Tris/HCl, pH 8.5) for 2 h at 4 °C. After centrifugation, supernatant was recovered and dialyzed in buffer A (2 mM $MgCl_2$, 2 mM KCl, 20 mM Tris/HCl, pH 8.5). The sample was loaded into an ion exchange column (Mono-Q) connected to a fast protein liquid chromatography system, APN was eluted using a 0–1 M NaCl gradient, and finally the eluted APN was visualized by SDS-PAGE and Western blot. The activity of purified APN was determined using L-leucine-*p*-nitroanilide as substrate as reported previously (32).

ELISA Binding Assay of Cry1Ab Toxins—ELISA plates were coated with 1 μg of either cadherin protein fragment (CR7–CR12 or CR12), APN from *M. sexta*, or scFv antibodies (scFv73 or scFv3L3) in 100 ml of PBS/well overnight at 4 °C. The plates were washed three times with PBS, blocked with 200 μl/well PBS-M for 2 h at 37 °C, and washed three times with PBS. Different non-saturated concentrations of monomeric or oligomeric Cry1Ab were used in the different binding assays as indicated throughout. The unbound toxins were removed by three washes with PBS-T and three washes with PBS. The bound toxins were detected using rabbit anti-Cry1Ab and anti-rabbit conjugated with horseradish peroxidase antibodies. Finally, *ortho*-phenylenediamine (Sigma) plus H_2O_2 was used as substrate for detection. The reaction was stopped adding 50 μl of 1 M H_2SO_4 and measured at 490 nm using an ELISA microplate reader. Data were analyzed using GraphPad Prism software (version 5.0b), and data curves were transformed by the Scatchard equation for obtaining relative binding affinities (K_d).

Insect Bioassay—Bioassays were performed with *M. sexta* neonate larvae by the surface contamination method (2). Different doses of toxin-activated proteins (from 0.1 to 2000 ng/cm^2) were applied onto the diet surface contained in 24-well polystyrene plates (Cell Wells, Corning Glass). A total of 24 larvae/plaque were fed with different doses of trypsin-activated toxins. The plates were incubated at 28 °C with 65 ± 5% relative humidity and a light/dark photoperiod of 16/8 h. Mortality was recorded after 7 days, and the 50% lethal concentration (LC_{50}) was analyzed with Probit software. For single dose assays, 2 ng/cm^2 of pure oligomer or 25 ng/cm^2 of monomer samples were used with 24 larvae per concentration, and mortality was recorded after 5 days.

RESULTS

Construction of Cry1Ab Loop 3 Mutants—Previously, we reported that loop 3 of Cry1Ab toxin showed a hydropathic complementary pattern with the binding epitope of *H. virescens* cadherin, suggesting a putative interaction through a complementary hydropathic profile (17). Here we introduce amino acid substitutions in loop 3 of Cry1Ab toxin designed to disrupt the hydropathic profile of this region. Three mutants were constructed, a single point mutant S446V (named MS), a double mutant S441R/N442V (MD), and the combination of these substitutions in a triple mutant S441R/N442V/S446V (named MT). After mutagenesis, plasmids were sequenced and transformed into an acrystalliferous *B. thuringiensis* strain, and cells were sporulated to produce crystal proteins. The crystalline inclusions produced by the loop 3 mutants, MS, MD, and MT, and the Cry1Ab toxin were solubilized and activated with trypsin. Fig. 1*A* shows that trypsin activation of the loop 3 mutants produced a 65-kDa protein similar to the Cry1Ab toxin. To determine whether these mutations affect oligomer formation we activated mutant protoxins with *M. sexta* midgut juice in the presence of scFv73 antibody. Antibody scFv73 was previously shown to mimic a cadherin binding region and facilitates formation of the oligomer structure when the Cry1Ab protoxin was proteolytically activated in the presence of this molecule (2, 24). Fig. 1*B* shows the Cry1Ab oligomers revealed by Western blot using a Cry1Ab antibody that recognizes both the monomeric and the oligomeric structures. The MS and MD mutants produced 40% lower yields of oligomer than the Cry1Ab protein, as revealed by scanning the optical density of the 250-kDa oligomer band (Fig. 1*B*). However, the MT mutant produced significantly lower levels of oligomer than Cry1Ab or MS and MD proteins (Fig. 1*B*).

To determine if loop 3 mutations affect the structure of other regions of domain II, we analyzed the binding of two anti-domain II antibodies (scFv73 and scFv3L3) that recognize either domain II loop 2 or loop 3, respectively, and compete with binding of Cry1Ab with Bt-R_1 in toxin overlay assays (16, 24, 33). Anti-loop 2 scFv73 antibody bound to the trypsin-activated mutants and to Cry1Ab toxin, indicating the same toxin conformation in this binding epitope (Fig. 1*C*). In contrast, the anti-loop 3 scFv3L3 antibody only recognized the Cry1Ab toxin, indicating that loop 3 mutations specifically affected the binding capacities of the loop 3 amino acid region (Fig. 1*D*).

Binding Assays of Cry1Ab Loop 3 Mutants with M. sexta BBMV Proteins—To determine the effect of loop 3 mutations in binding to both cadherin and aminopeptidase receptors, toxin overlay assays were performed. In these assays, BBMV proteins were separated by SDS-PAGE and blotted to polyvinylidene

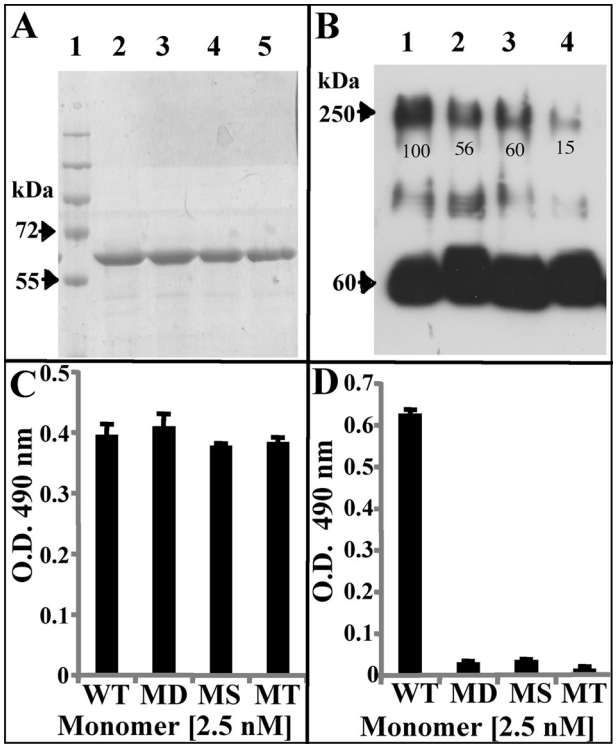

FIGURE 1. **Cry1Ab domain II loop 3 mutants are structurally stable.** *A*, SDS-PAGE electrophoresis pattern of trypsin-activated Cry1Ab (*lane 2*), MS (*lane 3*), MD (*lane 4*), and MT (*lane 5*) toxins. *Lane 1*, molecular weight marker. *B*, Western blot of toxin-activated samples in the presence of scFv73 antibody, Cry1Ab (*lane 1*), MS (*lane 2*), MD (*lane 3*), and MT (*lane 4*). The 250-kDa oligomer and 60-kDa monomer bands are shown. *Numbers below* the 250 kDa band represent the percentage of oligomer concentration after scanning this band. *C* and *D*, ELISA binding analysis of 2.5 nM trypsin-activated Cry1Ab loop 3 mutants to anti-loop 2 scFv73 antibody (*C*) or anti-loop 3 scFv3L3 (*D*).

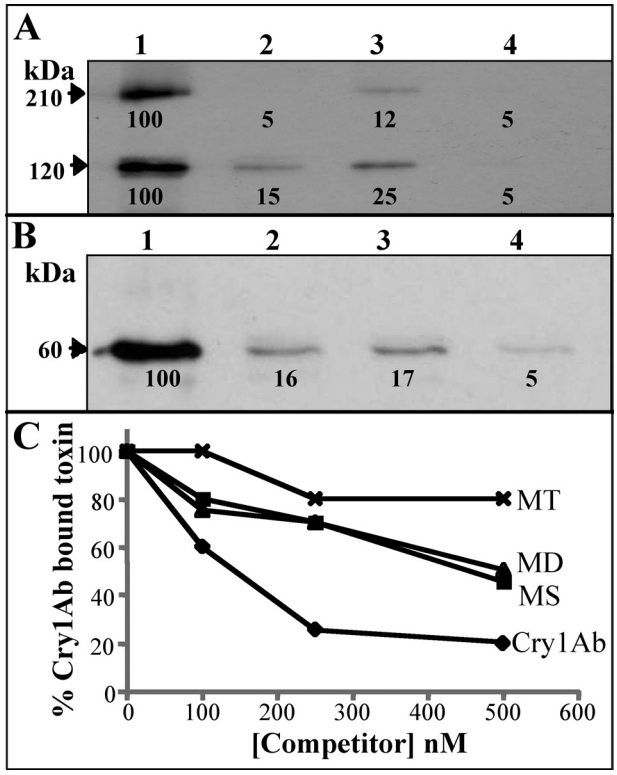

FIGURE 2. **Cry1Ab loop 3 mutants are affected in binding to *M. sexta* BBMV proteins.** *A*, toxin overlay binding assays of Cry1Ab (*lane 1*), MS (*lane 2*), MD (*lane 3*), and MT (*lane 4*) toxins to blotted *M. sexta* BBMV proteins. The 210-kDa protein corresponds to Bt-R_1, and the 120-kDa protein corresponds to APN. The *numbers* represent the percentage of binding after scanning bands. *B*, binding assays of 10 nM Cry1Ab (*lane 1*), MS (*lane 2*), MD (*lane 3*), and MT (*lane 4*) toxins with *M. sexta* BBMV. The 65-kDa protein corresponds to bound toxins recovered after centrifugation of BBMV samples and revealed with antiCry1Ab antibody as described under "Materials and Methods." The *numbers* represent the percentage of binding after scanning bands. *C*, binding competitions of biotinylated Cry1Ab toxin to BBMV using different excess of unlabeled Cry1Ab (♦), MS (■), MD (▲), and MT (×) proteins.

difluoride membranes. BBMV proteins that bind monomeric Cry1Ab toxin were identified after incubation with Cry1Ab proteins and revealed with a polyclonal anti-Cry1Ab antibody. Fig. 2*A* shows that the Cry1Ab monomeric toxin bound with 210- and 120-kDa BBMV proteins that were previously identified as Bt-R_1 and APN, respectively (8, 24, 31). In contrast, loop 3 mutants were affected in binding both 210- and 120-kDa BBMV proteins (Fig. 2*A*). The MT mutant was the most affected because it barely bound to Bt-R_1 or APN (Fig. 2*A*, *lane 4*). These results indicate the loop 3 mutations affect the binding of Cry1Ab to both Bt-R_1 and APN receptor molecules.

To determine the effect of Cry1Ab loop 3 mutations on the binding to *M. sexta* BBMV, Cry1Ab and loop 3 mutant proteins were incubated with BBMV, and bound labeled proteins were observed using an anti-Cry1Ab polyclonal antibody. Fig. 2*B* shows that the three loop 3 mutants were affected in binding to BBMV. Binding competition experiments of biotinylated Cry1Ab to BBMV using Cry1Ab or loop 3 mutants as unlabeled competitors show that the three mutants did not compete with the binding of Cry1Ab, suggesting that they bound BBMV with lower affinity than Cry1Ab and that the MT mutant was the most affected in binding (Fig. 2*C*).

Binding Assays of Cry1Ab Loop 3 Mutants with Bt-R_1 and APN—Toxin overlay assays determined binding of Cry toxins to partially unfolded proteins after SDS-PAGE. To analyze the effect of loop 3 mutations on toxin interaction with Bt-R_1 and APN in native conformation, we performed ELISA binding saturation assays of the activated Cry1Ab, MS, MD, and MT proteins to two cadherin fragment proteins produced in *E. coli* and to APN protein purified from *M. sexta* midgut tissue. Previously, it was shown that the apparent binding dissociation constant of Cry1Ab monomeric toxin with Bt-R_1 was in the range of 1 nM (8). Also, it was shown that binding with APN was in the range of 100 nM (20). We previously cloned and produced in *E. coli* two cadherin fragments corresponding to CR7–CR12 (residues Met^{810}–Ala^{1485}) and to CR12 (residues Gly^{1370}–Ala^{1485}) of *M. sexta* Bt-R1 (7, 25, 26). It was reported that Cry1Ab bound to a cadherin peptide (CR12-MPED) similar to CR12 with a binding affinity of 9.5 nM (34). Fig. 3 shows the analysis of folding of cadherin fragments CR7–CR12 and CR12 by circular dichroism spectra, indicating that both polypeptides have a similar content of α-helices and β-strand structures, with the β-fold structure the most abundant secondary structure. Fig. 4 shows that the Cry1Ab loop 3 mutants were not affected in binding to CR7–CR12 cadherin fragment but were affected in binding to CR12 and APN. Calculation of apparent binding affinities by Scatchard plots (not shown) revealed that Cry1Ab and the three loop 3 mutants bound CR7–CR12 with very high binding affinity (K_d = 0.2 nM). In the case of CR12, the

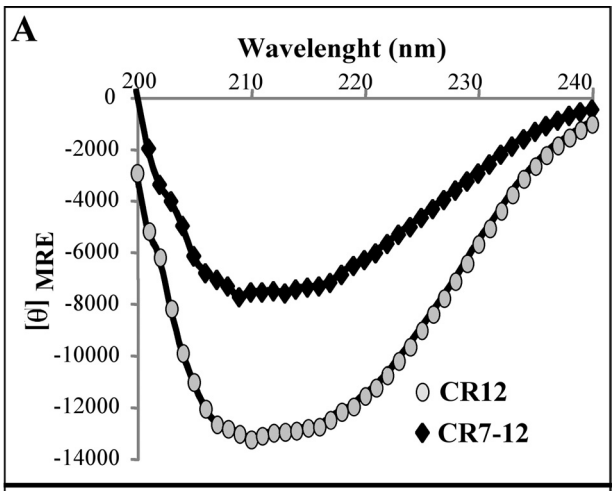

B

	helix	β-strand	turn	unordered
CR12	18%	31%	26%	21%
CR7-CR12	14%	36%	23%	27%

FIGURE 3. **Analysis of secondary structure composition of cadherin fragments by CD spectra.** *A*, CD spectra of cadherin fragments CR12 (♦) and CR7–CR12 (●). *MRE*, mean residue ellipticity. *B*, prediction of content in percentage of different secondary structures.

MT mutant showed a 250-fold reduction on binding affinity, whereas MT and MD showed a 70- and 80-fold reduction in binding in comparison with Cry1Ab (K_d = 9.5 nM). Finally, the MS, MD, and MT mutants were severely affected upon binding with APN, showing a 28-, 14-, and 23-fold reduction in binding affinity to APN, respectively, in comparison with Cry1Ab (K_d = 85 nM). The apparent binding affinities obtained by the saturation ELISA binding assays are in the range of those previously reported for cadherin fragment CR12-MPED and APN (20, 34). However, binding to CR7–CR12 showed a very high apparent dissociation of 0.2 nM, 5-fold higher than the reported binding affinity of 1 nM for Bt-R_1 (8). In any case, the data clearly show that Cry1Ab loop 3 mutations affected binding with CR12 and APN but not with CR7–CR12.

Interaction of Cry1Ab Loop 3 Mutant Oligomers with M. sexta Bt-R_1—In the proposed model of the mode of action of Cry1Ab, binding of Cry1Ab to Bt-R_1 and APN depends on the oligomeric state of the toxin (3). To determine the effect of the loop 3 mutations characterized here on the binding of the oligomeric structure with both receptors, we performed oligomerization assays of Cry1Ab, MS, MD, and MT proteins and further purified the oligomers by size exclusion chromatography. Despite the lower yields of oligomer formation by the MT mutant (Fig. 1*B*), we obtained sufficient amounts of oligomer proteins (Fig. 5*A*) to perform binding assays with both Bt-R_1 and APN.

We performed ELISA binding assays of both oligomeric and monomeric structures of Cry1Ab proteins with cadherin fragment proteins produced in *E. coli*. Non-saturated concentrations of oligomers were used in the comparison with the binding of the loop 3 mutants as judged by saturation binding assays of Cry1Ab oligomer with both cadherin fragments and APN.[3] The binding of 0.1 nM Cry1Ab and loop 3 mutant oligomers with the cadherin fragments revealed that the loop 3 mutations affected significantly the binding of the oligomer with both CR7–CR12 and CR12 cadherin fragments (Fig. 5, *B* and *C*). As controls, we performed ELISA binding assays using monomers that confirmed that loop 3 mutations affected monomer binding with CR12 but not with CR7–CR12 (Fig. 5, *D* and *E*).

Interaction of Cry1Ab Loop 3 Mutant Oligomers with M. sexta APN—To determine the effect of the loop 3 mutations on the binding of Cry1Ab oligomer with APN, we performed ELISA binding assays with APN purified from *M. sexta* BBMV, using either oligomeric or monomeric structures of each mutant and of Cry1Ab. As above, non-saturated concentrations were used in the ELISA binding assays. Fig. 6*A* shows that 0.1 nM Cry1Ab, MD, MS, and MT oligomers bound similarly to APN protein. In contrast, 25 nM monomeric MD, MS, and MT proteins were affected in binding to APN in contrast to the wild type Cry1Ab monomer (Fig. 6*B*).

Toxicity Effects of Cry1Ab Loop 3 Mutations—We determined the effect of the Cry1Ab loop 3 mutations on toxicity against *M. sexta* larvae. Table 1 shows that the activated MS and MD mutants had a 9-fold reduction in mortality, whereas MT had a 70-fold reduction in mortality when the LC_{50} lethal values were compared with activated Cry1Ab protein. To determine the effect on mortality in the context of both monomeric and oligomeric structures, we performed a single dose toxicity assay of pure monomer or oligomeric structures. Table 1 shows that a single dose of Cry1Ab monomer (25 ng/cm^2) or Cry1Ab oligomer (2 ng/cm^2) resulted in 95% larval mortality. In contrast, the same doses of monomeric and oligomeric structures of the three loop 3 mutants were severely affected in toxicity to *M. sexta* larvae (Table 1).

DISCUSSION

Interaction of pathogens with their target cells involves specific recognition of surface molecules to modulate cell recognition, membrane insertion, or cell internalization. In the case of bacterial pore-forming toxins, the interaction of single receptors seems to be a general strategy, although in the case of several toxins, such as diphtheria, anthrax protective antigen, or aerolysin, more than one surface molecule is involved in the binding and mode of action of these toxins (35–37). With viruses, sequential interaction with several surface molecules is important for infection where structural changes of the viral proteins are involved in target cell interactions (38, 39).

Regarding insecticidal Cry1A toxins, membrane insertion is the result of the sequential interaction with at least two receptor molecules in the lepidopteran *M. sexta*, Bt-R_1 and APN (3). Binding of Cry1Ab toxin with Bt-R_1 facilitates removal of helix α-1, triggering toxin oligomerization (2). The oligomer gains binding affinity to the second receptor, APN, and this interaction enhances insertion of the oligomer into the membrane (3, 40). We previously hypothesized that sequential interaction of the Cry1Ab toxin with the two receptors involves structural changes of binding epitopes upon oligomerization (16). By use

[3] I. Arenas and I. Gómez, unpublished data.

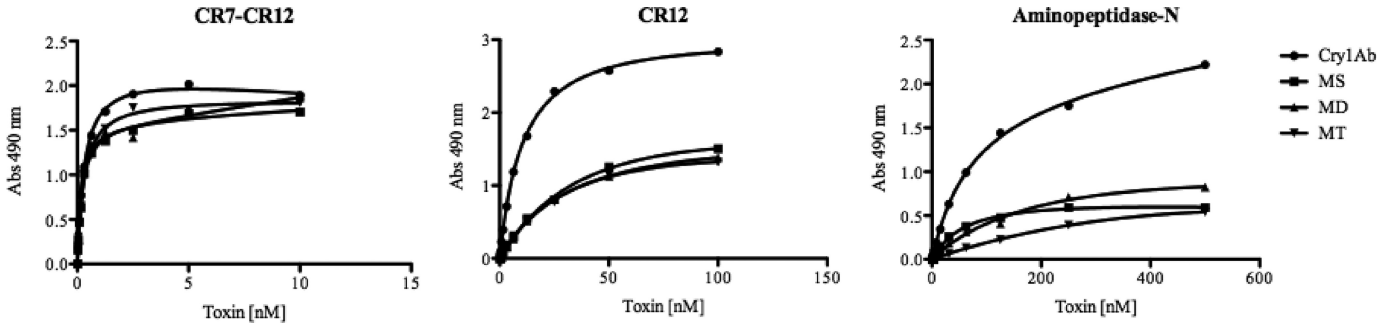

FIGURE 4. **ELISA saturation binding assays of Cry1Ab, MS, MD, and MT toxins to cadherin fragments CR7–CR12, CR12, and APN.**

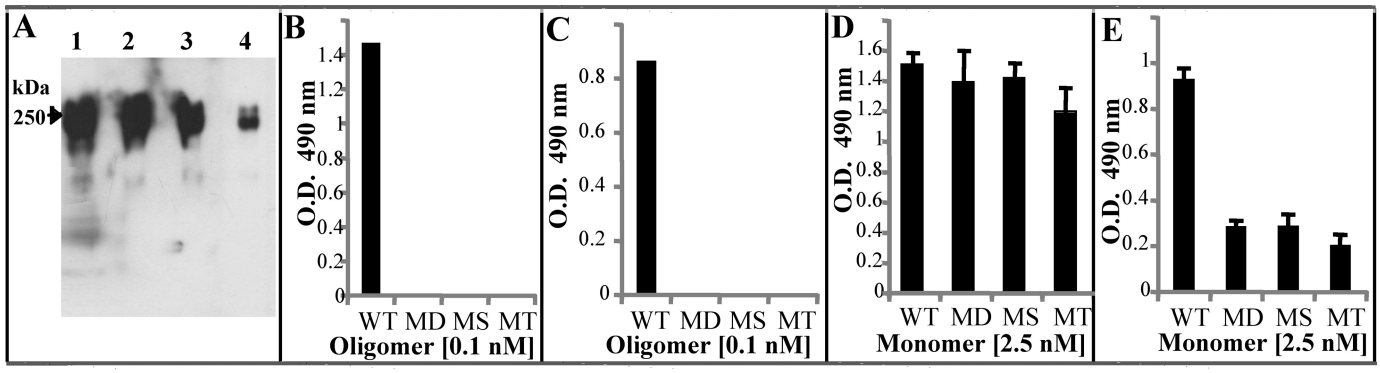

FIGURE 5. **Binding analysis of Cry1Ab and loop 3 mutants to cadherin fragments.** *A*, Western blot of pure oligomer samples obtained after size exclusion chromatography of toxin samples activated in the presence of scFv73 antibody, Cry1Ab (*lane 1*), MS (*lane 2*), MD (*lane 3*), and MT (*lane 4*). *B*, ELISA binding assays of 0.1 nM Cry1Ab (wild type (*WT*)), MS, MD, and MT oligomeric structures to cadherin fragment CR7–CR12. *C*, ELISA binding assays of 0.1 nM Cry1Ab, MS, MD, and MT oligomeric structures to cadherin fragment CR12. *D*, ELISA binding assays of 2.5 nM Cry1Ab, MS, MD, and MT monomeric structures to cadherin fragment CR7-CR12. *E*, ELISA binding assays of 2.5 nM Cry1Ab, MS, MD, and MT monomeric structures to cadherin fragment CR12.

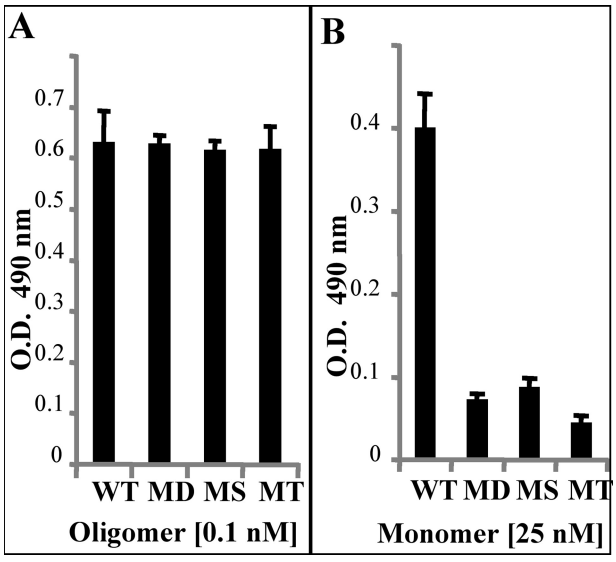

FIGURE 6. **Binding analysis of Cry1Ab and loop 3 mutants to APN.** *A*, ELISA binding assays of 0.1 nM Cry1Ab (wild type (*WT*)), MS, MD, and MT oligomeric structures to APN. *B*, ELISA binding assays of 25 nM Cry1Ab, MS, MD, and MT monomeric structures to APN.

TABLE 1
Toxicity of Cry1Ab toxin to *M. sexta* larvae

	LC_{50}[a]	LC_{50}(mutant)/ LC_{50}(wild type)	Monomer sample (25 ng/cm^2) mortality	Oligomer sample (2 ng/cm^2) mortality
	ng/cm^2		%	%
Cry1Ab	10.3 (8.9–11.9)	ND[b]	95	95
MS	94.7 (73–119.7)	9.19	5	5
MD	91.7 (75.7–113.7)	8.9	5	5
MT	723 (341.1–2148.9)	70.12	0	0

[a] 50% lethal concentration of trypsin-activated Cry1Ab proteins.
[b] ND, not determined.

of scFv antibodies that bind with two different domain II loop regions, loop 2 and loop 3, or with the domain III $\beta16-\beta22$ region, we showed that antibodies to domain II loop recognized preferentially the monomeric structure rather than the oligomer, in contrast to the anti-domain III scFv molecule that recognized equally both structures. This finding suggests a subtle structural change in domain II loop 2 and 3 binding regions upon oligomerization of the toxin (16). Here we show that the loop 3 mutations have a differential effect on binding to both Bt-R_1 and APN, depending on the oligomeric state of the toxin (monomer *versus* oligomer structures). Thus, structural changes that occur upon oligomerization also affect Cry1Ab toxin binding capacities.

In this study, we mutagenized domain II loop 3 to determine its role in the *in vivo* binding to both Bt-R_1 and APN receptors. Published data regarding the role of this binding region in the interaction with both receptor molecules are incomplete because binding of loop 3 mutant oligomers with the two receptor molecules was not previously analyzed. Mutagenesis studies of Cry1Ab and Cry1Ac loop 3 previously performed indicated that this amino acid region was important for binding with *M. sexta* BBMV and toxicity (40, 41). In addition, alanine substitutions of loop 3 residues in Cry1Ab and Cry1Ac toxins showed a correlative effect on APN binding, suggesting that their effects on toxicity were due to defects in this binding (22, 23). However, it was also shown that loop 3 is the cognate bind-

ing region of CR12 in *H. virescens* cadherin and in Bt-R_1 receptors (17) (Fig. 4), suggesting that this toxin region may be involved in the interaction with both Bt-R_1 and APN receptors.

Toxin overlay binding analysis of loop 3 mutants confirmed the hypothesis that this amino acid region may be involved in the interaction with both Bt-R_1 and APN receptors because binding with both of these proteins was greatly reduced, data that correlated with the observed reduced binding with *M. sexta* BBMV. However, binding analysis of monomeric or oligomeric structures to non-denatured Bt-R_1 fragment or APN revealed unexpected results that indicate that the mode of action of Cry1Ab toxin may involve multiple binding interactions with both receptor molecules during the intoxication process. ELISA binding assays showed that loop 3 mutations had a significant effect on the binding of monomeric toxin with APN. In the case of aerolysin, another pore-forming toxin, the first binding event with the target cell involves binding with a high abundance low affinity binding molecule and then with a low abundance but high affinity binding site (37). APN has been shown to be an abundant molecule in *M. sexta* midgut, in contrast with Bt-R_1 that is present in much lower concentrations (42). We therefore speculate that monomeric Cry1Ab binds first with the high abundance low affinity APN site before the high affinity interaction with Bt-R_1.

Regarding the interaction of Cry1Ab monomer with Bt-R_1 receptor, previous work showed that domain II, loop α-8, loop 2, and loop 3 are involved in the binding of Cry1Ab toxin to this receptor (2, 16, 32). Loop 2 was the cognate binding epitope of the CR7 region (^{869}HITDTNNK^{876}) (33); loop α8 and loop 2 interact with the CR11 region (^{1331}IPLPASILTVTV^{1342}) (15), whereas loop 3 binds to the CR12 region of the cadherin receptors in *H. virescens* and *B. mori* (17, 18). Monomeric structures of the three loop 3 mutants characterized here were only affected in the binding with the CR12 fragment of Bt-R_1 and not with a Bt-R_1 fragment corresponding to CR7–CR12 (Fig. 4), confirming that Cry1Ab loop 3 binds CR12 and that binding with the CR7–CR12 fragment also involves loops α-8 and 2.

Loop 3 mutations had no effect on the binding interaction of the Cry1Ab oligomeric structure with APN but had a significant effect on oligomer binding with Bt-R_1 (Figs. 5 and 6). These results suggest that when oligomer is formed after interaction with Bt-R_1, it remains bound with Bt-R_1 through loop 3 and that oligomer interaction with APN involves other regions as previously reported, corresponding to the domain III β16–β-22 region (16, 21). Furthermore, the formation of such a protein complex (Bt-R_1-Cry1Ab-APN complex) was previously suggested because Bt-R_1 was mobilized into lipid rafts after toxin interaction (5). What could be the role of such a protein complex (Bt-R_1-oligomer-APN) in Cry1Ab toxicity? Loop 3 mutations severely affected the toxicity of Cry1Ab oligomer, suggesting that this protein complex may be important for toxicity. However, engineered Cry1Ab- and Cry1Ac-modified toxins (Cry1AbMod and Cry1AcMod) lacking helix α-1 formed oligomers in the absence of cadherin interaction and killed *M. sexta* larvae that were silenced for the cadherin gene, showing that cadherin interaction is not important for toxicity mediated by Cry1Ab oligomer (25). Therefore, the effect of loop 3 mutations on oligomer toxicity should be due to postbinding APN events.

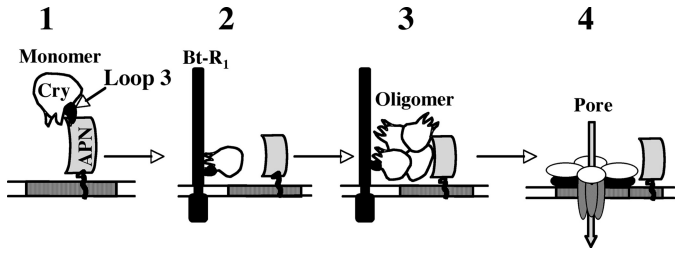

FIGURE 7. **Ping pong binding model of Cry1Ab toxin interaction with APN and Bt-R_1 receptors.** *1*, binding of 65-kDa Cry1Ab monomer to APN through domain II loop 3. *2*, the monomer binds Bt-R_1 through domain II loops α-8, 2, and 3. *3*, formation of a 250-kDa oligomer that binds Bt-R_1 through loop 3 and to APN through domain III. *4*, membrane insertion of the 250-kDa oligomer and pore formation after APN interaction.

Previously, it was shown that the APN binding through *N*-acetylgaloctosamine moieties enhances membrane insertion of Cry1Ac toxin (43). It is possible that domain II loop 3 mutations affect structural changes that are triggered by APN and necessary for membrane insertion of the Cry1Ab oligomer. In this regard, it has been shown that mutations in domain II loop 2 Phe^{371} retain binding with *M. sexta* BBMV but are affected in membrane insertion (44, 45).

The results shown here indicate that Cry1Ab toxin specificity is determined by a complex binding mechanism with two different receptor molecules that depends on the oligomeric state of the toxin. A "ping pong" binding mechanism may occur where domain II loop 3 may be involved in the first binding event with the high abundance low affinity APN receptor. This interaction is followed by a high affinity binding to Bt-R_1 receptor that involves participation of other regions of domain II in addition to loop 3, such as loops α-8 and 2. Interaction with Bt-R_1 triggers cleavage of helix α-1 and oligomer formation. The oligomeric structure gains binding affinity with APN through other regions of the toxin, such as the domain III β16–β22 region, but remains bound with Bt-R_1 through loop 3. Finally, residues in domain II loop 3 may be also involved in post-APN binding events important for toxicity, such as oligomer membrane insertion (Fig. 7).

Acknowledgment—We thank Lizbeth Cabrera for technical assistance.

REFERENCES

1. Bravo, A., Gill, S. S., and Soberón, M. (2007) *Toxicon* **49,** 423–435
2. Gómez, I., Sánchez, J., Miranda, R., Bravo, A., and Soberón, M. (2002) *FEBS Lett.* **513,** 242–246
3. Bravo, A., Gómez, I., Conde, J., Muñoz-Garay, C., Sánchez, J., Miranda, R., Zhuang, M., Gill, S. S., and Soberón, M. (2004) *Biochim. Biophys. Acta* **1667,** 38–46
4. Jurat-Fuentes, J. L., and Adang, M. J. (2004) *Eur. J. Biochem.* **271,** 3127–3135
5. Zhuang, M., Oltean, D. I., Gómez, I., Pullikuth, A. K., Soberón, M., Bravo, A., and Gill, S. S. (2002) *J. Biol. Chem.* **277,** 13863–13872
6. Griffitts, J. S., Haslam, S. M., Yang, T., Garczynski, S. F., Mulloy, B., Morris, H., Cremer, P. S., Dell, A., Adang, M. J., and Aroian, R. V. (2005) *Science* **307,** 922–925
7. Jiménez-Juárez, N., Muñoz-Garay, C., Gómez, I., Saab-Rincon, G., Damian-Almazo, J. Y., Gill, S. S., Soberón, M., and Bravo, A. (2007) *J. Biol. Chem.* **282,** 21222–21229
8. Vadlamudi, R. K., Weber, E., Ji, I., Ji, T. H., and Bulla, L. A., Jr. (1995) *J. Biol.*

Chem. **270,** 5490–5494
9. Nagamatsu, Y., Toda, S., Koike, T., Miyoshi, Y., Shigematsu, S., and Kogure, M. (1998) *Biosci. Biotechnol. Biochem.* **62,** 727–734
10. Gahan, L. J., Gould, F., and Heckel, D. G. (2001) *Science* **293,** 857–860
11. Xu, X., Yu, L., and Wu, Y. (2005) *Appl. Environ. Microbiol.* **71,** 948–954
12. Morin, S., Biggs, R. W., Sisterson, M. S., Shriver, L., Ellers-Kirk, C., Higginson, D., Holley, D., Gahan, L. J., Heckel, D. G., Carrière, Y., Dennehy, T. J., Brown, J. K., and Tabashnik, B. E. (2003) *Proc. Nat. Acad. Sci. U.S.A.* **100,** 5004–5009
13. Flannagan, R. D., Yu, C. G., Mathis, J. P., Meyer, T. E., Shi, X., Siqueira, H. A., and Siegfried, B. D. (2005) *Insect. Biochem. Mol. Biol.* **35,** 33–40
14. Bel, Y., and Escriche, B. (2006) *Gene* **381,** 71–80
15. Gómez, I., Dean, D. H., Bravo, A., and Soberón, M. (2003) *Biochemistry* **42,** 10482–10489
16. Gómez, I., Arenas, I., Benitez, I., Miranda-Ríos, J., Becerril, B., Grande, R., Almagro, J. C., Bravo, A., and Soberón, M. (2006) *J. Biol. Chem.* **281,** 34032–34039
17. Xie, R., Zhuang, M., Ross, L. S., Gomez, I., Oltean, D. I., Bravo, A., Soberon, M., and Gill, S. S. (2005) *J. Biol. Chem.* **280,** 8416–8425
18. Atsumi, S., Inoue, Y., Ishizaka, T., Mizuno, E., Yoshizawa, Y., Kitami, M., and Sato, R. (2008) *FEBS J.* **275,** 4913–4926
19. Hua, G., Jurat-Fuentes, J. L., and Adang, M. J. (2004) *J. Biol. Chem.* **279,** 28051–28056
20. Masson, L., Lu, Y. J., Mazza, A., Brousseau, R., and Adang, M. J. (1995) *J. Biol. Chem.* **270,** 20309–20315
21. Atsumi, S., Mizuno, E., Hara, H., Nakanishi, K., Kitami, M., Miura, N., Tabunoki, H., Watanabe, A., and Sato, R. (2005) *Appl. Environ. Microbiol.* **71,** 3966–3977
22. Jenkins, J. L., and Dean, D. H. (2000) in *Genetic Engineering: Principles and Methods*, Vol. 22 (Setlow, J. K., ed) pp. 33–54, Plenum Press, New York
23. Jenkins, J. L., Lee, M. K., Valaitis, A. P., Curtiss, A., and Dean, D. H. (2000) *J. Biol. Chem.* **275,** 14423–14431
24. Gómez, I., Oltean, D. I., Gill, S. S., Bravo, A., and Soberón, M. (2001) *J. Biol. Chem.* **276,** 28906–28912
25. Soberón, M., Pardo-López, L., López, I., Gómez, I., Tabashnik, B. E., and Bravo, A. (2007) *Science* **318,** 1640–1642
26. Pacheco, S., Gómez, I., Gill, S. S., Bravo, A., and Soberón, M. (2009) *Peptides* **30,** 583–588
27. Sreerama, N., and Woody, R. W. (2000) *Anal. Biochem.* **287,** 252–260
28. Whitmore, L., and Wallace, B. A. (2004) *Nucleic Acids Res.* **32,** W668–W673
29. Whitmore, L., and Wallace, B. A. (2008) *Biopolymers* **89,** 392–400
30. Wolfersberger, M., Lüthy, P., Maurer, A., Parenti, P., Sacchi, F. V., Giordana, B., and Hanozet, G. M. (1987) *Comp. Biochem. Physiol.* **86A,** 301–308
31. Sangadala, S., Azadi, P., Carlson, R., and Adang, M. J. (2001) *Insect. Biochem. Mol. Biol.* **32,** 97–107
32. Lorence, A., Darszon, A., and Bravo, A. (1997) *FEBS Lett.* **414,** 303–307
33. Gómez, I., Miranda-Rios, J., Rudiño-Piñera, E., Oltean, D. I., Gill, S. S., Bravo, A., and Soberón, M. (2002b) *J. Biol. Chem.* **277,** 30137–30143
34. Chen, J., Hua, G., Jurat-Fuentes, J. L., Abdullah, M. A., and Adang, M. J. (2007) *Proc. Natl. Acad. Sci. U.S.A.* **104,** 13901–13906
35. Hasuwa, H., Shishido, Y., Yamazaki, A., Kobayashi, T., Yu, X., and Mekada, E. (2001) *Biochem. Biophys. Res. Commun.* **289,** 782–790
36. Scobie, H. M., Rainey, G. J., Bradley, K. A., and Young, J. A. (2003) *Proc. Natl. Acad. Sci. U.S.A.* **100,** 5170–5174
37. Abrami, L., Fivaz, M., Glauser, P. E., Sugimoto, N., Zurzolo, C., and van der Goot, F. G. (2003) *Infect. Immun.* **71,** 739–746
38. Bartosch, B., Vitelli, A., Granier, C., Goujon, C., Dubuisson, J., Pascale, S., Scarselli, E., Cortese, R., Nicosia, A., and Cosset, F. L. (2003) *J. Biol. Chem.* **278,** 41624–41630
39. López, S., and Arias, C. F. (2004) *Trends Microbiol.* **12,** 271–278
40. Rajamohan, F., Hussain, S. R., Cotrill, J. A., Gould, F., and Dean, D. H. (1996) *J. Biol. Chem.* **271,** 25220–25226
41. Smedley, D. P., and Ellar, D. J. (1996) *Microbiology* **142,** 1617–1624
42. Chen, J., Brown, M. R., Hua, G., and Adang, M. J. (2005) *Cell Tissue Res.* **321,** 123–129
43. Pardo-López, L., Gómez, I., Rausell, C., Sanchez, J., Soberón, M., and Bravo, A. (2006) *Biochemistry* **45,** 10329–10336
44. Rajamohan, F., Alcantara, E., Lee, M. K., Chen, X. J., Curtiss, A., and Dean, D. H. (1995) *J. Bacteriol.* **177,** 2276–2282
45. Nair, M. S., and Dean, D. H. (2008) *J. Biol. Chem.* **283,** 26324–26331

Biochimica et Biophysica Acta 1788 (2009) 2229–2237

Contents lists available at ScienceDirect

Biochimica et Biophysica Acta

journal homepage: www.elsevier.com/locate/bbamem

Characterization of the mechanism of action of the genetically modified Cry1AbMod toxin that is active against Cry1Ab-resistant insects

Carlos Muñóz-Garay [a], Leivi Portugal [a], Liliana Pardo-López [a], Nuria Jiménez-Juárez [a], Ivan Arenas [a], Isabel Gómez [a], Rosana Sánchez-López [a], Raquel Arroyo [a], Andreas Holzenburg [b,c], Christos G. Savva [c], Mario Soberón [a], Alejandra Bravo [a,*]

[a] Instituto de Biotecnología, Universidad Nacional Autónoma de México. Apdo. postal 510-3, Cuernavaca 62250, Morelos, Mexico
[b] Department of Biology and Department of Biochemistry and Biophysics, Texas A&M University. College Station, Texas 77843-2257, USA
[c] Microscopy and Imaging Center, Texas A&M University. College Station, Texas 77843-2257, USA

ARTICLE INFO

Article history:
Received 4 May 2009
Received in revised form 16 June 2009
Accepted 17 June 2009
Available online 24 June 2009

Keywords:
Bacillus thuringiensis
Cry toxin
Insect resistance
Mode of action
Oligomerization
Pore formation
Aminopeptidase

ABSTRACT

Bacillus thuringiensis Cry toxins are used in the control of insect pests. They are pore-forming toxins with a complex mechanism that involves the sequential interaction with receptors. They are produced as protoxins, which are activated by midgut proteases. Activated toxin binds to cadherin receptor, inducing an extra cleavage including helix α-1, facilitating the formation of a pre-pore oligomer. The toxin oligomer binds to secondary receptors such as aminopeptidase and inserts into lipid rafts forming pores and causing larval death. The primary threat to efficacy of Bt-toxins is the evolution of insect resistance. Engineered Cry1AMod toxins, devoid of helix α-1, could be used for the control of resistance in lepidopterans by bypassing the altered cadherin receptor, killing resistant insects affected in this receptor. Here we analyzed the mechanism of action of Cry1AbMod. We found that alkaline pH and the presence of membrane lipids facilitates the oligomerization of Cry1AbMod. In addition, tryptophan fluorescence emission spectra, ELISA binding to pure aminopeptidase receptor, calcein release assay and analysis of ionic-conductance in planar lipid bilayers, indicated that the secondary steps in mode of action that take place after interaction with cadherin receptor such as oligomerization, receptor binding and pore formation are similar in the Cry1AbMod and in the wild type Cry1Ab. Finally, the membrane-associated structure of Cry1AbMod oligomer was analyzed by electron crystallography showing that it forms a complex with a trimeric organization.

1. Introduction

Bacillus thuringiensis (Bt) bacteria produce insecticidal Cry proteins that are toxic to different insect orders, but harmless to vertebrates and other organisms [1]. Cry toxins are produced as crystal inclusions during the sporulation phase of the bacteria. They are pore-forming toxins that kill susceptible insects by destroying the cells of their midgut epithelium [1,2]. The crystal inclusions are ingested by the larvae and solubilized in the midgut lumen due to the alkaline and reducing environment that is present in the larval gut [1–3]. The soluble protoxins are activated by midgut proteases producing monomeric toxins. The activated toxins must undergo conformational changes in order to insert into the target membrane forming ionic pores [1,2]. In a previous study, it was demonstrated that binding of monomeric Cry1Ac to brush border membrane vesicles isolated from susceptible *Manduca sexta* larvae induce aggregation of the toxin and that the toxin becomes highly resistant to digestion with protease K since only 60 amino acids in amino terminal region including helix α-1 were cleaved [4]. Later we showed that in the case of Cry1A toxins the interaction with the primary cadherin receptor facilitates this additional cleavage at the N-terminal end of the toxin, which eliminates helix α-1 of domain I [5]. This cleavage induces the assembly of the toxin into an oligomeric pre-pore structure [5,6]. The oligomeric toxin then binds to secondary receptors, which are glycosyl phosphatidylinositol (GPI)-anchored proteins, such as aminopeptidase N (APN) or alkaline phosphatase [6–8]. Compared with toxin monomers, the Cry toxin oligomers have increased binding affinity to the secondary receptors [6]. After binding to the secondary receptor, the Cry toxin oligomer localizes into membrane-microdomains or lipid rafts, where it inserts into the membrane forming pores that cause ion leakage, cell lysis and insect death [6]. The toxin oligomer produces stable channels in black lipid bilayers with high open probability, in contrast to the monomeric toxin structure [9]. Point mutations affecting oligomerization of Cry1Ab toxin were unaffected in their binding interaction with cadherin receptor but were severely

Abbreviations: Bt, *Bacillus thuringiensis*; Cry, crystal proteins; SUV, small unilamellar vesicles; PC, phosphatidylcholine; AFU, arbitrary fluorescence units; PMSF, Phenylmethanesulphonyl fluoride; PVDF, polyvinylidene difluoride; HRP, horseradish peroxidase; ELISA, enzyme linked immunosorbent assay; 2D, two-dimensional; OTG, octyl-β-D-1-thioglucopyranoside

* Corresponding author. Tel.: +52 777 3291635.
E-mail address: bravo@ibt.unam.mx (A. Bravo).

0005-2736/$ – see front matter © 2009 Elsevier B.V. All rights reserved.
doi:10.1016/j.bbamem.2009.06.014

impaired in its pore formation activity and in its toxicity against susceptible insect larvae [4,10], suggesting that the oligomeric toxin pore plays a major role in the mode of action of Cry toxins in lepidopteran larvae.

Different Cry toxins active against different insect orders showed a similar mechanism of action, since they also form oligomeric structures after interaction with their protein receptors [5,11–16]. In the case of other pore-forming toxins produced by other bacteria, an oligomeric pre-pore structure is also produced after receptor binding. This oligomeric structure represents a toxin intermediate before insertion into the membrane [17].

The primary threat to the long-term efficacy of Bt-toxins is the evolution of resistance by pests. Previously we showed that engineered variants of Cry1A toxins modified to lack amino terminal end, including helix α-1 (Cry1AbMod and Cry1AcMod) are able to form oligomers after proteolysis in the absence of cadherin receptor [18]. These Cry1AMod toxins kill resistant insects affected in cadherin gene such as *Pectinophora gossypiella*. Cry1AMod toxins also kill *M. sexta* larvae with reduced cadherin expression after RNA interference using a cadherin-dsRNA [18]. However, the mechanism of action of Cry1AMod toxins was not previously analyzed. In order to propose the use of Cry1AMod toxins in the field as an alternative to control insect resistance to Cry toxins, it is important to demonstrate that they work with a similar mechanism as the approved unmodified Cry1A toxins. In this regard it is important to characterize the different steps in Cry toxin action that take place after cadherin interaction such as binding to GPI-anchored receptors, structural organization of oligomers and pore formation activity.

In this work we took advantage that Cry1AMod toxins oligomerize in the absence of primary receptor interaction to study the limiting factors affecting oligomer formation. We characterized the oligomer of Cry1AbMod by analyzing binding to aminopeptidase N receptor and its pore formation activity and determined some structural aspect of the membrane-associated oligomer by tryptophan fluorescence spectroscopy and by negative staining of 2D crystals showing that they form a complex with a trimeric organization.

2. Experimental procedures

2.1. Preparation of liposomes

Egg-yolk phosphatidylcholine (PC) at 2.6 μmol final concentration from a chloroform stock (Avanti Polar Lipids, Alabaster, AL), was dried by argon flow evaporation followed by overnight storage under vacuum to remove residual chloroform. The lipids were hydrated in 2.6 ml of 150 mM KCl, and 10 mM CHES at pH 9, for 5 min followed by vortex. To prepare small unilamellar vesicles (SUV) the lipid suspension was subjected to sonication three times for 3 min in a Branson-1200 bath sonicator (Danbury, CT). Liposomes were used within 48 h upon their preparation, where they remained stable and showed similar capacitance values. Liposomes were prepared by keeping the total lipid concentration at 1 mM and diluted to the required concentration just before use. Calcein containing vesicles were prepared by sonication of the SUV liposomes in 80 mM calcein (Molecular Probes, Eugene Oregon), three times for 3 min, dissolved in 150 mM KCl, and 10 mM CHES at pH 9. In order to remove the non-entrapped calcein, 650 μl of the calcein-vesicle suspension were loaded to a gel filtration Sephadex G-50 column (1×15 cm) and eluted with the same buffer.

2.2. Purification of Cry1AbMod and wild type Cry1Ab toxins

Bt transformants containing cry1AbMod or cry1Ab genes were grown for 3 days at 30 °C in HCT sporulation medium supplemented with 10 μg/ml erythromycin. The HCT medium contained ($g\,l^{-1}$): Bacto Tryptone (Difco), 5; Casamino acids (Difco), 2; KH_2PO_4, 3.4; $MgSO_4.7H_2O$, 0.012; $MnSO_4.4H_2O$, 0.0003; $ZnSO_4.7H_2O$, 0.0028; the pH was adjusted to 7.2. After sterilization $Fe(SO_4).7H_2O$, 0.02; $CaCl_2.2H_2O$ 0.147 and glucose 3; were added ($g\,l^{-1}$). The Bt strain expressing Cry1AbMod toxin produced bipyramidal crystals similar to the wild type Cry1Ab toxin. After sporulation, Cry1AbMod and Cry1Ab crystals were purified by sucrose gradients [19] and protoxins were solubilized in different pH conditions, as follows: 100 mM Tris–HCl, 0.2% β-mercaptoethanol pH 8.5; or 100 mM CHES, 0.2% β-mercaptoethanol pH 9.0; 80 mM $NaHCO_3$, 20 mM Na_2CO_3, 0.2% β-mercaptoethanol pH 10 or pH 10.5; 100 mM piperidine 0.2% β-mercaptoethanol pH 11, 100 mM NaH_2PO_4, 0.2% β-mercaptoethanol pH 12 or 100 mM NaOH pH 12. Protoxin activation was performed by 1 h incubation with trypsin at 37 °C at different pHs as indicated in the results section, either in the presence or in the absence of PC-SUV (5000:1 lipid:protein ratio). Proteolysis was stopped by adding 1 mM phenylmethylsulfonyl fluoride (PMSF). For the production of wild type Cry1Ab oligomer, Cry1Ab protoxin was activated with 0.5% *M. sexta* midgut juice in the presence of scFv73 antibody (1:4 protein:antibody ratio) as reported previously [5]. For pore formation assays in black lipid bilayers the Cry1Ab or Cry1AbMod oligomeric structures were produced in the presence of PC-SUV to recover membrane-inserted oligomer as previously described [10]. For ELISA binding assays or tryptophan fluorescence determinations, oligomer was prepared in the absence of PC-SUV to recover soluble oligomer. The oligomeric structure was further purified by size-exclusion chromatography with a Superdex 200 HR 10/30 (Amersham Pharmacia Biotech, Uppsala, Sweden) FPLC size-exclusion column as described [5]. The purified Cry1Ab and Cry1AbMod oligomeric structure eluted in fractions 9–11 of the column, while monomeric structure eluted in fractions 16–18 as previously reported [5,10]. Protein concentration was determined by the Bradford assay using bovine serum albumin as standard and the extinction coefficient method where $E_m^{280} = 5700\ M^{-1}/cm^{-1}$ for Cry1Ab toxin.

2.3. Western blot

Protein samples were boiled for 5 min in Laemmli sample loading buffer, separated in SDS-PAGE and electrotransferred onto PVDF membrane (Millipore, Bedford, MA). The Cry1Ab and Cry1AbMod proteins were detected using polyclonal anti-Cry1Ab antibody (1/15,000, for 1 h) followed by a secondary antibody coupled with horseradish peroxidase (HRP) (Sigma, St Louis, MO) (1/5000, 1 h). This polyclonal anti-Cry1Ab antibody was obtained as reported [20] from a New Zealand white rabbit immunized with a Cry1Ab sample containing a mixture of Cry1Ab monomeric and oligomeric structures obtained after proteolytical activation in the presence of scFv73 antibody. This antiserum readily recognized the 250-kDa oligomer and the 60 kDa monomeric toxin, in contrast to other polyclonal antibodies obtained by immunizing with trypsin activated Cry1Ab toxin. Blots were revealed with luminol (ECL; Amersham Pharmacia Biotech) as described by the manufacturers. Molecular weight markers used in all SDS-PAGE were precision pre-stained plus standards all blue (BioRad, Hercules CA).

2.4. Tryptophan fluorescence emission assays

Analysis of the Trp fluorescence emission of Cry1Ab or Cry1AbMod oligomer inserted in SUV membranes was done by adding SUV to the protein suspension of pure soluble-oligomer in the cuvette to get a ratio of 5000 (lipid:protein). After liposome addition, 1 h of incubation at room temperature was allowed before liposome vesicles were recovered by ultracentrifugation at 100,000 ×*g* and suspended in the same volume. The Trp emission spectra were performed as previously described [9], three to four scans were recorded and corrected for background and dilution. The membrane suspension was subject to spectrum acquisition. Controls of oligomeric Cry1AbMod incubated in the absence of membrane was performed, showing that protein remain in solution under these experimental conditions. Control

spectra from SUV alone were performed under the same conditions and subtracted from the respective protein spectra.

2.5. Purification of aminopeptidase N (APN)

The brush border membrane APN was purified from *M. sexta* BBMV [21] isolated from 5th instar larvae. The BBMV were solubilized 2 h at 4 °C in 20 mM Tris–HCl at pH 8.5 containing 100 mM NaCl, 5 mM EDTA, 1 mM PMSF, and 1% CHAPS. After detergent solubilization of BBMV the APN protein was purified using a mono-Q column as previously reported [22]. Briefly, the samples were centrifuged 1 h at 90,000 ×*g* and the supernatants containing the CHAPS-solubilized proteins were concentrated by Amicon YM-50 ultrafiltration. A 2 ml aliquot was applied to a HR 5/10 mono-Q column equilibrated with 20 mM Tris–HCl at pH 8.5 buffer containing 2 mM $MgCl_2$, 2 mM KCl. The column was eluted with a NaCl gradient (0.5–1 M) with a flow rate of 1 ml per min for 40 min. APN activity was assayed using L-leucine-*p*-nitroanilide (LpNA) as substrate [23]. Fractions containing APN activity were pooled and concentrated by Amicon YM-50 ultrafiltration. Quality of APN purification was observed in SDS-PAGE.

2.6. Toxin overlay assays

Protein blot analysis was done as described previously [20]. The pure APN protein sample (1.3 μg) was separated by 10% SDS-PAGE and electrotransferred to nitrocellulose membranes PVDF (Millipore, Bedford MA). After renaturation and blocking, blots were incubated for 2 h with 10 nM of biotinylated Cry1A toxins in washing buffer (1% Tween 20 in PBS) at room temperature. Unbound toxin was removed by washing three times for 10 min in washing buffer (1 ml) and bound toxin was identified by streptavidin-peroxidase conjugate (1:5000) for 1 h and visualized using luminol (ECL, Amersham) as described by manufacturers.

2.7. ELISA binding assays

ELISA plates, 96-wells, were coated with 10 ng of the purified APN in PBS buffer. After 12 h incubation at 4 °C, 200 μl PBS containing 2% non-fat dry milk was added to each well and incubated for 2 h at 37 °C. The ELISA plate was washed three times with PBS buffer, followed by 1 h incubation with different concentrations (0.6–5 nM) of oligomeric Cry1Ab or Cry1AbMod toxins at 37 °C. The unbound toxin was removed by three times washing and the ELISA plate was incubated 1 h with anti-Cry1Ab antibody (1:20,000) at 37 °C. After three times washing, the secondary antibody coupled to HRP-peroxidase (1:10,000) was added for 1 h at 37 °C. ELISA plates were finally washed three times. The HRP enzymatic activity was revealed with a freshly prepared substrate (40 mg of *o*-phenylenediamine, 18 ml of H_2O_2 in 100 ml of 100 mM NaH_2PO_4, at pH 5.0). The enzymatic reaction was stopped with 6 N HCl and the absorbance read at 490 nm with a Pharmacia LKB Ultraspec II. Binding of monomeric Cry1Ab was used as control in these experiments showing no binding under this concentration range (data not shown).

2.8. Pore formation activity with calcein release assay

Calcein leakage experiments were performed as described [9]. Briefly, 10 μl of calcein-loaded liposomes were added to 900 μl of 150 mM KCl, CHES 10 mM, and 2.5 mM $CaCl_2$, at pH 9. Calcein fluorescence was excited at 490 nm and monitored at 520 nm (4 nm slit) with an Aminco Bowman Luminescence Spectrometer (Urbana IL). The soluble oligomeric toxin samples were added and the release of calcein was analyzed. The released calcein induced an increase in fluorescence due to the dequenching of the dye after release into the external medium. Maximal leakage at the end of each experiment was assessed by adding 0.1% Triton-X-100 that clarify the SUV solution. All fluorescence experiments were performed in quadruplicate at 20 °C.

2.9. Pore forming activity in black lipid bilayers

Black lipid bilayers were made as previously reported [9,24] with egg derived PC. Bilayer capacitance values were between 250 and 300 pF. Buffers 300 mM KCl, and 10 mM CHES, at pH 9 and 10 mM KCl, and 10 mM CHES, at pH 9 were added to the cis and trans compartments, respectively. Once a bilayer was formed, the activated Cry1AbMod or Cry1Ab toxins in SUV were added to the cis compartment; the trans compartment was held as reference ground. All experiments were performed at room temperature. Single-channel currents were recorded with a Dagan 3900A patch-clamp amplifier (Dagan Corp.; Minneapolis, MN). Currents were filtered at 200 or 500 Hz, digitalized on-line at 1 or 2 kHz, and analyzed using a Digidata 1200 interface and Axotape and pClamp software (Axon Instruments, Foster City, CA).

2.10. 2D crystallization of Cry1AbMod oligomers

Purified Cry1AbMod protoxin was diluted to a final concentration of 1.5 mg/ml in 80 mM $NaHCO_3$, and 20 mM Na_2CO_3, at pH 10.5 containing trypsin at a final dilution of 1:20 (trypsin:protoxin) and a PC-SUV to protein mass ratio of 0.5 in a total volume of 100 μl. The reaction was incubated 2 h at 37 °C with slow agitation. Reaction was stopped with PMSF 0.1 mM (final concentration) and centrifuged 1 h at 100,000 ×*g*, 4 °C. The membrane pellet was suspended in 80 mM $NaHCO_3$, 20 mM Na_2CO_3, and 50 mM octyl-β-D-1-thioglucopyranoside (OTG) at pH 10.5. Finally detergent was removed by adding 0.015 g biobeads SM2 (25–50 mesh from BioRad Hercules CA) every 4 h during 24 h (6 additions) at 16 °C with slow agitation.

2.11. Electron microscopy

Five microliters of the protein samples was placed onto carbon-formvar-coated copper grids G400/Cu 400 mesh square, excess liquid was drained off with filter paper upon which the specimen was stained with 20 μl of 2% (w/v) uranyl acetate (pH 4.25) for a few seconds and blotted dry. Specimens were observed in a Jeol 1200 EX transmission electronmicroscope operated at 100 kV. Electron micrographs were recorded at a calibrated magnification of 37,800×. Selected micrographs were digitized at increments so that one pixel corresponded to 5.29 Å at the specimen level. Images were analyzed and projection maps calculated using the software package CRISP [25].

2.12. Bioassays

Insect toxicity of Cry1Ab and Cry1AbMod toxins was assayed with first instar *M. sexta* larvae by the diet-surface contamination procedure. The protoxins Cry1Ab and Cry1AbMod were solubilized at pH 10.5. A constant volume of the sample dilutions in water (35 μl) was applied onto the diet surface contained in 24-well polystyrene plates (Cell Wells, Corning Glass Works, Corning NY). One first instar larva was added per well and one 24-well plate was used per toxin concentration. The plates were incubated at 28 °C, 65 ± 5% of relative humidity, and a light:dark photoperiod of 16:8 h. Mortality of *M. sexta* larvae was recorded after seven days. *Aedes aegypti* and *Anopheles albimanus* mosquitoes were reared at 28 °C, 87% RH and 12:12 h light: dark photoperiod. Twenty early fourth-instar larvae were placed in 100 ml of dechlorinated water. Spore–crystal complex of Cry1Ab or Cry1AbMod were used in the mosquito-bioassays (three repetitions). A negative control of dechlorinated water was included. *A. aegypti* and *A. albimanus* larvae were incubated at 28 °C and mortality was examined after 24 h. A positive control of *Bt subsp. israelensis* was included in the bioassay. The mean lethal concentration (LC_{50}) was

estimated by Probit analysis using statistical parameters [26] after four independent assays (Polo-PC LeOra Software).

3. Results

3.1. Effect of pH on the oligomerization of Cry1AbMod toxin

We have previously shown that Cry1AbMod protoxin forms oligomers when activated with trypsin in the absence of cadherin receptor in contrast with Cry1Ab toxin [18]. Since pH is an important determinant of protein flexibility, we analyzed the effect of pH in toxin oligomerization. In the case of the wild type Cry1Ab toxin, it was previously shown that alkaline pH increased the flexibility of monomeric toxin [9]. The pH of the midgut lumen of lepidopteran insect *M. sexta* was measured and shown to be alkaline pH 10. In order to analyze the effect of pH on the formation of oligomeric structure, the Cry1AbMod toxin was proteolytically activated with trypsin at different pH. Oligomerization was analyzed as the formation of SDS-resistant aggregates of 250 kDa in SDS-PAGE as previously reported for different Cry toxins [5,11–16]. Several bacterial pore-forming toxins such as PA-anthrax toxin, aerolysin and α-toxin also formed oligomeric structures that could be observed in SDS-PAGE [17]. Fig. 1

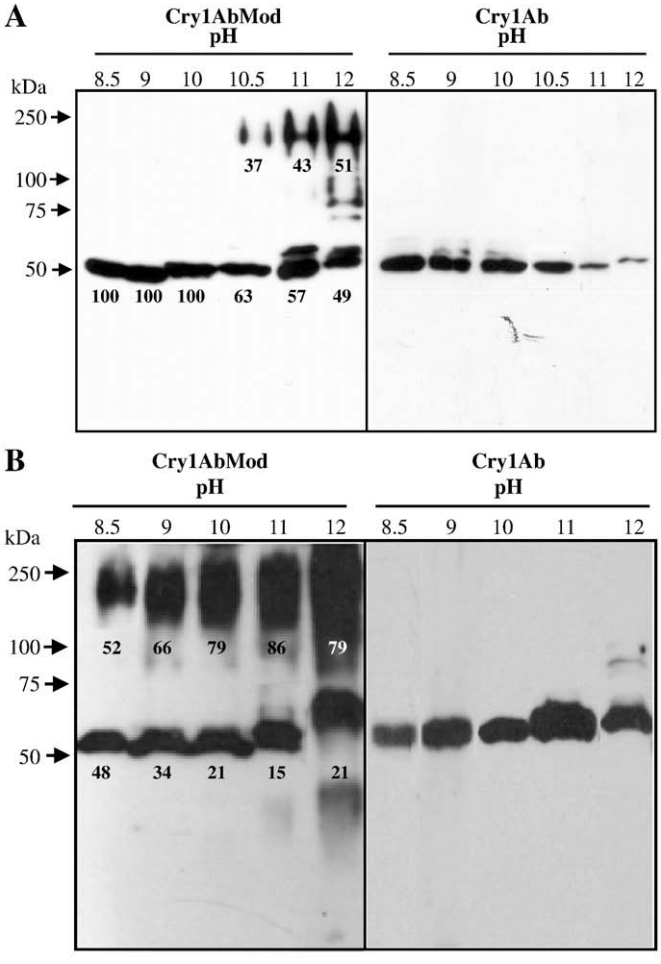

Fig. 1. Activation of Cry1AbMod and Cry1Ab with trypsin at different pH. The presence of 250 kDa oligomeric structure was evaluated by western blot assay using specific anti-Cry1Ab polyclonal antibody. Activation pH is indicated on the top of each lane. Five micrograms of protein was loaded in each lane (SDS-PAGE 8% poyacrylamide gels). Panel A activation in solution. Panel B activation in the presence of PC-SUV liposomes at a 5000:1 lipid:protein ratio. Numbers within the images represent the percentage of signal of oligomeric vs. monomeric bands determined by scanning optical density of bands in the blots.

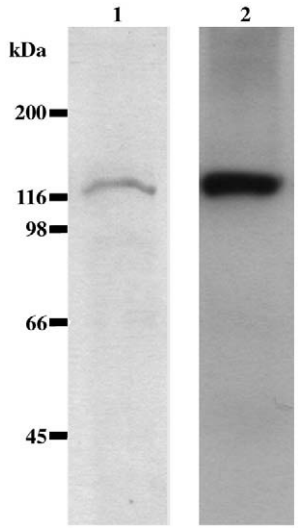

Fig. 2. Analysis of APN purification from *Manduca sexta* BBMV. Lane 1, SDS-PAGE 10% polyacrylamide electrophoresis of purified APN sample stained with coomasie blue staining. Lane 2, binding of biotinylated Cry1Ab to APN sample in toxin overlay assay revealed after incubation with streptavidin-peroxidase conjugate and visualized with luminol as described in Experimental procedures.

shows that Cry1AbMod toxin could form oligomeric structures after trypsin activation in the absence cadherin receptors. This figure also shows that the oligomerization of this protein increased when incubation was done at high pH in contrast with incubations at pH 8.5. As expected, the wild type Cry1Ab toxin did not form oligomeric structures after activation with trypsin (Fig. 1A). In addition, we found that the presence of PC-SUV during toxin activation provide a membrane substrate in which the toxin could bind and form pores, facilitating the production of the oligomeric structure (Fig. 1B). The relative proportion the oligomeric and the monomeric structures of Cry1AbMod after activation in the presence or absence of PC-SUV was determined by scanning optical density of the bands in the blots, showing that in the presence of PC-SUV the ratio of oligomeric/monomeric structure was enhanced.

3.2. Fluorescence Trp emission of Cry1AbMod oligomer

In order to analyze if the Cry1AbMod oligomer is structurally similar to the oligomeric structure of the wild type Cry1Ab, the Trp fluorescence emission of this protein was analyzed in the soluble pre-pore and in the membrane-associated state. The emission maximum of the oligomeric structure of Cry1AbMod in solution was at 333 nm, which corresponds exactly with the previously reported emission maximum for the oligomer of Cry1Ab toxin [9].

The emission spectrum of Cry1AbMod membrane-associated oligomer, was performed after incubation of the oligomeric structure with PC-SUV using a lipid:protein ratio of 5000 since it was previously reported that the threshold limit for partition of Cry1Ab oligomer into the SUV was a lipid:protein ratio of 3000 [9]. The membrane fraction was separated by ultracentrifugation and fluorescence spectra were recorded in the pellet fraction. The oligomeric Cry1AbMod has a blue shift of 5 nm in the emission spectrum λ_{max} from 333 nm in solution to 328 nm when inserted into SUV liposomes, indicating a more hydrophobic environment for some of the Trp residues. A similar shift in the maximal emission spectrum of the wild type Cry1Ab membrane-inserted oligomer was also observed. These data indicate that structure of the oligomer formed by the Cry1AbMod toxin is similar to that of the wild type Cry1Ab toxin.

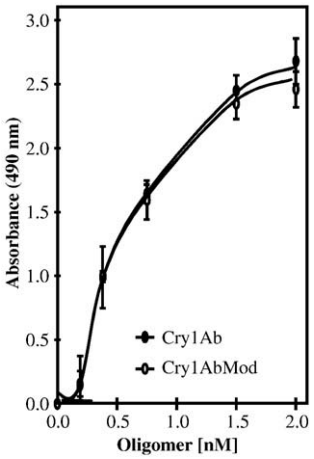

Fig. 3. ELISA binding of Cry1Ab and Cry1AbMod oligomers to purified APN from *Manduca sexta* midgut microvilli. ELISA plates were coated with purified APN and then incubated with different concentrations of Cry1Ab or Cry1AbMod oligomers (0.6–5 nM). Bound Cry1Ab oligomer (black squares ■) or Cry1AbMod oligomer (white squares □) were detected with anti-Cry1Ab antibody followed by a secondary goat-anti-rabbit-HRP antibody.

3.3. Binding of Cry1AbMod and Cry1Ab oligomeric structures to APN receptor

We have previously reported that Cry1Ab oligomer binds a protein extract enriched in *M. sexta* APN activity with 0.7 nM apparent binding affinity (K_D). In contrast, the monomeric toxin binds this protein extract with 160 nM K_D [6]. We purified APN protein from 5th instar larvae as described in experimental procedures and the fractions with APN activity were analyzed by SDS-PAGE 10% polyacrylamide revealing a single band of 120 kDa (Fig. 2, lane 1). This sample lacks alkaline phosphatase activity (data not shown). The quality of the purified APN sample was also tested by analyzing the binding of biotinylated Cry1Ab toxin, in toxin overlay assays, showing that Cry1Ab only binds to the 120-kDa band indicating that no other Cry1Ab-binding proteins were present in the APN sample (Fig. 2, lane 2). To study the interaction of Cry1Ab and Cry1AbMod oligomeric structures with the purified APN sample, the binding of different concentrations of these proteins was analyzed by ELISA assays. Fig. 3 shows that both, Cry1Ab or Cry1AbMod oligomeric structures bound to the *M. sexta* APN with a similar high affinity indicating also that the Cry1AbMod oligomer is structurally similar to that of Cry1Ab.

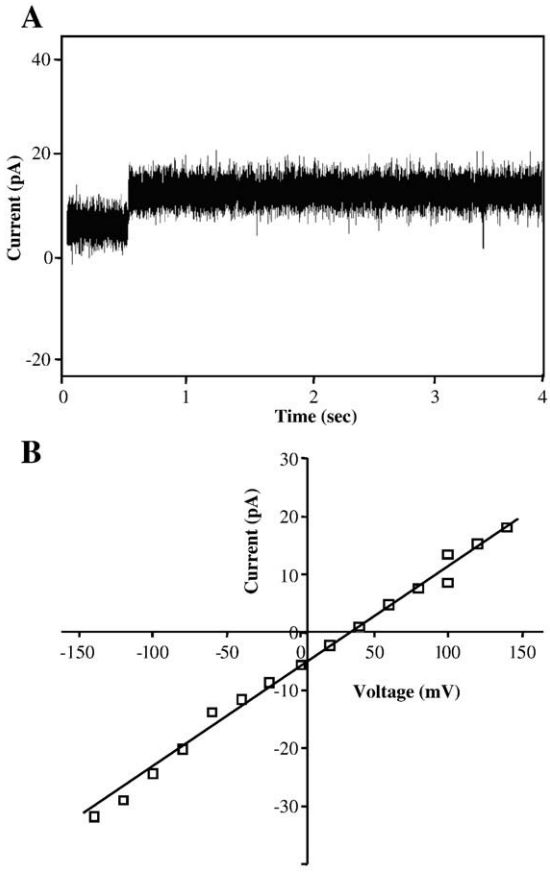

Fig. 5. Ionic currents induced by oligomeric structure of Cry1AbMod in planar lipid bilayers. Panel A, Representative ionic channel records of most common transitions induced by Cry1AbMod toxins in lipid bilayers. The observed responses showed stable channels with high open probability. Records were obtained in 300:10 mM KCl (cis: trans), 10 mM CHES pH 9. Panel B, Current/voltage (I/V) relationship of currents induced by the Cry1AbMod toxin.

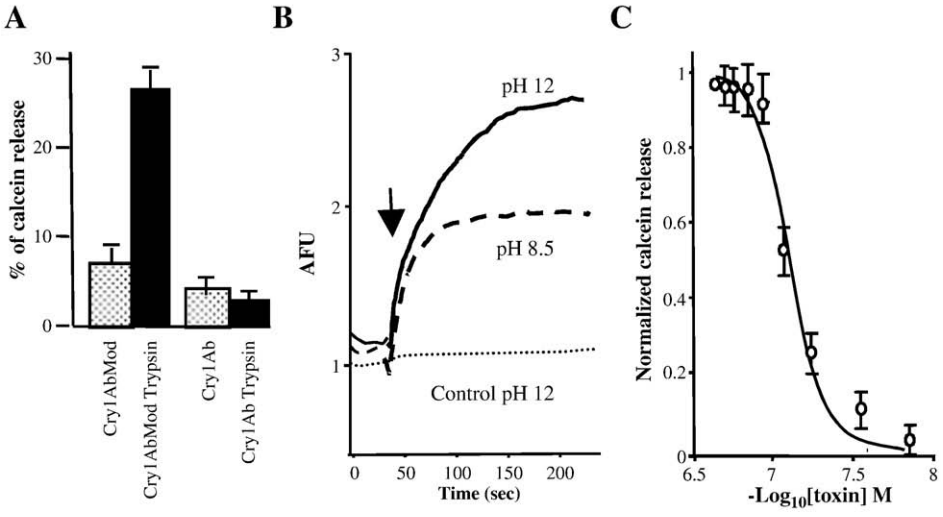

Fig. 4. Pore formation activity of Cry1Ab or Cry1AbMod analyzed by calcein release assays. Panel A, analysis of calcein released by trypsin activated samples of Cry1Ab or Cry1AbMod at pH 10.5. 50 nM of Cry1Ab or Cry1AbMod protoxins (dotted bars) or trypsin activated proteins (black bars) were used in these experiments. Maximal leakage at the end of each experiment was assessed with 0.1% Triton-X-100. Panel B, Pore formation activity of the Cry1AbMod as a function of the pH used during toxin activation. The effect of Cry1AbMod on the integrity of lipid membrane vesicles was determined by the calcein release assay performed at pH 9.0 using toxin samples activated at different pH with trypsin as stated in the figure. Control is same amount of buffer. Arrow indicates toxin addition. Panel C, Dose–response curve of Cry1AbMod toxin activated at pH 10.5 with trypsin and analyzed using the calcein release assay at pH 9.0.

3.4. Pore formation activity of activated Cry1AbMod

To further analyze the functionality of Cry1AbMod oligomer, we analyzed its pore formation activity using two different procedures, the calcein release assay and measurement of ionic-conductance in planar lipid bilayers. We first analyzed the release of entrapped calcein from liposomes due to the formation of pores by toxin oligomers. The dequenching of the calcein fluorescence was monitored continuously as an increase in the fluorescence intensity. Data are expressed as percentage of the maximal fluorescence release, obtained with the positive control 1% Triton-X-100. The analysis of calcein release induced by trypsin activated-Cry1AbMod is shown in Fig. 4. Cry1AbMod trypsin activated toxin induced a significant release of calcein from loaded liposomes. In contrast the Cry1AbMod protoxin, Cry1Ab protoxin and the Cry1Ab trypsin activated protein showed a minor response (Fig. 4A). We then assayed the pore formation activity of the Cry1AbMod samples activated with trypsin at different pH, in order to analyze if oligomer formation correlated with pore formation activity. Fig. 4B shows that Cry1AbMod toxin showed a more efficient response after activation at pH 12 in contrast to pH 8.5, correlating with the increased production of oligomeric structure in this condition. Finally, the dose–response curve of Cry1AbMod toxin that was activated at pH 10.5 is presented in Fig. 4C. A direct correlation of calcein released from the SUV with the concentration of Cry1AbMod toxin showed that the half maximal effective concentration at which 50% of calcein has been released (EC_{50}) was 54.2 nM.

In addition, the induced ionic channel activity Cry1AbMod was also examined in synthetic planar lipid bilayers. We recorded the current amplitude using protein samples that were activated with trypsin at pH 10.5 in the presence of SUV liposomes. Control sample containing only SUV gave a no-response. These experiments were performed in a KCl gradient 300/10 mM in the cis/trans compartments to facilitate liposome fusion in the bilayer. The conductance of Cry1AbMod was 6.0 pS similar to the wild type toxin that showed a value of 7.5 pS [9]. The ionic currents in these experiments revealed that oligomeric structure of Cry1AbMod produced stable channels with high open probability (Fig. 5) that are similar to the previously described pores induced by Cry1Ab wild type oligomer [9].

3.5. Lipid associated structure of Cry1AbMod oligomer

Since the results reported so far indicated that the oligomeric structure of Cry1AbMod analyzed by Trp emission, pore formation and receptor interaction resembles that of the wild type Cry1Ab oligomer,

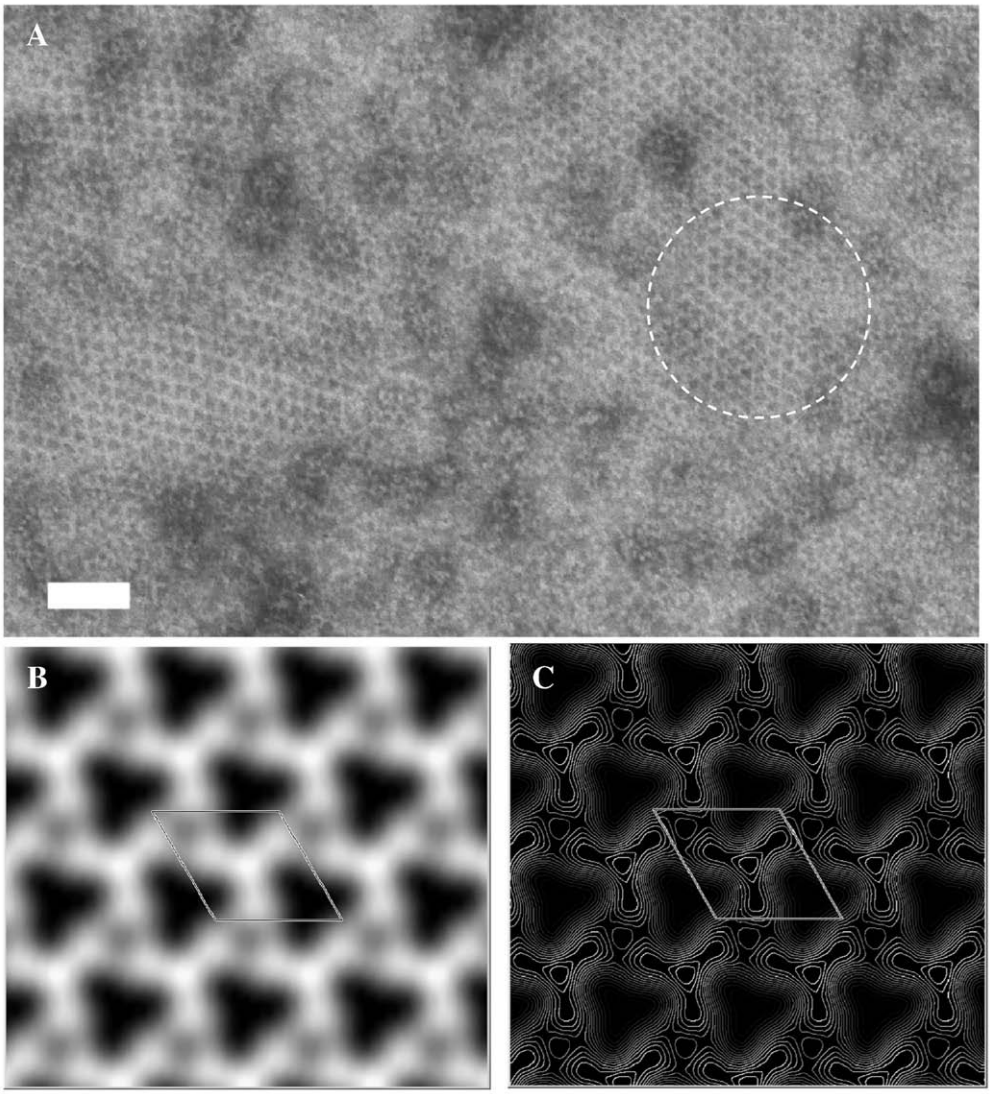

Fig. 6. Analysis of the structure of the lipid associated Cry1AbMod oligomer. Panel A, Electron micrograph of negatively stained 2D crystals. The scale corresponds to 50 nm and the area marked by a dashed circle was used for calculating the Fourier projection map shown in panel B (half tone) and panel C (contour lines). There is one trimer per $a = b = 107$ Å unit cell.

Table 1
Toxicity of wild type Cry1Ab and modified Cry1AbMod toxins against *Manduca sexta*, *Anopheles albimanus* and *Aedes aegypti* larvae.

δ-endotoxin	*Manduca sexta* ng/cm^2 (95% confidence limits)	*Anopheles albimanus* μg/ml	*Aedes aegypti* μg/ml
Cry1Ab	1.9 (0.99–2.47)	>10	>10
Cry1AbMod	3.2 (1.4–5.4)	>10	>10

we decide to use the Cry1AbMod toxin to analyze the membrane-associated structure of the oligomer by electron crystallography. We took advantage that Cry1AbMod toxin forms oligomeric structure in the absence of any other protein as cadherin receptor that could potentially interfere with the formation of ordered arrays. We induced the formation of two-dimensional (2D) crystal of Cry1AbMod that allow us to determine the structural organization of the membrane-inserted pore. The 2D crystals were obtained after toxin insertion into PC membrane as reported in experimental procedures section. This method involves removing the detergent from the micellar solution containing the protein and the lipids. We used hydrophobic adsorption of detergent onto polystyrene Bio-beads SM2 as previously described [27]. Ordered arrays of the membrane-associated toxin were observed with $a = b = 107$ Å and $\gamma = 120°$ calculated in p3, and the calculated projection map displayed an organization resembling a trimeric propeller (Fig. 6).

3.6. Toxicity of Cry1AbMod toxin

The Cry1AbMod toxin was tested in bioassays against the lepidopteran larvae, *M. sexta*. We also analyzed toxicity against two different dipteran larvae, *A. aegypti* and *A. albimanus*. The specificity of Cry1AbMod did not change since no toxicity was observed against *A. aegypti* or *A. albimanus* mosquito larvae and similar toxicity of the Cry1Ab was observed against *M. sexta* larvae (Table 1).

4. Discussion

The Cry1AbMod is essentially identical to its parental Cry1Ab protoxin with the exception that 56 amino acids from the amino terminal end were removed by genetic engineering [18]. The most important characteristic of these Cry1AMod toxins is that they are able to kill resistant insects that are affected in cadherin gene, representing a viable alternative in the control of insects that become resistant to wild type Cry1A toxins. Although it was demonstrated that Cry1AMod toxins formed oligomeric structures in the absence of cadherin receptor, the other steps in the toxin mode of action such as binding interaction with the APN receptor and its pore formation activity were not analyzed before. In this work we analyzed these parameters and also analyzed the structural conformation of the membrane-inserted oligomer.

4.1. Analysis of oligomerization of Cry1AbMod toxin

Our results show that the oligomerization process is facilitated by alkaline pH and in the presence of membrane lipids. These data are interesting since the *in vivo* pH of the midgut lumen of Lepidopteran insects is also highly alkaline (up to pH 11) [3], suggesting that pH may play an important role during toxin activation and oligomerization *in vivo*.

It was previously demonstrated that alkaline pH increase the flexibility of the monomeric and oligomeric form of Cry1Ab toxin [28,29], by showing that Cry1Ab toxin was highly susceptible to denaturation with low urea concentrations only at alkaline pH [28,29]. These data suggest that alkaline pH in the midgut lumen of susceptible larvae may facilitate a looser conformation of the Cry1Ab toxin that is important to trigger oligomerization and therefore for active channel formation. Interestingly, in the case of colepteran specific Cry3A toxin, the acidic pH that induced unfolding of this toxin correlated with the acidic pH that is present in the midgut lumen of susceptible Coleopteran larvae [30]. Similarly, in the case of other pore-forming toxins active against mammalian cells, it was shown that they must partially unfold to facilitate pre-pore formation [17,31–33]. These toxins unfold under acidic pH conditions, correlating with the acidic pH that these toxins encounter upon cell internalization in acidic membrane compartments [17,31–33].

Other Cry toxins besides Cry1A toxins form oligomeric structures when they were activated in the presence of their natural receptor. This is the case of Cry1Aa, Cry1Ab, Cry1Ca, Cry1 Da, Cry1Ea and Cry1Fa toxins active against *M. sexta*, that form oligomers after activation in the presence of *M. sexta* BBMV [4,5,7,11–13]. An oligomeric structure of Cry1C was observed when it was activated in the presence of *Spodoptera exigua* BBMV [13] and oligomers of Cry1Aa were observed when activated in the presence of *Bombyx mori* BBMV [34]. The colepteran specific Cry3 toxins, formed oligomeric structures after activation in the presence of the susceptible insect *Leptinotarsa decemlineata* BBMV [14]. Finally, in the case of the dipteran specific toxins, the Cry11Aa form oligomers of 250 kDa after activation in the presence of the mosquito *A. aegypti* BBMV [15]. The Cry4Ba also formed oligomeric structures after activation [16]. In all cases the presence of oligomers correlated with higher K^+ permeability, in contrast with monomeric toxins [5,9,11,14,15]. These data support the hypothesis that the formation of a pre-pore oligomer is a conserved mechanism on different members of the Cry family and that is an intermediate responsible for pore formation.

4.2. Characterization of oligomeric structure of Cry1AbMod

In this work we show that the Cry1AbMod oligomer has a similar conformation as the wild type Cry1Ab oligomer structure both in solution and in the membrane-inserted state as judged by tryptophan fluorescence emission analysis. We are also reporting that Cry1AbMod oligomer binds APN with high affinity as the wild type Cry1Ab oligomer and that they show similar pore formation activity. The Cry1AbMod toxin produces stable channels in black lipid bilayers with high open probability and similar conductance to the previously reported pores of Cry1Ab toxin [9]. These data confirm that Cry1AbMod toxin shares a similar mode of action as Cry1Ab toxin.

We took advantage that Cry1AMod toxins are more efficient to form oligomeric structure *in vitro* in absence of receptor protein to improve oligomer formation and to study its conformation by electron crystallography. The composition of the Cry1Ab oligomer was previously suggested to be comprised of four monomers based on molecular weight of the oligomeric structure as determined by SDS-PAGE [5]. However, 2D crystallographic analysis performed here, show a trimeric organization of the membrane-associated structure of the Cry1AbMod. These results are in agreement with the previously described organization of the membrane-associated Cry4Ba [35], where calculated projection structures from 2D crystal patches analyzed by electron crystallography at 17 Å resolution showed also a trimeric organization [35]. The projection map presented herein highlights propeller-like densities similar to the ones reported by Ounjai et al. [35] albeit with distal domains that are somewhat narrower. This overall architecture and assembly pattern is in contrast to the structure of Cry1Aa trypsin activated-toxin analyzed by Atomic Force Microscopy (AFM), for which a structure composed of four subunits surrounding a 1.5 nm diameter central depression was reported [36]. However, it is important to mention that the AFM studies were performed with Cry1Aa inserted into monolayer membranes, which may cause some artifacts.

Recently, based on sensitivity of membrane-inserted toxin to protease and determination of fluorescence quenching measurements

of fluorescent-labeled cysteine mutants in different regions of Cry1Ab toxin, it was suggested that the three domains of this protein insert into the membrane [37]. However, other studies suggest that only domain I may be inserted into the membrane and that domain III is exposed to the solvent [28,38]. Specifically, quenching studies of Trp fluorescence of Cry1Ac with the soluble quencher KI clearly demonstrate that at least Trp545 located in domain III is exposed to the solvent when the oligomeric Cry1Ac toxin is inserted into the membrane [38]. Evidently more studies are necessary and the description of the structure of the membrane-inserted pore of Cry1A toxins is necessary to determine the exact architecture of the pore and define the regions of the toxin that participate in membrane insertion.

4.3. Insecticidal activity of Cry1AbMod

The Cry1AbMod toxin was shown to kill a *P. gossypiella* resistant population whose resistance was linked to deletions in the cadherin gene [18,39]. We show here that Cry1AbMod is not toxic to mosquito larvae and retain similar toxicity against the susceptible *M. sexta* larvae, indicating that the spectrum of action of Cry1AbMod toxins was not drastically modified. The toxicity of Cry1AbMod against *M. sexta* was slightly lower but since 95% confidential limits are overlapping, we may conclude that both proteins showed similar insecticidal activity. These results suggest that although the modified Cry1AbMod do not require interaction with the primary cadherin receptor, they did not become unspecific. It is possible that their specific interaction with the secondary GPI-anchored receptors such as APN play an important role in Cry1A toxins toxicity (Table 1).

4.4. Concluding remarks

The Cry1AMod toxins are toxic against insect pests that developed resistance to natural Cry1A toxins. In order to develop transgenic crops producing Cry1AMod toxins to counter insect resistance, it is important to show that the mechanism of action of Cry1AMod toxins is similar to the approved unmodified Cry1A toxins, that are currently used in different transgenic crops. Here we show that secondary steps in mode of action of Cry1Ab toxin, that take place after interaction with cadherin receptor, such as binding to aminopeptidase, oligomerization and pore formation of both proteins, Cry1A and Cry1AMod, are similar in Cry1AbMod toxin. This knowledge will be important for the future application of Cry1AMod toxins to counteract resistance to Bt-crops that may assure a long-term use of this environmental friendly technology, avoiding the use of harmful chemical pesticides in agriculture.

Acknowledgments

This work was supported in part by CONACyT U48631-Q, J45863-Q, J44962, 83135, and DGAPA IN222308 and NRI 2008-03980.

References

[1] A. Bravo, S.S. Gill, M. Soberón, Mode of action of *Bacillus thuringiensis* toxins and their potential for insect control, Toxicon 49 (2007) 423–435.
[2] E. Schnepf, N. Crickmore, J. Van Rie, D. Lereclus, J. Baum, J. Feitelson, D.R. Zeigler, D. H. Dean, *Bacillus thuringiensis* and its pesticidal crystal proteins Microbiol, Mol. Biol. Rev. 62 (1998) 775–806.
[3] J.A.T. Dow, Insect midgut function, Adv. Insect Physiol. 19 (1986) 187–238.
[4] A.I. Aronson, C. Geng, L. Wu, Aggregation of *Bacillus thuringiensis* Cry1A toxin upon binding to target insect larval midgut vesicles, Appl. Environ. Microbiol. 65 (1999) 2503–2507.
[5] I. Gómez, J. Sánchez, R. Miranda, A. Bravo, M. Soberón, Cadherin-like receptor binding facilitates proteolytic cleavage of helix α-1 in domain I and oligomer pre-pore formation of *Bacillus thuringiensis* Cry1Ab toxin, FEBS Lett. 513 (2002) 242–246.
[6] A. Bravo, I. Gómez, J. Conde, C. Muñoz-Garay, J. Sánchez, R. Miranda, M. Zhuang, S.S. Gill, M. Soberón, Oligomerization triggers binding of a *Bacillus thuringiensis* Cry1Ab pore-forming toxin to aminopeptidase N receptor leading to insertion into membrane microdomains, Biochim. Biophys. Acta 1667 (2004) 38–46.
[7] P.J. Knight, N. Crickmore, D.J. Ellar, The receptor for *Bacillus thuringiensis* Cry1Ac delta-endotoxin in the brush border membrane of the lepidopteran *Manduca sexta* is aminopeptidase N Mol, Microbiol. 11 (1994) 429–436.
[8] J.L. Jurat-Fuentes, M.J. Adang, Characterization of a Cry1Ac-receptor alkaline phosphatase in susceptible and resistant *Heliothis virescens* larvae, Eur. J. Biochem. 271 (2004) 3127–3135.
[9] C. Rausell, C. Muñoz-Garay, R. Miranda-CassoLuengo, I. Gómez, E. Rudiño-Piñera, M. Soberón, A. Bravo, Tryptophan spectroscopy studies and black lipid bilayer analysis indicate that the oligomeric structure of Cry1Ab toxin from *Bacillus thuringiensis* is the membrane-insertion intermediate, Biochemistry 43 (2004) 166–174.
[10] N. Jiménez-Juárez, C. Muñoz-Garay, I. Gómez, G. Saab-Rincon, J.Y. Damian-Alamazo, S.S. Gill, M. Soberón, A. Bravo, *Bacillus thuringiensis* Cry1Ab mutants affecting oligomer formation are non toxic to *Manduca sexta* larvae, J. Biol. Chem. 282 (2007) 21222–21229.
[11] C. Muñoz-Garay, J. Sánchez, A. Darszon, R.A. de Maagd, P.L. Bakker, M. Soberón, A. Bravo, Permeability changes of *Manduca sexta* midgut brush border membranes induced by oligomeric structures of different Cry toxins, J. Membr. Biol. 212 (2006) 61–68.
[12] N.J. Tigue, J. Jacoby, D.J. Ellar, The alpha-helix 4 residue, Asn135, is involved in the oligomerization of Cry1Ac1 and Cry1Ab5 *Bacillus thuringiensis* toxins, Appl. Environ. Microbiol. 67 (2001) 5715–5720.
[13] S. Herrero, J. González-Cabrera, J. Ferré, P.L. Bakker, R. de Maagd, Mutations in the *Bacillus thuringiensis* Cry1Ca toxin demonstrate the role of domains II and III in specificity towards *Spodoptera exigua* larvae, Biochem. J. 384 (2004) 507–513.
[14] C. Rausell, I. García-Robles, J. Sánchez, C. Muñoz-Garay, A.C. Martínez-Ramírez, M.D. Real, A. Bravo, Role of toxin activation on binding and pore formation activity of the *Bacillus thuringiensis* Cry3 toxins in membranes of *Leptinotarsa decemlineata* [Say], Biochem. Biophys. Acta 1660 (2004) 99–105.
[15] C. Pérez, C. Muñoz-Garay, L.C. Portugal, J. Sánchez, S.S. Gill, M. Soberón, A. Bravo, *Bacillus thuringiensis* subsp. *israelensis* Cyt1Aa enhances activity of Cry11Aa toxin by facilitating the formation of a pre-pore oligomeric structure, Cell. Microbiol. 9 (2007) 2931–2937.
[16] S. Likitvivatanavong, G. Katzenmeier, Ch. Angsuthanasombat, Asn183 in α5 is essential fro oligomerization and toxicity of the *Bacillus thuringiensis* Cry4Ba toxin, Arch. Biochem. Biophys. 445 (2006) 46–55.
[17] M.W. Parker, S.C. Feil, Pore-forming proteins: from structure to function, Progress Biophys. Mol. Biol. 88 (2005) 91–124.
[18] M. Soberón, L. Pardo-López, I. López, I. Gómez, B. Tabashnik, A. Bravo, Engineering modified Bt toxins to counter insect resistance, Science 318 (2007) 1640–1642.
[19] W.E. Thomas, D.J. Ellar, *Bacillus thuringiensis* var *israelensis* crystal δ-endotoxin: effect in insect and mammalian cells *in vitro*, J. Cell Sci. 60 (1983) 181–197.
[20] I. Gómez, I. Arenas, I. Benitez, J. Miranda-Ríos, B. Becerril, R. Grande, J.C. Almagro, A. Bravo, M. Soberón, Specific epitopes of Domains II and III of *Bacillus thuringiensis* Cry1Ab toxin involved in the sequential interaction with cadherin and aminopeptidase-N receptors in *Manduca sexta*, J. Biol. Chem. 281 (2006) 34032–34039.
[21] M. Wolfersberger, P. Lüthy, A. Maurer, P. Parenti, F.V. Sacchi, B. Giordana, G.M. Hanozet, Preparation and partial characterization of amino acid transporting brush border membrane vesicles from the larval midgut of the cabbage butterfly (*Pieris brassicae*), Comp. Biochem. Physiol. 86A (1987) 301–308.
[22] S. Sangadala, P. Azadi, R. Carlson, M.J. Adang, Carbohydrate analyses of *Manduca sexta* aminopeptidase N, co-purifying neutral lipids and their functional interaction with *Bacillus thuringiensis* Cry1Ac toxin, Insect Biochem. Mol. Biol. 32 (2001) 97–107.
[23] A. Lorence, A. Darszon, A. Bravo, The pore formation activity of *Bacillus thuringiensis* Cry1Ac toxin on *Trichoplusia ni* membranes depends on the presence of aminopeptidase N, FEBS Lett. 414 (1997) 303–307.
[24] P. Müeller, D.O. Rudin, H.T. Tien, W.C. Westcott, Reconstitution of cell membrane structure *in vitro* and its transformation into an excitable system, Nature 194 (1962) 979–980.
[25] S. Hovmöller, CRISP: crystallographic image processing on a personal computer, Ultramicroscopy 41 (1992) 121–135.
[26] D. Finney, Probit Analysis, Cambridge University Press, 1971, pp. 50–80.
[27] J.L. Rigaud, G. Mosser, J.J. Lacarpere, A. Olofsson, D. Levy, J.L. Ranck, Bio-Beads: and efficient strategy for two-dimensional crystallization of membrane proteins, J. Structural Biol. 118 (1997) 226–235.
[28] C. Rausell, L. Pardo-López, J. Sánchez, C. Muñoz-Garay, C. Morera, M. Soberón, A. Bravo, Unfolding events in the water-soluble monomeric Cry1Ab toxin during transition to oligomeric pre-pore and membrane inserted pore channel, J. Biol. Chem. 279 (2004) 55168–55175.
[29] D. Convents, M. Cherlet, J. Van Damme, L. Lasters, M. Lauwereys, Two structural domains as a general fold of the toxic fragment of the *Bacillus thuringiensis* delta-endotoxin, Eur. J. Biochem. 195 (1991) 631–635.
[30] P. Ort, I.A. Zalunin, V.S. Gasparov, G.G. Chestukhina, V.M. Stepanov, Domain organization of *Bacillus thuringiensis* CryIIIA delta-endotoxin studied by denaturation in guanidine hydrochloride solutions and limited proteolysis, J. Prot. Chem. 14 (1995) 241–249.
[31] A. Muga, J.M. Gonzalez-Mañas, J.H. Lakey, F. Pattus, W.K. Surewicz, pH-dependent stability and membrane interaction of the pore-forming domain of colicin A, J. Biol. Chem. 268 (1993) 1553–1557.
[32] L.J. Evans, M.L. Goble, K.A. Hales, J.H. Lakey, Different sensitivities to acid denaturation within a family of proteins: implications for acid unfolding and membrane translocation, Biochemistry 35 (1996) 13180–13185.

[33] J. Ren, K. Kachel, H. Kim, S.E. Malenbaum, R.J. Collier, E. London, Interaction of diphtheria toxin T domain with molten-globule-like proteins and its implications for translocation, Science 284 (1999) 955–957.
[34] H. Ihara, M. Himeno, Study of irreversible binding of *Bacillus thuringiensis* Cry1Aa to brush border membrane vesicles from *Bombyx mori* midgut, J. Invertebr. Pathol. 98 (2008) 177–183.
[35] P. Ounjai, V.M. Unger, F.J. Sigworth, C. Angsuthanasombat, Two conformational states of the membrane-associated *Bacillus thuringiensis* Cry4Ba delta-endotoxin complex revealed by electron crystallography: implications for toxin-pore formation, Biochem. Biophys. Res. Commun. 361 (2007) 890–895.
[36] V. Vié, N. Van Mau, P. Pomarède, C. Dance, J.L. Schwartz, R. Laprade, R. Frutos, C. Rang, L. Masson, F. Heitz, C. Le Grimellec, Lipid-induced pore formation of the *Bacillus thuringiensis* Cry1Aa insecticidal toxin, J. Membr, Biol. 180 (2001) 195–203.
[37] M.S. Nair, D.H. Dean, All domains of Cry1A toxins insert into insect brush border membranes, J. Biol. Chem. 283 (2008) 26324–263231.
[38] L. Pardo-López, I. Gómez, C. Rausell, J. Sánchez, M. Soberón, A. Bravo, Structural changes of the Cry1Ac oligomeric pre-pore from *Bacillus thuringiensis* induced by *N*-acetylgalactosamine facilitates toxin membrane insertion, Biochemistry 45 (2006) 10329–10336.
[39] S. Morin, R.W. Biggs, L. Shriver, C. Ellers-Kirk, D. Higginson, D. Holley, D.G. Gahan, Heckel, Y. Carriere, T.J. Dennehy, J.K. Brown, B.E. Tabashnik, Three cadherin alleles associated with resistance to *Bacillus thuringiensis* in pink bollworm, Proc. Nat. Acad. Sci. U. S. A. 100 (2003) 5004–5009.

PEPTIDES 29 (2008) 324–329

available at www.sciencedirect.com

ScienceDirect

journal homepage: www.elsevier.com/locate/peptides

Review

Employing phage display to study the mode of action of *Bacillus thuringiensis* Cry toxins

Luisa Elena Fernández [a], *Isabel Gómez* [a], *Sabino Pacheco* [a], *Iván Arenas* [a], *Sarjeet S. Gilla* [b], *Alejandra Bravo* [a], *Mario Soberón* [a,*]

[a] *Instituto de Biotecnología, Universidad Nacional Autónoma de México, Apdo. Postal 510-3, Cuernavaca, Morelos 62250, Mexico*
[b] *Department of Cell Biology and Neuroscience, University of California, Riverside, CA 92521, USA*

ARTICLE INFO

Article history:
Received 8 March 2007
Accepted 10 July 2007
Published on line 14 December 2007

Keywords:
Phage display
Bacillus thuringiensis
Cry toxin

ABSTRACT

Phage display is an *in vitro* method for selecting polypeptides with desired properties from a large collection of variants. The insecticidal Cry toxins produced by *Bacillus thuringiensis* are highly specific to different insects. Various proteins such as cadherin, aminopeptidase-N (APN) and alkaline phosphatase (ALP) have been characterized as potential Cry-receptors. We used phage display to characterize the Cry toxin–receptor interaction(s). By employing phage-libraries that display single-chain antibodies (scFv) from humans or from immunized rabbits with Cry1Ab toxin or random 12-residues peptides, we have identified the epitopes that mediate binding of lepidopteran Cry1Ab toxin with cadherin and APN receptors from *Manduca sexta* and the interaction of dipteran Cry11Aa toxin with the ALP receptor from *Aedes aegypti*. Finally we displayed in phages the Cry1Ac toxin and discuss the potential for selecting Cry variants with improved toxicity or different specificity.

Contents

* *Corresponding author*. Tel.: +52 777 3291618; fax: +52 777 3291624.
E-mail address: mario@ibt.unam.mx (M. Soberón).
0196-9781/$ – see front matter
doi:10.1016/j.peptides.2007.07.035

1. Introduction

Bacillus thuringiensis (Bt) is an aerobic, spore-forming bacterium from the *Bacillus cereus* group that is distinguished due to its capacity to produce δ-endotoxins that have insecticidal activity. δ-Endotoxins are produced as crystalline inclusions during the sporulation phase [4]. The δ-endotoxins, or Cry proteins, are specifically toxic to the following insect Orders: Lepidoptera, Coleoptera, Hymenoptera and Diptera [4,31]. One feature that distinguishes Cry toxins is their remarkable specificity, and therefore they are harmless to non-target insects or vertebrates. Cry toxins are being used worldwide for the control of vectors of human diseases or insect agricultural pests as insecticidal sprays or in transgenic plants [4].

2. Bt Cry toxins

Cry toxins belong to the group of pore-forming toxins (PFT) and it is widely accepted that their toxic effect is due to the formation of ionic pores in the membrane of insect epithelial midgut cells, which leads to cell swelling and death. To exert its toxic effect, crystals are ingested by susceptible larvae and solubilized by the alkaline pH and reducing conditions of the midgut. Midgut proteases act on the protoxin giving rise to a protease-resistant 55–60 kDa toxin fragment. The toxin fragment binds to specific midgut membrane-associated proteins resulting in the oligomerization and membrane insertion of the toxin [4]. Toxin–receptor interaction is a key step that determines insect specificity [4,31]. Even more, the principal mechanism of resistance to Cry toxins are mutations that affect toxin–receptor interaction [8]. Different proteins such as cadherins, aminopeptidase-N (APN), and alkaline phosphatase (ALP) have been characterized as Cry-receptors in different insect species [17,18,21,33]. Thus, understanding the molecular basis of the interaction of Cry toxins with their receptor molecules would be useful not only for engineering Cry proteins with different specificities or with enhanced insecticidal activity but also for coping with the problem of insect resistance in the field.

The three-dimensional structures of six Cry toxins with different insect specificities have been solved [2,3,9,15,22,26]. These toxins are composed of three domains—domain I, a seven α-helix bundle involved in membrane insertion, oligomer formation and pore formation [4]; domain II, a three anti-parallel β-sheets packed around a hydrophobic core in a ''β-prism'' involved in receptor interaction [4]; and domain III, a β-sandwich of two antiparallel β-sheets also involved in receptor interaction [4].

3. Phage display

For the past few years we characterized Cry toxin–receptor interaction in lepidopteran and dipteran insects to understand the molecular basis of insect specificity of these toxins. For this purpose we have employed a molecular technique known as phage display. Phage display, first developed in 1985 [32], displays recombinant peptides or proteins on the surface of phage particles, that can be screened by enabling the phage to interact with ligands that are immobilized in tubes (panning). This is a very powerful technique since the selected phages maintain a physical link between the displayed protein (phenotype) and the encoding gene (genotype). Filamentous phages, like M13, have been extensively used to develop different types of phage display libraries that display millions of variants of peptides or antibodies. Phage display involves the fusion of foreign DNA sequences to a coat protein gene enabling the fusion protein to be displayed on the surface of the phage. Most commonly, phage display libraries are constructed using vectors called phagemids, which are hybrids of phage and plasmid vectors. These phagemids contain the origins of replication from the M13 phage and *E. coli*; the gene coat protein III or gene coat IV for protein fusion, and an antibiotic resistance gene [1,25]. To display the fusion protein, *E. coli* cells harboring the phagemids are infected with a helper phage that provides all the necessary components for phage assembly.

In this review we will summarize the types of libraries and the panning procedures used to characterize the Cry toxin–receptor interaction. Our experimental approach has been to select, by panning, ligands of the toxin or the receptor that compete the toxin–receptor interaction. This approach has enabled us to map the binding epitopes in the Cry toxins and in the receptors, identify novel receptor molecules, study receptor localization in the insect gut and most importantly, to determine how receptors promote toxicity. Finally, we will discuss the potential of displaying Cry toxins on the surface of phages as a way to select toxins with different specificities or that overcome insect resistance to Cry toxins.

4. A synthetic human scFv library—selection of an scFv molecule that mimics a cadherin receptor

Our first attempt to characterize the amino acid epitopes involved in the interaction of Cry toxins with their receptor molecules was with the lepidopteran insect *Manduca sexta* and the Cry1Ab toxin [10]. At that time, two *M. sexta* proteins that bind Cry1A toxins had been cloned and characterized, a 210 kDa cadherin protein known as Bt-R_1 and a 120 kDa glycosylphosphatidyl-inositol (GPI)-anchored aminopeptidase-N [21,33]. As a way to determine which was the functional receptor and the amino acid epitopes involved in the toxin–receptor interaction, we decided to select by phage display peptides that bind Cry1Ab toxin and identify those that competed toxin interaction with both receptor molecules, then we used these phages as tools to determine the role of both *M. sexta* proteins in toxicity. Also, we expected that some of the peptides that competed the interaction of Cry toxins with their receptor could share sequence similarity with discrete receptor amino acid sequences that were involved in toxin binding as has been shown for several examples of interacting proteins [20]. For the first panning procedure we used the Nissim synthetic phage-antibody library. This library, with a diversity of 1×10^8, contains a diverse repertoire of *in vitro* rearranged human variable heavy (VH) genes containing a random VH-CDR3 of 4–12 amino acids residues in length [27]. Antigen-recognition by antibodies is determined mainly by

CDR regions in the variable light (VL) and VH fragments. To facilitate the display of antibody molecules in phages, the VL and VH fragments are assembled as single-chain molecules with a $(Gly_4Ser)_3$ linker peptide resulting in the construction of scFv genes fused to the pIII gene in phagemids [1,27]. scFv antibodies are likely to retain the binding properties of the whole antibody molecule [1,27]. For the panning procedure, we immobilized Cry1Ab toxin in immunotubes and after several panning rounds of selection we identified three scFv phages that bound specifically to Cry1Ab toxin. Using ligand blots assays and by competing the binding of Cry1Ab toxin with *M. sexta* brush border membrane vesicles (BBMV) blotted proteins, we identified one scFv (scFv73) that competed the binding of Cry1Ab with the 210 kDa Bt-R_1 molecule but not with the 120 kDa APN [10]. Antibody scFv73 inhibited the toxicity of Cry1Ab toxin in bioassays. Sequence analysis of the CDR3 region of scFv73 led to the identification of a eight amino acid region ($_{869}$HITDTNNK$_{876}$) in cadherin repeat 7 of Bt-R_1 [10]. Synthetic peptides corresponding to the Bt-R_1 amino acid region or to scFv73 CDR3 competed the binding of Cry1Ab with Bt-R_1 [10].

Use of the scFv73 antibody was also very important to map the cognate-binding region in the Cry1Ab toxin [11]. Previous work of other groups demonstrated by site directed mutagenesis that domain II loops located in the apex of the β-prism were important for receptor recognition [4,31]. We determined if these loop regions were involved in the interaction of Cry1Ab toxin with scFv73. To do this, we performed binding competition of scFv73 binding with Cry1Ab toxin in Western blots using synthetic peptides corresponding to each of the Cry1Ab loop regions (loop 1–loop 3) [11]. Only loop 2 peptide competed the binding of scFv73 with Cry1Ab toxin [11]. Interestingly a mutant loop 2 synthetic peptide that contained two-amino acid residue changes that in the context of the whole toxin affected binding and toxicity did not compete the binding of scFv73 with Cry1Ab [11]. These results indicate that the Cry1Ab domain II loop 2 region interacts with the Bt-R_1 $_{869}$HITDTNNK$_{876}$ amino acid region [11] (Fig. 1).

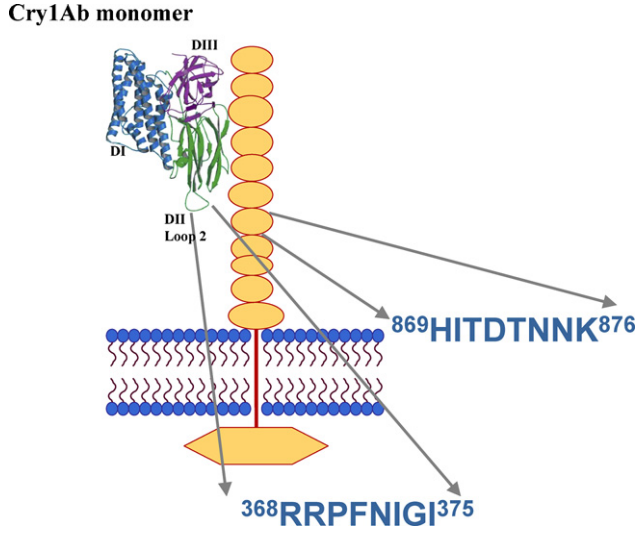

Fig. 1 – Cry1Ab toxin binds *Manduca sexta* cadherin repeat 7 by means of domain II loop 2.

Antibody scFv73 was also very useful to determine the role of the cadherin receptor in promoting toxicity. For several other pore-forming toxins, binding to a receptor facilitates a proteolytic cleavage that finally induces the formation of oligomeric structures that are capable of inserting into membranes [29]. Using scFv73 as a surrogate of Bt-R_1, we demonstrated that Cry1Ab toxin forms a soluble 250 kDa oligomer when activated *in vitro* by *M. sexta* midgut-proteases in the presence of scFv73 [12]. Subsequently, we demonstrated that the 250 kDa oligomer is membrane insertion competent and forms stable pores with high conductances and open probability, in contrast to the 60 kDa monomeric structure that barely inserts into membranes and induces unstable low-conductance pores in black lipid bilayers [30]. Also, we demonstrated that the 250 kDa oligomer is formed in the presence of cadherin fragments containing the toxin binding regions [13]. These results led us to propose that binding to cadherin facilitates the formation of a pre-pore oligomer that is membrane insertion competent (Fig. 2).

5. An immune rabbit scFv library—mapping the binding epitopes of oligomeric toxin and APN receptor

In order to determine the role of other Cry1Ab toxin regions in binding to the receptor molecules, we attempted to isolate other scFv antibodies that recognize other domain II loop regions or domain III, previously shown to be involved in receptor interaction [4,31]. Nevertheless, different attempts of panning using the Nissim library were unsuccessful. Therefore we decided to construct a new scFv phage display library that would be enriched in scFv molecules that recognize Cry1Ab toxin. For this purpose, phage display libraries constructed from a host immunized with the target antigen favors selection of high-affinity, specific antibodies generated during immunization process [14]. A Cry1Ab-immune M13 phage-repertoire was constructed using antibody gene transcripts of bone marrow and spleen from a rabbit immunized with Cry1Ab toxin [14]. These were the first immune-libraries described against Cry toxins.

We also used novel panning protocols to identify antibodies that recognize exposed regions of domain II and III. scFv-antibodies to domain II loop 3 were selected by panning against a domain II loop 3 synthetic peptide. Anti-domain III-scFv molecules were identified by selecting scFv phages that bound Cry1Ab toxin in the presence of soluble Cry1Ac toxin, which has similar domains I and II to Cry1Ab, but a non-related domain III. Then, toxin overlay binding competition assays in the presence of synthetic peptides were used to show that domain II loop 3 of Cry1Ab is an important epitope for interaction with the Bt-R_1 receptor. This interaction between the toxin and the anti-domain II loop 3 scFv antibody also promoted the formation of the pre-pore oligomer as a previously observed with an anti-domain II loop 2 scFv73 antibody [14]. The selected anti-loop 3 antibody (scFvL3-3) molecule lowered the toxicity of Cry1Ab to *M. sexta* larvae in bioassays.

The Cry1Ab epitopes involved in the interaction of the oligomeric structure with APN were also mapped by ELISA and

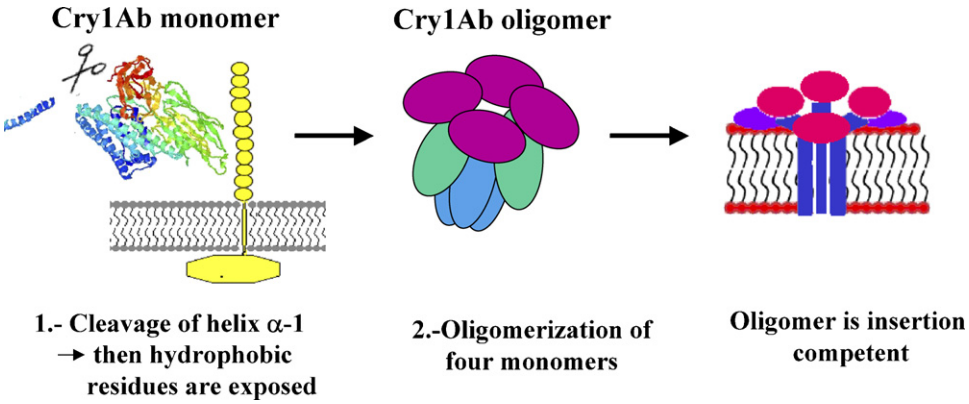

Fig. 2 – Binding of Cry1Ab toxin to the *Manduca sexta* cadherin receptor promotes cleavage of helix α-1 in domain I and the subsequent formation of a pre-pore oligomeric structure that is membrane insertion competent.

toxin overlay binding competition assays. The β16 and β22 from domain III play an important role in this interaction since a scFv-antibody that recognizes these regions (scFvM22) inhibited the interaction of the pre-pore oligomeric structure with APN and lowered the toxicity of Cry1Ab to *M. sexta* larvae in bioassays [14]. scFvM22 did not promote the *in vitro* formation of a pre-pore oligomeric structure. Our results show that interaction with both receptors is important for *in vivo* toxicity.

Finally, we found that scFvL3-3 and scFv73 antibodies preferentially recognized the monomeric toxin rather than the pre-pore structure, suggesting a conformational change in the domain II loop regions is recognized by these antibodies [14]. Overall, these results indicated that the first interaction of Cry1Ab with Bt-R_1 through domain II loop regions, promotes the formation of the pre-pore oligomeric structure with a subtle change in the structure of these exposed domain II loops; then the pre-pore interacts with APN through a different domain III region (β16) (Fig. 3).

6. Random peptide library—identification of an ALP receptor and its interaction with Cry toxins in mosquitoes

In the case of mosquitocidal toxins we decided to work with a Cry11Aa toxin that is particularly toxic to *Aedes aegypti* that is

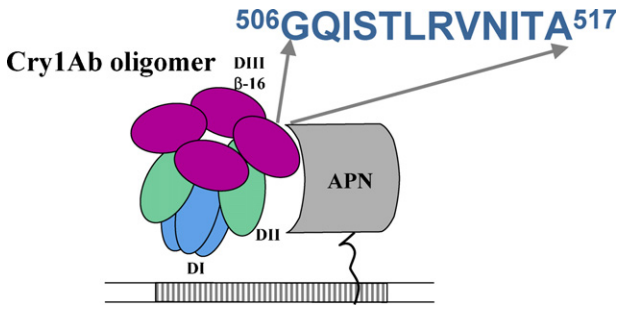

Fig. 3 – The Cry1Ab pre-pore oligomer binds aminopeptidase-N (APN) from *Manduca sexta* by means of β-16 in domain III.

the vector of dengue in humans. *Bacillus thuringiensis* subs *israelensis* (Bti) produces a crystal inclusion composed of six toxins: Cry4Aa, Cry4Ba, Cry10Aa, Cry11Aa, Cyt1Aa and Cyt2Ba that are highly active against dipteran insects, vectors of human diseases [23]. In contrast to *M. sexta* and Cry1Ab, no receptor molecules had been identified in *Ae. aegypti* nor the binding regions in the toxin. We decided to perform panning against Cry11Aa to select molecules that competed for the binding of the toxin with *Ae. aegypti* BBMV and also panning against the BBMV to select molecules that bind the receptor. This is an example that shows that molecules that bind to a receptor molecule can be selected without the need of having a pure preparation of this receptor [7]. We used a commercial phage-peptides library obtained from New England BioLabs Inc. (Ph.D.-12 Phage Display Peptide Library Kit). This library has a complexity of 2.7×10^9 transformants, and is based on a combinatorial library of random 12-mers fused to the coat protein pIII of the M13 phage. We demonstrated that the putative exposed loop α-8 of Cry11Aa toxin, located in domain II, is an important epitope involved in receptor interaction and toxicity. Four exposed loops and three putative exposed regions in domain II of Cry11A were predicted by modeling the three-dimensional structure of the mosquitocidal Cry11Aa toxin [6]. Synthetic peptides corresponding to these regions were used in heterologous binding competition assays of Cry11Aa to *Ae. aegypti* BBMV. We identified three regions of Cry11A toxin, corresponding to loop α-8, β4 and loop 3 that are involved in binding of this toxin to the BBMV [6]. We isolated peptide-displaying phages that bind to Cry11Aa toxin (P5.tox) or to *Ae. aegypti* BBMV (P1.BBMV) [6,7]. These phages interfered with the interaction of the toxin with the BBMV and attenuated the toxicity of Cry11Aa in bioassays [6,7]. The binding of both phages was competed by loop α-8 synthetic peptide, suggesting that phage P5.tox binds the toxin by interacting with loop α-8 while P1.BBMV interacts with the receptor by using an epitope similar to this region [6,7].

A 65 kDa GPI-anchored ALP was identified as a binding Cry11Aa protein in *Ae. aegypti* BBMV. P1.BBMV bound specifically to ALP demonstrating that ALP is a functional receptor of Cry11Aa [7]. On the other hand, immunocytochemical localization of the binding of phage P1.BBMV and Cry11Aa toxin to midgut tissue sections from the mosquito

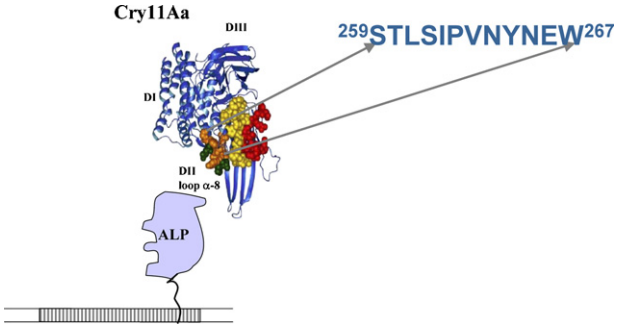

Fig. 4 – The Cry11Aa toxin binds *Aedes aegypti* alkaline phosphatase (ALP) by means of the α-8 loop in domain II.

revealed that Cry11Aa and P1.BBMV strongly recognized the same regions in the midgut tissue. These regions corresponded to the microvilli membrane from the caeca and from the posterior part of the midgut indicating that ALP colocalizes with the binding sites of Cry11Aa [7]. Our results identify domain II loop α-8 as a key determinant for the binding of Cry11Aa toxin to GPI-anchored ALP [6,7] (Fig. 4).

7. Displaying Cry toxins in phages and selection of novel variants

One of the most important features of phage display is that it allows a rapid selection of variants with improved binding characteristics [1,25]. Even more, further mutagenesis and selection by panning allows *in vitro* molecular evolution of proteins [5]. This seems particularly interesting for Cry toxins since for many insect pests there are no Cry toxins available for their control. Also, a major threat for the use of Bt toxins in transgenic plants is the appearance of insect resistance. It has been demonstrated that a single nucleotide change in the *Heliothis virescens* cadherin receptor gene produces an amino acid change that abolishes Cry1A toxin binding [35]. Therefore the need of developing an efficient method that allows genetic evolution of Cry toxins to kill novel targets or to recover toxicity to resistant insects, in the case of the appearance of resistance in the field, will be greatly desirable.

Cry1A toxins have been displayed in three different phages. The first attempts to display Cry1A toxins were using M13 phages [19,24]. In the case of the filamentous M13 experiments, the Cry1Aa toxin was not properly displayed resulting in deletions of the fused protein [24]. A complete Cry1Ac was efficiently displayed in M13 showing toxicity to *M. sexta* larvae, however, the displayed Cry1Ac protein did not bind to functional receptors *in vitro* suggesting structural constraints of the displayed toxin [19]. M13 phage display systems have an intrinsic problem in displaying big proteins since fusion proteins have to be transported into the *E. coli* periplasm where phage assembly occurs.

To circumvent this problem, λ and T7 phages have been used to display Cry1Ac toxin since the assembling of phage particles in both systems occur in the cytoplasm of bacterial cells, thus allowing the display of bigger proteins [28,34]. In the case of λ, the Cry1Ac protein was fused with the capsid protein D and displayed on the surface of phage particles. The displayed Cry1Ac toxin retained toxicity and the capacity to interact with the *M. sexta* APN receptor [34]. More recently we described the use of T7 phage display system to display Cry1Ac toxin [28]. The *cry1Ac* gene was fused to the 3′ end of the T7 10B capsid protein gene and the chimeric protein was displayed on the surface of T7 phage. The T7-Cry1Ac bind receptors recognized by Cry1Ac toxin and retained toxicity against *M. sexta* larvae. Also, we showed that T7-Cry1Ac phage particles bind specifically to *M. sexta* BBMV that contain the native receptor molecules [28]. Nevertheless, a problem with both λ and T7 displaying systems is that for displaying the fusion protein both systems rely on *in vitro* packaging systems that under the best scenario allow for the production of up to 10^7 to 10^8 recombinant phage particles/μg of DNA, making the construction of libraries with large number of variants inefficient. Recently the T7 system was used successfully to select Cry1Aa toxin variants with higher toxicity by selecting phages by panning domain II loop 2 variants that bound the *B. mori* cadherin protein (Bt-R_{175}) with higher affinity [16]. This result shows that it is possible to select novel Cry toxins with desirable binding properties from a pool of variants.

8. Concluding remarks

To exert their toxic effect, Cry toxins interact with several receptor proteins and undergo drastic structural changes allowing a soluble protoxin molecule to insert as oligomers in the membranes of their target cells, thus forming ionic pores. Several receptor molecules in different insect species have been shown to be involved in this complex process. We have exploited the potential of phage display methodology to determine the identity and localization of one receptor molecule in mosquitoes and to determine the sequential participation of two receptor molecules leading to pore formation in lepidopteran insects. We believe that phage display will also be useful for the *in vitro* evolution of Cry toxins for selecting toxins with novel specificities and for selecting toxin mutants that kill resistant insects. Such a system will be of great value to assure long-term use of Bt toxins for insect management; this is highly desirable since the use of these toxins is recognized as an environmentally friendly technology.

Acknowledgments

The research work of our groups was supported in part by CONACyT U48631-Q and 46176-Q, USDA 2007-35607-17780 and NIH 1R01 AI066014.

REFERENCES

[1] Azzazy HME, Highsmith JWE. Phage display technology: clinical applications and recent innovations. Clin Biochem 2002;35:425–45.
[2] Boonserm P, Mo M, Angsuthanasombat Ch, Lescar J. Structure of the functional form of the mosquito larvicidal

Cry4Aa toxin from *Bacillus thuringiensis* at a 2 8-angstrom resolution. J Bacteriol 2006;188:3391–401.
[3] Boonserm P, Davis P, Ellar DJ, Li J. Crystal structure of the mosquito-larvicidal toxin Cry4Ba and its biological implications. J Mol Biol 2005;348:363–82.
[4] Bravo A, Gill SS, Soberón M. *Bacillus thuringiensis* mechanisms and use. In: Gilbert LI, Iatrou K, Gill SS, editors. Comprehensive molecular insect science. Elsevier B.V.; 2005. p. 175–206.
[5] Droge MJ, Ruggeberg CJ, van der Sloot AM, Schimmel J, Dijkstra DW, Verhaert RMD, et al. Binding of phage display *Bacillus subtilis* lipase A to a phosphonate suicide inhibitor. J Biotechnol 2003;101:19–28.
[6] Fernández LE, Pérez C, Segovia L, Rodríguez MH, Gill SS, Bravo A, et al. Cry11Aa toxin from *Bacillus thuringiensis* binds its receptor in *Aedes aegypti* mosquito larvae through loop α-8 of domain II. FEBS Lett 2005;79:3508–14.
[7] Fernández LE, Aimanova KG, Gill SS, Bravo A, Soberón MA. GPI-anchored alkaline phosphatase is a functional midgut receptor of Cry11Aa toxin in *Aedes aegypti* larvae. Biochem J 2006;394:77–84.
[8] Ferré J, Van Rie J. Biochemistry and genetics of insect resistance to *Bacillus thuringiensis*. Annu Rev Entomol 2002;47:501–33.
[9] Galitsky N, Cody V, Wojtczak A, Ghosh D, Luft JR, Pangborn W, et al. Structure of the insecticidal bacterial δ-endotoxin Cry3Bb1 of *Bacillus thuringiensis*. Acta Crystallogr D 2001;57:1101–9.
[10] Gómez I, Oltean D, Gill SS, Bravo A, Soberón M. Mapping the epitope in cadherin like receptors involved in *Bacillus thuringiensis* Cry1A toxin interaction using phage display. J Biol Chem 2001;276:28906–12.
[11] Gómez I, Miranda-Rios J, Rudiño-Piñera E, Oltean DI, Gill SS, Bravo A, et al. Hydropathic complementarity determines interaction of epitope ^{869}HITDTNNK^{876} in *Manduca sexta* Bt-R_1 receptor with loop 2 of domain II of *Bacillus thuringiensis* Cry1A toxins. J Biol Chem 2002;277:30137–43.
[12] Gómez I, Sánchez J, Miranda R, Bravo A, Soberón M. Cadherin-like receptor binding facilitates proteolytic cleavage of helix α-1 in domain I and oligomer pre-pore formation of *Bacillus thuringiensis* Cry1Ab toxin. FEBS Lett 2002;513:242–6.
[13] Gómez I, Dean DH, Bravo A, Soberón M. Molecular basis for *Bacillus thuringiensis* Cry1Ab toxin specificity: Two structural determinants in the *Manduca sexta* Bt-R1 receptor interact with loops α-8 and 2 in domain II of Cy1Ab toxin. Biochemistry 2003;42:10482–9.
[14] Gómez I, Arenas I, Benitez I, Miranda-Ríos J, Becerril B, Grande G, et al. Specific epitopes of Domains II and III of *Bacillus thuringiensis* Cry1Ab toxin involved in the sequential interaction with cadherin and aminopeptidase-N receptors in *Manduca sexta*. J Biol Chem 2006;281:34032–9.
[15] Grochulski P, Masson L, Borisova S, Pusztai-Carey M, Schwartz JL, Brousseau R, et al. *Bacillus thuringiensis* CryIA(a) insecticidal toxin: crystal structure and channel formation. J Mol Biol 1995;254:447–64.
[16] Ishikawa H, Hoshino Y, Motoki Y, Kawahara T, Kitajima M, Kitami M, et al. A system for the directed evolution of the insecticidal protein from *Bacillus thuringiensis*. Mol Biotechnol 2007;36:90–101.
[17] Jurat-Fuentes JL, Adang MJ. Characterization of a Cry1Ac-receptor alkaline phosphatase in susceptible and resistant *Heliothis virescens* larvae. Eur J Biochem 2004;271:3127–35.
[18] Jurat-Fuentes JL, Adang MJ. Cry toxin mode of action in susceptible and resistant *Heliothis virescens* larvae. J Invertebr Pathol 2006;92:166–71.
[19] Kasman LM, Lukowiak AA, Garcynski SF, McNall RJ, Youngman P, Adang MJ. Phage display of a biologically active *Bacillus thuringiensis* toxin. Appl Environ Microbiol 1998;64:2995–3003.
[20] Kay BK, Kasanov J, Knight S, Kurakin A. Convergent evolution with combinatorial peptides. FEBS Lett 2000;480:55–62.
[21] Knight P, Crickmore N, Ellar DJ. The receptor for *Bacillus thuringiensis* CryIA(c) delta-endotoxin in the brush border membrane of the lepidopteran *Manduca sexta* is aminopeptidase. Mol Microbiol 1994;11:429–36.
[22] Li J, Carroll J, Ellar DJ. Crystal structure of insecticidal delta-endotoxin from *Bacillus thuringiensis* at 2.5 Å resolution. Nature 1991;353:815–21.
[23] Margalith Y, Ben-Dov E. In: Rechcigl JE, Rechcigl NA, editors. Insect pest management: techniques for environmental protection. CRC Press; 2000. p. 243.
[24] Marzari R, Edomi P, Bhatnagar RK, Ahmad S, Selvapandiyan A, Bradbury A. Phage display of *Bacillus thuringiensis* CryIA(a) insecticidal toxin. FEBS Lett 1997;411:27–31.
[25] Mullen LM, Nair SP, Ward JM, Rycroft AN, Henderson. Phage display in the study of infectious diseases. Trends Microbiol 2006;14:141–7.
[26] Morse RJ, Yamamoto T, Stroud RM. Structure of Cry2Aa suggests an unexpected receptor binding epitope. Structure 2001;9:409–17.
[27] Nissim A, Hoogenboom HR, Tomlinson IM, Flynn G, Lidgley C, Lane D, et al. Antibody fragments from a 'single pot' phage display library as immunochemical reagents. EMBO J 1994;13:692–8.
[28] Pacheco S, Gómez I, Sato R, Bravo A, Soberón M. Functional display of *Bacillus thuringiensis* Cry1Ac toxin on T7 phage. J Invert Pathol 2006;92:45–9.
[29] Parker MW, Feil SC. Pore-forming proteins: from structure to function. Prog Biophys Mol Biol 2005;88:91–124.
[30] Rausell C, Muñoz-Garay C, Miranda-CassoLuengo R, Gómez I, Rudiño-Piñera E, Soberón M, et al. Tryptophan spectroscopy studies and black lipid bilayer analysis indicate that the oligomeric structure of Cry1Ab toxin from *Bacillus thuringiensis* is the membrane-insertion intermediate. Biochemistry 2004;43:166–74.
[31] Schnepf E, Crickmore N, Van Rie J, Lereclus D, Baum JR, Feitelson J, et al. *Bacillus thuringiensis* and its pesticidal crystal proteins. Microbiol Mol Biol Rev 1998;62:705–806.
[32] Smith GP. Filamentous fusion phage-novel expression vectors that display cloned antigens on the virion surface. Science 1985;228:1315–7.
[33] Vadlamudi RK, Weber E, Ji I, Ji TH, Bulla Jr LA. Cloning and expression of a receptor for an insecticidal toxin of *Bacillus thuringiensis*. J Biol Chem 1995;270:5490–4.
[34] Vílchez S, Jacoby J, Ellar DJ. Display of biologically functional insecticidal toxin on the surface of λ phage. Appl Environ Microbiol 2004;70:6587–94.
[35] Xie R, Zhuang M, Ross LS, Gómez I, Oltean DI, Bravo A, et al. Single amino acid mutations in the cadherin receptor from *Heliothis virescens* affect its toxin binding ability to Cry1A toxins. J Biol Chem 2005;280:8416–25.

THE JOURNAL OF BIOLOGICAL CHEMISTRY VOL. 281, NO. 45, pp. 34032–34039, November 10, 2006

Specific Epitopes of Domains II and III of *Bacillus thuringiensis* Cry1Ab Toxin Involved in the Sequential Interaction with Cadherin and Aminopeptidase-N Receptors in *Manduca sexta*[*]

Received for publication, May 17, 2006, and in revised form, September 5, 2006 Published, JBC Papers in Press, September 12, 2006, DOI 10.1074/jbc.M604721200

Isabel Gómez[‡], Iván Arenas[‡], Itzel Benitez[‡], Juan Miranda-Ríos[‡], Baltazar Becerril[§], Ricardo Grande[¶], Juan Carlos Almagro[§], Alejandra Bravo[‡], and Mario Soberón[‡1]

From the Instituto de Biotecnología, UNAM, Departamento de [‡]Microbiología Molecular, [§]Medicina Molecular y Bioprocesos, and [¶]Ingeniería Celular y Biocatálisis, Apdo. Postal 510-3, Cuernavaca, Morelos 62250, México

The *Bacillus thuringiensis* Cry toxins are specific to different insects. In *Manduca sexta* cadherin (Bt-R_1) and aminopeptidase-N (APN) proteins are recognized as Cry1A receptors. Previous work showed that Cry1Ab binds to Bt-R_1 promoting the formation of a pre-pore oligomer that binds to APN leading to membrane insertion. In this work we characterized the binding epitopes involved in the sequential interaction of Cry1Ab with Bt-R_1 and APN. A Cry1Ab immune M13 phage repertoire was constructed using antibody gene transcripts of bone marrow or spleen from a rabbit immunized with Cry1Ab. We identified antibodies that recognize domain II loop 3 (scFvL3-3) or β16–β22 (scFvM22) in domain III. Enzyme-linked immunosorbent assay and toxin overlay binding competition assays in the presence of scFvL3-3, scFvM22, or synthetic peptides showed that domain II loop 3 is an important epitope for interaction with Bt-R_1 receptor, whereas domain III β16 is involved in the interaction with APN. Both scFvL3-3 and scFvM22 lowered the toxicity of Cry1Ab to *M. sexta* larvae indicating that interaction with both receptors is important for *in vivo* toxicity. scFvL3-3 and anti-loop2 scFv (scFv73) promoted the formation of the pre-pore oligomer in contrast to scFvM22. In addition, scFvL3-3 and scFv73 preferentially recognized the monomeric toxin rather than the pre-pore suggesting a conformational change in domain II loops upon oligomerization. These results indicate for the first time that both receptor molecules participate in Cry1Ab toxin action *in vivo*: first the monomeric toxin binds to Bt-R_1 through loops 2 and 3 of domain II promoting the formation of the pre-pore inducing some structural changes, then the pre-pore interacts with APN through β-16 of domain III promoting membrane insertion and cell death.

Crystal proteins (Cry)[2] are widely used as insecticides in agriculture, forestry, and vector transmission due to their high specificity and their safety for the environment. Cry proteins are produced as protoxins of 70–130 kDa that are toxic to larval forms of several insects of different orders as well as to other invertebrates (1). Proteolytic activation of protoxin by midgut proteases produces Cry toxin fragments of 60–65 kDa. Cry toxins then bind to the cell surface where they undergo large-scale irreversible conformational changes to convert them into an oligomeric form capable of inserting into the membrane, causing osmotic lysis of midgut cells and ultimately insect death (1). Receptor binding has been studied extensively as a key step determining insect specificity, toxicity, and resistance of Cry toxins (1, 2). In the case of the lepidopteran insect *Manduca sexta*, at least two Cry1A-binding proteins, a cadherin-like protein (Bt-R_1) and a glycosylphosphatidylinositol (GPI)-anchored aminopeptidase-N (APN), have been described as receptors of Cry1A toxins (3, 4). Previously, we provided evidence showing that binding of monomeric Cry1Ab toxin to Bt-R_1 promotes an additional proteolytic cleavage in the N-terminal end of the toxin (helix α1) facilitating the formation of a pre-pore oligomeric structure that is competent in membrane insertion and that oligomer formation is important for toxicity (5, 6). The pre-pore oligomer has a higher affinity to APN (7, 8). The oligomeric Cry1A structure then binds to the APN receptor leading to its insertion into membrane lipid rafts (7, 8) implying a sequential binding mechanism of Cry1A toxins with Bt-R_1 and APN receptor molecules (8). However, a different mechanism of action of Cry toxins based on the study of the effect of Cry1Ab toxin to cultured *Trichoplusi ni* H5 insect cells expressing *M. sexta* Bt-R_1 (9, 10) was recently proposed. It was proposed that the toxicity of Cry1Ab is mainly due to the interaction of monomeric Cy1Ab toxin with Bt-R_1 by activating a Mg^{+2}-dependent adenylyl cyclase/protein kinase A signaling pathway that leads to apoptosis and not to pore formation induced by insertion of oligomeric Cry1Ab into the membrane (9, 10). Therefore, additional experimental evidence is needed

* This work was supported by Consejo Nacional de Ciencia y Tecnologia contracts J46829-Q and 46176-Q, DGAPA-UNAM Grants IN206200 and IN216300, UC MEXUS-Consejo Nacional de Ciencia y Tecnologia, and United States Department of Agriculture Contract 2002-3502-1239. The costs of publication of this article were defrayed in part by the payment of page charges. This article must therefore be hereby marked "*advertisement*" in accordance with 18 U.S.C. Section 1734 solely to indicate this fact.

[1] To whom correspondence should be addressed. E-mail: mario@ibt.unam.mx.

[2] The abbreviations used are: Cry, crystal protein; BBMV, brush border membrane vesicles; Bt, *Bacillus thuringiensis*; ELISA, enzyme-liked immunosorbent assay; scFv, single-chain Fv antibody fragments; APN, aminopeptidase-N; Bt-R_1, cadherin; GPI, glycosylphosphatidylinositol; Ab, antibody; PBS, phosphate-buffered saline; VL, variable light chain; HL, heavy chain.

to discriminate between the two models of mode of action of Cry toxins, in particular evidence that determines the role of the APN receptor in toxicity of Cry1A toxins will be valuable.

To date, the tertiary structures of six different Cry proteins, Cry1Aa, Cry2Aa, Cry3Aa, Cry3Bb, Cry4Aa, and Cry4Ba, have been determined by x-ray crystallography (11–16). All these structures display a high degree of similarity with a three-domain organization, suggesting a similar mode of action of the Cry three-domain protein family. The N-terminal domain (domain I) is a bundle of seven α-helices in which the central helix-α5 is hydrophobic and is encircled by six other amphipathic helices, this helical domain is responsible for membrane insertion and pore formation (11–15). Domain II consists of three anti-parallel β-sheets with exposed loop regions, and domain III is a β-sandwich (11–15). Exposed regions in domains II and III are involved in receptor binding (1).

The Cry1Aa, Cry1Ab, and Cry1Ac proteins share more than 95% amino acid sequence identity as protoxins and are selectively toxic to some lepidopteran insect pests. These Cry1A toxins bind to the same receptor molecules in *M. sexta* (Bt-R_1 and APN) (17, 18). Domain I in the three toxins share more than 98% amino acid sequence identity. However, there are important differences in domains II and III of these toxins. Cry1Ab and Cry1Ac toxins share the same domain II in contrast to Cry1Aa that has a different domain II sharing only 69% identity. In particular, the loop regions involved in receptor interaction are different in Cry1Aa. In contrast, Cry1Aa and Cry1Ab share a very similar domain III, whereas domain III of Cry1Ac shares only 38% identity with both toxins. Because different lepidopteran insects show different sensitivity to these Cry1A toxins, it is likely that the differences in domains II and III influence the receptor binding affinities and the activity of these toxins.

The characterization of the epitopes involved in interaction of Cry toxins with their receptors could give clues on the molecular basis of insect specificity and resistance. In previous work, using a synthetic phage-antibody library, we isolated an scFv antibody (scFv73) that binds to domain II loop 2 (β6–β7 loop) of Cry1A toxins and inhibited binding of Cry1A toxins to Bt-R_1 but did not affect binding to APN (19, 20). Sequence analysis of the CDR3H region of scFv73 led to the identification of an 8-amino acid epitope in Bt-R_1 cadherin repeat 7 (CADR7, ^{869}HITDTNNK^{876}) involved in the binding to domain II loop 2 of Cry1A toxins (19, 20). A second binding epitope in Bt-R_1 CADR11 (^{1331}IPLPASILTVTV^{1342}) that interacts with domain II loop α8 (α8a–α8b loop) and loop 2 of Cry1Ab toxin (21) was recently described. Finally, a third region in CADR12 of Bt-R_1 (amino acids 1363–1464) involved in Cry1Ab interaction and toxicity was identified (22). In the case of the *Heliothis virescens* cadherin, this binding region was narrowed to residues 1422–1440 by mutagenesis and shown to bind Cry1Ac domain II loop 3 (β10–β11 loop) (23). Regarding interaction of Cry1A toxins with APN, Cry1Ac toxin binds to APN receptor by means of domain III that specifically recognizes *N*-acetylgalactosamine (GalNAc) moieties in contrast to Cry1Aa and Cry1Ab toxins that show no GalNAc binding capacities (18). Based on the use of monoclonal antibodies that competed binding of Cry1Aa with *Bombix mori* APN, the Cry1Aa-APN interacting epitopes were recently mapped in domain III β16 (^{508}STLRVN^{513}) and β22 (^{582}VFTLSAHV^{589}) residues, which are exposed and in close proximity in the three-dimensional structure (24, 25).

Binding of Cry1Ab toxin to anti-loop 2 scFv73 antibody or to Bt-R_1 CADR7 or CADR11 peptides facilitates the formation of the pre-pore oligomeric structure *in vitro*, showing that domain II interaction with Bt-R_1 is an important step in the formation of the pre-pore oligomer before toxin inserts into the membrane (6, 21).

Although some binding epitopes in the toxin have been characterized, little is known about the mechanism by which the Cry1A toxins undergo a sequential interaction with the two receptors molecules. The characterization of the binding epitopes in the pre-pore oligomer and the role of these binding sites in the interaction with both Bt-R_1 and APN is still missing. Furthermore, the characterization of possible structural changes in the toxin epitopes involved in receptor interaction could give clues on the mechanism of differential interaction of monomeric and pre-pore oligomeric structures with Bt-R_1 and APN. Also, the study of the role of the interaction of the pre-pore with APN in Cry1Ab toxicity will be important to determine the role of pre-pore formation in toxicity. In this study, we constructed immune libraries for Cry1Ab toxin and selected specific monoclonal scFv fragments that recognize Cry1Ab domain II loop 3 or domain III β16–β22 epitopes and demonstrated that both scFv molecules can inhibit the toxicity to *M. sexta* larvae. An anti-loop 3 antibody inhibited binding of Cry1Ab to Bt-R_1, whereas an anti-β16–β22 antibody inhibited interaction with APN. *In vitro* oligomer formation assays with the selected scFv antibodies showed that only binding of Cry1Ab domain II with Bt-R_1 is involved in oligomer formation in contrast to binding of domain III with APN that did not facilitate the formation of the pre-pore. Overall, these results suggest that interaction of Cry1Ab with both receptor molecules is important for toxicity. Also these data contribute to our understanding of the mechanism involved in the sequential interaction of Cry1Ab toxin with both receptor molecules.

MATERIALS AND METHODS

Purification of Monomeric Cry Toxins—The acrystalliferous Bt strain 407*cry*$^-$ (26) transformed with pHT409 plasmid harboring the *cry1Aa* gene (27) or pHT315-*cry1Ab* (19) were used for Cry1Aa and Cry1Ab production, respectively. Cry1Ac was produced from wild-type Bt strain HD73. Bt strains were grown for 3 days at 29 °C in nutrient broth sporulation medium (28) supplemented with 10 μg/ml erythromycin for Cry1Aa and Cry1Ab. After sporulation, crystals were purified by sucrose gradients as reported (19). The Cry1A protoxins were solubilized and proteolytically activated as reported (19).

Oligomer Formation Assay—For activation, 1–2 μg of Cry1Ab protoxin was incubated with scFv molecules in the presence of *M. sexta* midgut juice as previously reported (6). Purification of the activated toxins was done by size exclusion chromatography with Superdex 200 HR 10/30 (Amersham Biosciences) FPLC size exclusion as described (29). The oligomeric structure was detected by Western blot assays using Cry1Ab-polyclonal antibodies as reported (6).

Solubilization of GPI-anchored Proteins—*M. sexta* brush border membrane vesicles (BBMV) were treated with phospholipase C from *Bacillus cereus* (Sigma) as previously reported in Ref. 30. Membranes were recovered by ultracentrifugation (90,000 x *g* for 20 min), and the supernatant was analyzed for aminopeptidase activity. APN enzymatic activity was measured using 1 mg/ml leucine-*p*-nitroanilide (Sigma) as substrate. BBMV proteins (5 μg) were mixed with APN buffer (0.2 M Tris-HCl, pH 8, 0.25 M NaCl) containing 1 mM leucine-*p*-nitroanilide. APN enzymatic activity was monitored as change in the absorbance at 405 nm for 10 min at room temperature.

Rabbit Immunization—A New Zealand White rabbit was immunized subcutaneously with a mixture of oligomeric and monomeric Cry1Ab toxin structures obtained after proteolytical activation of Cry1Ab in the presence of scFv73. The rabbit was boosted three times with 1 mg of Cry1Ab toxin structure mixture, mixed with incomplete adjuvant, at 15-day intervals. The bone marrow and spleen were dissected 40 days after the primary immunization.

Phage Display Library Construction—Total RNA was prepared from spleen tissue and bone marrow as described (31). Total RNA and random primer were used for first strand cDNA synthesis using a kit (Roche Applied Sciences), according to the manufacturer's instructions. From cDNA, heavy and light chain DNA fragments were amplified separately and recombined by three subsequent PCR, essentially as described (31), except that PCR1 and PCR2 were done with Vent DNA polymerase (New England BioLabs, Beverly, MA). Primer sequences for amplification of VL and VH antibody regions have been described before (31). However, primers HH13, HH14, and HH15 sequences were corrected; HH13, 5′-GGCGGATCAGGAGGCGGAGGTTCTGGAGGTGGGAGTGMCCTCGATMTGACCCAGACTCCAGC-3′; HH14, 5′-GGCGGATCAGGAGGCGGAGGTTCTGGAGGTGGGAGTGMCCTCGTGMTGACCCAGACTCCAGC-3′; HH15, 5′-GGCGGATCAGGAGGCGGAGGTTCTGGAGGAGGTGGGAGTGMCCTCGTGMTGACCCAGACTCCATC-3′, where M = A/C.

To construct the scFv libraries, scFv PCR products and phagemid vectors pCANTAB 5E and pSyn2 were digested with restriction enzymes SfiI and NotI (New England BioLabs, Beverly, MA), gel purified, and ligated. The ligation products were purified by extraction with phenol/chloroform and ethanol precipitation. The purified DNA was electroporated into TG1 *Escherichia coli* cells. Each library was grown on TYE agar plates, supplemented with ampicillin (100 μg/ml) and glucose (1% w/w). After overnight incubation at 37 °C, grown colonies were scraped off the agar plates, mixed with glycerol (20%), and stored at −70 °C. Libraries of 2.0×10^6 members were obtained.

Selection and Characterization of Phage Displayed Antibodies—Preparation of phage particles for panning was done as described (19). Briefly, Maxisorp immunotubes (Nunc, Denmark) were coated with Cry1Ab and blocked (19). The tubes were incubated with phage antibodies (10^{11} phage particles in MPBS skim milk 2% in PBS) and washed 10 times to remove unbound phage Abs (19). The binders were eluted with triethylamine, and the eluant neutralized and mixed with 8.5 ml of exponentially growing TG1 cells to allow infection as described (19). Cells were resuspended in 1 ml of medium, and plated on three TYE agar plates (145-mm diameter) as described (19). After overnight growth at 37 °C, bacteria were harvested and phage were rescued to produce phagemids for the next selection cycle. This panning cycle was done three times, after which polyclonal phage Abs from each round of selection were tested for binding activity in a phage ELISA. In the case of the panning of anti-domain III Cry1Ab antibodies, the last panning round was performed in the presence of 25 μg/ml soluble Cry1Ac toxin.

Panning Selection Using Biotinylated Antigens—Streptavidin microtiter plates (Pierce) were coated with biotinylated Cry1Ab (10 nM) or biotin-loop 3 synthetic peptide (1 μM). Cry1Ab was biotinylated using biotinyl-*N*-hydroxysuccinimide ester (Amersham Biosciences) according to the manufacturer's instructions. Panning was carried out essentially as described above, except that volumes were adapted for microtiter plates. Synthetic peptides (Table 1) were purchased from Invitrogen.

Phage or scFv ELISA—For phage ELISA, the microtiter plates were coated with 2.5 μg of Cry1Ab toxin in 100 μl of carbonate buffer (50 mM, pH 9.6) per well overnight at 4 °C. For scFv ELISA the microtiter plates were coated with 100 ng of Cry1Ab monomer or 100 ng of oligomer in 100 μl of carbonate buffer per well overnight at 4 °C. The plates were washed 3 times with PBS and blocked with 200 μl/well of MPBS skim milk 2% in PBS for 2 h at 37 °C. For phage ELISA, 100 μl of phage Abs (1×10^8 plaque-forming units) were added and incubated for 90 min at 25 °C. After washing, 100 μl of horseradish peroxidase-conjugated sheep anti-M13 antibody (1:1000 in MPBS skim milk 2% in PBS) was added and incubated as before. For scFv ELISA, 200 nM pure scFv molecules were added to the Cry1Ab monomeric- or oligomeric-coated wells and incubated for 90 min at 25 °C. scFv antibodies were detected with horseradish peroxidase-conjugated anti-His antibody (Qiagen) (1:5000 dilution). After washing 3 times with TPBS and 3 times with PBS, *ortho*-phenylenediamine (Sigma) (0.5 mg/ml, 30% H_2O_2) was used as substrate for detection. Reaction was stopped with 100 μl of 1 M H_2SO_4 and measured at 490 nm using a microplate reader. For competition assays, 1 μg of synthetic peptides were added during the incubation with the selected scFv phages.

Nucleotide Sequence Determination and Fingerprint Analysis—To determine the diversity of the original libraries and clones after panning selection, we randomly picked infected TG1 colonies and amplified their scFv inserts with the PCR 5′ primer PSYN1 (ATACCTATTGCCTACGGC) and 3′ primer PSYN2 (TTACAACAGTCTATGCGG), or primers JK2 and AW1 (31). To obtain DNA fingerprint of the insert sequences, the PCR products were digested with AluI (New England Biosciences) and resolved on 8% acrylamide gels.

Expression and Purification of Soluble scFv Antibodies—The positive phage clones were subcloned into expression vector pET22b (Novagen). Recombinants were transformed into *E. coli* BL21(DE3) and induced with 1 mM isopropyl 1-thio-β-D-galactopyranoside. After incubation at 30 °C overnight, the proteins in the periplasm were collected using solution I (30 mM Tris-HCl, pH 8.0, 1 mM EDTA, 20% sucrose) and solution II (5

TABLE 1
Synthetic peptide sequences

Name	Sequence	Description
Biotin-loop 3	Biotin-SGSSG-FRSGFSNSSVS	Cry1Ab residues 436-379 fused to biotin-SGSSG peptide
Loop2	LYRRPFNIGINNQQ	Cry1Ab residues 366-379
Loop3	FRSGFSNSSVSIIR	Cry1Ab residues 436-449
DIII-1	GQISTLRVNITA	Cry1Ab residues 506-517
DIII-2	VFTLSAHVFN	Cry1Ab residues 583-592

mM $MgSO_4$), respectively. The scFv antibodies were purified using nickel-agarose columns as reported (19). The purified proteins were then detected by SDS-PAGE and Western blot.

Preparation of BBMV—M. sexta were reared on an artificial diet. BBMV from third instar *M. sexta* larvae were prepared as reported (32).

Toxin Binding Assays—Toxin overlay assays to BBMV were performed as described (19–21). To determine the ability of selected scFv to compete with the Cry1Ab toxin, different concentrations of scFv were incubated with biotinylated Cry1Ab toxin in washing buffer before adding the mixture to nitrocellulose membranes. Single gel blots were incubated with different competitors using the PR 150 mini deca-probe (Amersham Biosciences) that was designed to incubate each lane of the blot in different conditions avoiding the need of cutting lanes for different conditions.

For analysis of oligomer binding to GPI-anchored protein extract, microtiter plates were coated with 20 μg of GPI proteins as above. The plates were washed 3 times with PBS and blocked with 200 μl/well of skim milk 2% in PBS for 2 h at 37 °C. 10 nM pure Cry1Ab oligomer was added to the coated wells as above. Cry1Ab oligomer was detected using Cry1Ab polyclonal antibody (1:20,000 dilution) and then a secondary goat anti-rabbit antibody conjugated with horseradish peroxidase (Sigma) (1:5,000 dilution). Washing and reading of ELISA was done as described above. For competition assays, 10^{12} plaque forming units of scFv phages were added during incubation with the Cry1Ab oligomer.

Insect Bioassay—Bioassays were performed with *M. sexta* neonate larvae by the surface contamination method as previously described (19).

RESULTS

Phage Antibody Libraries, Construction, and Characterization—We constructed Cry1Ab-immune rabbit libraries in scFv format that could be used for selection of high-affinity and highly specific antibodies against Cry1Ab toxin. The scFv libraries were constructed as reported previously in three PCR steps using reported primers that allow the amplification of rabbit variable heavy and light chain cDNAs (31). Total RNA was extracted from the spleen and bone marrow of a New Zealand White rabbit previously immunized with a mixture containing both monomeric and oligomeric Cry1Ab toxin structures. After cDNA synthesis by reverse transcription, VH and VL DNA fragment repertoires were amplified separately by PCR using four pairs of primers for heavy chains and three pairs of primers for light chains as reported (31). In the second PCR, a DNA linker coding a $(Gly_4Ser)_3$ peptide linker sequence was added using modified 3′-heavy and 5′-light chain primers (31). However, reported primers HH13, HH14, and HH15 were modified because the reported primer sequence contained a misplaced glycine codon (31) (see "Materials and Methods" for primer sequence). Finally, a third PCR was performed to fuse the amplified VH and VL genes DNA fragments by overlapping extension. In the final PCR SfiI and NotI restriction sites were added to the 3′ and 5′ ends, respectively, using primers harboring these restriction sites as reported (31). PCR products of 800 bp from the final PCR were digested with SfiI and NotI restriction enzymes and cloned into the previously digested phagemid vectors pSyn2 or pCANtab that allows the display of the cloned fragment on the surface of M13 phage (19). After *E. coli* cell transformations, libraries of 2.0×10^6 members were obtained.

To examine the integrity and variability of the libraries, 20 clones of each library were picked at random and analyzed by PCR, 95% of the clones were found to contain scFv DNA fragments of the expected size (data not shown). The diversity of the libraries was determined by digestion of the amplified scFv fragment with the AluI restriction enzyme. The PCR fingerprinting analysis of bone marrow and spleen libraries showed that the libraries contain high variability because all restriction patterns analyzed were different (data not shown).

Identification of Anti-loop 3 and Anti-domain III Phage Antibodies—To study the role of domain II and III regions in the binding interaction with receptor molecules, we selected scFv-M13 phages by panning that recognize Cry1Ab-domain II loop 3 or domain III because these regions have been shown to be involved in interaction with Bt-R_1 or APN (23, 25). Previously we characterized an scFv antibody (scFv73) that binds domain II loop 2 and inhibits Cry1Ab toxin binding with Bt-R_1 but not with APN (19, 20).

Novel panning procedures were performed to select the desired specific scFv antibodies. For the identification of anti-loop 3 scFv antibodies, the panning procedure consisted in two panning rounds against whole Cry1Ab toxin and a third panning round against a biotinylated synthetic peptide with an amino acid sequence corresponding to Cry1Ab loop 3 (*biotin-loop3*, Table 1). Simultaneously, a third panning round was performed against biotinylated Cry1Ab toxin. After the third round of panning, scFv antibodies were preferentially retained by Cry1Ab as shown by the higher number of exit colony forming units obtained for biotinylated Cry1Ab (10^7 colony forming units/ml) in comparison to biotin-loop3 peptide (10^4 colony forming units/ml). Fingerprinting analysis of 20 clones selected against the biotin-loop 3 peptide revealed five different restriction patterns (Fig. 1). The five different scFv-M13 phages were tested in ELISA for binding to Cry1Aa or Cry1Ab toxins. Fig. 2*A* shows that all five clones bound to Cry1Ab toxin but not to Cry1Aa, which has a different loop 3 amino acid sequence. The scFv phage

scFv3-L3 was selected and Fig. 2*B* shows that binding of scFv3-L3 to Cry1Ab was competed by a loop 3 synthetic peptide but not by loop 2, β16 or β22 synthetic peptides (Fig. 2*B*).

To select scFv antibodies that recognize Cry1Ab domain III, we performed a panning procedure that counter-selected scFv-M13 phages that recognize Cry1Ac toxin that has a different domain III and very similar domains I and II. After two rounds of panning against Cry1Ab, a third round against Cry1Ac was performed. The non-binding Cry1Ac phages were recovered, amplified, and subjected to a final panning round against Cry1Ab in the presence of soluble Cry1Ac to ensure binding to Cry1Ab of phages that do not recognize Cry1Ac. Fifty colonies from the fourth round were amplified by PCR and characterized by fingerprinting. Five different restriction patterns were identified (Fig. 1). Analysis of binding to Cry1A proteins revealed that four of these scFv phages bind to Cry1Ab but not to Cry1Ac, suggesting that these scFv antibodies bind domain III of Cry1Ab (Fig. 2*C*). Previously it was demonstrated that Cry1Aa domain III ^{508}STLRVN^{513} and ^{582}VFTLSAHV^{589} residues, corresponding to β16 and β22, were involved in binding with *B. mori* APN (25). These amino acid regions are in close proximity in the Cry1Aa structure (25). To determine whether any of the selected anti-domain III scFv-M13 phages recognize these binding epitopes, binding of these five scFv-M13 phages to Cry1Ab was performed in the presence of synthetic peptides corresponding to the β16 or β22 regions of Cry1Ab. Fig. 2*B* shows that binding of phage scFvM22 to Cry1Ab was inhibited by the two domain III synthetic peptides corresponding to Cry1Ab β16 or β22 and not by the synthetic peptides of domain II loops, indicating that scFvM22 binds to this domain III amino acid epitope.

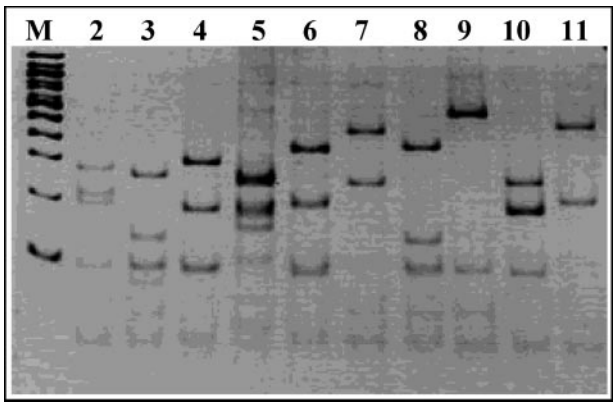

FIGURE 1. **Fingerprint analysis of scFv clones.** AluI restriction patterns of selected scFv DNA fragments after panning against loop 3 peptide (-3L1, 3L2, 3L3, 3L6 3L9, *lanes 2–6*) and against Cry1Ab in the presence of soluble Cry1Ac (-B2, B12, M2, M21, M22, *lanes 7–11*). *Lane 1* (M) is the molecular size marker (50-bp DNA ladder, Invitrogen).

Effect of Anti-loop 3 and Anti-β-16–β-22 scFv Molecules on Cry1Ab-Receptor Interaction—To determine whether the selected scFv protein fragments inhibit the Cry1Ab-receptor interaction, we performed toxin overlay assays using *M. sexta* BBMV. Fig. 3*A* shows that the anti-loop 3 scFvL3-3 phage particles inhibited binding of biotinylated Cry1Ab to Bt-R_1 (210 kDa) in contrast to the anti-β16–β22 scFvM22 phage particles that did not affect this interaction. Interestingly, APN (120 kDa) binding was competed by scFvM22 phage in contrast to scFvL3-3 phage that did not compete this interaction (Fig. 3*A*). To determine whether binding competition of scFv molecules was not due to steric hindrance due to the size of the scFv molecule, binding of Cry1Ab toxin with blotted BBMV proteins was performed in the presence of synthetic peptides corresponding to Cry1Ab binding epitopes. Fig. 3*B* shows that loop 3 synthetic peptide competed the binding of Cry1Ab to Bt-R_1 but not to APN. In contrast, synthetic peptide DIII-1 (corresponding to the β16) competed the binding of Cry1Ab to APN but had no effect on Bt-R_1 binding (Fig. 3*B*). Synthetic peptide DIII-2 (corresponding to β22) did not compete the binding of Cry1Ab to Bt-R_1 nor to APN. These results show that domain II loop 3 is involved in Bt-R_1 binding, whereas domain III β16 from Cry1Ab is important for the interaction with *M. sexta*-APN.

Oligomer Formation of Cry1Ab in the Presence of Anti-loop 3 or Anti-domain III scFv Antibodies—Previous work demonstrated that binding of Cry1Ab protoxin to Bt-R_1 peptides CADR7 or CADR11 or to scFv73 antibody, which mimics these cadherin epitopes (6, 19, 21), facilitated the proteolytic cleavage of domain I helix α1 resulting in the formation of a pre-pore oligomeric structure that is capable of membrane insertion (6, 21). To determine whether the scFvL3-3 or scFvM22 antibodies

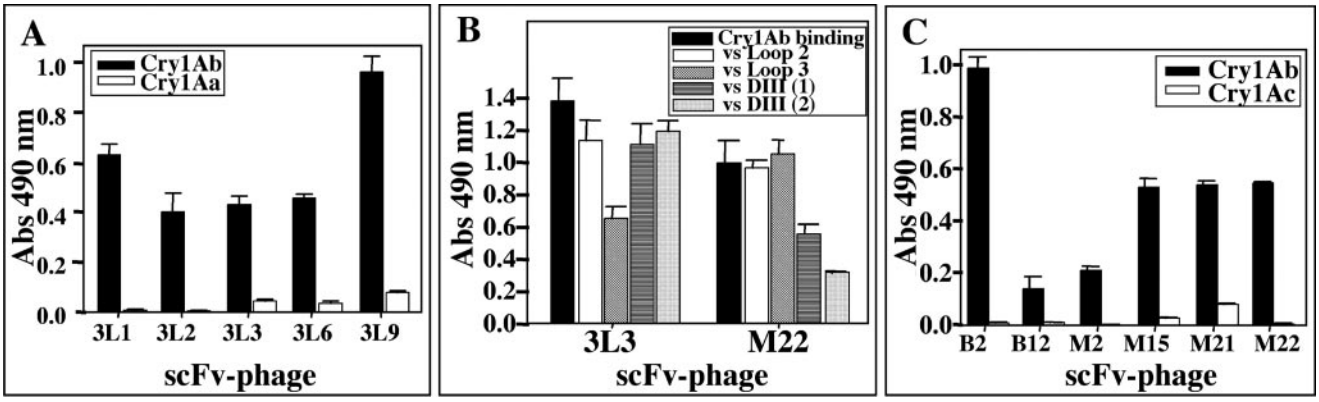

FIGURE 2. **ELISA binding analysis of scFv-M13 phages with Cry1A toxins.** *A*, binding of five different anti-loop 3 scFv phages to Cry1Ab or Cry1Aa toxins; *B*, binding of scFv3L-3 or scFvM22 phage particles to Cry1Ab in the presence of 1 μg of synthetic peptides corresponding to loop 2, loop 3, β16 (DIII-1), or β22 (DIII-2) amino acid sequences; *C*, binding of different anti-domain III scFv phages with Cry1Ab or Cry1Ac toxins. *Bars* are S.D. of three repetitions. Statistical significance: *A*, $p < 0.01$; *B*, $p < 0.05$; *C*, $p < 0.01$.

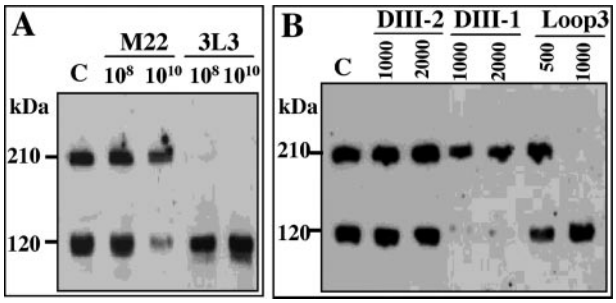

FIGURE 3. **Binding of Cry1Ab toxin to *M. sexta* BBMV proteins by toxin overlay assay.** *A*, toxin overlay assay in the presence of scFv phage particles as competitors (10^8 or 10^{10} plaque-forming units as competitors); *B*, toxin overlay assay in the presence of synthetic peptides as competitors. *Numbers* indicate the molar excess of each synthetic peptide; *lanes C*, control without competitor. Representative results of at least four repetitions.

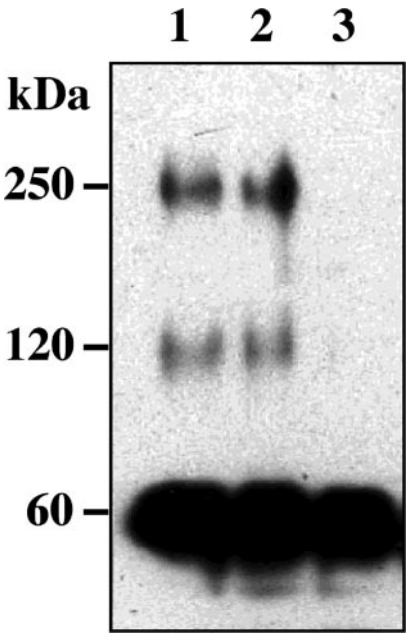

FIGURE 4. **Pre-pore oligomer formation induced by binding of Cry1Ab with selected scFv molecules.** Western blot of Cry1Ab toxin after incubation with scFv molecules (1/4 ratio) and activated with *M. sexta* midgut juice. Reaction was stopped with 1 mM phenylmethylsulfonyl fluoride and centrifuged 20 min at 12,000 × *g*. Supernatants were loaded into SDS-PAGE and Cry1Ab structures were detected with polyclonal anti-Cry1Ab antibody. *Lane 1*, proteolytic activation in the presence of anti-loop 2 scFv73 antibody; *lane 2*, activation in the presence of anti-loop 3 scFv3L-3 antibody; *lane 3*, activation in the presence of anti-domain III scFvM22 antibody.

facilitate the formation of the pre-pore structure, Cry1Ab protoxin was proteolytically activated in the presence of each one of these pure scFvL3-3 or scFvM22 molecules. Fig. 4 shows that when Cry1Ab protoxin was activated in the presence of scFvL3-3, a 250-kDa oligomer was produced. In contrast, when Cry1Ab protoxin was activated in the presence of the scFvM22 molecule only monomeric 60-kDa Cry1Ab toxin was produced (Fig. 4).

Binding of scFv to Cry1Ab Monomeric and Oligomeric Structures—The pre-pore oligomeric Cry1Ab structure gains 200-fold affinity to APN receptor suggesting some structural changes in the receptor-binding epitopes of the Cry1Ab toxin upon oligomerization (8). To determine whether domain II loops 2 and 3 or the domain III β16–β22 epitopes have a similar structure in the monomeric and oligomeric structures, binding

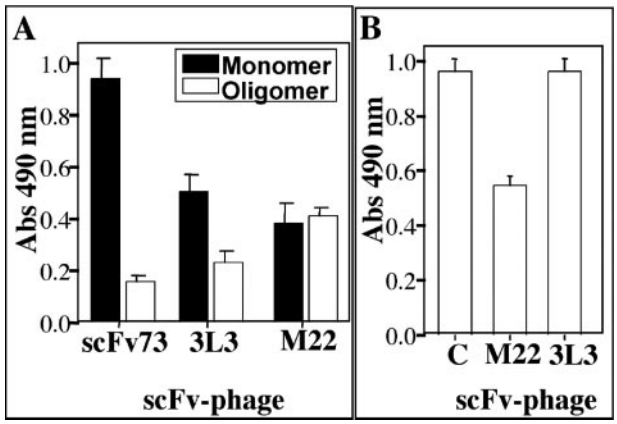

FIGURE 5. **Domain III β16–β22 epitope involved in Cry1Ab pre-pore interaction with APN.** *A*, binding of anti-loop 2 scFv73, anti-loop 3 scFv3L-3, or anti-domain III scFvM22 to pure Cry1Ab monomeric or oligomeric structures. *B*, binding of pure oligomer to GPI-anchored proteins from *M. sexta* BBMV without competitor (*C*) or in the presence of 10^{12} scFvM22 or scFvL3-3 phage particles. *Bars* are S.D. of three repetitions. Statistical significance: *A*, $p < 0.01$; *B*, $p < 0.05$.

of anti-domain II-loop 2 scFv73, anti-loop 3 scFvL3-3, or anti-domain III-scFvM22 molecules to pure monomeric or oligomeric Cry1Ab toxin structures was analyzed by ELISA. Fig. 5*A* shows that anti-loop 2 scFv73 or anti-loop 3 scFvL3-3 antibodies bound preferentially the monomeric toxin in contrast to the oligomeric structure. In contrast, the anti-β16–β22 scFvM22 recognized both Cry1Ab structures. These results suggest that domain II loops 2 and 3 of Cry1Ab might suffer a conformational change upon oligomerization or are buried in the oligomeric structure, in contrast to β16–β22 that has a similar conformation in both monomeric and oligomeric structures.

Domain III β16 Is Involved in the Interaction of Cry1Ab Pre-pore Oligomer with M. sexta GPI-anchored Proteins—The results shown so far demonstrated that the Cry1Ab monomer interacts with APN by domain III β16 and that this binding epitope has a similar structure in both monomeric and oligomeric structures. To determine whether domain III β16 was involved in the interaction of the Cry1Ab pre-pore to APN, binding of pure oligomeric Cry1Ab pre-pore to proteins obtained after phosphatidylinositol-phospholipase C treatment of BBMV was performed in the presence of scFvM22 or scFvL3-3 phages as competitors. APN is GPI-anchored and phosphatidylinositol-phospholipase C cleaves out GPI anchored proteins (4, 30). Fig. 5*B* shows that scFvM22-phage competed the binding of Cry1Ab oligomer to GPI-anchored proteins in contrast to scFvL3-3 phage that had no effect in this interaction.

Effect of scFv Phage on Toxicity of Cry1Ab Toxin in M. sexta Larvae—To test the effects of selected scFv phages on the toxicity of Cry1Ab toxin to *M. sexta* larvae, bioassays were performed using the different scFv phages in combination with Cry1Ab toxin. First instar *M. sexta* larvae were fed Cry1Ab toxin either alone or with the Cry1Ab toxin preincubated with 10^9 phage particles of the different monoclonal scFv antibodies. As control we included an scFv phage particle (scFvS1) that was selected by biopanning against Cry1Ab toxin and that showed similar binding to Cry1Aa, Cry1Ab, or Cry1Ac in ELISA (data not shown). None of the phages were toxic to *M. sexta* larvae

TABLE 2
Toxicity of Cry1Ab toxin to *M. sexta* larvae in the presence of scFv-phages competitors

Treatment	Mortality[a]
	%
Cry1Ab	95 ± 0.8
Cry1Ab + scFv3L-3	17 ± 1.6
Cry1Ab + scFvM22	30 ± 5.5
Cry1Ab + scFvS1	96 ± 1
H_2O	0

[a] Expressed as mean ± S.D. ($n = 3$) using 24 larvae. For each treatment 10 ng/cm^2 of Cry1Ab toxin plus 10^9 colony forming units of scFv-displaying phage were used.

(data not shown). Table 2 shows that both scFvL3-3-M13 and scFvM22-M13 phages inhibited 70–80% toxicity of the Cry1Ab toxin. In contrast, scFvS1 phage particles had no effect on Cry1Ab toxicity.

DISCUSSION

We have previously proposed a model involving the sequential interaction of Cry1A toxins with cadherin-like protein (Bt-R_1) and GPI-anchored APN receptor molecules. First, the interaction of monomeric Cry1A toxins with Bt-R_1 facilitates the formation of a pre-pore oligomeric structure that gains binding affinity to APN, after APN binding the Cry1A pre-pore inserts into lipid rafts inducing osmotic unbalance and cell swelling (8). However, the molecular mechanism that determines the sequential interaction of monomeric and pre-pore oligomeric structures with both receptors is not understood. In this work we identify the binding epitopes of monomeric and oligomeric Cry1Ab structures to their corresponding receptor (cadherin Bt-R_1 for the monomeric structure and APN for the oligomeric structure) and determined for the first time the important role of both receptors in the Cry1Ab toxicity *in vivo*.

In the case of Bt-R_1, domain II loops α8, 2, and 3 have been shown to have an important role in Bt-R_1 recognition (19–21, 23). In agreement with this, anti-loop 3 scFvL3-3 antibody, or the previously reported anti-loop 2 scFv73, inhibited the interaction with Bt-R_1 (19, 20). Sequence analysis of the five anti-loop 3 antibodies revealed that all of them shared a similar CDR1 of the variable light chain. Binding competition analysis of anti-loop 3 antibodies to Cry1Ab toxin using synthetic peptides corresponding to the amino acid sequences of the six predicted CDR regions in scFvL3-3 revealed that only peptide CDR1-L competed the binding indicating that anti-loop 3 binds Cry1Ab loop 3 using the CDR1-L region. The CDR1-L amino acid sequence (^{162}QASQSIVS^{169}) showed a similar hydropathic profile to the Bt-R_1 sequence (^{1412}NAQTGVLT^{1419}) located in CADR12. This amino acid region corresponds to the loop 3-binding epitope of *H. virescens* cadherin ^{1421}QTGVLTLNFQ^{1431} (23), suggesting that both *M. sexta* and *H. virescens* cadherins recognize loop 3 by similar binding epitopes.

Data from several laboratories, including this report, have recognized that Cry1A domain III has an important role in APN recognition (25, 33). Cry1Ac toxin binds *M. sexta* APN receptors through domain III binding to GalNAc residues (18, 33), whereas it was proposed that Cry1Aa binds *B. mori* APN through domain III β16 (^{508}STLRVN^{513}) and β22 (^{582}VFTLSAHV^{589}) residues (25). In this work we show that Cry1Ab binds *M. sexta* APN principally by the domain III β16 epitope because scFvM22 antibody that binds β16 and β22 amino acid regions competed the binding of Cry1Ab with APN. Nevertheless, Cry1Ab binding competitions with synthetic peptides DIII-1 (corresponding to β16 residues) or DIII-2 (corresponding to β22) revealed that only the β16 region is involved in interaction with APN in contrast to the β22 region. Mutagenesis of β16 residues will be helpful to further narrow this APN binding epitope. Interestingly, the β16–β22 epitope has a similar structure in both the monomeric and oligomeric structures because scFvM22 recognized both toxin structures with similar efficiencies and scFvM22 inhibited the interaction of the pre-pore oligomer with GPI-anchored protein extracts. These results indicate that this domain III epitope is involved in the interaction of the oligomer with APN.

SPR binding studies of Cry1Ab mutants with pure *M. sexta* APN showed that domain II loops 2 and 3 are also involved in APN recognition (34). These data seem to be in disagreement with the finding that an anti-loop 2 scFv73 or anti-loop 3 scFvL3-3 phages did not inhibit the interaction of monomeric Cry1Ab with APN and the oligomeric pre-pore with soluble GPI-anchored proteins. In the case of the lepidopteran insect *Lymantria dispar*, a sequential binding mechanism was proposed in the interaction of Cry1Ac with APN (35). Cry1Ac domain III first interacts with APN GalNAc sugar moieties facilitating the subsequent interaction of domain II loop regions with another region in this receptor (35). This binding mechanism could explain the binding competition of anti-domain III scFvM22 phage particles to APN in contrast to anti-domain II loop antibodies scFv73 and scFvL3-3, because competing the first binding event will inhibit the binding of domain II loop regions.

The scFv molecules characterized in this work were useful in determining the role of Cry1Ab binding to both receptor molecules in the formation of the pre-pore oligomeric structure. Anti-domain II loop scFv molecules, scFv73 or scFvL3-3, facilitated the formation of the pre-pore oligomeric structure. Because these scFv molecules inhibited Bt-R_1 binding and not APN recognition, these data are in agreement with a model where binding of monomeric Cry1Ab toxin to Bt-R_1 through domain II loop regions induces a conformational change resulting in the formation of the pre-pore structure. In contrast, anti-domain III antibody scFvM22 did not facilitate the formation of the oligomeric structure, suggesting that the interaction of monomeric Cry1Ab with APN has no consequence in pre-pore formation.

Previous work demonstrated that Cry1Ab pre-pore oligomer bound APN with a 200-fold increased apparent binding affinity in comparison to monomeric Cry1Ab, suggesting that structural changes of certain binding epitopes in the toxin occur upon oligomerization (8). Interestingly, the anti-loop 2 scFv73 and anti-loop 3 scFvL3-3 antibodies bound preferentially the Cry1Ab monomeric structure in comparison to the oligomeric structure, suggesting a possible conformational change upon oligomerization in the domain II loop 2 and 3 regions. Because domain II loops 2 and 3 seems to suffer a conformational change upon oligomerization that affects recognition by specific monoclonal antibodies, it could be possible that changes in domain II loops 2 and 3 may be involved in the sequential inter-

action with Bt-R_1 and APN. This structural change could lead to loose binding of oligomer to Bt-R_1 and enhance binding of oligomer to APN. The nature of the structural change of the domain II loop region in the oligomer remains to be characterized, we cannot rule out that domain II loop regions may be buried into the pre-pore oligomer affecting the interaction of monoclonal antibodies (scFv73 and scFvL3-3) that mimic the Bt-R_1 binding sites. Determination of binding affinities of pure pre-pore oligomeric structures of several point mutants in domain II loop regions of Cry1Ab to APN and Bt-R_1 will be helpful in understanding the role of these regions on Cry1Ab pre-pore binding to APN. Overall these results show that the constructed immune scFv libraries against Cry1Ab toxin are a valuable resource for identifying regions in the toxin involved in different steps of the toxin mode of action.

Finally, it was recently proposed that the toxicity of Cry1Ab is mainly due to the interaction of monomeric toxin with Bt-R_1 by apparently activating a Mg^{2+}-dependent adenylyl cyclase/protein kinase A signaling pathway in midgut cells that leads to apoptosis and not to lytic pore formation induced by oligomer membrane insertion (9, 10). This was proposed based on the study of the effect of Cry1Ab toxin to cultured *Trichoplusi ni* H5 insect cells expressing *M. sexta* Bt-R_1 (9, 10). Although not recognized by the authors, the data presented by Zhang *et al.* (9) showed that toxicity of Cry1Ab toxin to H5 cells expressing *Ms*-Bt-R_1 correlated with increased oligomer formation. In addition, these authors found that activation of adenylyl cyclase using a direct activator (forskolin) of membrane adenylyl cyclase does not affect cell viability even thought it was expected that the increased levels of cAMP would activate protein kinase A under treatment with forskolin. The authors concluded that other effectors could be involved in Cry1Ab toxicity (10). In any case, it should be pointed out that the situation *in vivo* on intact larvae midgut cells could be very different from cultured insect cells. Our data show that scFvM22, which specifically blocks binding of Cry1Ab to APN without affecting the interaction of Cry1Ab with Bt-R_1, severely attenuated the toxicity of Cry1Ab toxin *in vivo*, indicating that the interaction of Cry1Ab toxin with Bt-R_1 is not enough to kill the larvae and that interaction with both receptor molecules is necessary for complete toxicity in *M. sexta* larvae. These data are in agreement with the model of the sequential participation of Bt-R_1 and APN in toxin membrane insertion, pore formation, and toxicity of Cry1A toxins.

Acknowledgments—We are indebted to Dr. H. Hawlisch for valuable advice. We thank Jorge Sánchez, Oswaldo López and Lizbeth Cabrera for technical assistance, and Elizabeth Mata and Sergio González for veterinary services.

REFERENCES

1. Bravo, A., Soberón, M., and Gill, S. S. (2005) in *Comprehensive Molecular Insect Science* (Gilbert, L. I., Iatrou, K., and Gill, S. S., eds) Vol. 6, pp. 175–206, Elsevier, Amsterdam
2. Ferré, J., and Van Rie, J. (2002) *Annu. Rev. Entomol.* **47,** 501–533
3. Vadlamudi, R. K., Weber, E., Ji, I., Ji, T. H., and Bulla, L. A. (1995) *J. Biol. Chem.* **270,** 5490–5494
4. Knight, P., Crickmore, N., and Ellar, D. J. (1994) *Mol. Microbiol.* **11,** 429–436
5. Soberón, M., Perez, R. V., Nuñez-Valdéz, M. E., Lorence, A., Gómez, I., Sánchez, J., and Bravo, A. (2000) *FEMS Microbiol. Lett.* **191,** 221–225
6. Gómez, I., Sánchez, J., Miranda, R., Bravo A., and Soberón, M. (2002) *FEBS Lett.* **513,** 242–246
7. Zhuang, M., Oltean, D. I., Gómez, I., Pullikuth, A. K., Soberón, M., Bravo, A., and Gill, S. S. (2002) *J. Biol. Chem.* **277,** 13863–13872
8. Bravo, A., Gómez, I., Conde, J., Muñoz-Garay, C., Sánchez, J., Zhuang, M., Gill, S. S., and Soberón, M. (2004) *Biochem. Biopphys. Acta* **1667,** 38–46
9. Zhang, X., Candas, M., Griko, N. B., Rose-Young, L., and Bulla, L. A., Jr. (2005) *Cell Death Differ.* **12,** 1407–1416
10. Zhang, X., Candas, M., Griko, N. B., Taussig, R., and Bulla, L. A., Jr. (2006) *Proc. Natl. Acad. Sci. U. S. A.* **103,** 9897–9902
11. Grochulski, P., Masson, L., Borisova, S., Pusztai-Carey, M., Schwartz, J. L., Brousseau, R., and Cygler, M. (1995) *J. Mol. Biol.* **254,** 447–464
12. Morse, R. J., Yamamoto, T., and Stroud, R. M. (2001) *Structure* (*Camb.*) **9,** 409–417
13. Li, J., Carroll, J., and Ellar, D. J. (1991) *Nature* **353,** 815–821
14. Galitsky, N., Cody, V., Wojtczak, A., Ghosh, D., Luft, J. R., Pangborn, W., and English, L. (2001) *Acta Crystallogr. Sect. D Biol. Crystallogr.* **57,** 1101–1109
15. Boonserm, P., Mo, M., Angsuthanasombat, C., and Lescar, J. (2006) *J. Bacteriol.* **188,** 3391–3401
16. Boonserm, P., Davis, P., Ellar, D. J., and Li, J. (2005) *J. Mol. Biol.* **348,** 363–382
17. Keeton, T. P., Francis, B. R., Maaty, W. S., and Bulla, L. A. (1998) *Appl. Envionm. Microbiol.* **64,** 2158–2165
18. Masson, L., Lu, Y.-J., Mazza, A., Brosseau, R., and Adang, M. J. (1995) *J. Biol. Chem.* **270,** 20309–20315
19. Gómez, I., Oltean, D. I., Sanchez, J., Bravo, A., Gill, S., and Soberón, M. (2001) *J. Biol. Chem.* **276,** 28906–28912
20. Gómez, I., Miranda-Rios, J., Rudiño-Piñera, E., Oltean, D. I., Gill, S. S., Bravo, A., and Soberón, M. (2002) *J. Biol. Chem.* **277,** 30137–30143
21. Gómez, I., Dean, D. H., Bravo, A., and Soberón, M. (2003) *Biochemistry* **42,** 10482–10489
22. Hua, G., Jurat-Fuentes, J. L., and Adang, M. J. (2004) *J. Biol. Chem.* **279,** 28051–28056
23. Xie, R., Zhuang, M., Ross, L. S., Gómez, I., Oltean, D. I., Bravo, A., Soberón, M., and Gill, S. S. (2005) *J. Biol. Chem.* **280,** 8416–8425
24. Nakanishi, K., Yaoi, K., Nagino, Y., Hara, H., Kitami, M., Atsumi, S., Miura, N., and Sato, R. (2002) *FEBS Lett.* **519,** 215–220
25. Atsumi, S., Mizuno, E., Hara, H., Nakanishi, K., Kitami, M., Miura, N., Tabunoki, H., Watanabe, A., and Sato, R. (2005) *Appl. Environm. Microbiol.* **71,** 3966–3977
26. Lereclus, D., Arantès, O., Chaufax, J., and Lecadet, M.-M. (1989) *FEMS Microbiol. Lett.* **60,** 211–218
27. Arantès, O., and Lereclus, D. (1991) *Gene* (*Amst.*) **108,** 115–119
28. Lereclus, D., Agaisse, H., Gominet, M., and Chaufaux, J. (1995) *Bio/Technology* **13,** 67–71
29. Rausell, C., Muñoz-Garay, C., Miranda-CassoLuengo, R., Gómez, I., Rudiño-Piñera, E., Soberón, M., and Bravo, A. (2004) *Biochemistry* **43,** 166–174
30. Lorence, A., Darszon, A., and Bravo, A. (1997) *FEBS Lett.* **414,** 303–307
31. Hawlisch, H., Meyer zu Vilsendorf, A., Bautsch, W., Klos, A., and Kohl, J. (2000) *J. Immunol. Methods* **236,** 117–131
32. Bravo, A., Miranda, R., Gómez, I., and Soberón, M. (2002) *Biochim. Biophys. Acta* **1562,** 63–69
33. Lee, M. K., You, T. H., Gould, F. L., and Dean, D. H. (1999) *Appl. Environ. Microbiol.* **65,** 4513–4520
34. Jenkins, J. L., and Dean, D. H. (2000) *Genet. Eng.* **22,** 33–54
35. Jenkins, J. L., Lee, M. K., Valaitis, A. P., Curtiss, A., and Dean, D. H. (2000) *J. Biol. Chem.* **275,** 14423–14431

ANEXO III

Colaboración del estudiante en capítulos de libros.

Identification of scFv molecules that recognize loop 3 of domain II and domain III of *Bacillus thuringiensis*.

Gómez, I., Miranda-Ríos, J., **Arenas, I.**, Grande, R., Becerril, B., Bravo A. and Soberón, M.

6th Pacific Rim Conference on the biotechnology of *Bacillus thuringiensis* and its environmental impact.

Vincent, C. Montreal. Erudit. 12-14

6th Pacific Rim Conference on the Biotechnology of Bacillus thuringiensis *and its Environmental Impact*, Victoria BC, 2005
Côté, J.-C., Otvos, I.S., Schwartz, J.-L. and Vincent, C. (eds)

Identification of scFv Molecules that Recognize Loop 3 of Domain II and Domain III of Cry1Ab Toxin from *Bacillus thuringiensis*

Isabel Gómez[1], Juan Miranda-Ríos[1], Iván Arenas[1], Ricardo Grande[2], Baltazar Becerril[3], Alejandra Bravo[1], and Mario Soberón[1*]

Instituto de Biotecnología, [1]Depto. de Microbiología Molecular, Universidad Nacional Autónoma de México, Cuernavaca, Morelos, Mexico, 62250. [2]Depto. de Ing. Celular y Biocatálisis, Universidad Nacional Autónoma de México, Cuernavaca, Morelos, Mexico, 62250. [3]Depto. de Medicina Molecular y Bioprocesos. Universidad Nacional Autónoma de México, Cuernavaca, Morelos, Mexico, 62250.

A phage repertoire was constructed using antibody genes from the bone marrow and the spleen of a rabbit immunized with Cry1Ab toxin. Biopanning against either the Cry1Ab toxin or a domain II loop 3 synthetic peptide resulted in the identification of monoclonal antibodies in scFv format. They inhibited binding and toxicity of Cry1Ab toxin against *Manduca sexta*. Toxin overlay assays, using the scFv antibodies as competitors, revealed that the anti-loop 3 molecule competed with Cry1Ab toxin binding to the cadherin receptor (Bt-R_1) of *M. sexta*, while anti-domain III antibodies interfered with the binding of Cry1Ab toxin to the aminopeptidase N (APN) receptor of this insect.

Introduction

Insecticidal Cry1 proteins from *Bacillus thuringiensis* (Bt) are used in biopesticides and transgenic crops (2). In susceptible insects, proteinases in the alkaline midgut activate the Cry protein to a toxin that binds with high affinity to receptors of the brush border epithelium membrane. In the case of the cadherin receptor Bt-R_1, toxin binding initiates a conformational change that results in the assembly of a pre-pore toxin oligomer (5). Aminopeptidases also bind Cry1 toxins and facilitate toxin-induced pore formation (8). An emerging model suggests that after binding cadherins, toxins bind aminopeptidases and insert into membrane microdomains called lipid rafts (3). Domain II determines specificity, because it represents the most divergent part of the toxin sequence, and exchanging domain II, or domains II and III, between closely related toxins resulted in active hybrids showing altered specificity (4,6).

Materials and methods

Phage display libraries construction. Total RNA from spleen tissue and bone marrow of an immunized rabbit was used for first strand cDNA synthesis. Heavy- and light-chain genes were amplified separately and recombined by three subsequent PCR, essentially as described (7). In order to construct the scFv libraries, scFv DNA and phagemid vector were digested with *Sfi*I and *Not*I (New England BioLabs, Beverly, MA, USA), and ligated. The purified DNA was electroporated into TG1 electrocompetent cells. Each library was grown on large TYE AMP GLU agar plates. For panning, phage preparations were purified and concentrated by polyethylene glycol precipitation.

Selection and characterization of phage-displayed antibodies. Panning was carried out essentially as described previously (7) using 50 μg of Cry1Ab. 10^{11} phage were used in each round of selection. Binders were eluted with 1 ml of triethylamine (100 mM) and the eluant was neutralized and mixed with 8.5 ml of exponentially growing TG-1 cells. An aliquot was removed for titration, measured as colony forming units on agar plates. Infected bacteria were plated on TYE AMP GLU agar plates and bacteria were harvested after ON growth at 37°C. Phages were rescued for the next selection cycle.

Insect bioassay. Bioassays were performed on *M. sexta* neonate larvae by the surface contamination method. The toxin solution was preincubated with selected phages for 1 h then poured on the diet surface and allowed to dry. Neonate *M. sexta* larvae were placed on the dried surface and mortality was monitored after 7 days.

Results

Phage antibody library construction and characterization. After cDNA synthesis by reverse transcription from spleen and bone marrow RNA samples, the VH and VL region gene repertoires were amplified separately by PCR. In the second PCR reaction, a DNA linker coding a $(Gly_4Ser)_3$ peptide linker sequence was added using

* Corresponding auhtor. Mailing address: Instituto de Biotecnología, Universidad Nacional Autónoma de México, 2001 Av. Universidad, Col. Chamilpa, Apdo. postal 510-3, Cuernavaca, Morelos, Mexico, 62250. Tel: 52 73 11-4900. Fax: 52 73 17-2388. Email: mario@ibt.unam.mx.

modified 3′-heavy and 5′-light chains primers. Finally, a third PCR reaction was performed to fuse heavy and light chain genes by overlapping extension. PCR products from the third PCR reaction were digested with *Sfi*I and *Not*I, and cloned into phagemid vectors pSyn2 or pCANTAB that allow the display of the cloned fragment on M13 phage. After transformation, libraries sizes of 2.0×10^6 members were obtained.

To examine the integrity of the libraries, 20 clones of each library were picked at random and 95% of the clones were found by PCR to contain scFv genes having the expected size. To determine the diversity of the gene content of the libraries, cloned scFv genes were amplified from the same colonies and digested with the *Alu*I restriction enzyme. PCR fingerprinting analysis of bone marrow and spleen libraries showed that the libraries were diverse since all restriction patterns analyzed were different.

Identification of anti-loop 3 and anti-domain III phage antibodies. For the identification of anti-loop 3 scFv antibodies, the libraries were panned against a synthetic biotinylated peptide with a sequence corresponding to the Cry1Ab loop 3. The panning procedure consisted in two selection rounds against the whole Cry1Ab toxin and a third panning round against the biotinylated loop 3 synthetic peptide. Fingerprinting analysis revealed five different restriction patterns. In ELISA, all clones bound to Cry1Ab and Cry1Ac, but did not bind to Cry1Aa which has a different loop 3 amino acid sequence, suggesting that these scFv bind loop 3 of Cry1Ab. After two rounds of panning against Cry1Ab, a final panning round was conducted against Cry1Ab in the presence of soluble Cry1Ac to ensure binding to Cry1Ab toxin of phages that do not recognize Cry1Ac. Fifty colonies from the fourth round were amplified by PCR and characterized by fingerprinting analysis. Five different restriction patterns were identified. Analysis of binding to the three Cry1A proteins revealed that three scFv phages bound to Cry1Ab, but not to Cry1Ac which has a different domain III sequence, suggesting that these scFv antibodies bind Cry1Ab toxin through domain III.

Effect of phage antibodies on toxicity of Cry1Ab toxin to *M. sexta* larvae. First instar larvae were fed Cry1Ab toxin either alone or Cry1Ab pre-incubated with 10^8 phage preparation of the different monoclonal scFv antibodies selected after four rounds of selection. None of the phages were toxic to *M. sexta* larvae. All of the anti-loop 3 phages reduced the toxicity of Cry1Ab to 30-60% while the two anti-domain III phages reduced it to 10-20%.

Discussion

The striking dissimilarity between domain II and domain III amino acid sequences of different Cry toxins motivated us to investigate the role of these regions in insect specificity, toxicity and binding using phage display antibodies against these regions. We generated immune libraries in the scFv format that could be used for efficient selection of high-affinity and specific scFv antibodies against Cry1Ab toxin. We identified scFv phages that recognized domain II loop 3 or domain III, since these regions are likely to be involved in receptor interaction (1, 6).

Rabbit immune repertoires from spleen or bone marrow yielded a great diversity. Using phage display technology, after three or four rounds of panning using Cry1Ab toxin, we isolated specific scFv antibodies from the pool of the two libraries, that inhibited toxicity. Among these, antibody M22 was particularly interesting. M22, in contrast to the other anti-Cry1Ab scFv molecules analyzed, recognized Cry1Ab but did not bind to Cry1Ac. Therefore, scFv M22 most likely recognized a certain domain III region involved in toxicity, since this antibody reduced the toxicity of Cry1Ab toxin. In the case of Cry1Ac toxin, domain III is important on APN binding (4). We were able also to obtain five specific scFv antibodies against loop 3 of domain II. All anti-loop 3 scFv molecules analyzed recognized Cry1Ab but did not bind to Cry1Aa, consistent with the fact that these toxins do not share sequence similarity in the loop 3 region. Our results show the efficacy of our libraries for the generation of highly specific reagents against specific regions of Cry toxins to study toxin-receptor interaction. Our set of recombinant scFv antibodies against Cry1Ab toxin represents the first demonstration of the recombinant-antibody approach to the study of toxin-receptor and structure-function relations. With these tools it should be possible now to characterize more thoroughly the toxin-receptor interactions of Cry proteins and to ascertain the role of these interactions in the mode of action of these important toxins.

Acknowledgments

The authors are indebted to Dr. H. Hawlisch for valuable advice. We thank Jorge Sánchez, Oswaldo López and Lizbeth Cabrera for technical assistance, and Elizabeth Mata and Sergio González for veterinary services. This work was supported by CONACyT contract no. G36505-N, DGAPA-UNAM IN206200 and IN216300, UC MEXUS-CONACYT, and the United States Department of Agriculture, USDA 2002-3502-1239.

References

1. **Atsumi, S., E. Mizuno, H. Hara, K. Nakanishi, M. Kitami, N. Miura, H. Tabunoki, A. Watanabe, and R. Sato.** 2005. Location of the *Bombyx mori* aminopeptidase N type I binding site on *Bacillus thuringiensis* Cry1Aa toxin. Appl. Environ. Microbiol. **71**:3966-3977.

2. **Bravo, A., M. Soberón and S.S. Gill.** 2005. *Bacillus thuringiensis* mechanisms and use, p. 175-206. *In* L. I. Gilbert, K. Iatrou, and S. S. Gill (ed.), Comprehensive Molecular Insect Science, Vol. 6, Elsevier, New York, NY, USA.

3. **Bravo, A., I. Gómez, J. Conde, C. Muñoz-Garay, J. Sánchez, M. Zhuang, S. S Gill, and M. Soberón.** 2004. Oligomerization triggers differential binding of a pore-forming toxin to a different receptor leading to efficient interaction with membrane microdomains. Biochim. Biophys. Acta **1667**:38-46.

4. **de Maagd, R. A., P. Bakker, L. Masson, M. J. Adang, S. Sangadala, W. Stiekema, and D. Bosch.** 1999. Domain III of the *Bacillus thuringiensis* delta-endotoxin Cry1Ac is involved in binding to *Manduca sexta* brush border membranes and to its purified aminopeptidase N. Mol. Microbiol. **31**:463-471.

5. **Gómez, I., J. Sánchez, R. Miranda, A. Bravo, and M. Soberón.** 2002. Cadherin-like receptor binding facilitates proteolytic cleavage of helix α-1 in domain I and oligomer pre-pore formation of *Bacillus thuringiensis* Cry1Ab toxin. FEBS Lett. **513**:242-246.

6. **Gómez, I., J. Miranda-Rios, E. Rudiño-Piñera, D. I. Oltean, S. S. Gill, A. Bravo, and M. Soberón.** 2002. Hydropathic complementarity determines interaction of epitope ^{869}HITDTNNK^{876} in *Manduca sexta* Bt-R_1 receptor with loop 2 of domain II of *Bacillus thuringiensis* Cry1A toxins. J. Biol. Chem. **277**:30137-30143.

7. **Hawlisch, H., A. Meyer zu Vilsendorf, W. Bautsch, A. Klos, and J. Kohl.** 2000. Guinea pig C3 specific rabbit single chain Fv antibodies from bone marrow, spleen and blood derived phage libraries. J. Immunol. Methods **236**:117-31.

8. **Zhuang, M., D.I. Oltean, I. Gómez, A.K. Pullikuth, M. Soberón, A. Bravo, and S. S. Gill.** 2002. *Heliothis virescens* and *Manduca sexta* lipid rafts are involved in Cry1A toxin binding to the midgut epithelium and subsequent pore formation. J. Biol. Chem. **277**:13863-13872.